# Acidic Deposition:

# State of Science and Technology

**Report 24**

## *Visibility: Existing and Historical Conditions – Causes and Effects*


NATIONAL ACID PRECIPITATION ASSESSMENT PROGRAM

This Report is one from the series of Final Assessment Reports of the National Acid Precipitation Assessment Program

# Acidic Deposition: State of Science and Technology, Volumes I - IV

## Volume I — Emissions, Atmospheric Processes and Deposition

Report 1 — *Emissions Involved in Acidic Deposition Processes*
Report 2 — *Atmospheric Processes Research and Process Model Development*
Report 3 — *Regional Acid Deposition Modeling*
Report 4 — *The Regional Acid Deposition Model and Engineering Model*
Report 5 — *Evaluation of Regional Acidic Deposition Models*
Report 6 — *Deposition Monitoring: Methods and Results*
Report 7 — *Air Quality Measurements and Characterizations for Terrestrial Effects Research*
Report 8 — *Relationships Between Atmospheric Emissions and Deposition/Air Quality*

## Volume II — Aquatic Processes and Effects

Report 9 — *Current Status of Surface Water Acid-Base Chemistry*
Report 10 — *Watershed and Lake Processes Affecting Surface Water Acid-Base Chemistry*
Report 11 — *Historical Changes in Surface Water Acid-Base Chemistry in Response to Acidic Deposition*
Report 12 — *Episodic Acidification of Surface Waters Due to Acidic Deposition*
Report 13 — *Biological Effects of Changes in Surface Water Acid-Base Chemistry*
Report 14 — *Methods for Projecting Future Changes in Surface Water Acid-Base Chemistry*
Report 15 — *Liming Acidic Surface Waters*

## Volume III — Terrestrial, Materials, Health and Visibility Effects

Report 16 — *Changes in Forest Health and Productivity in the United States and Canada*
Report 17 — *Development and Use of Tree and Forest Response Models*
Report 18 — *Response of Vegetation to Atmospheric Deposition and Air Pollution*
Report 19 — *Effects of Acidic Deposition on Materials*
Report 20 — *Processes of Deposition to Structures*
Report 21 — *Distribution of Materials Potentially at Risk from Acidic Deposition*
Report 22 — *Direct Health Effects of Air Pollutants Associated with Acidic Precursor Emissions*
Report 23 — *Indirect Health Effects Associated with Acidic Deposition*
Report 24 — *Visibility: Existing and Historical Conditions – Causes and Effects*

## Volume IV — Control Technologies, Future Emissions, and Effects Valuation

Report 25 — *Technologies and Other Measures for Controlling Emissions: Performance, Costs and Applicability*
Report 26 — *Methods for Modeling Future Emissions and Control Costs*
Report 27 — *Methods for Valuing Acidic Deposition and Air Pollution Effects*

Volumes I - IV can be purchased from:
Superintendent of Documents
Government Printing Office
Washington, DC 20402-9325
(202) 783-3238

# NAPAP REPORT 24

# VISIBILITY: EXISTING AND HISTORICAL CONDITIONS—CAUSES AND EFFECTS


## Principal Author:

**John C. Trijonis**
Santa Fe Research Corporation
11200 Bloomington Ferry Road
Bloomington, MN 55438

## Primary Co-authors:

**William C. Malm**
National Park Service - Air
CIRA - Foothills Campus
Colorado State University
Fort Collins, CO 80523

**Marc Pitchford**
National Oceanic and Atmospheric Administration
Assigned to US EPA/EMSL
PO Box 93478
Las Vegas, NV 89193

**Warren H. White**
Campus Box 1124—CAPITA
Washington University
St Louis, MO 63130

## Contributing Authors:

**Robert Charlson (sections 2.3 & 3.6)**
Dept of Atmospheric Science
University of Washington
Seattle, WA 98195

**Rudolf Husar (section 3.4)**
Campus Box 1124—CAPITA
Washington University
St Louis, MO 63130



October 1990

## CONTENTS

## TABLES

## FIGURES[a]



[a] CP in a page number indicates a Color Plate at the end of the Report.

## DEFINITIONS

**Acid precipitation** - typically is rain with high concentrations of acids produced by the interaction of water with oxygenated compounds of sulfur and nitrogen which are the by-products of fossil fuel combustion.

**Aerosols** - gaseous suspension of ultramicroscopic particles of a liquid or a solid. Atmospheric aerosols govern variations in light extinction and, therefore, visibility reduction. Aerosol size distribution and chemistry are key parameters.

**Albedo** - the fraction of total light incident on a reflecting surface that is reflected back omnidirectionally.

**Anthropogenic** - refers to alteration to the natural environment caused by human activity, i.e. man-made.

**Apparent spectral contrast** - percent difference in radiant energy associated with an object and its background when the object is observed at some distance r.

**Apportionment** - the act of assessing the degree to which specific components contribute to light extinction or aerosol mass.

**Artifact** - any component of a signal or measurement that is extraneous to the variable represented by the signal or measurement.

**Atmospheric clarity** - is an optical property related to the visual quality of the landscape viewed from a distance (see optical depth and turbidity).

**Cloud condensation nuclei** - particles of liquids or solids upon which condensation of water vapor begins in the atmosphere.

**Contrast transmittance** - contrast transmittance is the ratio between apparent and inherent spectral contrast. When the object is darker than its background, it has a value between 0 and -1. For objects brighter than their background the value varies from 0 to infinity. When the contrast transmittance is equal to zero, the object cannot be seen.

**Current conditions** - refer to contemporary, or modern, atmospheric conditions that are affected by human activity.

**Deliquescence** - the process that occurs when the vapor pressure of the saturated aqueous solution of a substance is less than the vapor pressure of water in the ambient air. Water vapor is collected until the substance is dissolved and in equilibrium with its environment.

**Direct effects** - the optical effects of aerosols on climate modification referring to absorption and scattering of solar radiation by airborne particles.

**"ΔE" parameter** - an index of color and brightness differences for developed for colorimetry studies by Commission International de l'Eclairage.

**Edge sharpness** - describes a characteristic of landscape features. Landscape features with sharp edges contain scenic features with abrupt changes in brightness.

**Equilibration** - a balancing or counter balancing to create stability, often with a standard measure or constant.

**Equivalent contrast** - any scene can be fourier decomposed into light and dark bars of various frequencies and intensities modulated in accordance with a sine wave function. Equivalent contrast is the average contrast of those sine waves within a specified range of spatial frequencies.

**Externally mixed** - particulate species that co-exist as separate particles without co-mingling or combining.

**Hydrophobic** - lacking affinity for water, or failing to adsorb or absorb water.

**Hygroscopic** - an ability or tendency to rapidly accelerate condensation of water vapor around a nucleus. Also pertains to a substance (*e.g.* aerosols) which have an affinity for water and whose physical characteristics are appreciably altered by the effects of water.

**Indirect effects** - non-optical atmospheric effects of aerosols on cloud albedo and formation, e.g. as condensation nuclei for cloud droplets.

**Inherent spectral contrast** - percent difference in radiant energy associated with an object and its background at an observer distance equal to zero.

**Internally mixed** - refers to the situation where individual particles contain one or more species. For example, water is internally mixed with its hygroscopic hosts.

**Just noticeable change** - a variation of just noticeable difference that relates directly to human visual perception. A JNC corresponds to the amount of optical change in the atmosphere required to evoke human recognition of a change in a given landscape (scenic) appearance. The change in atmospheric optical properties may be expressed as the number of JNC's between views of a given scene at different intervals of time.

**Just noticeable difference** - is a measure of change in image appearance that affects image sharpness. Counting the number of JND's (detectable changes) in scene appearance is regarded as an alternative method of quantifying visibility reduction (light extinction).

**Koschmeider constant** - the constant in the reciprocal relationship between standard visual range and the extinction coefficient (see standard visual range).

**Light extinction** - the attenuation of light per unit distance due to absorption and scattering by the gases and particles in the atmosphere.

**Liquid water** - the water present within a cloud expressed as a percent of total cloud constitutents, or liquid phase water in an aerosol.

**Mie scattering** - the attenuation of light in the atmosphere by scattering due to particles of a size comparable to the wavelength of the incident light. This is the phenomenon largely responsible for the reduction of atmospheric visibility. Visible solar radiation falls into the range from 0.4 to 0.8 μm, roughly, with a maximum intensity around 0.52 μm.

**Modulation transfer function (MTF)** - is a mathematical function which describes contrast transmittance in spatial-frequency space. It is the ratio between scene equivalent contrast at the observer and equivalent contrast at the object. When the object of interest is small compared to its surroundings, the modulation transfer function and contrast transmittance reduce to the same value.

**Natural conditions** - refer to prehistoric and pristine atmospheric states, *i.e.* atmospheric conditions that are not affected by human activities.

**Nephelometer** - an instrument used to measure the light scattering component of light extinction.

**Optical depth** - the degree to which a cloud or haze prevents light from passing through it. It is a function of physical composition, size distribution, and particle concentration. Often used interchangeably with "turbidity".

**Path radiance** - or "airlight", is a radiometric property of the air resulting from light scattering processes along the sight line, or path, between a viewer and the object (target).

**Primary particles** - primary particles are suspended in the atmosphere as particles from the time of emission (*e.g.* dust and soot).

**Pyranometer** - an instrument that measures directly the loss of total solar radiance under clear sky conditions.

**Quadratic detection model** - is a model used to predict the amount of change in equivalent contrast or perceived landscape structure required to evoke a single just noticeable change in landscape appearance.

**Rayleigh scattering** - refers to the scattering of light by air molecules, also called blue-sky scatter.

**Secondary particles** - are formed in the atmosphere by a gas-to-particle conversion process.

**Spatial frequency** - is the reciprocal of the distance between sine wave crests (or troughs) measured in degrees of angular subtense of a sine wave grating. Spatial frequency is a general term for the frequencies associated with the image radiance in a scene along the path of radiance (path of sight). Landscape features contain multiple landscape scenic elements. Each element generates its own image radiance with its own frequency and intensity.

**Standard visual range** - is the reciprocal of the extinction coefficient. The distance under daylight and uniform lighting conditions at which the apparent contrast between a specified target and its background becomes just equal to the threshold contrast of an observer, assumed to be 0.02.

**Telephotometer** - a photometer designed to measure the radiant energy arriving from a scene weighted in accordance with the response of the human eye brain system to spectral radiance.

**Threshold contrast** - a measure of human eye sensitivity to contrast. It is the smallest increment of contrast preceptible by the human eye.

**Transmissometer** - an instrument that measures atmospheric transmittance. From transmittance, the atmospheric extinction coefficient can be derived.

**Transmittance** - the fraction of initial light from a light source that is transmitted through the atmosphere. Light is attenuated by scattering and absorption from gases and particles.

**Turbidity** - a condition that reduces atmospheric transparency to radiation, especially light. The degree of cloudiness, or haziness, caused by the presence of aerosols, gases, and dust.

**Visibility** - refers to the visual quality of the view, or scene, in daylight with respect to color rendition and contrast definition. The ability to perceive form, color, and texture.

**Visibility indexes** - have been formalized for aerosol, optical, and scenic attributes. Aerosol indexes include mass concentrations, particle compositions, physical characteristics, and size distributions. The optical indexes include coefficients for scattering, extinction, and absorption. Scenic indexes comprise visual range, contrast, radiance, color, and just noticeable changes.

**Visibility reduction** - is the impairment or degradation of atmospheric clarity. Becomes significant when the color and contrast values of a scene to the horizon are altered or distorted by airborne impurities.

**Visual image processing** - the digitizing, calibration, modeling, and display of the effects of atmospheric optical parameters on a scene. The process starts with a photograph of landscape features viewed in clean atmospheric conditions and models the effects of changes in atmospheric composition.

## ACRONYMS

| | |
|---|---|
| **ACHEX** | California Aerosol Characterization Study |
| **BAPMON** | Background Air Pollution Monitoring Network |
| **CARB** | California Air Resources Board |
| **CCN** | cloud condensation nuclei |
| **CIE** | Commission International de l'Eclairage |
| **CPD** | cycles per degree |
| **EFPVN** | Eastern Fine Particle Visibility Network |
| **EPA** | U.S. Environmental Protection Agency |
| **ERAQS** | Eastern Regional Air Quality Studies |
| **GCM** | global circulation models |
| **GMCC** | Geophysical Monitoring for Climatic Change |
| **HI-VOLS** | high volume samplers |
| **IMPROVE** | Interagency Monitoring of Protected Visual Environments |
| **IN** | ice nuclei |
| **IP** | Inhalable Particle network |
| **JNC** | just noticeable change |
| **JND** | just noticeable difference |
| **MTF** | modulation transfer function |
| **NAPAP** | National Acid Precipitation Assessment Program |
| **NASN** | National Air Surveillance Network |
| **NOAA** | National Oceanic and Atmospheric Administration |
| **NPS** | National Park Service |
| **PACS** | Portland Aerosol Characterization Study |
| **PANORAMAS** | Pacific Northwest Regional Aerosol Mass Apportionment Study |
| **QDM** | quadratic detection model |
| **RAPS** | Regional Air Pollution Study |

| | |
|---|---|
| **RESOLVE** | Desert Visibility Study |
| **RH** | relative humidity |
| **SBE** | scenic beauty |
| **SCENES** | Subregional Cooperative Electric Utility, Department of Defense, National Park Service, Environmental Protection Agency Study |
| **SOS/T** | State of Science/Technology |
| **SURE** | Sulfate Regional Experiment |
| **TVA** | Tennessee Valley Authority |
| **VAQ** | visual air quality |
| **VIPS** | Visibility Image Processing System |
| **WMO** | World Meteorological Organization |
| **WRAQS** | Western Regional Air Quality Study |

# SECTION 1

# INTRODUCTION

One of the important effects associated with acid precipitation related pollutants is interference with radiation transfer (light transmission) in the atmosphere. An obvious result of such interference is visibility degradation—the impairment of atmospheric clarity or of the ability to perceive form, texture, and color. Climate modification constitutes another, somewhat less obvious, result. The purpose of this NAPAP State of Science/Technology report is to summarize current knowledge regarding these radiation transfer effects. Although this report focuses mainly on visibility issues, it does encompass the emerging field of climate modification.

The links between the acid rain problem and radiation transfer effects, although indirect, are quite strong. The principal link is through sulfur dioxide emissions and sulfate aerosols. Sulfur dioxide, a major contributor to acid deposition, produces sulfate aerosol (itself a fundamental component of acid deposition). Sulfate aerosol, in turn, is an important contributor to visibility reduction—in fact, the dominant contributor in the eastern United States. A secondary link occurs through nitrogen oxide emissions. Nitrogen oxide emissions—also a major contributor to acid deposition—produce gaseous nitrogen dioxide and, in combination with ammonia (which may be the controlling precursor emission), fine ammonium nitrate particles. Ammonium nitrate aerosol sometimes accounts for a significant fraction of visibility degradation, and nitrogen dioxide typically contributes a few percent of visibility reduction.

## 1.1 BASIC CONCEPTS

*J.C. Trijonis*

The terminology, concepts, and theory related to radiation transfer in the atmosphere are explained in detail in Section 2. Here, as an introduction to the scope and direction of this report, it is useful to review a few concepts concerning visibility and atmospheric light extinction.

Visibility does not have a precise, universally accepted, scientific definition. Its implied meanings are as diverse as the various disciplines which investigate the ability to see objects either in the laboratory or under natural conditions. Webster's dictionary defines visibility as "the quality or state of being visible; the degree of clearness of the atmosphere—the greatest distance toward the horizon that prominent objects can be identified visually with the naked eye."

Historically, much of the interest in visibility came from aviation and military operations, where the most important aspect of visibility was the furthest distance at which an object could be discerned. Pilots needed to have some minimum visual range to land their airplanes, bombardiers needed to know the greatest distance at which they could first see a target, fighter pilots were interested in the distance they could first observe other aircraft, and observers on warships needed to know the farthest distance that they could first spot an enemy vessel. Consequently, early on, visibility became synonymous with visual range—the maximum distance at which an observer could identify an object against a uniform background. This concept of visibility is reflected in the definition by the World Meteorological Organization, which is as follows:

> "Meteorological visibility by day is defined as the greatest distance at which a black object of suitable dimensions, situated near the ground, can be seen and recognized when observed against a background fog or sky."

Currently, much of the concern about visibility is related to the aesthetic damage from air pollution. From an aesthetic perspective, visibility represents not just visual range but rather the overall visual experience of an observer viewing a scene. Once the atmosphere has become sufficiently hazy so that an object is just perceptible, the object has lost all color and texture and—for all practical purposes—all its scenic value. Aesthetically, the main issues are whether an observer can clearly see the form, color, and texture of features that are at distances less than the visual range, and whether an observer can discern the atmospheric haze in and of itself.

This report is mostly concerned with this later concept of visibility, *i.e.*, degradation of aesthetics by air pollution. However, because of the historical significance, ease of understanding, popularity among researchers, and continued importance to aviation of visual range, the visual range concept is also used. Also, it should be stressed that aesthetics and visual range are not unrelated, both are tied closely to light transmittance in the atmosphere.

Under a variety of viewing conditions, "visibility reduction" or "haziness" is directly proportional to reduction in atmospheric light transmittance. Light transmittance in the atmosphere is attenuated by scattering and absorption from both gases and particles. The extinction coefficient

(**B**ext), which measures the total fraction of light that is attenuated per unit distance, is simply the sum of these four components, **B**ext = **B**sg + **B**ag + **B**sp + **B**ap. Here,

**B**sg = light scattering by gases (Rayleigh or natural blue-sky scatter by air molecules). This term is on the order of 10 to 12 $Mm^{-1}$, depending on altitude.

**B**ag = light absorption by gases. Nitrogen dioxide ($NO_2$) is the only common gaseous species that significantly absorbs light. Light absorption by $NO_2$ typically contributes only a few percent of total extinction in regional or urban hazes, but it is sometimes important to discoloration by plumes because $NO_2$ preferentially absorbs blue light.

**B**sp = light scattering by particles. Except under extremely clean conditions, when Rayleigh scatter predominates, this term is usually the largest component of light extinction. Light scattering is dominated by *fine* particles because scattering efficiency per unit particle mass exhibits a pronounced peak in the size range of 0.1 to 1.0 μm.

**B**ap = light absorption by particles. This term arises nearly entirely from elemental carbon (soot particles).

Because extinction coefficient is a fundamental optical variable that under a variety of viewing conditions relates directly to how well a landscape feature can be seen, many of the discussions in this report will center around the concept of light extinction.

Another important issue to emphasize is that particles (aerosols) tend to dominate total light extinction except under extremely clean conditions (when Rayleigh scatter predominates). Thus, a state-of-science assessment for visibility requires, to some degree, a similar assessment regarding knowledge about aerosols. Therefore, in this report, a great deal of attention will be focused on aerosols (in terms of monitoring methods, data bases, existing concentrations, background conditions, origins, *etc.*).

Compared to many other effects of air pollutants, visibility is fairly well understood. Unlike certain acid deposition effects that are multi-media, involve cumulative buildup, or are delayed, atmospheric optical parameters are instantaneous properties of atmospheric composition. The fundamental physics relating light extinction (and other optical parameters) to atmospheric gases and particles is well established. Also, light extinction is a simple linear sum of scattering and absorption by gases and particles. Furthermore, additional sub-divisions of light extinction contributions are either exactly additive (*e.g.* coarse versus fine particles) or approximately additive (*e.g.* allocations among chemical species). In fact, even before the past decade of visibility research, visibility was called the "best understood and most easily measured effect of air pollution" (Council on Environmental Quality, 1978).

## 1.2 SPATIAL AND TEMPORAL SCALES
*J.C. Trijonis*

Although much of acid precipitation research focuses on the eastern United States, the spatial scope of this report is the entire continental United States. Parts of the report even involve expanded spatial coverage. For example, the spatial/seasonal patterns for visibility (Section 3.3) include some data for Canada, and the climate analyses (Sections 3.6 and 5.2) include considerations of global effects.

Within the overall national scope of this report, regional differences are characterized whenever possible. One obvious dichotomy that exists in aerosol concentrations and visibility is East versus West—most vividly, the area east of the Mississippi and south of the Great Lakes versus the mountain/desert West. This dichotomy is acknowledged and treated in most parts of the report. Sometimes, further regional subdivisions are considered, *e.g.*, Pacific Northwest, California coast, *etc.*, in the West; or New England, Appalachian mountains, *etc.*, in the East.

Another spatial issue involves the distinction between metropolitan (urban) versus nonmetropolitan (nonurban). This report considers both urban and nonurban areas, although the emphasis is slightly on the latter because acid precipitation is basically a large-scale, regional phenomenon. With respect to visibility field studies, the distinction between urban versus nonurban is usually rather easy to make because such studies typically have been carried out either in very large metropolitan centers or in rural/remote areas.

When discussing uncertainties associated with visibility (or light extinction) levels, we have adopted a special notation related to spatial variability versus potential estimation errors. Unless otherwise specified, a range of numbers (*e.g.*, 20 - 35 km current visual range in the East) represents both spatial variation and estimation uncertainty, while a plus-or-minus (such as 150 ± 45 km natural visual range averaged over the East) represents estimation uncertainty only.

With respect to temporal considerations, the initial thrust of nearly all the analyses in this report is to characterize annual values, either as annual averages or annual medians. After that, in many cases, seasonal aspects are addressed in terms of quarterly averages or quarterly medians. Except where otherwise noted, the quarters are seasonal (*i.e.*, Dec - Feb, Mar - May, *etc.*) rather than calendrical (Jan - Mar, Apr - Jun, *etc.*) In some instances,

worst-case conditions (*i.e.*, 90th, 95th, or 99th percentiles) are considered in addition to averages or medians.

## 1.3 REPORT CONTENTS, SCOPE, AND PHILOSOPHY

*J.C. Trijonis*

This report is organized into seven sections. The present section provides an introduction and a statement of scope and philosophy. Section 2 discusses basic concepts and theories regarding aerosol air quality, radiation transfer, visibility effects, and climatic effects. Section 3 characterizes existing and historical conditions; it includes a survey of methods and data, a description of geographical/temporal patterns, an analysis of historical trends, and an assessment of natural background. In Section 4, light extinction levels are apportioned with respect to the contributions from gases and various aerosol components. Section 5 describes the current level of visibility effects and climate effects. Section 6 presents a summary of conclusions, and Section 7 presents recommendations.

The basic purpose of this document is to review, evaluate, and synthesize the current scientific information regarding visibility (including climate). In working toward this purpose, several guidelines are followed. First, an attempt is made to rely, as much as possible, on peer-reviewed publications. In some instances, however, nonpeer-reviewed data are sufficiently important to be included. The nonpeer-reviewed sources are marked by an asterisk in the reference list. Second, an effort is made to include both quantitative and qualitative assessments of uncertainty. The qualitative uncertainties attached to major conclusions (Section 6.2) follow the NAPAP uncertainty classification scheme of

- o = no basis,
- * = limited information with major uncertainties,
- ** = broad information with large or unknown uncertainty or limited information with low uncertainty,
- *** = broad information with known but sometimes large uncertainty, and
- **** = ample and certain information.

Third, although the discussions include conflicting views and alternative explanations, the main thrust is to work toward conclusions, not to focus only on unknowns. Fourth, in line with the structure of NAPAP, this report is concerned with the effect (visibility) and the relationship of visibility to air quality. The report does not address the economics of visibility nor does it consider (with the exception of historical trend studies) the relationship of emissions to air quality. Also, in characterizing the effect, most of the concern is with optical variables and perception, with only minor discussions extending further to psychological issues and the science of human judgment. Lastly, this report is intended to lay the groundwork for visibility impact calculations in the Integrated Assessment phase of NAPAP. The extinction allocations of Section 4 and visibility effects modeling of Section 5 should provide the theoretical framework for linking visibility effects to air quality changes.

This report—like all the NAPAP State of Science/Technology documents—is directed toward scientific experts rather than a lay audience. The intent is to provide a technically sound, peer-reviewed summary of the state of visibility science for use by NAPAP in addressing visibility issues. For additional material on visibility, the reader is referred to the Visibility Report to Congress (EPA, 1979), the proceedings of three major visibility conferences (Atmospheric Environment, 1981; Bhardwaja *et al.*, 1987; Mathai *et al.*, 1990), and the various publications cited within this document.

# SECTION 2

# CONCEPTS AND THEORIES

The purpose of this section is to present the important definitions, concepts, and theories relevant to this report. The conceptual and theoretical framework is organized in three parts: aerosol air quality (Section 2.1), radiation transfer theory and visibility effects (Section 2.2), and climate effects (Section 2.3).

## 2.1 CONCEPTS OF AEROSOL AIR QUALITY

*J.C. Trijonis*

As noted in the Introduction, suspended particles in the atmosphere (*i.e.*, aerosols) usually account for the dominant part of light extinction. Accordingly, understanding visibility requires understanding the basic concepts and definitions of aerosol air quality.

One important set of definitions concerns the origins of atmospheric particles. Particle origins can be either *anthropogenic* (man-made) or *natural*. Another origin classification is *primary* versus *secondary*. Primary particles are those that are emitted into the atmosphere as particles, such as organic and soot particles in smoke plumes or soil dust particles. Secondary particles are those that are formed from gas-to-particle conversion in the atmosphere, such as sulfates (from $SO_2$), nitrates (from $NO_x$), and secondary organics (from gaseous hydrocarbons).

Size distribution is another critical aspect of atmospheric particles. Figure 24-1 presents an example of a typical number/surface/volume (mass) distribution (Whitby *et al.*, 1972). With respect to particle size, aerosols tend to

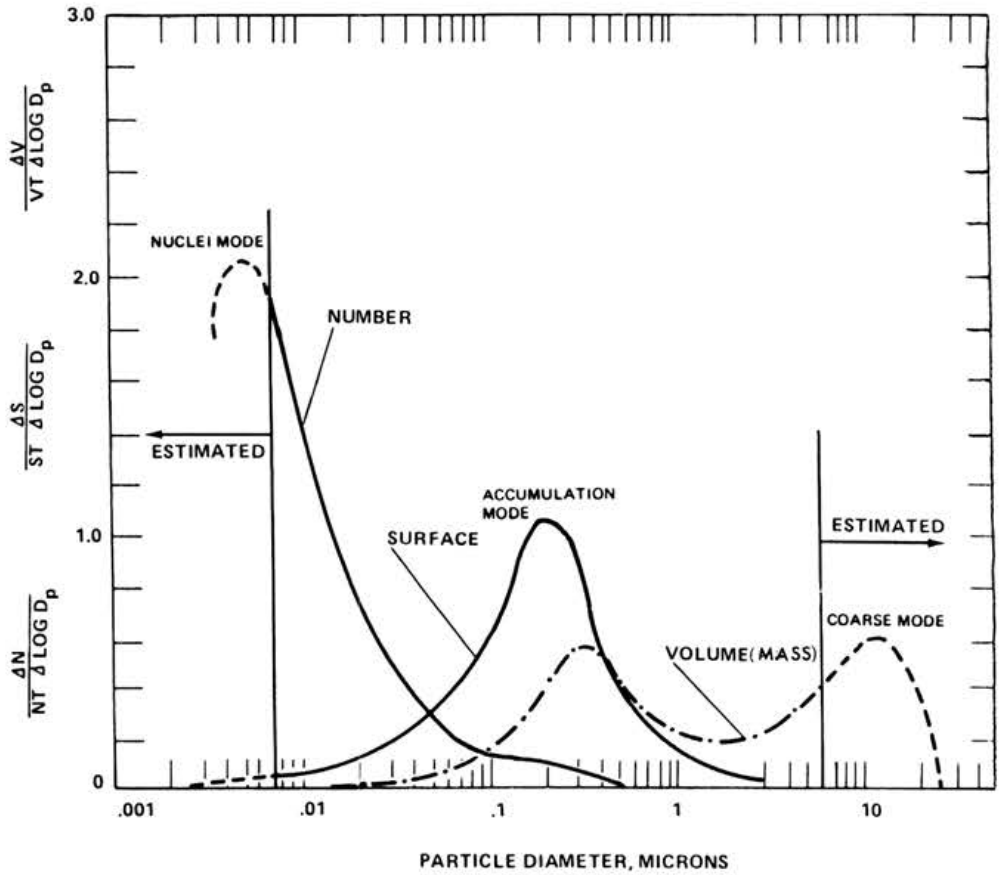


*Figure 24-1 Number, surface, and volume (mass) distributions for typical aerosols in the lower atmosphere (Whitby et al., 1972).*

occur in three modes: the *nuclei* mode (*0.005* to *0.1* μm diameter), *accumulation* mode (*0.1 to 1-3* μm), and *coarse* mode (*1-3 to 50-100* μm). Figure 24-2 illustrates the principal sources, formation processes, and removal mechanisms for each mode (Whitby and Cantrell, 1976).

The nuclei mode dominates with respect to numbers of particles but contributes very little to particle mass because the particles are so small. This mode forms from the condensation and coagulation of hot supersaturated vapors during combustion and from homogeneous nucleation of secondary aerosols (nucleation that forms new particles). The accumulation mode predominates with respect to surface area and contributes substantially to aerosol mass. This mode forms from two processes: coagulation of smaller particles and heterogeneous nucleation of secondary particles (condensation of one material on another, *i.e.*, on existing particles). Because of the decrease in particle numbers and surface area at the upper size range of the accumulation mode, particles in this mode do not tend to grow significantly into the coarse mode. The coarse mode, rather, comes from natural and man-made mechanical processes, such as suspension of dust.

Because of marked difference in origin, behavior, effects, and removal processes, it is often worthwhile to consider the coarse mode separately from the nuclei and accumulation modes. Accordingly, the latest routine methods for sampling particle mass allow the distinction of fine particle mass (≤ *2.5* μm) from *coarse particle mass* (*2.5* μm to a selected upper bound).

Another important aspect of aerosol air quality is chemical composition which, as one could expect from the

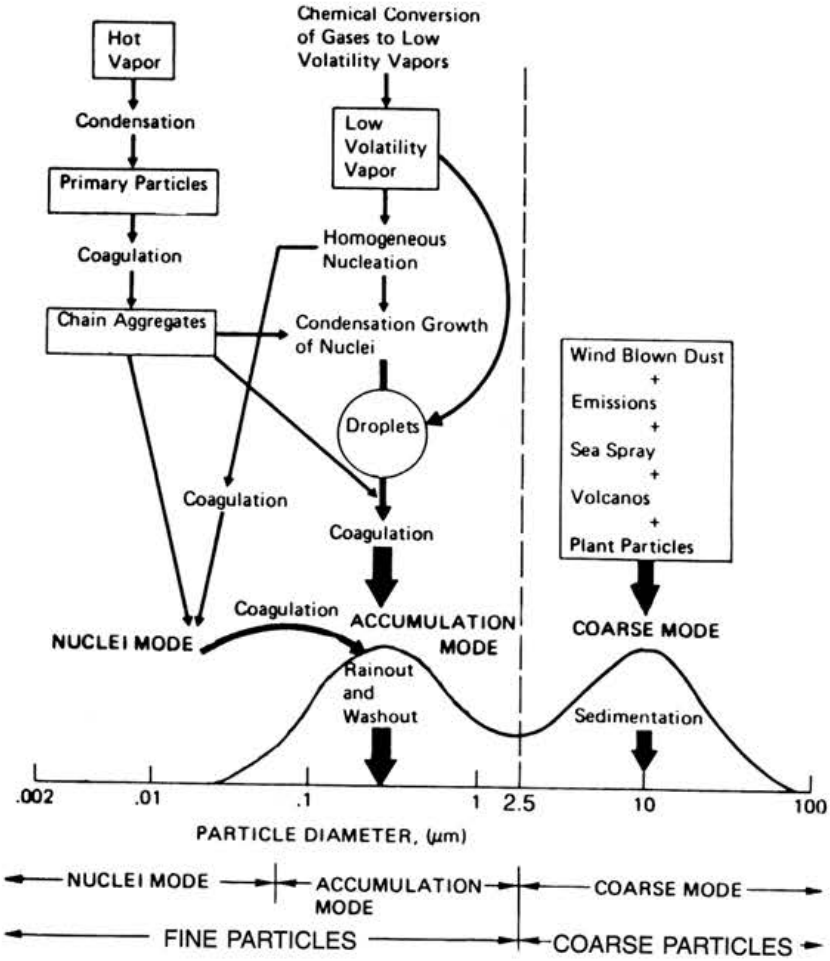


*Figure 24-2 Diagram of hypothetical mass distribution for particles showing the three particle modes as well as sources, atmospheric mechanisms, and removal processes (Whitby and Cantrell, 1976).*

above discussions, bears a strong interrelationship to particle size. In almost all cases, dry fine particle mass is dominated by just five types of chemical species: sulfates (typically with ammonium and/or hydrogen cations), organics, ammonium nitrate, soil dust (from the lower tail of the coarse mode), and elemental carbon. The two largest contributors are usually sulfates and organics, which together typically account for about *60* to *80%* of average dry fine mass (Eldred *et al.*, 1987; Trijonis, 1982a; also see particle composition data in Section 4.2 and Appendix A).

Under ambient conditions, aerosol water constitutes a very important sixth component of fine particle mass. At high relative humidities (*e.g.* above *80%*), water often contributes the majority of ambient fine aerosol mass (Covert *et al.*, 1972; Winkler, 1973; Ho *et al.*, 1974; Stelson and Seinfeld, 1981; Tang *et al.*, 1981). Most of this water is drawn into the aerosol phase by the hygroscopic (or deliquescent) properties of sulfates, nitrates, and some organics. Reducing the atmospheric concentrations of these hygroscopic species would reduce the concentrations of ambient aerosol water.

Coarse mass tends to be dominated by soil dust (*e.g.*, oxides and other salts of *Si, Al, Fe, Ca, etc.*) Other, usually lesser, contributions to coarse mass come from sea spray (*Na, Cl, etc.*), plant particles (organics), reactions of gaseous nitric acid with soil dust or sea salt particles (nitrates), and the upper tail of the accumulation mode particles (*e.g.*, sulfates and organics).

Because of the dichotomy in chemical and physical natures, fine particles and coarse particles exhibit pronounced differences in terms of effects (such as health, corrosion, soiling, visibility, and climatology). The effects of concern to this report are visibility and climatology, *i.e.*, the radiation transfer effects. As will be explained later in this chapter, fine particles tend to dominate over coarse particles in terms of impacts on radiation transfer.

## 2.2 THEORY OF RADIATION TRANSFER AND VISIBILITY

*W.C. Malm*

The response of the human eye to radiant energy of different wavelengths is shown in Figure 24-3. The maximum response to a unit of energy is at *0.55* microns. When radiant energy is discussed in terms of the response of the human eye, *photometric* concepts and units are conventionally used. Conversely, when the entire radiation field of the sky is modeled or measured, *radiometric* units are employed. Usually, but not always, photometric parameters are derived from the more fundamental radiometric variables. Table 24-1 lists the various radiometric and corresponding photometric variables typically employed in radiation transfer calculations.

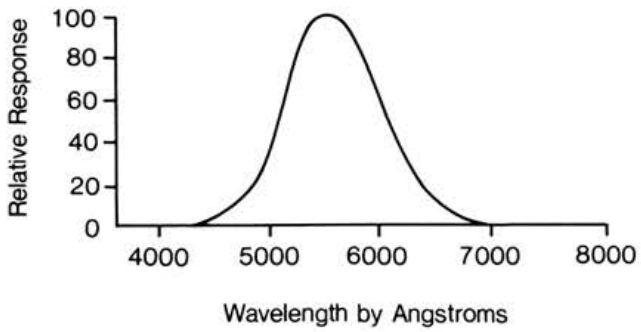


*Figure 24-3 Spectral response of the human eye.*

*Table 24-1. Radiometric and Photometric Concepts and Units*

| Radiometric | Symbol | Units | Photometric | Symbol | Units |
|---|---|---|---|---|---|
| Radiant energy | U | joule | Luminous energy | Q | talbot |
| Radiant flux | P | watt | Luminous flux | F | lumen |
| Radiant intensity | J | watt/steradian | Luminous intensity | I | lumen/steradian |
| Radiance | N | watt/$m^2$ steradian | Luminance | B | lumen/$m^2$ steradian |
| Irradiance | H | watt/$m^2$ | Illuminance | E | lumen/$m^2$ |

The alteration of radiant energy as it passes through the atmosphere is due to scattering and absorption by gases and particles. The sum of scattering and absorption is referred to as the extinction coefficient. The effect of the atmosphere on the visual properties of distant objects theoretically can be determined if the concentration and characteristics of air molecules, particles, and absorbing gases are known throughout the atmosphere and most importantly along the line of sight between the observer and object.

A schematic of how direct sunlight, reflected sunlight, and diffuse radiation affect the seeing of landscape features is shown in Figure 24-4. Image-forming information is lost by the scattering of imaging radiant energy out of the sight path and absorption within the sight path, while ambient light scattered into the sight path adds radiant energy to the observed radiation field. This process is described by

$$\frac{dN_r(\theta,\varphi,\vec{r})}{dr} = -B_{ext}N_r(\theta,\varphi,\vec{r}) + N_s(\theta,\varphi,\vec{r}) \qquad \textbf{(24-1)}$$

$$(loss) \qquad (gain)$$

where $N_r(\theta,\varphi,\vec{r})$ is the apparent radiance at some vector distance "$r$" from a landscape feature, $N_s(\theta,\varphi,\vec{r})$ (referred to as the path function) is the radiant energy gain within an incremental path segment, and $B_{ext}N_r(\theta,\varphi,\vec{r})$ is radiant energy lost within that same path segment. The atmospheric extinction coefficient ($B_{ext}$) is the sum of both atmospheric scattering ($B_s$) and absorption ($B_a$). Although not explicitly stated, it is assumed that each variable in, and each variable derived from, Equation 24-1 is wavelength dependent. The parenthetical variables $(\theta,\varphi,\vec{r})$ indi-

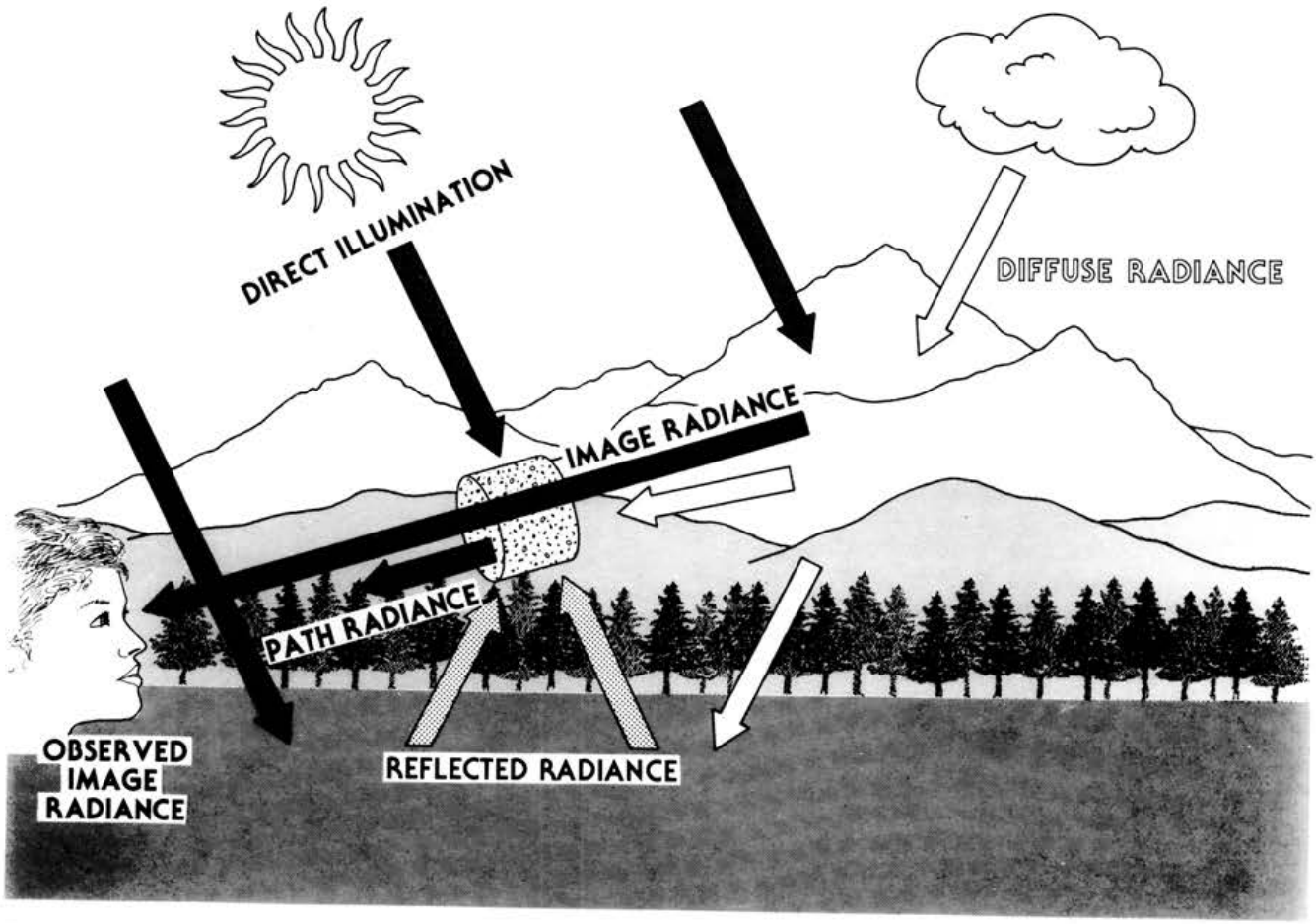


*Figure 24-4 Schematic diagram showing the interaction of direct and diffuse radiance with landscape features and atmospheric particles to produce image forming and path radiance.*

cate that $N_r$ and $N_*$ are dependent both on the direction of image transmission and on the position within the path segment. For the sake of brevity, the parenthetical variables will be dropped in following equations. When the postscript "$r$" is appended to any symbol, it denotes that the quantity pertains to a path of length $r$. The subscript "$o$" always refers to the hypothetical concept of any instrument located at zero distance from the object—as, for example, in denoting the inherent radiance of a surface. Prescripts identify the objects, the prescript "$b$" referring to background and "$t$" to target.

When $N_r$ has some special value, $N_q$, such that $B_{ext} N_q = N_*$, then $dN_q/dr = 0$. $N_q$ is independent of $r$ and is commonly referred to as the equilibrium radiance. Therefore, for every path segment

$$\frac{dN_r}{dr} = -B_{ext}(N_r - N_q). \qquad \textbf{(24-2)}$$

If $N_q$ is constant, Equation 24-2 can be integrated to yield

$$\frac{N_r - N_q}{N_o - N_q} = T_r \qquad \textbf{(24-3)}$$

where $T_r$ is the transmittance over path length $r$ and is given by

$$T_r = e^{-\int_o^r B_{ext}(r)dr}. \qquad \textbf{(24-4)}$$

Rearranging Equation 24-3 yields

$$N_r = N_o T_r + N_q(1 - T_r) \qquad \textbf{(24-5)}$$

where the first term on the right of Equation 24-5 is the residual image forming radiance, while the second term is the path radiance (airlight), $N_r^*$, which results from scattering processes throughout the sight path. The parameter $NN^*_\infty$ is the sky radiance

$$N_\infty^* = N_q(1 - T_\infty). \qquad \textbf{(24-6)}$$

If $T_\infty$ is approximately zero, then $N_q = N^*_\infty = N_s$ and

$$N_r^* = N_s(1 - T_r) \qquad \textbf{(24-7)}$$

where $N_s$ is sky radiance. Equation 24-7 allows for a simple approximation of $N_r^*$ when $N_s$ is known.

The explicit dependence of $N_r^*$ on illumination and directional scattering properties of the atmosphere is best examined by considering

$$N_r^* = \int_o^r N_* T_r dr \qquad \textbf{(24-8)}$$

where

$$N_* = h_s\sigma + \int_{4\pi} N\sigma d\Omega. \qquad \textbf{(24-9)}$$

The second term on the right-hand side is the contribution to $N_*$ from sky, cloud, and earth radiance and $d\Omega$ is an element of solid angle. The parameter $h_s$ is sun irradiance, and $\sigma$ is the volume scattering function defined in such a way that

$$B_s = \int_{4\pi} \sigma d\Omega \qquad \textbf{(24-10)}$$

Therefore, $\sigma$ describes the amount of radiant energy (light) scattered in some direction, while the sum of radiant energy scattered in all directions is proportional to the scattering coefficient $B_s$. The amount of energy scattered out of and into a sight path over some incremental distance, $\Delta_r$, is proportional to $B_s$. It is a fundamental optical property of the atmosphere. Its measurement (see Section 3.1) and characterization (see Section 4.3) have been the focus of a number of studies.

### 2.2.1 Contrast Transmittance in Real Space

Any landscape feature can be thought of as consisting of many small pieces, or elements, with a variety of physical characteristics. For instance, the reflectivity of an element as a function of wavelength, along with characteristics of the incident radiation, determines its color and brightness. The brightness of a scenic element at some observing distance and at one wavelength is referred to as monochromatic apparent spectral radiance. The monochromatic apparent spectral radiance of any scenic element is given according to Equation 24-5 by

$${}_sN_r = T_r\,{}_sN_o + N_r^* \qquad \textbf{(24-11)}$$

where $N_r^*$ is substituted explicitly for $N_q(1-T_r)$. The subscript $s$ indicates that the radiance is associated with a specific uniform scenic element.

A scenic element is always seen against some background, such as the sky or another landscape feature. The apparent and inherent background radiance are related by an expression similar to Equation 24-11

$${}_bN_r = T_r\,{}_bN_o + N_r^*. \qquad \textbf{(24-12)}$$

Subtracting Equation 24-12 from Equation 24-11 yields the relation

$$[{}_sN_r - {}_bN_r] = T_r[{}_sN_o - {}_bN_o]. \qquad \textbf{(24-13)}$$

Thus, *radiance differences* are transmitted along *any* path with the same attenuation as that experienced by each

image-forming ray. This important result is the basis for measuring extinction using transmissometer methods (see Section 3.1).

The image-transmitting properties of the atmosphere can be separated from the optical properties of the object by the introduction of the contrast concept. The *inherent spectral contrast*, $C_o$, of a scenic element is, by definition,

$$C_o=[{}_sN_o-{}_bN_o]/{}_bN_o. \quad \textbf{(24-14)}$$

The corresponding definition for *apparent spectral contrast* at some distance $r$ is

$$C_r=[{}_sN_r-{}_bN_r]/{}_bN_r. \quad \textbf{(24-15)}$$

If Equation 24-13 is divided by the apparent radiance of the background ${}_bN_r$ and combined with Equations 24-14 and 24-15, the result can be written as

$$C_r=C_o\frac{{}_bN_o}{{}_bN_r}T_r. \quad \textbf{(24-16)}$$

Substituting Equation 24-12 for ${}_bN_r$ and rearranging yields

$$\tau_r\equiv C_r/C_o=1/[1+N_r^*/{}_bN_o\,T_r]. \quad \textbf{(24-17)}$$

The right-hand member of Equation 24-17 is an expression for the *contrast transmittance*, $\tau_r$, of the path of sight. Equation 24-17 is the *law of contrast reduction by the atmosphere* expressed in the most general form. It should be emphasized that Equation 24-17 is completely general and applies rigorously to any path of sight regardless of the extent to which the scattering and absorbing properties of the atmosphere or the distribution of lighting exhibit non-uniformities from point to point. It is shown in Appendix C that $\tau_r$ can also be interpreted as the modulation transfer function of the atmosphere, $M_{tf,a}$. The concept of modulation transfer is necessary when the sensitivity of the eye-brain system to textural content of landscape features is considered. These concepts are discussed in Section 2.2.3.1.

## 2.2.2 Visual Range Concept

Substituting Equation 24-4 into Equation 24-16 yields

$$C_r=C_o\frac{{}_bN_o}{{}_bN_r}e^{-B_{ext}r}. \quad \textbf{(24-18)}$$

If an object is viewed against a background sky under uniform illumination conditions and through a uniform haze ${}_bN_r/{}_bN_r=1$ and Equation 24-18 becomes

$$B_{ext}=-\frac{1}{r}\ln C_r/C_o. \quad \textbf{(24-19)}$$

Equation 24-19 forms the basis for using teleradiometer contrast measurements for approximating the extinction coefficient. If $C_o$ and distance $r$ are known, $B_{ext}$ can be calculated.

The distance at which $C_r$ approaches a threshold contrast of between *-0.02* or *-0.05* defines the visual range, $V_r$. If $|C_o|=1$ (black object) and *-0.02* is taken to be a threshold contrast, then Equation 24-19 becomes

$$V_r=3.912/B_{ext}. \quad \textbf{(24-20)}$$

Equation 24-20 allows visual range data to be interpreted in terms of extinction and vice versa, extinction measurements to be interpreted in terms of visual range. There is some debate as to what threshold contrast to use. Appendix B presents a discussion of threshold measurements as well as a more complete derivation of Equation 24-20.

## 2.2.3 Equivalent Contrast

The above mathematical formalism is limited in that it does not account for human visual system response to edge sharpness between adjacent scenic features or to changes in contiguous contrast for features with varying size. More modern psychophysical perception threshold formalisms can be constructed to incorporate the eye brain system response to variations in edge sharpness between landscape features as well as variation in spatial frequency of landscape scenic elements (Carlson and Cohen, 1978; Campbell and Robson, 1964; Campbell *et al.*, 1968; Campbell and Kulikowski, 1986; Henry, 1977; Malm, 1985; Malm *et al.*, 1987c). Any approach which incorporates the human response to spatial frequencies (size and shape effects) is most easily handled using linear system theory. A first step is to develop a quantitative descriptor of the scene itself.

A scene can be further decomposed into light and dark bars of various spatial frequencies and intensities whose brightness change is proportional to a sine wave function. Equivalent contrast, $C_{eq}$, is just the average contrast of those sine waves within specified frequencies. Therefore, equivalent contrast can be calculated either for all spatial frequencies or only for those frequencies that the human visual system responds to. (See Appendix C for a more detailed derivation of equivalent contrast.) $C_{eq}$ can then be used in human visual system models to estimate the probability that a human observer will notice a change in the appearance of a landscape feature as aerosols are added or removed from the atmosphere.

### 2.2.3.1 Contrast Transmittance in Spatial Frequency Space (Modulation Transfer Function)

In a derivation similar to the contrast transmittance derivation (see Appendix C), it can be shown that the transmittance of equivalent contrast through the atmosphere in the presence of aerosols is given by

$$C_{eq,r}=C_{eq,o}\ M_{tf,a} \qquad \textbf{(24-21)}$$

where

$$M_{tf,a}=\frac{1}{1+\dfrac{N_r^*}{a_\infty T_r}}. \qquad \textbf{(24-22)}$$

$C_{eq,r}$ and $C_{eq,o}$ are the equivalent contrast at distance $r$ and $o$, respectively, while $M_{tf,a}$ is the atmospheric modulation transfer function. The parameter $a_\infty$, the average scene radiance, is the zero order term in a two dimensional fourier decomposition of the scene radiance field.

Comparison of Equations 24-17 and 24-22 shows that if ${}_bN_o=a_\infty$, then contrast transmittance in real and spatial frequency space is identical. In most cases, the feature within the image of interest is small compared with its surroundings, and average radiance "$a_\infty$" is very nearly the same as background radiance ${}_bN_o$. This is a very satisfying result. Whether one is interested in using modern psychophysical spatial frequency models to examine how much aerosol can be introduced into the atmosphere before it is noticed or how image contrast is changed as a function of aerosol load, the calculation is reduced to understanding the dependence of the atmospheric modulation transfer function, or contrast transmittance, on aerosol chemical and physical properties.

## 2.2.4 Dependence of Contrast Transmittance ($\tau_r$) on Atmospheric Optical Variables

Since the contrast transmittance is the one variable that contains all the information required to describe how various physical descriptors of scenic landscape features are modified as a function of aerosol loading, illumination, and observer-vista geometry, it is of interest to examine how sensitive $\tau_r$ is to changes in atmospheric aerosol loading as a function of aerosol mass and average scene radiance. The average scene radiance, $\overline{N}_o$, was identified as "$a_\infty$" in Equation 24-22.

Malm and Henry (1987) examined how the $\tau_r$ changes with changing image reflectivity, image distance, aerosol size distribution, and aerosol mass loading. For a sulfate aerosol, $B_{ext}$ is almost entirely due to scattering and, as such, $B_{ext}$ is proportional to aerosol mass. Therefore, the variation of $\tau_r$ with respect to $B_{ext}$ is proportional to its variation with respect to aerosol mass. Figures 24-5a and 24-5b show $s \equiv |\Delta\tau_r/\Delta B_{ext}|$ as a function of $B_{ext}$.

Figure 24-5a corresponds to a typical sulfate aerosol mass size distribution, scattering angle $\theta_s=15°$, and $\overline{N}_o=0.13\ N_s$, where $N_s$ is the Rayleigh sky radiance. Figure 24-5b is also for a sulfate aerosol but with $\theta_s=125°$ and $\overline{N}_o=0.5\ N_s$. An immediately evident trend shown in Figures 24-5a and 24-5b is that there is a distance where $S$ is maximum. $S$ decreases to zero as $R \rightarrow 0$ and $R \rightarrow \infty$. Second, the distance at which $S$ is maximum increases as $\overline{N}_o$ increases (brighter landscapes). In a forward scattering situation where landscapes are in a shadow ($C_o \approx -0.90$), $S$ is maximum in the *5* to *10 km* range. Although not explicitly shown in Figure 24-5a, in a backscatter geometry ($\theta_s=125°$), the most sensitive distance is still around *5-10 km* if the landscape is dark.

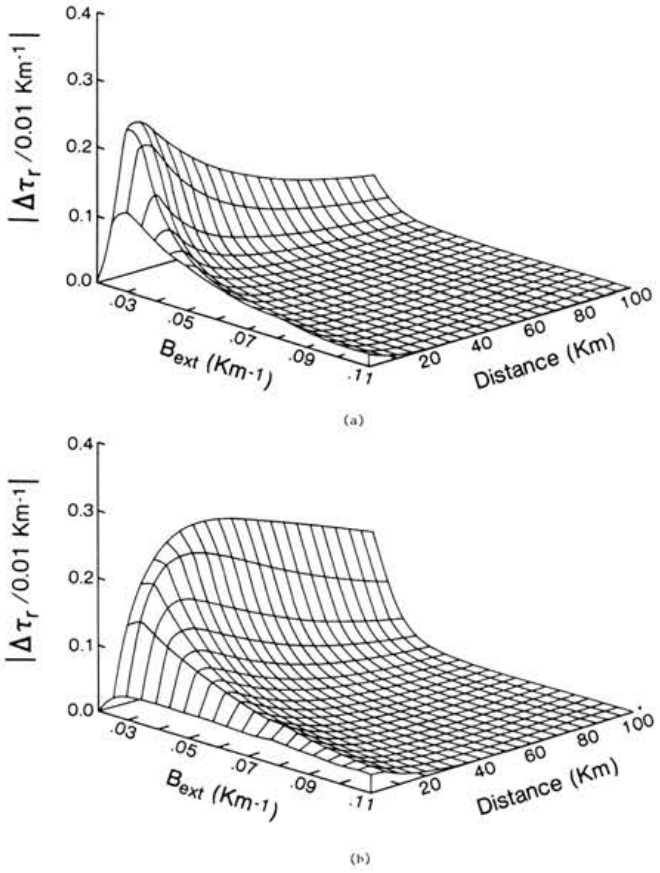


*Figure 24-5 The sensitivity of the absolute value of contrast transmittance ($\Delta\tau_r/\Delta B_{ext}$) plotted as a function of extinction coefficient and distance to landscape feature. Figure A is for a scattering angle $\theta_s$ = 15°, shadowed vista $\overline{N}_o$ = 0.13 $N_s$, and sulfate aerosol, whereas Figure B corresponds to $\theta_s$= 125°, and $\overline{N}_o$ = 0.5 $N_s$, and sulfate aerosol.*

However, the maximum sensitivity drops by about a factor of two and is not nearly as sensitive to distance. On the other hand, Figure 24-5b shows that when the landscape is highly reflective and illuminated ($C_o \approx 0.50$ and $\theta_s = 125°$) the distance of maximum sensitivity increases, is quite sensitive to background $B_{ext}$, and remains sensitive to changes in $B_{ext}$ long after dark targets have lost their sensitivity (dark targets will have disappeared, while bright targets can still be seen).

Figure 24-6 examines in more detail the relative contribution of $N_r^*$ and $T$ to $S$. Figure 24-6a shows contributions of $N_r^*$ and $T$ to $S$ for the case shown in Figure 24-5a at $R = 10$ km (forward scattering, sulfate aerosol, and dark target). Changes in $N_r^*$ are primarily responsible for changes in $M_{tf,a}$ as aerosol is added or subtracted from a clean atmosphere. As background aerosol loading is increased (larger $B_{ext}$), the relative importance of $T$ to $S$ increases to a point where $T$ dominates the effect on $S$. However, it should be emphasized that this only occurs after the $M_{tf,a}$ has increased to a point where landscape features would be barely visible. Figure 24-6b shows $N_r^*$ and $T$ contributions to $S$ for the Figure 24-5b case at $R = 70$ km (backscatter, sulfate aerosol, and bright target). With this geometry, attenuation of image-forming information, $T$, is responsible for much of the change in $M_{tf,a}$. In fact, $N_r^*$ can decrease as $B_{ext}$ increases and compensate slightly (contribute to cause $M_{tf,a}$ to increase) for decreases in $T$.

The foregoing discussion shows that the effect of increasing $B_{ext}$ (aerosol concentration) for a scattering aerosol in almost all situations causes $M_{tf,a}$ to decrease. However, under forward scattering situations where targets tend to be dark, $N_r^*$ dominates changes in $M_{tf,a}$. On the other hand, when looking at brightly colored landscape features with the sun behind the observer's back (backscatter), the relative importance of $N_r^*$ to visibility becomes smaller and changes in $N_r$ as a result of increased $B_{ext}$ are more dependent on image forming radiance being attenuated over the sight path. However, for a specific scene under static illumination conditions, contributions of $N_r^*$ and $T$ to change in $M_{tf,a}$ as a function of aerosol concentration tend to track each other.

Because most research to date has focused on apportionment of $B_{ext}$, and therefore $T$, to aerosol species, it is fortunate that, for scattering aerosols such as sulfates, an understanding of this relationship yields significant insight into how aerosols affect visibility under a wide range of viewing conditions. However, under not uncommon circumstances, the major cause of visibility degradation can be associated with path radiance, and path radiance explicitly requires a knowledge of the volume scattering function in addition to $B_{ext}$. Almost no effort has been expended on examining how path radiance is affected as a function of aerosol characteristics or on apportioning path radiance to aerosol species. Aerosols that absorb light contribute to path radiance differently than aerosols that only scatter light (such as sulfates), so the impact of scatterers and absorbers on path radiance is not additive. Conversely, the effect of scattering and absorbers in $B_{ext}$ is additive. Therefore, when appreciable concentrations of light-absorbing particles or gases are present, a knowledge of just $B_{ext}$ (transmittance) may not be adequate to describe changes in visibility.

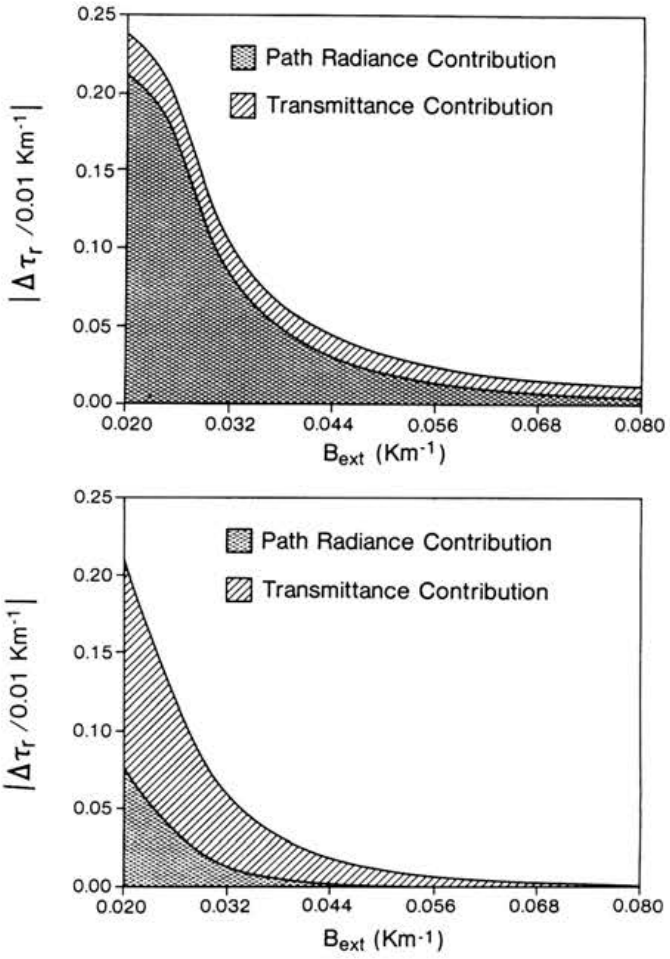


*Figure 24-6 Sensitivity (**S**) expressed as changes in the modulation transfer function per increase of $\mathbf{B}_{ext} = 0.01\ km^{-1}$ plotted against $\mathbf{B}_{ext}$ for a sulfate aerosol. In Figure A, $\theta_s = 15°$, $R = 70$ km, and $\overline{N}_o = 0.13\ N_s$, while in Figure B, $\theta_s = 125°$, $R = 70$ km, and $\overline{N}_o = 0.5\ N_s$. The figures show the relative contributions of path radiance and atmospheric transmittance to changes in $M_{tf,a}$ as a function of $\mathbf{B}_{ext}$.*

### 2.2.5 Relationship of Aerosol Physical Chemical Properties to Atmospheric Optical Properties

The extinction coefficient is made up of particle and gas scattering and absorption:

$$B_{ext}=B_{sg}+B_{ag}+B_{sp}+B_{ap} \qquad \textbf{(24-23)}$$

where *s, a, g,* and *p* refer to scattering, absorption, gases, and particles respectively. The volume scattering function consists of scattering by gases and particles.

Light scattering by gases is described by the Rayleigh scattering theory (van deHulst, 1981). Important characteristics of Rayleigh scattering are

- its proportionality to molecular number density ($B_{sg}$ = *12* $Mm^{-1}$ at sea level and at *0.55* $\mu m$)
- the amount of scattered light varies as $1/\lambda^4$ where $\lambda$ is the wavelength of light
- equal amounts of light are scattered in forward and backward directions
- light scattered at 90° is nearly completely polarized.

The only gas that is normally found in the atmosphere and absorbs light is nitrogen dioxide, $NO_2$. Absorption by $NO_2$ at 550 nm is $B_{ag}=330[NO_2]$, where the units of $B_{ag}$ are $Mm^{-1}$ and the units of $[NO_2]$ are ppm (Nixon, 1940; Hodkinson, 1966). Furthermore, $NO_2$ absorbs more in the blue portion of the spectra than in the red portion. Therefore, $NO_2$ appears brown or yellowish if viewed against a background sky.

In most instances, particle scattering and absorption are primarily responsible for visibility reduction. Single particle scattering and absorption properties can, with a number of limiting assumptions, be calculated using Mie theory (van deHulst, 1981; Mie, 1908). However, before such calculations are carried out, appropriate boundary conditions must be specified. Typically aerosol models assume:

- *External mixtures* - particles exist in the atmosphere as pure chemical species which are mixed without interaction;
- *Multi-component aerosols* - single particles are made up of two or more species. If the chemical species are combined in fixed proportions independent of particle size, the aerosol is referred to as internally mixed. Another multi-component aerosol model assumes a solid core encased by a deposited shell of various thickness and composition.

As outlined in Figure 24-7, a necessary step in the calculation of the atmospheric $M_{tf,a}$ is relating $B_{ext}$ to aerosol chemical and physical characteristics.

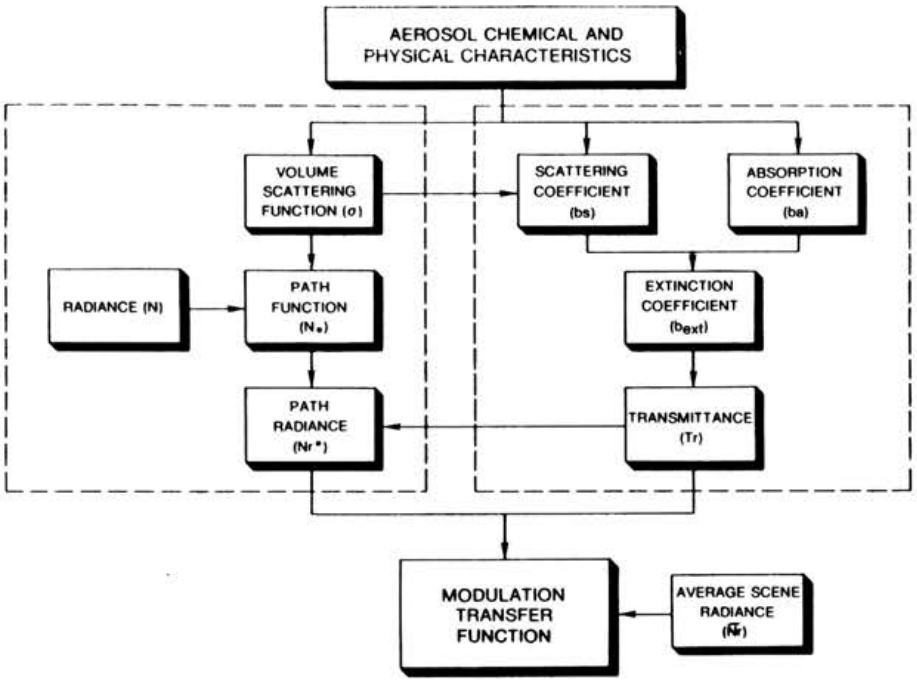


*Figure 24-7 Flow diagram showing how aerosol physical-chemical characteristics relate to the optical variables required to completely specify the atmospheric modulation transfer function.*

### 2.2.5.1 Externally Mixed Aerosols

For an externally mixed aerosol

$$B_{ext,i}=\frac{\pi}{4}\int_{o}^{\infty}D^2Q_e(m_i,\chi)n_i(D)d(D) \qquad \textbf{(24-24)}$$

where $Q_e$ (typically determined by Mie calculations) is the aerosol extinction efficiency; $n_i(D)$ is the aerosol number size distribution of the $i^{th}$ species; and $D$, $m_i$, and $\chi$ are the aerosol diameter, complex index of refraction, and size parameter, $\chi=\pi d/\lambda$, respectively (van deHulst, 1981). Since many aerosol measurement programs are designed to measure mass size distribution, it is convenient to rewrite Equation 24-24 as

$$B_{ext,i}=\int_{-\infty}^{\infty} E(m_i,x,\lambda)\bar{f}_i(x)dx \qquad \textbf{(24-25)}$$

where $E_e$ is mass extinction efficiency, $\bar{f}_i(x)$ is the aerosol mass distribution $dm/dx$ of the $i^{th}$ species, $x=ln[D/Do]$, and $\lambda$ is the wavelength (Ouimette and Flagan, 1982). Equation 24-25 can be rewritten as

$$B_{ext,i}=\alpha_i\, m_i \qquad \textbf{(24-26)}$$

where

$$\alpha_i=\int_{o}^{\infty}E_e(m_i,x,\lambda)\bar{f}_i(x)dx \qquad \textbf{(24-27)}$$

The function $\bar{f}_i(x)$ is the normalized mass distribution given by $\bar{f}_i(x)=f_i(x)/M_i$ where $M_i$ is total mass concentration of the $i^{th}$ species. Thus, the aerosol extinction coefficient is simply (Ouimette and Flagan, 1982):

$$B_{ext}=\sum_i \alpha_i m_i \qquad \textbf{(24-28)}$$

A number of investigators have taken advantage of the form of Equation 24-28 to construct a multi-lineal regression model with $B_{ext}$ as the independent variable and the measured aerosol mass concentration of species "$i$" as the independent variables. The regression coefficients are then interpreted as extinction to mass efficiencies. Results and limitations of these types of analysis will be discussed in following sections.

To understand the functional dependence of $Ee(m_i,x,\lambda)$ on index of refraction, wavelength, and aerosol size, it is worthwhile to examine extinction efficiencies for a number of idealized mass size distributions. Figure 24-8 shows mass scattering efficiencies as a function of single particle size for elemental carbon, iron, silica, and water. In all cases $\lambda=0.55$ $\mu m$. For $D<<\lambda$, $E$ is proportional to $D^3$, and for $D<<\lambda$, $E$ is proportional to $D^{-1}$. Silica and water show the typical resonant peaks around $D\approx\lambda$

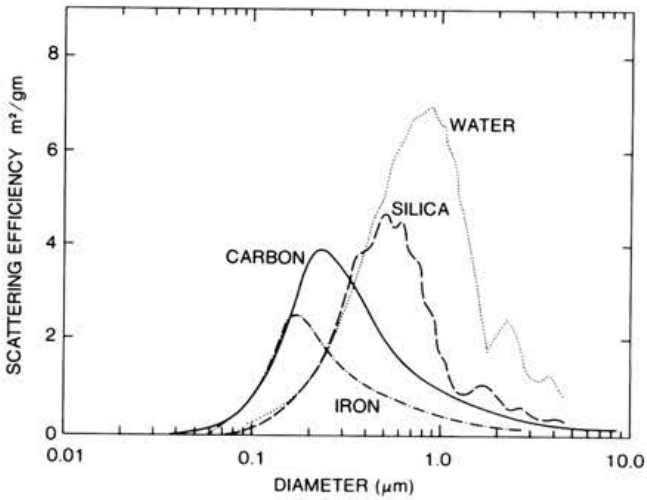


*Figure 24-8 The calculated scattering cross section per unit mass at wavelength of 0.55 μm for absorbing and nonabsorbing materials as a function of diameter for single-sized particles. The following refractive indexes and densities (g/cm³) were used: carbon: m = 1.96 - 0.66i, ρ = 20; iron: m = 3.51 - 3.95i, ρ = 7.86; silica: m = 1.55, ρ = 2.66; and water: m = 1.33, ρ = 1.0.*

(Faxvog and Roessler, 1975). On a per unit mass basis, it is clear that both large and small particles are very inefficient scatterers as compared to aerosols with sizes between approximately *0.1* μm and *1.0* μm.

If the aerosol is absorbing (such as elemental carbon) then $m$ is complex, and Figure 24-8 shows only part of the story. Figure 24-9 shows the scattering, absorption, and extinction (sum of scattering and absorption) efficiency as a function of mass mean diameter for a hypothetical aerosol with a complex index of refraction $m=2.0+0.5i$, particle density $\rho=1.5$ g/cm³, and wavelength $\lambda=0.55$ μm. Also shown is the scattering albedo $\omega=B_s/B_{ext}$. The aerosols were assumed to be log normally distributed with geometric standard deviation of $\sigma_g=2.0$. Notice that—at mass mean diameters $\bar{D}_g>0.2$ μm—scattering and absorption efficiencies are nearly equal, while for $\bar{D}_g<0.1$ μm aerosol absorption dominates and approaches a constant value for $\bar{D}_g<<\lambda$. Therefore, for small absorbing aerosols, extinction efficiencies become independent of size. The scattering efficiency reaches a maximum of approximately *3* m²/gm for a mass mean diameter of approximately *0.2* μm. This is typical for most naturally occurring aerosols with commonly found size distributions.

Previous discussions showed that the path radiance $N_r'$ is as important as transmittance to understanding how

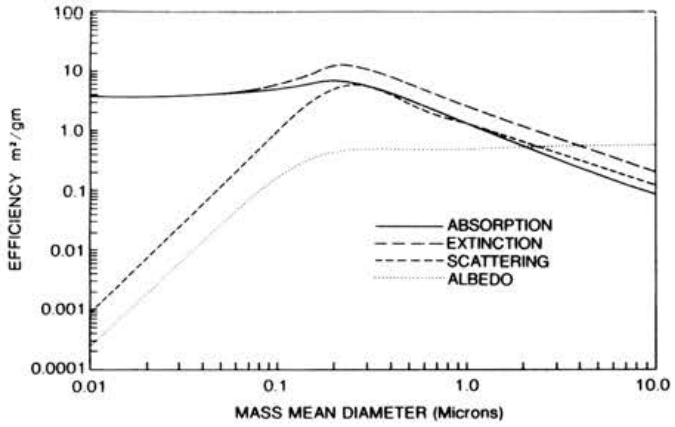


*Figure 24-9 Calculated scattering, absorption, albedo, and extinction efficiencies per unit mass at the wavelength of 0.55 μm for absorbing spheres as a function of mass mean diameter. A log normal particle size distribution was assumed with geometric standard deviation σg = 2.0, refractive index m = 2.0 + 0.5i, and density ρ = 1.5 g/cm³.*

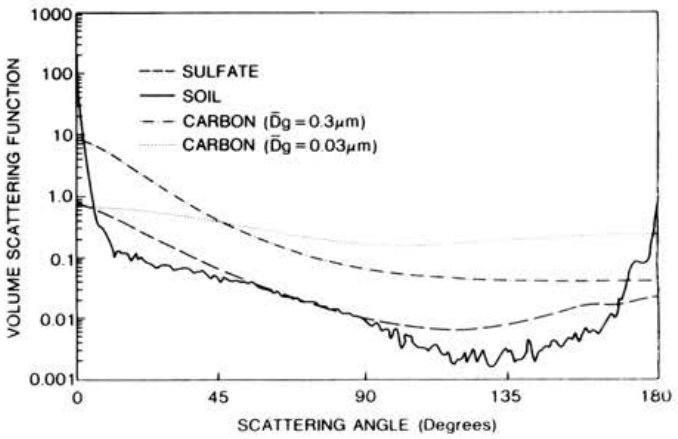


*Figure 24-10 Calculated volume scattering functions at wavelength of 0.55 μm for a sulfate, soil, and two carbon aerosol log normal mass size distributions. The following refractive indexes, diameters, geometric standard deviations, and mean mass diameters were used: sulfate: m = 1.53, ρ = 1.7 g/cm³, σg = 2.0, $\overline{D}g$ = 0.4 μm; soil: m = 1.55, ρ = 1.66 g/cm³, σg = 2.0, $\overline{D}g$ = 10.0 μm; and carbon: m = 1.5 + 1.0i, ρ = 2.0 g/cm³, σg = 2.0, $\overline{D}g$ = 0.03 μm.*

increases in aerosol loadings affect the transfer of image forming information. Equations 24-8 and 24-9 show that $N'_i$ explicitly depends on the volume scattering function. For external mixtures equations similar to 24-33 through 24-35 can be developed for path radiance at any one angle and will be explicitly dependent on the volume scattering function. Figure 24-10 shows typical volume scattering functions for mass size distributions associated with a sulfate and two absorbing aerosols.

Figure 24-10 indicates that large soil type aerosols scatter radiant energy in the forward direction many times (10-1000) more efficiently than aerosols that are less than *1.0 μm* in size. All aerosols in the efficient light scattering mode between *0.1 μm* and *1.0 μm* scatter more light in forward directions than backward, while the minimum light scattering is somewhere between 90° and 130°.

### 2.2.5.2 Multicomponent Aerosols

For an internal mixture (where the chemical species are mixed in a fixed proportion to each other), the index of refraction is not a function of composition or size, and the aerosol density is independent of volume. Aerosol extinction can again be related in a linear fashion to particle mass concentration. However, most aerosol growth models that are representative of ambient atmospheric conditions suggest that these assumptions are not very realistic and may be rarely met (Sloane, 1985).

Figure 24-11 shows a model where aerosol growth involves deposition of a dry hygroscopic shell under low relative humidity conditions and the subsequent interaction of that hygroscopic component with water. If the condensate (hygroscopic) species is increased or decreased, the relative proportion of one species to another is changed, and a basic assumption required for a linear relationship between aerosol scattering and mass concentration is violated. Extinction will not be linearly proportional to mass change. This can be easily seen on a purely physical basis. As condensate mass is increased or decreased, the number of particles stays constant, while mean mass size distribution increases or decreases; *i.e.*, the aerosol size distribution changes. As the size distribution shifts, the extinction efficiency will necessarily change. A similar process will take place at high relative humidities where the condensate has absorbed water. However, under high RH conditions, as the condensate mass changes, so will the associated mass of water. The net result is to change the size distribution even more significantly than in the dry condensate case. An important implication of the above aerosol model is "individual" extinction efficiencies are not constants and as such do not satisfy $B_{ext}=\sum \alpha_i\ m_i$. A change in mass need not be linearly related to the change in atmospheric extinction.

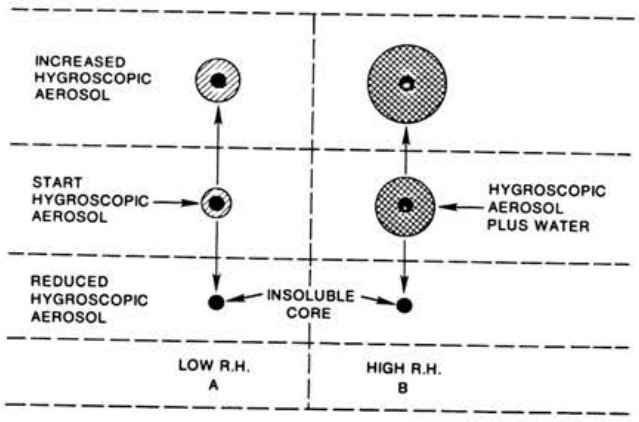


*Figure 24-11 Schematic diagram of a hygroscopic aerosol coating an insoluble core. The left side of the figure shows three different mass levels of the hygroscopic aerosol, while the right side shows how the aerosol would grow with increased relative humidity.*

Hygroscopic inorganic salt aerosols such as ammonium sulfate and ammonium nitrate will undergo sudden phase transitions from solid particles to solution droplets when the relative humidity (RH) rises above a threshold value. The threshold or deliquescence points are approximately *80%* RH for pure ammonium sulfate and *62%* RH for pure ammonium nitrate. When the relative humidity decreases after being above the deliquescence point, the droplet size decreases at approximately the same rate it grew until the relative humidity again falls below the deliquescence point. The size then continues to decrease, but at a lesser rate than it initially grew (hysteresis). The decrease in size continues until the particle reaches the "dry" size at approximately *30%* RH. If the aerosol is a mixed salt, the growth rates are complicated further because the particle may go through several stages of multi-phase equilibria before forming a homogenous droplet (Tang *et al.*, 1981). The inflation of $B_{sp}$ as a function of RH is a direct result of RH-induced particle growth. Figure 24-18 shows how $B_{sp}$ is increased as RH increases.

The light extinction efficiencies of aerosols depend on the ratios of the aerosol radii to the light wavelength and on the aerosol refractive indexes. A change in relative humidity can produce changes in both. Sloane (1984a), Tang *et al.* (1981), and Hanel (1976) have published curves of mean particle sizes as functions of relative humidity. Particle radii increase by a factor of as much as 2.5 when relative humidity approaches 100%. Bullrich (1964) and Hanel (1976) have shown that the refractive index of a hygroscopic aerosol will decrease in proportion to the increase in particle radius and will approach 1.33 (the refractive index of water) as the relative humidity approaches 100%. The real parts of the refractive indexes for ammonium sulfate and ammonium nitrate are approximately 1.52 and 1.60, respectively when the relative humidity is low. The net result of increasing relative humidity is that the scattering coefficient for hygroscopic aerosols can be as much as a factor of 15-20 higher when the relative humidity is near *100%* than if it is below *30%*.

If one is concerned with anything more than calculating standard visual range, then the path radiance is also important. Very little work has been done on relating multicomponent aerosols to volume scattering functions. Ultimately, we should understand not only how changes in multicomponent aerosols affect the scattering function, but also how they affect path radiance.

One theoretical investigation by Ackerman and Toon (1981) did look at normalized volume scattering function, $\sigma_N$, for carbon containing aerosols. They considered a log normal mass size distribution soot-only aerosol ($\overline{S}_g$ *=0.03* $\mu m$, $\sigma_g$*=1.7*), sulfate-only aerosol ($\overline{D}_g$*=0.4* $\mu m$, $\sigma_g$*=2.0*), external mixture with *10%* soot by volume (same size distribution), and shell mixture with sulfate as a core and soot as an external shell and still *10%* soot by volume. The complex index of refraction for soot and ammonium sulfate was set equal to $m=1.94\text{-}0.66i$ *and* $1.53\text{-}10^{-7}i$, respectively. Figure 24-12 shows the results of their calculations. The normalized volume scattering function for the external mixture is almost indistinguishable from sulfate-only scattering because sulfates dominate the scattering processes. For the shell mixture, forward scattering, which is dominated by diffraction effects, is determined primarily by size of the particle and is therefore similar to sulfate-only aerosol. However, in the backscatter region, $\theta_s > 120°$, the shell mixture deviates significantly from sulfate-only aerosols. Since path radiance tracks the volume scattering functions, one would expect that $N_r^*$ in the backscatter mode would be reduced for a sulfate aerosol with an elemental carbon coating and as such could yield an increase in the atmospheric $M_{tf,a}$. Consequently, under these circumstances, failure to explicitly consider path radiance could overestimate the effect of the aerosol on visibility reduction.

### 2.2.6 Visibility Impairment

Aerosols introduced into the atmosphere can result in visibility impairment that is manifested in two distinct ways: first, as a general alteration in the appearance of landscape features such as color, contiguous contrast between adjacent geologic features, etc., and second the aerosol haze may become visible in and of itself. Haze may be

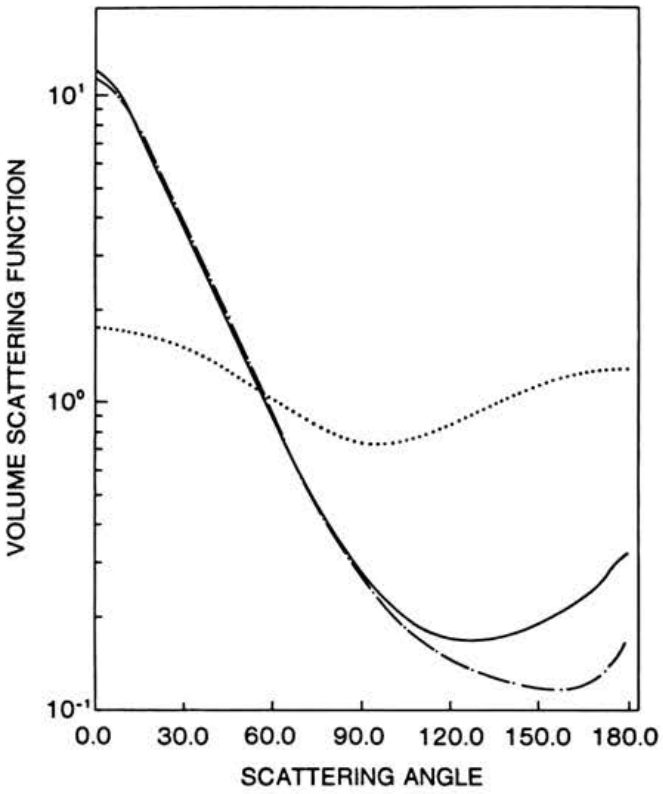


*Figure 24-12 Normalized volume scattering function, calculated for pure sulfate _____, elemental carbon ···, and an extremely mixed carbon-sulfate aerosol —·— See text for size parameters and aerosol physical characteristics.*

visible by the contrast or color difference between itself and its background, or (at great enough optical depths) uniform haze manifests itself as a semi-transparent curtain which can be seen or perceived as a separate hazy entity disassociated from landscape features. Henry has referred to the phenomenon as atmospheric transparency, which is psychophysical in nature, and different from atmospheric transmittance (Henry, 1987).

### 2.2.6.1 Perceptibility Parameters for Quantification of Layered Haze (Plume Blight)

Figure 24-13 illustrates two situations in which a layered haze is visible: (a) when viewed against the sky, and (b) when viewed against terrain features. In both cases, the layered haze will be visible as a distinct, horizontal layer if it is sufficiently brighter or darker than the viewing background.

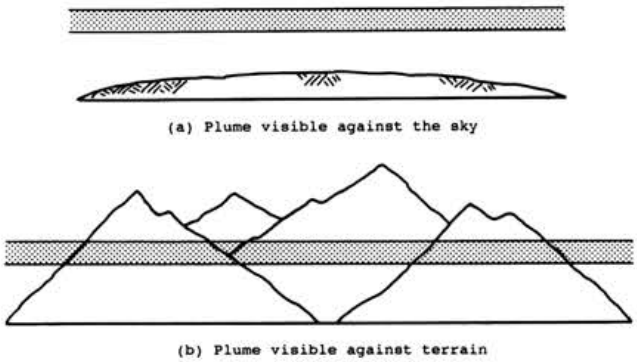


*Figure 24-13 Two viewing situations in which plumes may be visible.*

The simplest way to characterize the relative brightness (or darkness) of plumes is through the use of plume contrast:

$$C = \frac{{}_pN_r - {}_bN_r}{{}_bN_r} \qquad \textbf{(24-29)}$$

where ${}_pN_r$ and ${}_bN_r$ are the spectral radiances of the plume and its background, at some distance, $r$, and at wavelengths in the visible spectrum ($0.4<\lambda<0.7$ $\mu m$). A plume is visually perceptible only if it creates a non-zero contrast at different wavelengths in the visible spectrum greater than an observer's perceptibility threshold (generally in the range of $\pm 0.01$ *to* $0.05$).

An object can be perceived because it has a brightness different from that of the background or because it has a different color. Gases and particles in the atmosphere can give rise to coloration by their light scattering properties (blue sky or white clouds) or by altering the color of objects seen through them (brown coloration due to $NO_2$). Several schemes have been used to quantify color. The Commission Internationale de l'Eclairage (CIE) has set colorimeter standards that form the basis of the CIE system of color specification. The most popular CIE index is the so-called $\Delta E$ parameter that not only quantifies differences in color but also differences in brightness. However, the CIE method, while accurate and acceptable for a laboratory situation, may not adequately represent color differences in a natural setting. In any case, a $\Delta E$ of one is a just noticeable difference in color and/or brightness in a laboratory setting and $\Delta E$ of four can be easily seen by the casual observer. The CIE system, as well as other color quantification procedures, are outlined in Appendix G.

**Layered Haze Thresholds**

Recent psychophysical research (Cornsweet, 1970; Hall and Hall, 1977; Faugeras, 1979; Howell and Hess, 1978; Malm *et al.*, 1987c; Henry, 1986) has documented the

fact that the human eye/brain system is most sensitive to spatial frequencies of approximately three cycles/degree (*cpd*). Spatial frequency is defined as the reciprocal of the distance between sine-wave crests (or troughs) measured in degrees of angular subtense of a sine-wave grating. Thus, spatial frequency has units of cycles/degree. Any pattern of light intensities, whether it is a sine-wave, square-wave, step-function or any other pattern, can be resolved by Fourier analysis into a sum of sine-wave curves of different magnitude and frequency. For instance, a rough estimate of the primary spatial frequency of a Gaussian plume can be made as follows. If it is assumed that a Gaussian distribution is nearly identical to a sine-wave pattern, the 2° width of the plume would correspond to the period of the sine-wave. The spatial frequency would be the inverse of this, or *0.5 cpd*. Figure 24-14 illustrates several estimates of the sensitivity of the human visual system to sine/square-wave gratings with various spatial frequencies.

The sensitivity of the human eye-brain system drops off significantly at high spatial frequency (due to visual acuity) and also to a lesser extent at low spatial frequency (*i.e.*, broad, diffuse objects). The human visual system is more sensitive to images with sharp, distinct edges (*e.g.*, square-waves) than to images with diffuse, indistinct edges (*e.g.*, sine waves or Gaussian plumes).

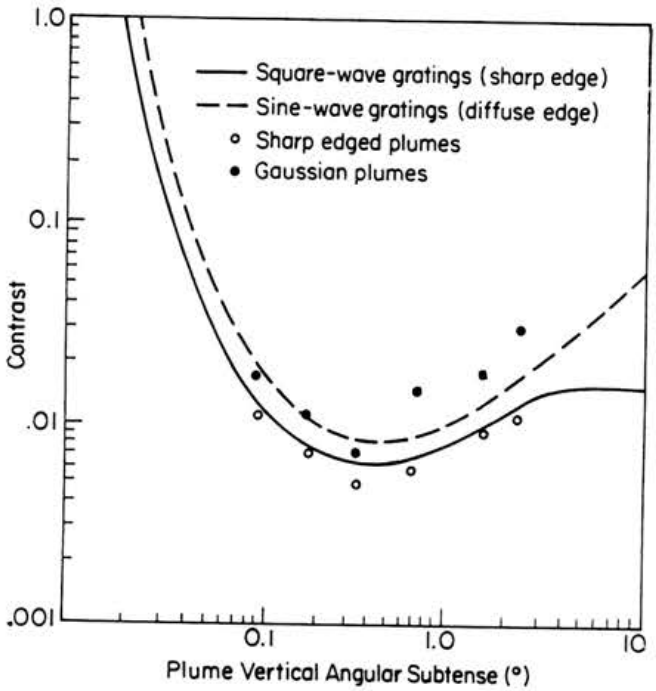


*Figure 24-14 Sensitivity curves as reported by Howell and Hess (1978) for sine and square wave gratings and for sharp edged (Malm et al., 1987) and Gaussian plumes (Ross et al., 1990).*

Malm *et al.* (1987c) found that the detection thresholds for computer generated square-wave plumes were a relatively strong function of plume width (Figure 24-14). The highest visual sensitivity was found for *0.36°* plumes, which is consistent with the previously noted maximum sensitivity for square wave gratings at a spatial frequency of three cycles/degree. These thresholds were defined at the *70%* probability of detection point. This threshold contrast of *0.005* is consistent with the *0.007* value of Howell and Hess (1978).

Ross *et al.* (1988) repeated the experiment using Gaussian plumes as seen against a blue sky background. Their results are also presented in Figure 24-14. The sensitivity is greatest at a threshold contrast of *0.007*.

Table 24-2 summarizes the research described previously. Under laboratory conditions in which observers are attentive and trained, the detection threshold (for *50%* detection) for objects of optimum size with distinct edges is in the range *0.003 - 0.007*. For conditions in which the stimulus has a diffuse edge (such as would be the case with a Gaussian plume) or is different from the optimum-sensitivity size, threshold contrasts are higher.

Ross *et al.* (1988) identified a *70%* detection threshold contrast of 0.02 using photographs of a natural scene with light-colored layered hazes which varied in size. The evidence for $\Delta E$ thresholds is not as clear-cut. The data of Jaeckel (1973) and Malm, Kleine, and Kelley (1980a) support *70%* detection thresholds for $\Delta E$ of three, while the estimates of Latimer *et al.* (1978) and the more recent data of Malm *et al.* (1987c) and Henry and Matamala (1989) suggest a $\Delta E$ threshold of less than one.

### 2.2.6.2 Perceptibility Parameters for Quantification of Uniform Haze Impairment

Whereas work discussed in the previous sections has emphasized detection thresholds of layered hazes, specifically plumes, other researchers have concentrated their efforts in establishing the change in image appearance required to just notice a difference in image sharpness.

Early work focussed on establishing the just noticeable difference between a scene where an object viewed against the same background could just be seen and one where that object could not be identified. This threshold work was carried out in the context of establishing the "threshold" contrast for visual range determination, and is discussed in section (2.2.6.1).

More recent work has been directed toward incorporating results of basic psychophysical measurements into models

*Table 24-2. Summary of Contrast and Color Change Threshold Data*

| Contrast | Δ E | Percent Detection | Edge | Reference |
|---|---|---|---|---|
| 0.003[a] | -- | 50 | Sharp | Blackwell (1946) |
| 0.014 | -- | ? | Sharp | Lowry (1931 & 1951) |
| 0.007[b] | -- | ? | Sharp | Howell and Hess (1978) |
| 0.009[b] | -- | ? | Diffuse | |
| 0.016[c] | -- | ? | Sharp | |
| -- | 1 | 30 | Sharp | Jaeckel (1973) |
| -- | 2 | 50 | Sharp | |
| -- | 3 | 70 | Sharp | |
| -- | 4 | 90 | Sharp | |
| 0.006 | 1 | 10 | Diffuse | Malm, Kleine, and |
| 0.009 | 1.5 | 25 | Diffuse | Kelley (1980) |
| 0.014 | 2.3 | 50 | Diffuse | |
| 0.02 | 3.3 | 75 | Diffuse | |
| 0.025 | 4.2 | 90 | Diffuse | |
| 0.01 | -- | 90 | Sharp | Loomis et al. (1985) |
| 0.005[d] | -- | 70 | Sharp | Malm et al. (1986) |
| 0.010[e] | -- | 70 | Sharp | |
| 0.020[f] | -- | 70 | Diffuse | Ross et al. (1988) |
| 0.007[d] | -- | 70 | Diffuse | Ross et al. (1990) |
| 0.025[e] | -- | 70 | Diffuse | |

[a] The most sensitive contrast reported for largest size of stimulus and largest luminance and longest response time evaluated (probably the minimum possible threshold).

[b] The most sensitive contrast reported at a spatial frequency of 3 cycles/degree.

[c] Threshold contrast for sharp objects at low spatial frequencies.

[d] Minimum threshold for 0.36° wide plumes.

[e] Maximum threshold for all size plumes tested.

[f] Threshold contrast reported for light-colored, diffuse edge hazes of varying size.

which will predict the change in display modulation transfer function (MTF) required to evoke a one just noticeable difference (JND) in display image sharpness.[1] The model, referred to as the quadratic detection model (QDM) is outlined in Appendix D. An integral component of the QDM calculation is the establishment of the image mean square luminance fluctuation, termed the image modulation depth. Henry (1979; Henry *et al.*, 1981) has suggested that modulation depths may be appropriate visibility indices because they incorporate all of the information content contained in a scenic vista.

Malm and Pitchford (1989) have suggested using the concept of a just noticeable change (JNC) in the appearance of a landscape feature as a psychophysical variable that relates directly to human perception. A JNC corresponds to the amount of absorbing gas or atmospheric particular matter required to evoke a noticeable change in the appearance of a particular landscape. The effect of a change in aerosol concentration can then be expressed as the number of JNC's between landscape appearance under current conditions versus the appearance after a change in emissions. Malm and Pitchford (1989) have suggested using the QDM to predict a JNC, however, any psycho-physical model relating changes in aerosol concentration to human eye-brain visual thresholds could be used for this purpose. It is emphasized that none of the currently used psycho-physical models have been field validated. JNC's calculated using the QDM model will be one approach used to quantify visibility effects, both in this report (Section 5) and in the NAPAP Integrated Assessment.

### 2.2.6.3 Application of the Quadratic Detection Model

Typical scenes are made up of features that are quite varied with respect to size, shape, and luminance level. However, some attempts have been made to classify scenic structure into broad categories such as form, line, and texture. Form refers to large shapes seen either against sky or other uniform background, while line is usually associated with appearance of rivers or similar geological features. Texture refers to the periodic contrast associated with sparsely populated trees seen against a uniform background, varied geologic features, or other similar higher frequency scenic structures.

Studies investigating eye fixation and eye motion as observers look at pictures shows that pictorial areas with little modulation receive very little attention, while higher modulated scenic features receive more (Boswell, 1975). Since high contrast edges are most sensitive to changes in atmospheric modulation transfer function and since the discrimination of an atmospheric modulation change in a frequency specific channel is a minimum when the contrast in that channel is largest, it can be concluded that high contrast edges are good patterns for predicting the relationship between just noticeable changes in scenic appearance and increases in atmospheric aerosol load.

For many typical scenes, a JNC is equivalent to a change in atmospheric modulation of approximately *0.06*. Figure 24-15 shows a typical JNC surface for an 80% reduction in atmospheric extinction as a function of observer dis-

[1] Displays of interest were television-type video displays.

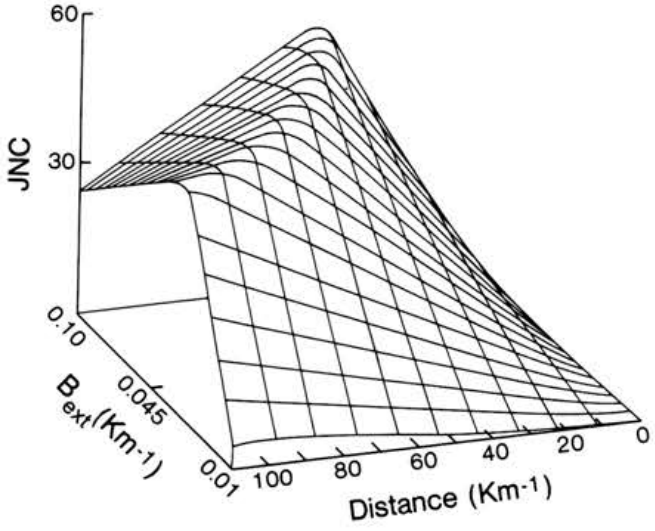


*Figure 24-15 Just noticeable change surface plotted as a function of observer distance and atmospheric background extinction. The surface corresponds to a reduction of background extinction of 80%. See text for details.*

tance and atmospheric extinction, assuming a change in MTF of 0.06 is perceptible. The scattering angle is 15 degrees, $a_\infty=N_s$ where $N_s$ is sky brightness, and the initial contrast, $C_o$, is equal to *-1.0*. A typical aerosol mass size distribution with typical chemical properties was assumed.

There are some general features that show up in all JNC surfaces. For any given distance there is a background extinction that is most sensitive to an incremental change in extinction, and for any given extinction there is observer distance that is most sensitive to extinction change. Secondly, for any given observer distance the sensitivity of a scene to incremental reductions in atmospheric extinction drastically reduces as background extinction increases; and finally the distance where the scene is most sensitive to a change in extinction decreases as background extinction increases.

### 2.2.7. Human Judgments of Visual Air Quality

The previous section discussed methodologies for establishing the change in atmospheric particulate loading required to be noticeable either as a layered haze or as a change in scenic quality. It should be emphasized that calculations of detection thresholds and JNC's are statements about changes in information content in an image. JNC changes in the appearance of an image are not necessarily good indicators of judged image quality. For instance, a change in 10 JNC's in a scene with low overall contrast may not be judged to have the same change in image quality as 10 JNC's in a high contrast scene.

Studies by Malm *et al.* (1980a and 1981), Latimer *et al.* (1980 and 1983), Middleton *et al.* (1983 and 1984), Stewart *et al.* (1983), and Hill (1989) have established relationships between judgments of image quality of natural scenes and various atmospheric and vista parameters such as mountain/sky contrast, solar angle, extinction coefficient, sky color and percent cloud cover. Latimer *et al.* (1980) had observers judge scenic beauty (SBE) and visual air quality (VAQ) for a number of eastern and western national park vistas as they appeared under a variety of illumination and meteorological conditions. The results of their study were mixed and in some cases contradictory. In Latimer *et al.* (1980), they conclude "To different extents for different vistas, ratings of VAQ and SBE both increase with increasing visual range." In the Latimer *et al.* (1983) paper, they conclude "Ratings of SBE of a given vista were independent of visual range unless there was a dominant distant landscape feature in the landscape scenery." Since the visual range calculation "normalizes" out specific unique characteristics of vistas, these results are not surprising. The Latimer studies did conclude that changes in illumination did have a considerable effect on SBE ratings. Middleton *et al.* (1984) also concluded that illumination was important to VAQ judgments and were able to show at one site that there is a good correlation between VAQ and ln (Bscat), where Bscat is the atmospheric scattering coefficient. Additionally, Hill (1989) emphasizes that color is extremely important to judgments of scenic beauty.

Malm *et al.* (1981) examined the relationship between VAQ and vista contrast. They showed that, under fixed illumination and meteorological conditions, apparent vista contrast of the most distant vista element was a good prediction of VAQ judgments. The study also showed that changes in foreground color (due to change in illumination), addition of clouds, or snow cover caused the VAQ ratings to be higher but did not cause the sensitivity of VAQ to change in vista contrast change. Malm *et al.* (1981) also presented a model of human perception of VAQ. The model is based on the observation that ratings of VAQ are proportional to the sum of the fraction of each scenic element subtended by various landscape features multiplied by the atmospheric transmittance between that landscape feature and observer. It was shown that when a single landscape feature, void of color and textural detail, dominates the perceived change in visual air quality, the model predicts a linear relationship between VAQ and the apparent contrast of that landscape feature (contrast of form).

Several researchers have found that judgments of photographs can be used as surrogates for judgments made in

the field provided the experiments have been properly designed. This is an important finding, since one way to reduce the per-observation cost of obtaining judgment based measurements of visual air quality is to use judgments of photographs rather than field observations. For example, Stewart *et al.* (1984) found that although visual air quality tends to be judged slightly worse in photographs than in the field, the relative differences among scenes are approximately the same whether visual air quality is judged from photographs or in the field.

The implication of the visual air quality perception research described in the preceding paragraphs is that there are a number of variables such as sun angle, cloud cover, and scene composition that are firmly integrated into judgments of aesthetic value of a scenic resource. Therefore, studies designed to assess social, psychological, or economical value associated with a given change in atmospheric particulate concentration must be designed in such a way that these confounding variables do not affect the outcome of the experiment. For instance, a number of experiments have been carried out using photographs of landscape features under a variety of air quality conditions as the stimulus. To avoid extraneous variables such as sun angle from affecting the study, it is essential that the study be carried out using photographs taken at the same time of day and under similar lighting conditions.

### 2.2.8 The Psychological Value of Good Visual Air Quality

Efforts to define and quantify the value of good visual air quality have generally followed two courses. One emphasis has been on monetary costs to resource degradation and human health. The other emphasis has been on the psychological value of visual air quality in the context of recreational and nonrecreational settings. Information regarding monetary effects can be found in Section 7, Methods for Valuing Acidic Deposition and Air Pollution Effects," SOS/T Report 27.

#### 2.2.8.1 Visual Air Quality in Nonrecreational Settings

Investigations into the psychological value of visual air quality in nonrecreational, or urban settings, have been sparse. The research which has been conducted in this area examined awareness of, and attitudes toward, visual air quality, and investigated relationships between visual air quality, stress, and human behavior.

**Public Perception of Visual Air Quality**
Survey research of public awareness of visual air quality using direct questioning typically reveals that *80%* or more of the respondents are aware of poor visual air quality, and that poor visibility and media publicity are the primary factors which precipitate the awareness (Cohen *et al.*, 1986). These surveys have also shown that awareness is not uniform across the general population of a given area. Persons with higher income and educational levels tend to be more aware of poor visual air quality than those with lower income and educational levels. Also, people are less aware of reduced visual air quality in their home communities compared to adjacent areas (Evans and Jacobs, 1982).

People are also less aware of pollution in their home area compared to awareness of pollution in areas adjacent to their home (Evans and Jacobs, 1982). A suggested explanation for this finding is that people cognitively adjust their awareness level to reduce the dissonance of living in a polluted area which they are otherwise satisfied with or might not be able to leave.

Attitudes toward poor visual air quality vary with socioeconomic status, health, and length of time an individual has lived in the area (Barker, 1976). Affluent and well-educated people consider poor visual air quality to be a more serious problem than others. People who are not economically tied to sources of air pollution, have respiratory ailments, or are new to an area also show the strongest negative reactions to reduced VAQ.

**Visual Air Quality and Stress**
Reduced visual air quality is an ambient environmental stressor because it is a relatively constant and unchanging situation which one has little direct control over (Campbell, 1983). The associated stress and lack of control is chronic, not salient, and may be manifested in heightened levels of anxiety, tension, anger, fatigue, depression, and feelings of helplessness (Evans *et al.*, 1987; Zeidner and Schecter, 1988). How one deals with this stress is dependent on coping behavior and ability to adapt. The relationship between stress due to poor visual air quality and mental health is poorly understood. However, results from a study conducted by Rotton and Frey (1982) showed that as visual air quality decreased, emergency calls for psychiatric disturbances increased.

**Visual Air Quality and Behavior**
Evans *et al.* (1982) found that persons who recently moved to Los Angeles from areas with good visual air quality consistently reduced outdoor activities during periods of reduced visual air quality compared with longer-term residents. Studies have also reported reduced altruism and increased hostility and aggression during periods of poor air quality (Cunningham, 1979; Jones and Bogat, 1978; Rotton *et al.*, 1979). The relationship between aggression, hostility, and visual air quality is curvilinear with feelings of aggression and hostility increasing to a certain point and then dropping off and yielding to a desire to withdraw and escape from the situation. Evans and Cohen (1987) suggest that individuals

adjust to poor visual air quality through adaptation and coping behaviors by altering their judgment of air quality based on current and previous exposure.

### 2.2.8.2 Visual Air Quality in Recreational Settings

During the past decade, an experience-based demand model has been developed to assess demand for recreational opportunities. The model incorporates visitor demand for activities, for social/physical/managerial site attributes, and for the realization of specific psychological satisfactions.

The model was used to investigate the psychological value of good visual air quality at Grand Canyon, Mesa Verde, Great Smoky Mountains, Mount Rainier, and Everglades National Parks using on-site interviews and mailback surveys. The purpose was to evaluate the importance of visual air quality relative to other park attributes, to determine if visitors were accurately aware of changes in visibility, and to ascertain whether relationships existed between visual air quality and visitor satisfaction (Ross *et al.*, 1985 and 1987a).

**Importance of Good Visual Air Quality**

The importance of good visual air quality to park visitors was evaluated by having visitors rate how important specific park attributes were to their recreational experience. Cluster analysis was used to statistically identify similar types of attributes based on response patterns. Grand Canyon National Park's attributes, their corresponding mean importance scores, and cluster formation are shown in Table 24-3. The "clean, clear air" attribute ranked third in importance and combined with attributes which are descriptive of a clean, natural setting which, as a group, were slightly more important than the cluster of view-related attributes. This indicates that visitors interpret "clean, clear air" as being an integral part of the cleanliness of the park and as such, an important part of the overall recreational experience sought at Grand Canyon.

The importance of a natural, clean environment with clean air was not unique to Grand Canyon visitors. Figure 24-16 shows that similar findings resulted from the other studies regardless of park location or overall theme. The cleanliness attribute cluster, which included "clean, clear air", was the most important cluster at all five parks.

**Visitor Awareness of Visual Air Quality**

A random sample of nearly *1,800* visitors at Grand Canyon National Park were asked during an interview if they were aware of any haze and, if so, how hazy they thought it was. Results from correlation analysis between

*Table 24-3. Attributes, Attribute Mean Scores, Attribute Clusters and Attribute Cluster Mean Scores for the Grand Canyon National Park Visitor Survey*

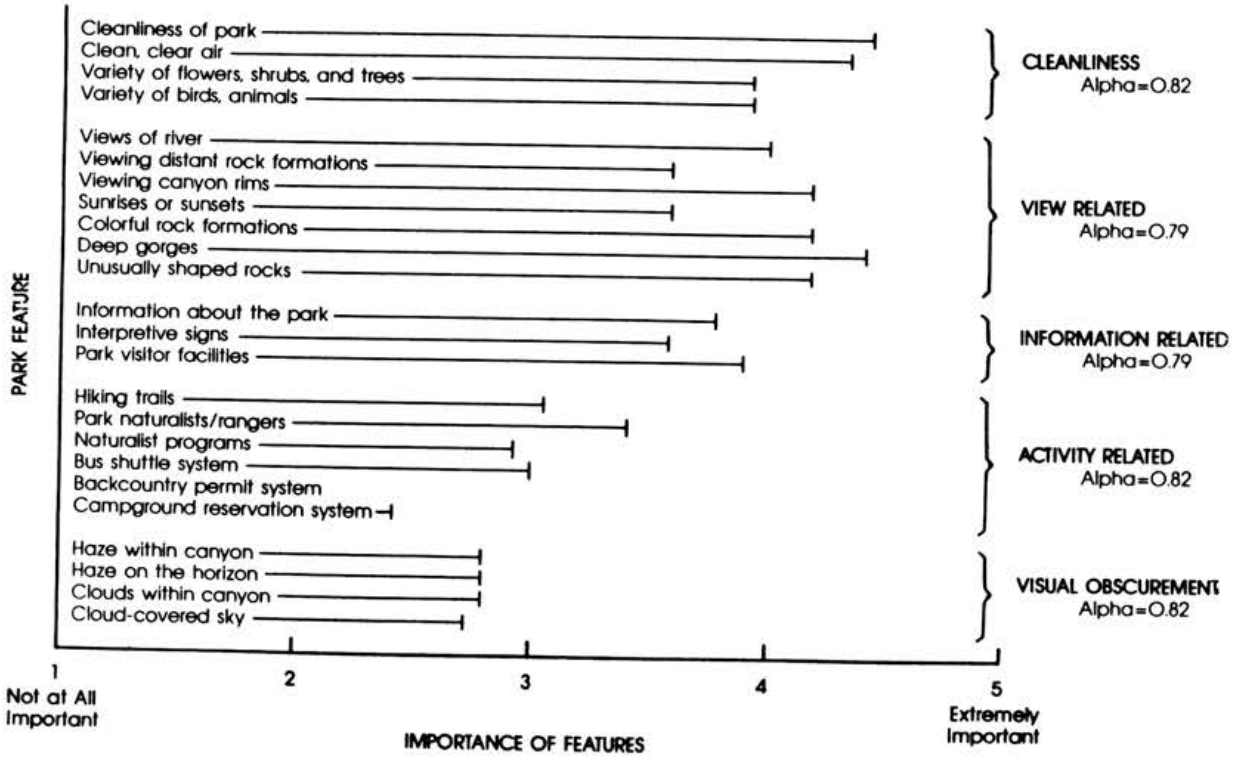

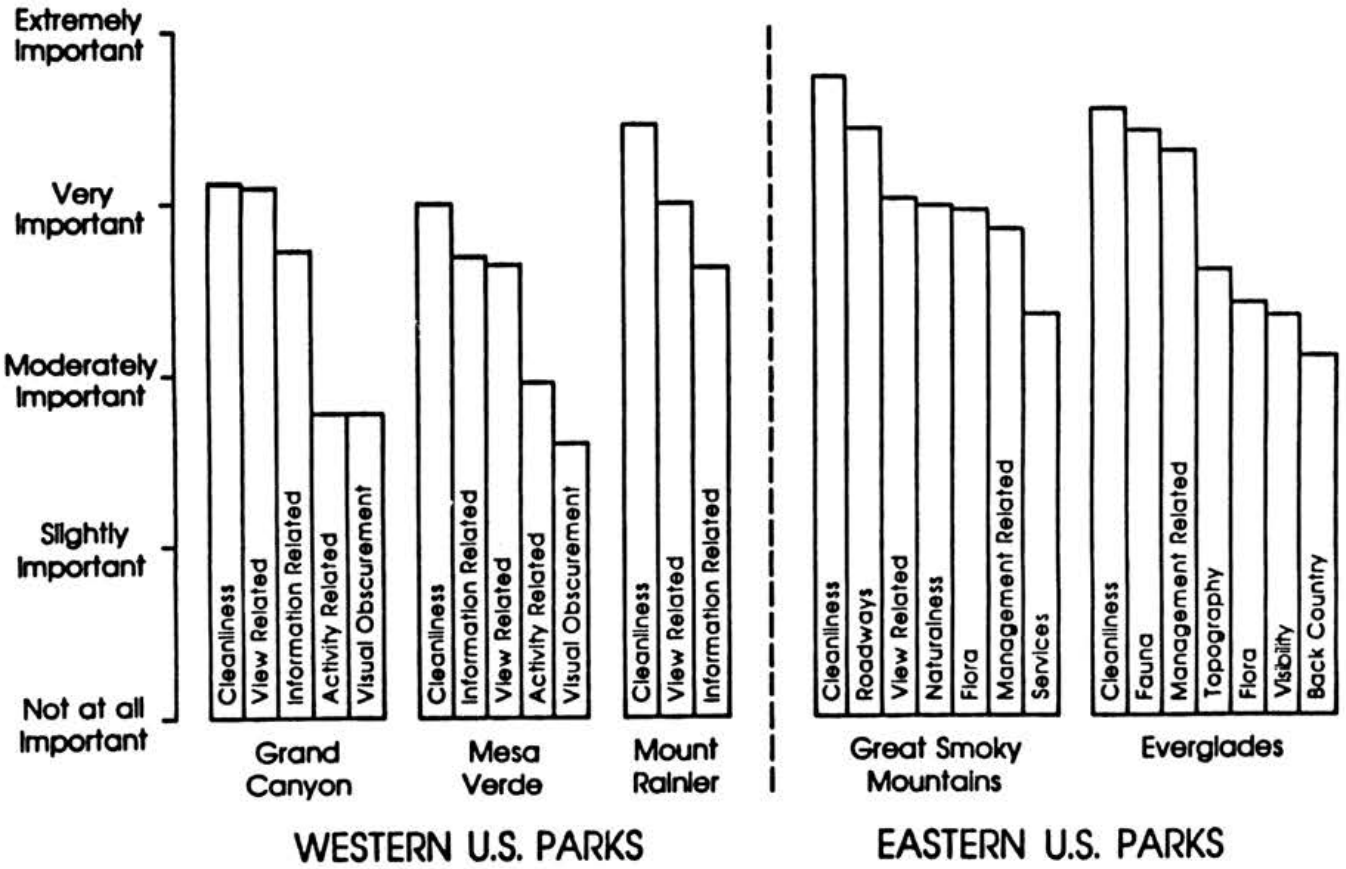


*Figure 24-16 Relative importance of attribute clusters at five national parks.*

awareness of haze and standard visual range measures showed that visitors' awareness of haze increased as visibility decreased. Correlation coefficients were also calculated between visitor awareness of haze and ratings on enjoyment of the view, impact of haze on overall park enjoyment, and satisfaction with the "clean, clear air" attribute. Results showed that as awareness of reduced visibility increased, enjoyment of the view, overall park enjoyment, and satisfaction with the "clean, clear air" attribute decreased.

**Visual Air Quality and Recreational Behavior**

A laboratory study conducted by Malm *et al.* (1984) at Grand Canyon National Park examined how visual air quality might affect visitor behavior. Participants examined sets of photographs with different levels of visual air quality and indicated how they would be willing to spend a given amount of time either driving to a lookout point or touring an archaeological site. The study concluded that subjects place a high value on visual air quality and would be willing to significantly alter behavior for increased visual air quality. For example, subjects would be willing to spend an additional *2.5* hours driving time to view a dominant distant landscape for a *0.01* $km^{-1}$ reduction in atmospheric extinction. The study also showed that vistas which lacked color and texture were insensitive to increases in atmospheric extinction.

## 2.3 THEORY OF CLIMATIC EFFECTS

*R. Charlson*

Among the important radiative effects of aerosols are those on climate. *Climate* is defined as the aggregate of all the physical/meteorological factors which are extant over a specific area. The spatial scale of the area (the scale of the climate) can be local, regional, or global. The important climatic variables that are influenced by aerosols include temperature, relative humidity, amount of condensed water (clouds or fog), amount and type of precipitation, albedo (of both clouds and clear air), as well as atmospheric optical extinction and optical depth.

Aerosol particles affect climate by scattering and absorbing solar radiation, absorbing infrared radiation, and act-

ing as nuclei for the formation of cloud droplets and ice particles. The optical effects are referred to collectively as *direct* effects, while the effects on clouds are referred to as *indirect*. The discussion below will be organized according to this subdivision. It should be noted that cloud effects being called indirect is not an indication that they are less important. Indeed, the highest sensitivity of regional and global heat balance to aerosols likely involves their interactions with clouds.

### 2.3.1 Direct Optical Effects

Direct climate effects include the scattering and absorption of visible (solar) radiation. The optical effects of particles on solar radiation are conventionally defined by using several variables: extinction, aerosol optical depth, turbidity, Angstrom turbidity, and phase function.

*Extinction*—the rate at which light intensity, $I$, is attenuated per unit path length, $dx$, of atmosphere—is given by the Beer-Lambert law for a given wavelength of light, $\lambda$

$$\frac{dI}{I} = -B_{ext}\, dx \qquad \textbf{(24-30)}$$

The extinction coefficient, $B_{ext}$, is a sum:

$$B_{ext} = B_{sp} + B_{ap} + B_{sg} + B_{ag} \qquad \textbf{(24-31)}$$

where: $B_{sp}$ is due to scattering by particles,
$B_{ap}$ is the absorption of particles,
$B_{sg}$ is Rayleigh scatter by gases,
$B_{ag}$ is the absorption by gases, and
all five terms are functions of wavelength, $\lambda$.

The particle effects, imbedded in the first two terms, are combined into the *albedo for single scatter*, $\omega_p$:

$$\omega_p = \frac{B_{sp}}{B_{sp} + B_{ap}} \qquad \textbf{(24-32)}$$

Extinction integrated over an atmospheric path yields an *aerosol optical depth*, $\delta_p$, usually defined over a vertical path, Z:

$$\delta_p = \int_o^z (B_{sp} + B_{ap})\, dz \qquad \textbf{(24-33)}$$

An archaic analogue of optical depth, *turbidity*, $\beta$, is extant in the older literature. Turbidity uses Base 10 rather than natural logarithms and $\beta = \delta_p/2.3$.

Aerosol particle optical depth, $\delta_{p\lambda}$, and turbidity, $\beta_\lambda$, for wavelength $\lambda$ are often defined formally in terms of measurable irradiances (where the subscript $\lambda$ denotes the quantity at that given wavelength of light):

$$I_\lambda S = I_{o\lambda} \exp[(\delta_{r\lambda} + \delta_{z\lambda} + \delta_{p\lambda})M] \qquad \textbf{(24-34)}$$

and

$$I_\lambda S = I_{o\lambda} 10[(\tau_{r\lambda} + \tau_{z\lambda} + \beta_\lambda)M] \qquad \textbf{(24-35)}$$

where:

$I_\lambda$ = solar irradiance at the observing site
$I_{o\lambda}$ = extraterrestrial solar irradiance at the mean sun-earth distance
$S$ = correction factor for sun-earth distance
$\delta_{r\lambda}$ = Rayleigh scatter optical depth of particle free air
$\delta_{z\lambda}$ = ozone absorption optical depth
$\delta_{p\lambda}$ = aerosol optical depth
$\tau_{r\lambda}$ = $\delta_{r\lambda}/2.3$
$\tau_{z\lambda}$ = $\delta_{z\lambda}/2.3$
$\beta_\lambda$ = turbidity = $\delta_{p\lambda}/2.3$, and
$M$ = number of optical air masses.

There are other variables as well, notably the angular scattering or *phase function*, $\beta(\phi)$:

$$B_{sp} = 2\pi \int_o^\pi \beta(\phi) \sin\phi\, d\phi \qquad \textbf{(24-36)}$$

A typical angular scattering function for a submicrometer atmospheric aerosol is given in Figure 24-17. Note that most of the light is scattered in a forward direction, *i.e.*, in the same direction as the transmitted beam. Typically, *10* to *20%* of the scattered energy is in the backward hemisphere which can result in solar energy being reflected away from the earth's surface.

The dependence of scattering on humidity, governed by the presence of hygroscopic and/or soluble materials in the particles is extremely important. This dependence can be determined empirically. A typical response is given in Figure 24-18; at *80%* RH the effect of water is to approximately double $B_{sp}$.

These relevant optical properties of particle ($B_{sp}$, $B_{ap}$, $\beta(\phi)$, $\delta_p$, *etc.*) can be utilized in model calculations to yield estimates of the effects on various meteorological quantities of interest, *i.e.*, local and regional albedo, amount of solar radiation reaching the ground, atmospheric heating rate, temperature, *etc.* However, it must be emphasized that ultimately it is this original set of relevant variables that control the direct effects. Therefore, understanding them is necessary to the understanding of the effects themselves.

The second direct climatic effect is absorption of infrared (terrestrial) radiation. While the same optical laws apply equally for visible and infrared radiation, the location, cause, and magnitude of effects is different in the two

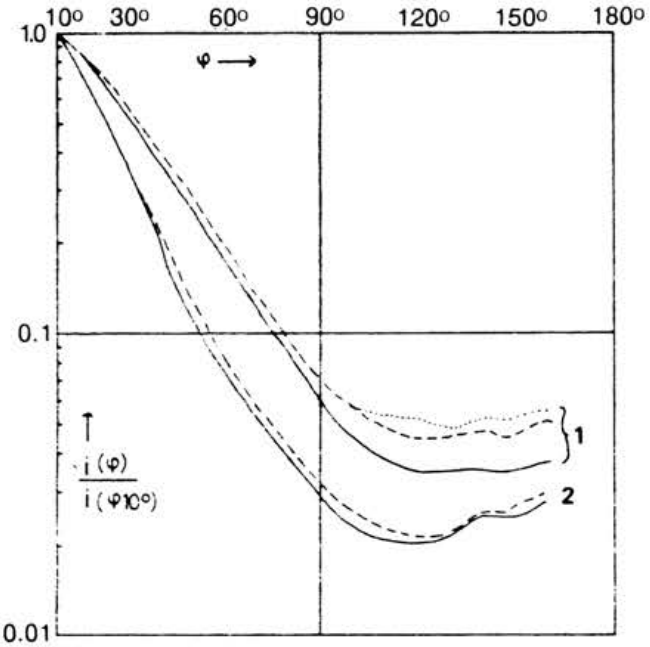


*Figure 24-17 Measured scattered light intensity as a function of angle (ϕ), relative to that at 10°. Solid line = blue light; dashed line = red light; and dotted line = 0.911 μm (Bullrich, 1964).*

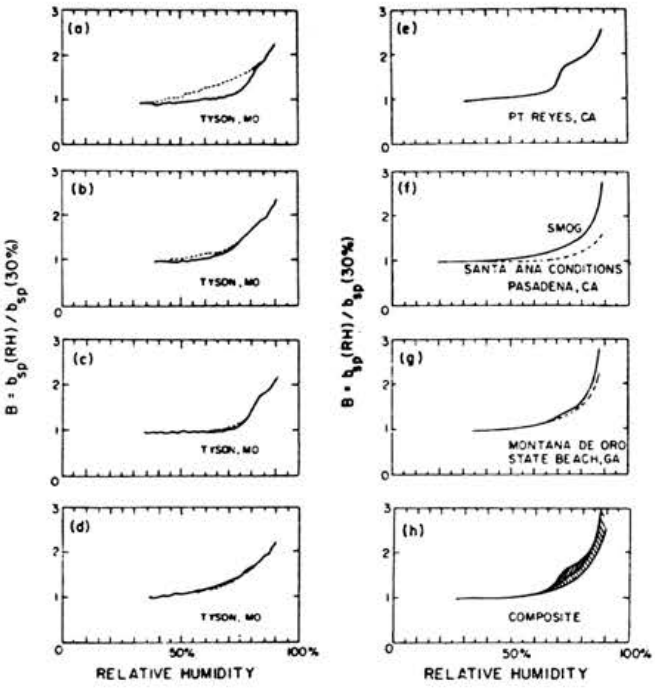


*Figure 24-18 Measured scattering component of extinction as a function of relative humidity relative to that at 30% relative humidity. R = **B**sp(RH)/**B**sp(30%) (Charlson et al., 1984).*

cases. It is widely accepted that the main effect on solar irradiance is scattering (causing both extinction of solar radiation and its backscatter to space) with absorption (*e.g.*, by soot) being significant but generally smaller. The main interactions with solar radiation occur for particle sizes close to the wavelength of light (*i.e.*, *0.5 μm*), which often are dominated by sulfates and organics that exhibit scattering but little absorption. In contrast, the infrared effects involve particles in the coarse mode, *i.e.* mechanically produced substances such as siliceous dust because these mineral compounds exhibit strong absorptivity of infrared radiation as does soot. As a result, mineral dust and soot may at times act to warm the earth's surface (Grassl, 1988).

It is important to consider direct effects in terms of their vertical distribution. Backscatter of light to space by particles causes a loss of energy from the earth-atmosphere system and hence cools the earth; the amount of cooling depending on the geographical location, time of day, and the albedo of the surface underlying the aerosol. The maximum effect is for a scattering aerosol over a dark surface (*e.g.*, the ocean which has an albedo at 500 nm wavelength of about 7%), while backscatter causes little or no effect over high-albedo surfaces such as snow or clouds. In the simplest non-cloud case over water, the altitude of the aerosol (*i.e.*, planetary boundary layer, free troposphere or stratosphere) is of almost no significance.

However, effects involving absorption of either visible or infrared radiation (*e.g.*, by soot and soil dust respectively) result in a transfer of the optical energy of light to thermal energy within the atmosphere. In principle, absorption thus causes a relocation from heating at the earth's surface to heating aloft with attendant changes in the vertical temperature profile, static stability, convection, and mixing.

The computer models that are used for calculating effects of aerosol particles range from simple to complex and local to global in extent. In general, they rely on fundamental notions of conversion of energy, mass, and momentum via the laws of classical physics. However, due to both insufficient data and finite computer capacity, these models necessarily rely on simplifying assumptions. It is of particular importance that such models be tested against data in order to demonstrate that they are correctly formulated and that the assumptions are realistic.

### 2.3.2 Indirect Effects

Indirect effects of aerosol particles occur when they act as cloud condensation nuclei (*CCN*) and ice nuclei (*IN*). Clouds of water droplets in the atmosphere require either *CCN* or *IN* for their formation. The theory, observation, and measurement of *CCN* are well developed (although there are no standard methods); while there is no agree-

ment on the fundamental nature of or the methods for measurement of *IN*. Hence, despite the obvious importance of the ice phase, it is necessary to simply designate *IN* as an important research topic and review what is known regarding *CCN*.

There is a growing, but as yet unproven, consensus that the main climatic influence of aerosol particles is on cloud albedo via the Twomey (1977) effect. For a given amount of liquid water in a cloud, its albedo depends on the droplet sizes which are determined by the number population of *CCN*. Since the amount of condensed water in the air is presumed to be controlled by factors other than *CCN* (*e.g.*, updraft velocity, total water content, and temperature), the *CCN* population is an external factor which, in principle, controls the albedo of clouds independently of other climatic forcings. Figure 24-19 shows the calculated sensitivity of cloud albedo at solar wavelength, *A*, to the *CCN* population as a function of cloud thickness. The highest sensitivity of *A* to *CCN* is for $0.3 \leq A \leq 0.7$, which (for realistic *CCN* populations of about *100* $cm^{-3}$) involves clouds of physical depth *0.1* to *1.0 km*. Marine stratus clouds have depths, albedos, and droplet populations in this range of values such that they are calculated to be peculiarly sensitive to changes in CCN content. Because these are the most common type of cloud, covering about *23%* of the earth's surface, they exert a

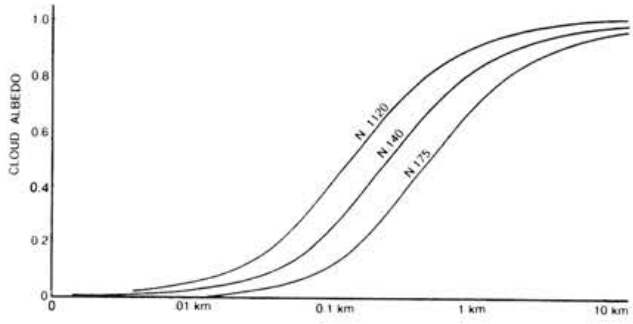


*Figure 24-19* *Calculated cloud albedo as a function of cloud depth (log scale) for three different cloud droplet (CCN) concentrations N* ($cm^{-3}$). *Note that the region where A is most sensitive to N lies between* $0.3 \leq A \leq 0.7$ *(Twomey, 1977).*

major influence on the average earth albedo. While no regional climate models have yet included *CCN* variation, global models indicate a high sensitivity. A change of $\pm$ *30%* in marine *CCN* influencing only marine stratiform clouds is calculated to cause a global temperature change on the order of $\pm$ *1°C* (Charlson *et al.*, 1987) with all other factors held constant.

# SECTION 3

# EXISTING CONDITIONS AND HISTORICAL TRENDS

The purpose of this part of the report is to describe patterns and trends for visibility and related aerosol concentrations. Sections 3.1 and 3.2 set the stage by discussing measurement methods and available data bases, respectively. Section 3.3 deals with current spatial, temporal, and statistical patterns. Historical visibility trends are described in Section 3.4, and natural background conditions are characterized in Section 3.5. Section 3.6 deals with existing and historical conditions for climate effects.

## 3.1 VISIBILITY AND AEROSOL MEASUREMENT METHODS

*M. Pitchford*

Any discussion of measurement methods must begin with a clear understanding of what is to be measured and how the information is to be used. As indicated in the previous section on concepts and theory, visibility is not well defined by a single parameter. It follows then that visibility monitoring is not well defined by a single method. Many of the indexes for characterizing visibility are not directly measurable but must be calculated from measurements using various assumptions. Furthermore, even if there were only one measurable index accepted as the definition of visibility, there would still be several methods that could be employed for monitoring.

Visibility related indexes can be separated into three groups: aerosol, optical, and scene. Table 24-4 includes some of the most useful indexes in each group. Aerosol indexes include the optically important chemical and physical characteristics of the particles that make up the atmosphere. Optical indexes characterize the fate of light traversing the atmosphere. In a sense, these indexes integrate the optical effects of the aerosol. Scene indexes characterize aspects of the appearance of the scene viewed through the atmosphere.

Monitoring methods can similarly be subdivided based upon the measured indexes. One source of confusion concerning this classification scheme for measurements is the common practice of converting measurement data to a different index (*e.g.*, scene measurements like contrast are converted to an optical index like extinction coefficient). Such conversions usually require models with assumptions that are not always met. Direct measurement of the indexes of interest avoids these concerns and has been the goal of many methods development efforts.

*Table 24-4. Visibility Related Indexes*

*AEROSOL:*
- Mass concentration of particle (e.g., total suspended particulate matter, particulate matter less than 10 microns, etc.).
- Particle composition (e.g., chemical, elemental, and ion concentrations).
- Physical characteristics (e.g., shape, structure, and index of refraction).
- Size distribution (i.e., the mass and/or chemical concentrations of particles in more than one size range.

*OPTICAL:*
- Extinction coefficient (often converted to visual range via Koschmieder formula).
- Scattering coefficient
- Absorption coefficient
- Scattering phase function

*SCENIC:*
- Observed visual range (furthest distance that a suitable object can be seen).
- Contrast (e.g., two points).
- Apparent radiance of scenic elements (e.g., photograph or video).
- Color (e.g., chromaticity or color contrast).
- Detail (e.g., scene modulation).

In the context of visibility, aerosol measurements are primarily used in conjunction with optical monitoring data to infer cause/effect relationships. In other words aerosol data are required to answer the question "What are the relative contributions to visibility impairment of various aerosol species?" In the absence of optical data, aerosol data can be used to estimate visibility levels by using generally accepted models (Mie scattering theory or literature values for extinction efficiencies). Usually the aerosol data are incomplete (*e.g.*, liquid water not being directly measured), uncertain in some aspects (*e.g.*, artifact loss or gain for organic carbon), and not necessarily representative (*e.g.*, surface based point measurements being used to represent elevated sight paths). This results in large uncertainty in the optical indexes calculated from aerosol information.

Most of the technical community associates visibility with atmospheric optical indexes (*e.g.*, extinction coefficient or scattering phase function). Since these indexes

integrate the effects of the aerosol yet are not dependent on scene-specific characteristics, they are useful for intercomparing visibility impact potential over time and space. As indicated above, if concurrent optical and aerosol measurements are available, an analysis of the relationship between visibility and the responsible aerosol components can be conducted. In addition, knowledge of optical properties is one of the factors required to predict the fate of light traversing the atmosphere. In practice, not all of the necessary optical measurements are made; so assumptions are required to predict effects on the appearance of scene.

To the person on the street (and to perception investigators), visibility is associated with changes in the appearance of scenic characteristics (*e.g.*, changes in color, loss of detail, or limits on the most distant visible feature). In addition to the optical characteristics of the atmosphere, lighting conditions and intrinsic scene characteristics control the appearance of scenes. Lighting conditions change continually due to variations in sun angle. Scene characteristics (*i.e.*, cloud cover, vegetation, snow cover, *etc.*) are more erratic than sun angle changes and are generally beyond quantitative measurement or prediction. Scene monitoring allows the effects of all factors that influence visibility to be documented. With a number of assumptions and for simple lighting conditions (*e.g.*, no clouds in the sky) scene measurements can be used to estimate optical indexes.

The following subsections will review the more commonly used measurement methods in each of the three groups of techniques. There are numerous monitoring techniques that will not be covered, and those that are covered are only briefly described. Additional information is available in the references cited within the text below. The references of Malm and Walther (1980); Lundgren *et al.* (1979); Bhardwaja (1987); Middleton (1952); and NOAA (1982) deserve special attention for the wealth of information they contain on visibility measurement techniques.

### 3.1.1. Aerosol Monitoring

The primary objective of visibility-related particle monitoring is to gather information required to establish the relative contributions of various species to visibility impairment. Though $NO_2$ absorbs light and all gases scatter light, monitoring of these gases is not the focus of this discussion. Standardized methods of monitoring $NO_2$ are described elsewhere (Stern, 1976). Light scattering by gases is basically constant except for a variation with elevation above sea level. The remainder of this discussion will concentrate on particle monitoring.

Size and composition are the two dimensions of particle characterization which are of most concern for visibility. Particle size and composition are both important factors affecting scattering efficiency. On a per unit mass basis, particles with diameters between 0.1 and 1.0 microns, the most efficient size range, are much more efficient at scattering light than larger or smaller particles. Chemical composition determines the index of refraction and the hygroscopic properties of the aerosol. Particle absorption efficiency is not as sensitive to size as scattering efficiency, but it does depend on particle composition (essentially on the amount of elemental carbon present).

Ideally, particle monitoring for visibility assessment would provide composition as a function of size. The composition information would include all of the significant components (*e.g.*, sulfates, nitrates, organics, elemental carbon, crustal material, and liquid water). The size resolution would be sufficient to characterize the shape of the particle size distribution for each species (*i.e.*, at least eight size ranges between 0.1 and 20 microns diameter).

Multistage particle samplers do allow some composition data as a function of size to be determined. These devices extract particles from the sample air according to particle aerodynamic size using inertial separation techniques. This is done in stages, with particles of ever-decreasing size being deposited on substrates for composition analysis. Particles from about 50 microns to 0.05 microns can be sized in this way. Multistage samplers usually have four to ten size ranges. The complexity of the samplers and the cost of the multistage sample analysis have discouraged the use of multistage samplers except for short-term research monitoring.

Particle size distributions without the corresponding composition data can be measured with a variety of particle size monitors. These monitors operate continuously or in relatively short cycles, determining size by one of several physical principles, such as electrical mobility or optical scattering properties (Lungren *et al.*, 1979). Though they are occasionally used in visibility research programs, these monitors are not suitable for unattended operation and hence are not employed for routine monitoring.

The most popular approach for particle monitoring uses any of a variety of samplers which separate the particles from the gases by filtration or inertial impaction. The particle samples are subsequently analyzed for mass and chemical composition.

Until the last decade, the majority of particle monitoring was conducted with high volume samplers (commonly called Hi-Vols). These samplers maintained a 40 cubic foot per minute flow for 24 hours through a high efficiency glass, quartz, or cellulose filter. The upper particle size cutoff for the Hi-Vols was about 50 microns diameter, depending on the wind speed and wind orientation with respect to the sampler. Several years ago, Hi-Vols

were largely replaced by inhalable particulate filter samplers which collect particles up to about 10 microns in size, independent of wind conditions. These PM-10 (particulate matter less than 10 microns diameter) samplers are not necessarily restricted to the high flow rates of the Hi-Vols, although they also generally collect 24-hour duration samples.

Samplers designed to collect in two size ranges, between 10 and 2.5 microns and less than 2.5 microns diameter (commonly called the coarse and fine particle size ranges), have been operated at numerous locations around the country. The original intent of the 2.5-micron size range was to allow investigation of the particles that can penetrate deeply into the respiratory tract and also to separate the two size modes of the typical bimodal particle mass distribution (see Section 2.1). This also represents an improvement from a visibility point of view, and most visibility monitoring programs have adopted the same two size ranges for consistency.

Numerous sampler designs have been developed to produce coarse and fine particle data. Table 24-5 lists the most common ones. Some collect separate PM-10 and PM-2.5 samples and characterize the coarse particles by subtraction, while others collect separate coarse and fine samples. The 10-micron size segregation is usually achieved at the sampler inlet which excludes particles greater than that size. Unlike earlier designs, most inlets in common use during the last five years have been wind tunnel tested to ensure that they operate independent of ambient wind conditions. The 2.5-micron size separation is usually accomplished by an inertial impactor or cyclone separator which removes larger particles from the sampling stream.

Sample analysis involves gravimetrical determination of mass and usually one or more types of chemical analysis—for ions, elements, and/or organic/elemental carbon. The analysis approach must be compatible with the filter substrate and the total amount of sample collected. Chemical analysis for all the significant particle components is relatively rare in the older monitoring programs. This is primarily due to the cost of the analysis and to the need for multiple samples on different filter materials. Typically mass and ions, or mass and elements, were analyzed. Until recently, though total carbon might be analyzed, separating black carbon from organic carbon was not considered important. The enhanced extinction efficiency of black carbon (due to its absorption characteristics) over that of organic carbon makes this separation important for visibility assessments.

Some of the historical particle composition data are of questionable quality due to sampling artifacts. Labile components, in particular nitrates and some organic compounds, have been shown to vaporize after collection on a filter (*i.e.*, negative artifact) and to deposit on filters during sampling from the gas phase (*i.e.*, positive artifact). The amount of positive or negative artifact depends upon the thermodynamic partition of the gas and liquid phases and upon the presence of chemical reaction sites on the filter or other material in the sample.

*Table 24-5. Commonly Used Two-Stage Particle Samplers*

| Sampler | References | Comments |
|---|---|---|
| Virtual Impactor (also called the Dichotomous Sampler) | Stevens et al., 1978 | Separate coarse and fine samples. Flow rate of about 17 L/min. Manual and automatic samplers available. One substrate per size per sampler. |
| IMPROVE Sampler | Eldred and Cahill, 1988 | System is configured to collect four simultaneous samples (usually 1 PM-10 and 3 PM-2.5). Flow rate of about 20 L/min. Two automatic filter changes. Nitrate denuder employed. |
| SCISAS | Mueller et al., 1986 | Collects one PM-15 and one PM-2.5 sample simultaneously. Flow rate of about 100 L/min. Up to six automatic filter changes. |
| Stacked Filter Unit | Eldred et al., 1986 | Collects PM-15 and PM-2.5 using series filtration for the fine particle separation. Flow rate of about 10 L/min. |
| Sequential Filter | Watson, 1990 | Collects PM-10 and PM-2.5 samples. Automatically sequences up to 12 sample periods. With 113 L/min flow, it can take as many as eight 3-hour samples per day. |

Sampling methods have been and are continuing to be developed to minimize these artifacts. However, these have only been employed in the last few years for nitrates, and a few preliminary approaches are just being field tested for organics. A discussion of the effects of artifacts and other measurement errors on visibility/aerosol relationships is contained in Section 4.

The most important labile component of ambient particles is the loosely bound liquid water associated with the hygroscopic aerosols (*e.g.*, sulfates and nitrates). The amount of liquid water (in the atmosphere or on the filter sample) is determined by the concentration and chemical nature of the particles, the ambient relative humidity, and to a lesser extent by the relative humidity history that the particles have experienced. The liquid water component during collection and analysis is constantly changing in response to changing relative humidity. Methods to measure liquid water in situ are under development, but no routinely used approach for such measurements is presently available. Until such techniques are available, the substantial role of liquid water in visibility impairment is estimated by models that require ambient relative humidity data. Relative humidity monitoring can therefore be considered an important component of aerosol monitoring for visibility assessment.

Until recently, nearly all particle monitoring was conducted on a 24-hour duration schedule. This allowed sufficient sample density on the filters for the analysis methods employed and was consistent with ambient particulate regulations. Visibility, unlike most other effects of air quality, manifests itself instantaneously and is of greatest significance during daylight hours. To relate visibility data with 24-hour particle data requires that the visibility data be averaged. This not only obscures short term (*i.e.*, hourly or less) fluctuations but also introduces errors because of the inability to account for the nonlinearities in the relationship between relative humidity (which has substantial diurnal variations) and aerosol water content (which can account for substantial light extinction). Several recent visibility monitoring programs have gone to shorter sampling schedules (*e.g.*, 8-hour duration) as a compromise between such concerns and the practical considerations of cost and sufficient sample mass for analysis.

### 3.1.2 Optical Monitoring

Determination of optical indexes such as extinction coefficient is one of the primary goals of most visibility monitoring programs. By integrating the optical effects of the aerosol and avoiding the complications of scene characterization, the optical indexes are ideal for spatial and temporal analysis of visibility effects. All of the optical indexes listed in Table 24-4 can be directly measured, though many programs employ scene monitoring techniques and convert the data to optical indexes.

All of the optical indexes are wavelength dependent. So in monitoring these indexes, consideration must be given to the wavelength of the measurement. As stated in Section 2, 550 nm is the wavelength of maximum eye response; thus it is the most desired wavelength for visibility related monitoring. The monitoring methods discussed below either involve measurements at about 550 nm or the measurements are adjusted to that wavelength. The remainder of this section will discuss the optical monitoring methods organized by optical index.

The path averaged extinction coefficient can be measured by transmissometers which monitor the intensity of light of known measured initial intensity after it has traversed a known distance. As indicated in Section 2.2, the ratio of these two intensities is the transmission,[1] which is the natural logarithm of the product of path averaged extinction coefficient and path length. The useful measurement range for a transmissometer is related to its precision and the path length over which it is operated. Longer path lengths are required for accurate measurements in cleaner air (*e.g.*, 10 km paths in remote western locations), while shorter paths are used in more polluted situations (*e.g.*, paths of less than a kilometer in the East). Short-path (250 to 500 foot path length) transmissometers have been used for years at many airports (NOAA, 1982). These have a useful range of measurement only up to a few kilometers visual range. Though useful for airport safety in fog or other severe conditions, such measurements are of little value for more general visibility monitoring.

The National Park Service has sponsored the development and testing of a long path (*i.e.*, to 15 km) transmissometer appropriate for the near pristine conditions of the remote West (Malm *et al.*, 1987b). Over path lengths greater than a few kilometers, successful transmissometer operation is particularly challenging due to light beam bending and distortion caused by atmospheric turbulence. A large part of the evaluation process dealt with determining whether turbulence interference was adequately minimized. After several years of field testing, deployment of these instruments was initiated in 1987 with about 20 presently in operation. Though most of the monitoring with these instruments is in the West, they are also employed at three eastern locations.

Another long-path instrument in the field testing stage is the rotating disk transmissometer (Richards and Stoelting, 1986). This instrument features an extended light source

[1] For uncollimated light sources the $r^2$ effect of distance on intensity must be included.

designed to minimize the effects of turbulence. The source is ambient light reflected by a disk that alternately exposes white and black sectors at a specific frequency. Because this instrument must measure the intensity variations caused by ambient lighting changes, it is restricted to daylight operations.

A number of instruments measure the light scattered by particles and gases from a light source of known intensity. They are classified according to the scattering angle that is measured: forward scattering, back scattering, polar, and integrating nephelometer.

Forward and back scattering instruments have been evaluated and used on limited basis by several federal government agencies for airport visibility and offshore fog monitoring purposes (NOAA, 1982). The simple design and good failure reliability of these instruments have made them popular candidates for automated visibility monitoring for transportation safety purposes. Since only a portion of the scattered light is measured and absorption is completely unaccounted for, these instruments must be calibrated for typical aerosol situations. As a result these devices will mismeasure visibility under atypical aerosol conditions (*e.g.*, unusual particle size or shape distributions, or unusual fractions of absorbing aerosol).

Integrating nephelometers (Charlson, 1969) measure scattering over nearly the entire range of angles from 0° to 180° (truncation at each extreme of about 10° is unavoidable). Unlike the forward and back scattering instruments, the nephelometer measurement is made in an enclosed cell through which sample air is continually being drawn by a pump. The nephelometer has been a popular method to monitor the variations of particle concentrations in air pollution studies. Originally, sample air heaters were usually employed to drive off the liquid water before the scattering measurement, so that the dry particle concentration could be better estimated. When used in this way the data are not representative of ambient scattering and therefore are of limited use for visibility monitoring. Recently, it has been found that even with the heaters removed, the nephelometer heats the sample air by about 7° C, causing some drying of the aerosol and an underestimate of scattering by liquid water associated with hygroscopic particles (Malm *et al.*, 1989). Nephelometer modifications can successfully minimize this inadvertent heating.

For nephelometers, the combination of scattering angle truncation error and particle loss from having to draw the sample into the enclosure for measurement results in a significant underestimation of the scattering due to coarse particles (*i.e.*, larger than 2.5 microns diameter). However, by coupling the nephelometer with a fine particle size-selective inlet, the instrumentation can provide valuable information on the fine particle component of the scattering component.

The polar nephelometer measures the light scattered from any chosen angle. This allows a direct measurement of the scattering phase function (light energy scattered as a function of solid angle), which is important for predicting the effects of aerosols on the appearance of a scene. Integration of these measurements over all angles yields the scattering coefficient. Unfortunately, polar nephelometers are not easily adapted to routine monitoring and have not seen much use except in laboratory situations.

Two instrumental approaches for monitoring the absorption coefficient, the aethelometer (Hansen *et al.*, 1988) and spectrophone (Szkarlat and Japar, 1981) have not been widely used in visibility monitoring programs. More commonly, light absorption measurements on filter samples are used as a measure of the atmospheric particle absorption coefficient. A number of methods have been devised to make this measurement, and efforts have been underway to intercompare and evaluate their relative merits. The common element in these methods is measurement of the change in the transmittance or reflectance of a filter before and after particle sampling. The sampled particles should be in a thin uniform layer on the filter for good quality measurements.

### 3.1.3 Scene Monitoring

Monitoring the appearance of a scene is the oldest form of visibility monitoring. (Since scenic appearance is the effect of interest, some would argue that it is the only form of visibility monitoring.) By every reasonable measure, the most extensive visibility monitoring data bases are those that employed scene monitoring. The commonly used monitoring methods that are described below include human observations of visual range, contrast measurements, and documentation of the scene by photography. As indicated earlier, it is common for scene measured data to be converted to extinction coefficient, an optical index. This section ends with a discussion of the concerns associated with these data transformations.

Airport observations of visual range have been made since 1919 and computer archived since 1947 (NOAA, 1982). One definition of visual range is the minimum distance that an observer would have to back away from an object before it disappears. In practice, this is not how the observation is made. Daylight observations involve viewing preselected visibility markers or targets (*i.e.*, dark colored objects) at known distances from the observation point to determine the most distant marker that is visible. At night the process is similar except that the markers are unfocused low to moderate intensity lights.

One of the more serious shortcomings of airport visual range observations is the availability of suitable targets at

reasonable distance intervals. Many observing locations have obstructed views (*e.g.*, treelines) or flat views (*e.g.*, airports on the plains or coasts) which limit the targets that can be used. It is not unusual for actual visual range to be greater than the most distant target for a substantial fraction of the time. In addition to target related problems, visual range observations also are plagued by inconsistencies in observation procedures, observer detection thresholds, and reporting practices. Also, there are perceptual difficulties associated with low light observation at dawn and dusk.

In spite of these shortcomings, visual range observation data have provided an impressive insight into national scale visibility patterns and trends. The large number of observation locations has allowed investigators the luxury of selecting subsets of airports with suitable targets and a history of consistent observations. Often only midday observations are used so that light levels are not a concern. Also, the "greater-than-or-equal-to" nature of observations can be accounted for by appropriate methods of compiling cumulative frequency distributions.

Contrast of distant targets against their background can be determined from direct measurements of the light from the target and background. A large variety of instruments have been developed to make such measurements (Malm and Walther, 1980), though only a few approaches have been routinely used. Of these, the most common are teleradiometers which have been employed widely in remote areas of the West over the last decade. (These are often confused with telephotometers which are the broad band pass equivalent.)

Teleradiometer measurements are made at one point on the target and another just above it in the sky. Target uniformity is important to ensure that slight misalignments are not a source of measurement error. Radiance measurements are typically made at 550 nm, although some programs have measured at several wavelengths in order to investigate the changes in color associated with visibility impairment.

Contrast can also be determined from microdensitometer measurements of targets and background sky images on photographic film. The overall accuracy of the technique is comparable to teleradiometer measurements, if the film density log exposure curve is well determined (Johnson *et al.*, 1984). For this reason and because of the additional information available with a photograph, this approach is replacing teleradiometers at many monitoring locations.

Photography has been an integral part of most visibility monitoring programs. The National Park Service alone has archived well over 100,000 color transparencies documenting daily changes in scenic appearance. Photography is usually the only technique that can provide information on the frequency, duration, intensity, and (occasionally) even the source of elevated pollutants (*i.e.*, those not in contact with the surface). Photographs are also valuable for identifying unusual events that can effect the performance or measurements of other instrumentation (*e.g.*, wild fires, dust storms, patchy fog, *etc.*) Finally, photographs are the single most important medium for communicating visibility conditions to the public and policy makers.

Scene monitoring data are often converted to optical indexes because of the usefulness of information in that form. Specifically, visual range observations and target contrast data are converted to extinction coefficient values. Such transformations require the use of a model (*e.g.*, Koschmieder's relationship) which relates the apparent contrast of a target as a function of distance to the extinction coefficient. This model requires a number of assumptions that are not always well met (Malm, 1986).

One key assumption that is often violated is the assumption that the inherent contrast (*i.e.*, the contrast at the target) is known. Target inherent contrast changes as a function of the sun position in the sky (*i.e.*, time of day and day of the year), cloud cover, and target cover (Pitchford and McGown, 1987). The assumption of a black target has been shown to be wrong except when a specially fabricated artificial target is employed. Another source of error is associated with cloud shading of the sight path but not the target. This nonuniform lighting condition will cause the extinction coefficient to be significantly underestimated.

For investigators interested only in long-term (*i.e.*, seasonal or annual) averages, the loss of precision associated with not knowing the correct inherent contrast can be tolerable. However, if short-term variations are important, as for example in trying to establish the relationship of the extinction coefficient to aerosol characteristics, then it is critical to reduce the uncertainty by estimating the inherent contrast as well as possible. Numerous approaches have been employed in attempting to handle this problem. Usually data associated with clouds in the sky are eliminated to reduce that source of uncertainty. Depending on the geographic location and time of year, eliminating cloudy days may seriously affect the size and representativeness of the data base.

## 3.2 VISIBILITY/AEROSOL DATA BASES
*M. Pitchford*

The purpose of this section is to catalogue major visibility and aerosol data bases. The information is presented in two tables. Table 24-6 summarizes the characteristics of long-term monitoring programs, while Table 24-7 describes short-term studies.

*Table 24-6. Long-term Visibility and Aerosol Data Bases*

| Study/Data Base | Reference | Air Sheds | Period | Type of Data[a] | Purpose of Study | Comments |
|---|---|---|---|---|---|---|
| | | | *National and Regional Networks* | | | |
| National Weather Service Airport Visibility Data | Trijonis (79, 82a & b)<br>Sloane (82a & b, 83b, 84)<br>Patterson et al. (80)<br>Husar & Patterson (84) | Rural & urban airports all over the nation. | 1918 to present | Human estimates of prevailing visibility mainly in support of aircraft operations. | To assess visibility trends; Assessment of the role of meteorology on visibility impairment. | Quality varies from site to site; natural causes of visibility impairment (rain, snow, fog) included in data. |
| Interagency Monitoring of Protected Visual Environments (IMPROVE) | Joseph et al. (86) | Twenty remote locations nationwide, though primarily in the West. | 1987 to present | Aerosol & visibility; PM-10 & fine particle mass. Fine particle elements, ions, organic & light absorbing carbon. **B**ext, **B**abs, & photography. | To establish baseline values & identify existing impairment in visibility protected federal Class I areas. | Employs "state-of-the-art" methods for long term routine monitoring. Operated jointly by EPA four federal land managers. |
| Eastern Fine Particle Visibility Network | Handler (89) | Five eastern rural locations. | 1988-89 Five sites after 1989 two sites | Aerosol & visibility; fine particle elements organic & soot carbon. **B**ext, **B**abs, & photography. | A research monitoring program to provide information needed to quality support development of a secondary fine particle standard. | An EPA operated network. Sites are collocated with other air monitoring programs. |
| National Park Service Network | Joseph (86) | About 37 remote locations nationwide, though primarily in the West. | 1978 to present Seventeen sites started in 1987. | Aerosol & visibility; 17 sites operated with IMPROVE measurements (see b). Other have some subset of the IMPROVE measurements. | To document visibility & aerosol levels & to identify sources of visibility impairment measurements in NPS. | Represents the longest period of record for visibility & aerosol monitoring at remote locations. |
| SCENES | McDade & Tombach (86) | Eleven rural & remote southwestern locations. | 1984-1989 | Aerosol & visibility; PM-15 & fine particle mass, elements, organic & light carbon at most sites. **B**ext or **B**scat, and photography at most sites. | To document levels & causes of visibility impairment in northern Arizona & southern Utah. | This cooperative research program included several intensive & special studies. An ambitious quality assurance protocol identified many monitoring method difficulties which new techniques ultimately solved. |

(Continued)

*Table 24-6. (Continued)*

| Study/Data Base | Reference | Air Sheds | Period | Type of Data[a] | Purpose of Study | Comments |
|---|---|---|---|---|---|---|
| Western Regional Air Quality Study (WRAQS) | Macias et al. (86) | Eleven nonurban locations in the western U.S. | 1981-1982 | Aerosol & visibility; PM-15 & fine particle mass, elements, ion. | To document background levels of visibility & related aerosols, organic & elemental carbon. **B**scat, observed visual range & photography. | Represents the highest times resolution for routinely collected filter samples (two four-hour samples each day). |
| National Air Surveillance Network (NASH) | Shah et al. (81)<br>Mueller & Hidy (83) | Urban & rural areas of U.S. | 1975 to present | Aerosol only; TSP ions, & some elements. | Air quality monitoring. | No size-fractioned data; collected only once every six days; artifact on filter possible. |
| Inhalable Particle Network (IP Network) | Pace et al. (81)<br>Watson et al. (81) | Urban & rural areas of U.S.<br>Evans (84)<br>Rodes & Evans (85) | June 1979 to present | Aerosol only; fine & coarse aerosol mass, PM-15 mass, elements, & ions (every fourth sample). | Charaterize inhalable particles | Discrepancy exists between PM-15 and IP mass (sum of fine & coarse). Screening of the data required to remove invalid data points (~25%). |
| Sulfate Regional Experiment (SURE) | Mueller & Hidy (83) | Nonurban areas of eastern U.S. (9 Class I sites & 45 Class II sites) | 1977-1978 | Aerosol only; TSP, fine & coarse aerosol mass, ions & elements. | Sulfate characterization pollutant source characterization. | Class I sites operated for 18 months continuously; Class II sites operated for one month every season for a total of six. |
| Eastern Regional Air Quality Studies (ERAQS) | Mueller & Watson (82)<br>Tombach & Allard (83) | Nine nonurban areas in north-eastern U.S. SURE Class I sites. | 1978-1979 | Aerosol & visibility; TSP, fine & coarse aerosol mass, ions, elements, **B**scat, **B**ext, & photography. | To characterize visibility (at two sites only) & air quality in the north-eastern U.S. region. | The only long-term instrumental visibility data set generated in the eastern U.S. Visibility monitored only at 2 sites; intercomparison of visibility measurement methods made. |
| Ohio River Valley Study | Shaw & Paur (83) | Three rural sites in Ohio River Valley. | May 1980-August 1981 | Aerosol only; fine & coarse aerosol mass & elements. | Characterization of fine & coarse aerosols in the region. | Portion of aerosol composition was not accounted for due to limitations in XRF analysis used. A long-term daily monitoring of aerosol in rural areas of the Ohio River Valley. |

(Continued)

*Table 24-6. (Continued)*

| Study/Data Base | Reference | Air Sheds | Period | Type of Data[a] | Purpose of Study | Comments |
|---|---|---|---|---|---|---|
| Harvard School of Public Health's Six Cities Study | Spengler & Thurston (83) | Portage, WI<br>Topeka, KS<br>Kingston, TN<br>Watertown, MA<br>St. Louis, MO<br>Steubenville, OH | Spring 1979 | Aerosol & visibility; fine & coarse aerosol mass, elements, $SO_4^=$, & **B**scat. | Mass & elemental characterization of aerosol & their temporal variations to assess health effects of air pollution. | Portion of aerosol composition was not accounted for due to limitations in XRF analysis used. |
| RESOLVE | Blumenthal et al. (86) | Seven remote sites in the California Mojave Desert | 1983-1985 | Aerosol & visibility; PM-10 & fine particle mass, elements, organic & elemental carbon, **B**ext, **B**scat, **B**abs, & photography. | To document levels & identify causes of visibility impairment in the R-2508 military air space. | DOD sponsored study to provide information needed to limit future additional degradation of military testing by visibility impairment. |
| | | *Single Air Shed Studies* | | | | |
| Great Smoky Mountain National Park Visibility & Air Quality Study (TVA) | Valente & Reisinger (83)<br>Reisinger & Valente (84 & 85) | Great Smoky Mountain National Park | 1980-1983 | Aerosol & visibility; fine & coarse aerosol mass & elements; **B**scat & **B**ext; photography. | Characterize visibility & aerosol. | Because of instrument problems, teleradiometer data were lost. Total particulate matter mass only estimated in some cases. PIXE analysis could not provide some major elemental data. |
| Regional Air Pollution Study (RAPS) | Jaklevic et al. (81)<br>Altshuller (82 & 85) | 100 km region around St. Louis, MO | 1974-1977 | Aerosol only; fine & coarse mass, $SO_4^=$, elements. | Develop & evaluate regional air quality models. | Comparison of Hi-Vol and dichotomous samplers. |
| Portland Aerosol Characterization Study (PACS) | Cooper & Watson (79)<br>Shah et al. (84) | Two rural & four urban areas in Portland, OR | July 1977-April 1978 | Visibility & aerosol; fine & coarse mass, TSP, ions, elements, **B**scat. | Aerosol characterization source apportionment. | Significant role of carbonaceous aerosols recorded. |

[a] Visibility data include light scattering and light extinction measurements using integrating nephelometer, teleradiometers, cameras, and human observers.

*Table 24-7. Short-term Intensive Visibility and Aerosol Studies*

| Study/Data Base | Reference | Air Sheds | Period | Type of Data[a] | Purpose of Study | Comments |
|---|---|---|---|---|---|---|
| | | | *Rural Studies* | | | |
| Allegheny Mountain Studies | Pierson et al. (80a & b) Pierson (personal communication, 1985) | Rural Allegheny Mountain site | 24 July-11 Aug 1977 & Aug 1983 | Visibility & aerosol; TSP, fine & coarse aerosol mass, ions, elements, **B**scat. | Characterization of visibility and $SO_4^=$ in the region. | Filter artifact investigated; no size fractionated data in 1977. |
| Shenandoah Valley Studies | Stevens et al. (84) Weiss et al. (82) Ferman et al. (81) Wolff et al. (83) | Rural Shenandoah Valley | 15 July-15 Aug 1980 | Visibility & aerosol; fine & coarse aerosol mass, ions, elements, **B**ext, human estimates of visibility. | To characterize visibility & aerosol in the rural eastern U.S. | Since three different groups performed the study, intercomparability of data possible. |
| Great Smoky Mountain Study (EPA) | Stevens et al. (80) | Great Smoky Mountain National Park | 20-26 Sept 1978 | Aerosol & gaseous pollutants; fine & coarse aerosol mass & elements. | Characterize aerosol in a rural area. | Comparison of day and night aerosol data made. |
| Research Triangle Park Visibility Study | Dzubay & Clubb (81) | Rural Research Triangle Park, NC | 8 June-3 Aug 1979 | Visibility & aerosol; fine & coarse aerosol mass, elements, **B**ext, **B**scat. | Characterize visibility & aerosol in the region. | Comparison of different visibility measurement methods studies. |
| Louisiana Gulf Coast Study | Wolff et al. (82a) | Gulf Coast | 8 Aug-7 Sept 1979 | Visibility & aerosol; fine & coarse aerosol mass, ions, elements, **B**scat. | Investigation of sources of $O_3$ and haze. | Calibration errors of MRI 1550 integrating nephelometer applied to data. |
| Atlantic Coastal Study | Wolff et al. (85a) | Lewes, DE | 1-31 Aug 82, 25 Jan-28 Feb 1983 | Visibility & aerosol; fine & coarse aerosol mass & chemistry, **B**scat. | Air quality & sources of haze. | |
| Pacific Northwest Regional Aerosol Mass Apportionment (PANORAMAS) | Core et al. (86) | Twenty-six rural & remote locations in Washington, Oregon, & Idaho | May-Nov 1984 | Visibility & aerosol; fine particle mass, elements, & ions. **B**ext, **B**abs, & photography. | To document the levels & sources of summer visibility impairment in the Northwest. | This cooperative monitoring program identified smoke as a major contributor to visibility impairment. |

(Continued)

*Table 24-7. (Continued)*

| Study/Data Base | Reference | Air Sheds | Period | Type of Data[a] | Purpose of Study | Comments |
|---|---|---|---|---|---|---|
| | | | *Urban Studies* | | | |
| California Aerosol Characterization Study (ACHEX) | Hidy (75)<br>Hidy et al. (80)<br>Charlson et al. (72) | Fourteen southern California cities | July-Nov 72, July-Oct 73 | Aerosol & visibility TSP, fine & coarse aerosol mass, ions, elements, **B**scat. | Characterization of urban aerosols in California. | The most complete classic aerosol experiment. New methods of sampling & analysis tested. |
| Denver Winter Haze Study I | Countess et al. (80 & 81)<br>Wolff et al. (81a)<br>Groblicki et al. (81)<br>Heisler et al. (80a & b) | Denver, CO | Nov-Dec 78 | Visibility & aerosol; fine & coarse aerosol mass, ions, elements, **B**scat, **B**ext. | Investigation of sources of Denver haze. | Role of local sources & the significant role of carbon in the air documented. |
| Denver Winter Haze Study II | Lewis & Stevens (83)<br>Hasan & Dzubay (85) | Denver, CO | Jan 1982 | Visibility & aerosol; fine & coarse aerosol mass, ions, elements, **B**scat. | Investigation of sources of Denver haze. | Role of local sources & the significant role of carbon in the air documented. |
| Metro Denver Brown Cloud Study | Watson et al. (88) | Denver, CO | Nov 1987-Jan 1988 | Visibility & aerosol; fine particle elements ions, organic & light absorbing carbon, **B**ext, **B**scat, **B**abs, & photography. | Investigate the sources of Denver haze. | Comprehensive spatial & temporal measurements included fuel switching to see effects of source modulation. |
| Detroit Visibility Study | Wolff et al. (82 & 85)<br>Sloane & Wolff (84a & 85) | Urban Detroit, MI | 15-21 July 1981 | Aerosol & visibility; fine & coarse aerosol mass, ions, elements, **B**scat. | Identification of chemical components of TSP. | Data from a major industrial & urban areas. |
| Houston Visibility Study | Dzubay et al. (82) | Houston, TX | 11-19 Sept 1980 | Visibility & aerosol; fine & coarse aerosol, ions, elements, **B**scat, **B**ext. | Characterization of visibility & aerosol. | Comparison of day & night aerosols & different visibility measurement devices made. |
| CARB Los Angeles Basin Study | Appel et al. (83) | Los Angeles Basin | Aug 1982 | Visibility & aerosol; fine & coarse aerosol mass, ions, & **B**scat. | Characterize visibility & aerosol in the basin. | Significant roles of $NO_3^-$ & organics shown; the importance of filter artifacts reported. |

(Continued)

*Table 24-7. (Continued)*

| Study/Data Base | Reference | Air Sheds | Period | Type of Data[a] | Purpose of Study | Comments |
|---|---|---|---|---|---|---|
| Northern New Jersey Air Pollution Study | Lioy et al. (83 & 85) | Newark, NJ<br>Elizabeth, NJ<br>Camden, NJ<br>Ringwood, NJ | Winter 1982-1983 | Aerosol only. | Inhalation toxicology studies. | Urban contributions of carbonaceous particles to air pollution episodes. |
| Willamette Valley Field & Slash Burning Study | Lyons & Tombach (79) | Willamette Valley, OR | Summer 1978 | Aerosol; fine & coarse mass, TSP, elements (carbon), ions. | Assessment of field & slash burning on air quality. | Significant role of carbonaceous particles in fine aerosol demonstrated. |
| San Joaquin Valley Aerosol Study | Heisler & Baskett (81) | San Joaquin Valley, CA | Nov-Dec 78, Jul & Sep 79 | Aerosol only; fine & coarse mass, ions. | Characterize ambient aerosols termittent data sets. | |

[a] Visibility data include light scattering and light extinction measurements using integrating nephelometer, teleradiometers, cameras, and human observers.

The long-term data bases are organized according to national/regional programs versus single airshed programs. The short-term studies are divided according to rural versus urban. For each data source, the tables include references, the location and duration of the monitoring, a summary of the types of data collected, and a description of the study purpose. These tables were adapted and updated from another report (Mathai and Tombach, 1985), which contains an extended summary for each of the studies it covers.

Most of the monitoring programs cited in the tables were conducted with visibility research as a primary goal. However, for a few programs, use of the data for visibility research is merely a fortunate byproduct. Airport visual range observations constitute the most notable example of this second category. Airport observations are made primarily for short-term use in support of aircraft operations. However, these data are the backbone of any attempt to assess national geographical patterns and historical visibility trends. None of the other data bases can compete in terms of the number of locations or period of record.

Though not of direct concern for this assessment, it is worth noting that manual airport observations are due to be discontinued within the next few years, to be replaced by instrumental visibility monitors. While this may represent an improvement in the quality of the data collected, it will also produce a break in the historical record of one of the longest air quality related data bases. Unfortunately this break will occur at about the time of anticipated sulfur reductions, thereby complicating the task of assessing the magnitude of associated visibility changes. It would be useful to have at least a year of overlap data for the two methods.

In Tables 24-6 and 24-7, there are few data sources which include aerosol measurements but no visibility data. Clearly these programs did not have visibility assessment as a primary goal. However, they can be used alone to identify spatial patterns and seasonal cycles, or they can be combined with the airport observations to investigate visibility/aerosol relationships.

The monitoring programs that include visibility as a primary focus usually have two major goals. These goals are to characterize visibility conditions (*e.g.*, spatial and temporal patterns) and to determine the causes of visibility degradation. The remainder of this section corresponds to the first goal, while Section 4 corresponds to the second.

## 3.3 EXISTING CONDITIONS FOR VISIBILITY/AEROSOLS

*J.C. Trijonis*

### 3.3.1 Spatial Patterns

Figure 24-20 presents an isopleth map of median mid-day airport visibilities at suburban/nonurban locations in the United States for the mid-1970's (Trijonis, 1982a). As discussed earlier in this section, airport data are subject to inconsistencies due to variations in reporting practices, observer detection thresholds, and visibility markers. However, Figure 24-20 should be representative of overall geographical patterns.

Figure 24-20 demonstrates that the mountainous Southwest experiences the best visibility in the country. Specifically, median airport visual range exceeds 70 miles in the region comprised of Utah, Colorado, Nevada, northern Arizona, northwestern New Mexico, and southwestern Wyoming. Airport visibility is also quite good, exceeding 45 miles, to the north and south of this region. Passing westward or eastward, fairly sharp gradients occur. Median airport visual range falls to less than 25 miles in a narrow band along the northern Pacific coast, less than 15 miles in the central valley of California, and less than 10 miles in the Los Angeles basin (Trijonis, 1982b). Although some parts of the East (*e.g.*, New England) experience moderate visibility levels (about 20 - 30 miles), median airport visual range is generally less than 15 miles in the area east of the Mississippi and south of the Great Lakes.

Figure 24-21 summarizes recent data for median visual range from the National Park Service (NPS) network of automated cameras (with contrast determined from densitometer measurements on the photographs). These data are not necessarily considered more accurate or consistent than airport data due to variations in film quality and uncertainties in initial sky radiance and initial contrast. However, they do agree rather well, in an overall general sense, with data from a prior NPS teleradiometer network (Air Resource Specialists, 1988; Dietich and Molinar, personal communication 1989).

Figure 24-21 verifies the general East/West dichotomy evident in the previous figure. With the NPS data set, median visual range in the mountain areas of the Southwest (about 160 km) is about three times greater than at the two sites in the Appalachians (about 50 km). The airport data indicate about the same factor of three: 70 - 80 miles (110 - 130 km) versus 15 - 30 miles (25 - 50 km). The reader should note from the previous discussions of Figure 24-20 that—in areas south of the Great Lakes and east of the Mississippi, but *excluding* the Appalachians—the dichotomy is more like a factor of six.

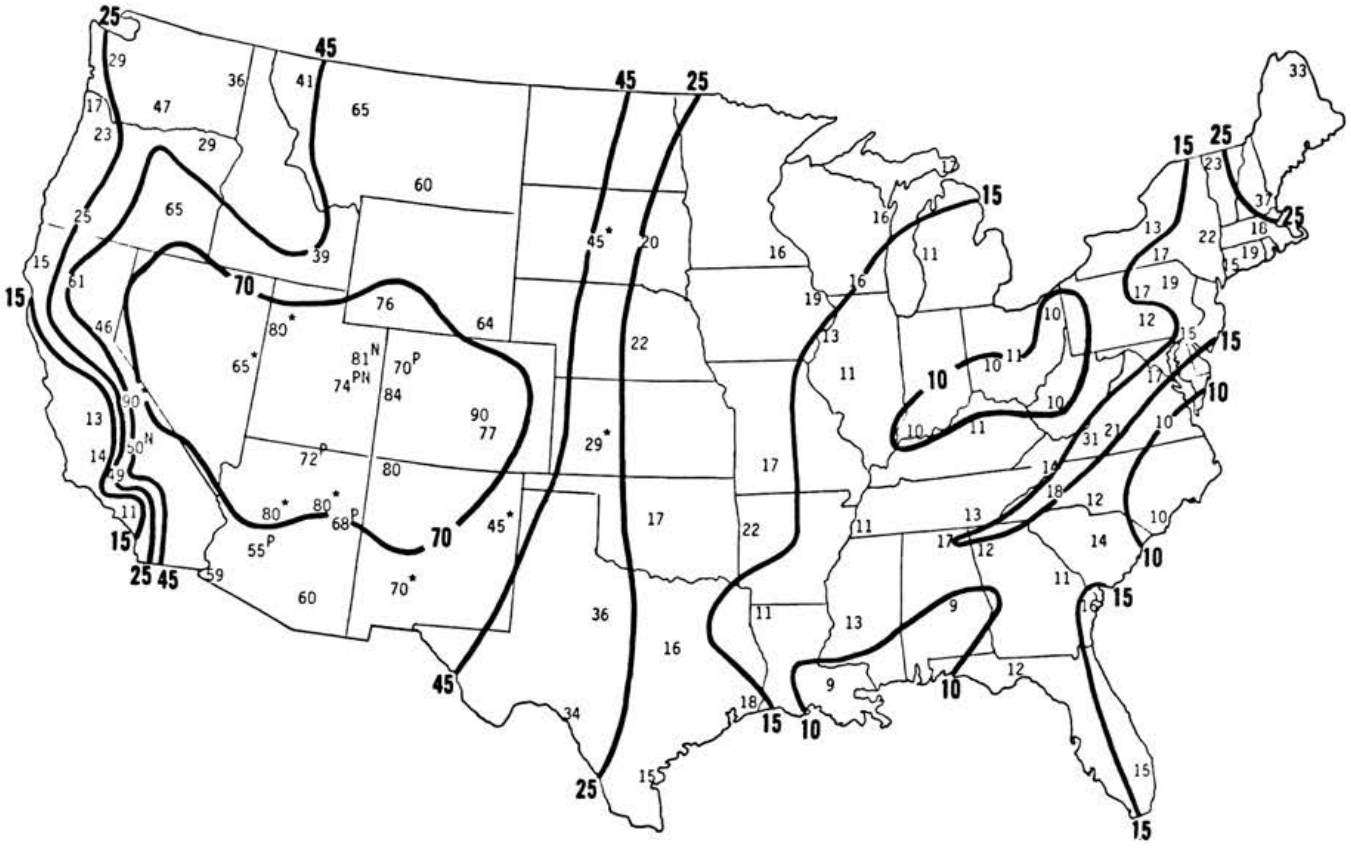

*Figure 24-20 Median mid-day visual range (in miles) at suburban/nonrural airports in the United States: 1974 - 1976 (Trijonis, 1982a). P: based on photographic photometry data; N: based on nephelometry data; *: based on uncertain extrapolation of visibility frequency distribution. Note: All data are included with no restrictions on meteorology.*

A disturbing feature of Figure 24-21 is that the NPS visual ranges are generally about 1.2 to 2.0 times greater than corresponding airport visual ranges. This discrepancy can be explained by two known biases between the data sets:

1. The NPS data pertain to *standard* visual range, the case of an observer contrast threshold of 0.02 or a Koschmeider constant of 3.9. Human observer airport data apparently correspond to a Koschmeider constant of about 3.0, equivalent to a 0.05 contrast detection threshold (Tombach and Allard, 1983; Douglas and Young, 1945; Malm, 1979; Middleton, 1952). This accounts for a factor of about 1.3 difference.

2. The NPS data are generally taken at higher altitudes than the airport data because many national parks are located within mountainous terrain. For a given region, the tendency for extinction coefficient to decrease with altitude is evident in the NPS data as well as in airport data (Trijonis, 1982b). Some of the strongest discrepancies in Figure 24-21—Pinnacles National Monument on the central California coast and Crater Lake National Park in Oregon—are thought to be caused basically by altitude differences (Dietrich and Molinar, personal communication 1989).

Some of the discrepancy might also be explained by the difference in years: 1974 - 1976 for the airport data versus 1986 - 1988 for the NPS data. However, because long-term trends tend to be rather gradual (see Section 3.4), the differences due to long-term trends should be relatively minor. Both the NPS and airport data represent midday conditions and both include all types of weather conditions (*i.e.*, no restrictions on meteorology). The NPS data exclude conditions when the target is visible and covered by snow, but include conditions when the target is invisible but snow covered. This can produce a *downward bias* of median visibility at some western NPS sites. Sensitivity analyses indicate that, at the worst-case sites, this bias can be as much as 10 - 20% in the winter and spring (as much as 5 - 10% annually) (Dietrich and Molinar, personal communication 1989).

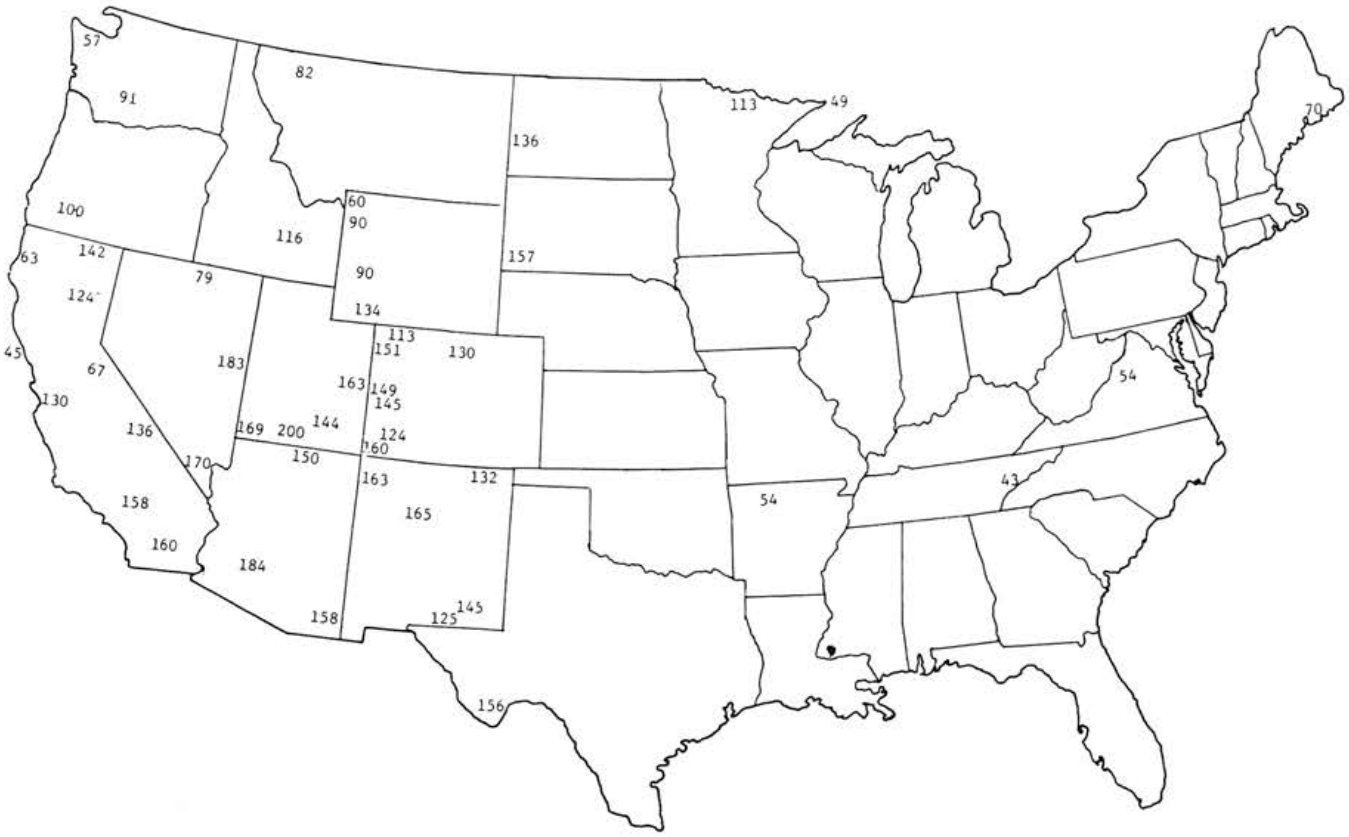


*Figure 24-21 Average of quarterly median range (km) for NPS automated camera sites. All data included except for observations of snow-covered targets. Quarterly medians are based on regressions fit to cumulative frequency data. (Air Resources Specialists, 1988; Dietrich and Molinar, personal communication 1989). See Appendix F for details.*

Figure 24-22 presents a map of median airport visibility at individual sites in the United States and Canada for the months of January and July during 1979 - 1983 (Husar, personal communication 1989). This map is not directly comparable to Figures 24-20 and 24-21 because it includes urban sites as well as rural sites (*e.g.*, note the unusually high western extinction values at Salt Lake City in Figure 24-22). Nonetheless, Figure 24-22 does confirm the strong dichotomy between the low visibilities of the eastern United States and the high visibilities of the mountainous/desert West.

This map further suggests that the only large region of the West with visibility as low as that found in the East is the region covered by the Los Angeles basin and the Central Valley of California (also see Trijonis, 1982b). Visibility in most of Canada appears to be fairly uniform and intermediate to the levels of the eastern United States and mountainous/desert western United States.

The above discussion has not yet answered the basic question: "What are typical annual levels of light extinction in the East and West?" A fairly consistent answer to this question is provided by four sources:

1. the review of field studies in Section 4.1
2. the literature review for the East by Mathai and Tombach (1987)
3. the extinction data sets published by Weiss (1980)
4. airport data sets used in conjunction with a 3.0 Koschmeider constant.

For the area of best visibility in the country—the desert Southwest—annual average extinction in rural areas is approximately 20 to 30 $Mm^{-1}$ (Trijonis, 1982a; Tombach *et al.*, 1987a; Lewis, personal communication 1989; also see various data sets in Section 4.1). For the area

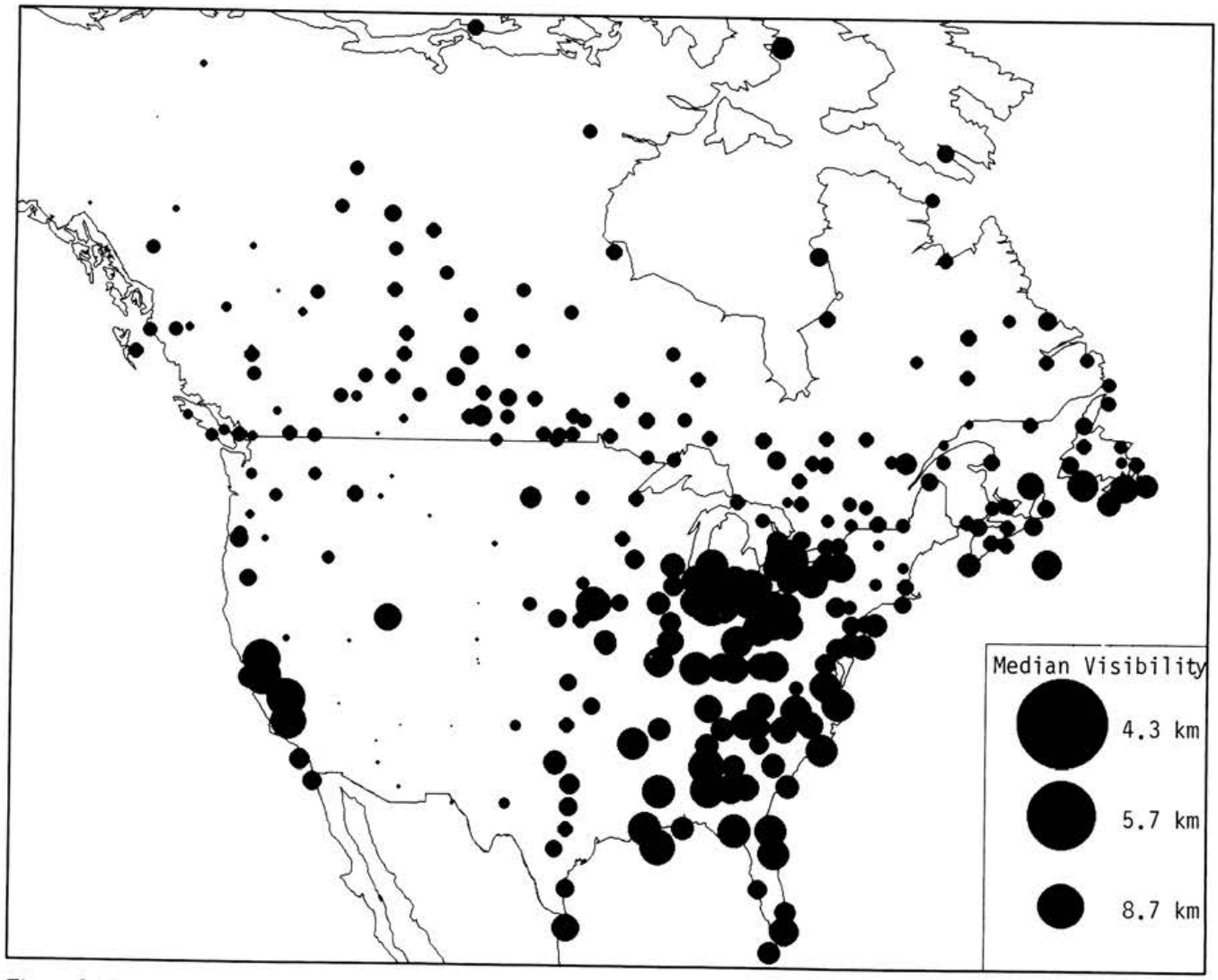


*Figure 24-22 Median airport visibilities at United States and Canadian stations averaged over January and July during 1979 - 1983 (Husar, personal communication 1989).*

south of the Great Lakes and east of the Mississippi (excluding the Appalachians), annual rural extinction is about 100 to 200 $Mm^{-1}$ (Trijonis, 1982a; Mathai and Tombach, 1987; also see data sets in Section 4.1).

The four data sources mentioned in the previous paragraph also provide extinction levels for several large urban centers. For large metropolitan areas in the East, average extinction is apparently on the order of 150 - 300 $Mm^{-1}$ (Trijonis and Yuan, 1978; Weiss, 1980; also see data sets in Section 4.1). This latter value is also typical of Los Angeles, but other large metropolitan areas of the West tend to exhibit extinction levels on the order of 50 - 200 $Mm^{-1}$ (Trijonis, 1979 & 1982b; Weiss, 1980; also see data sets in Section 4.1).

Figures 24-23a through 24-23f summarize geographical patterns in the National Park Service data for annual average particle concentrations. The figures include maps for fine mass, sulfur, elemental carbon, soil, remaining mass, and nonsulfate hydrogen (the latter two parameters might be qualitatively suggestive of spatial patterns for organic aerosols).[2] These figures, as well as the various rural data sets reported in Section 4.2 (Tables 24-13 and 24-15), support the following conclusions regarding the air quality dichotomy that exists between the rural West

[2] Note that the quality of the absorption data (Figure 24-23d) and nonsulfate hydrogen data (Figure 24-23f) are open to question.

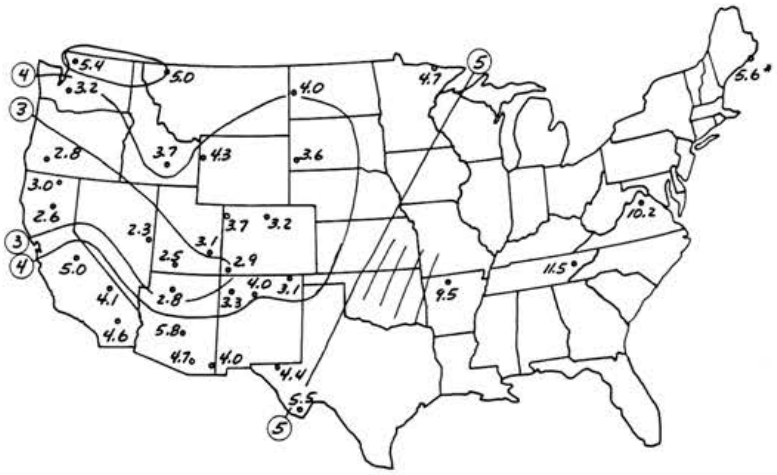


*Figure 24-23a Average concentrations of fine particle mass (μg/m³) from the NPS network, 1983 - 1986 (Eldred et al., 1987).*

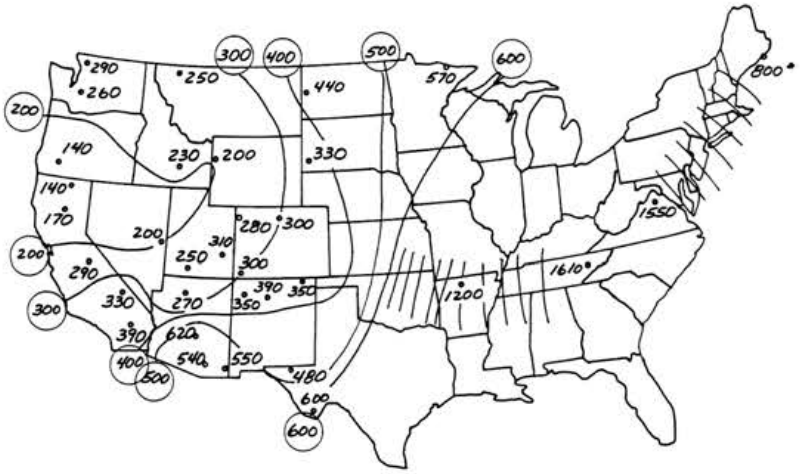


*Figure 24-23b Average concentration of fine particle sulfur (ng/m³) from the NPS network, 1983 - 1986 (Eldred et al., 1987).*

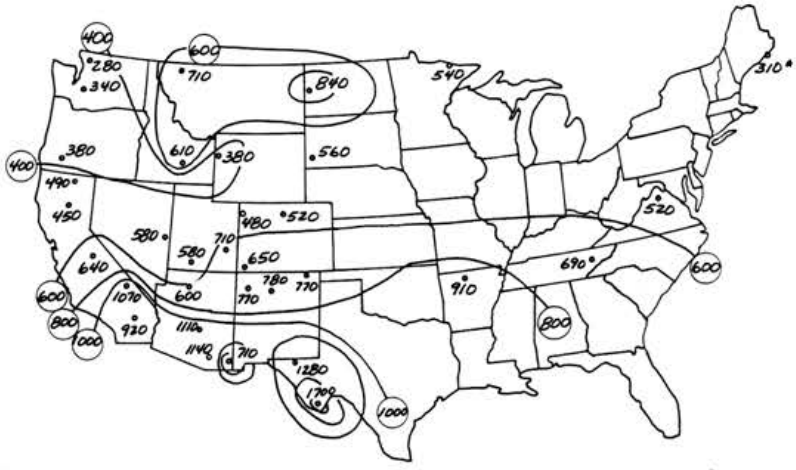


*Figure 24-23c Average concentration of fine particle soil (ng/m³) from the NPS network, 1983 - 1986 (Eldred et al., 1987).*

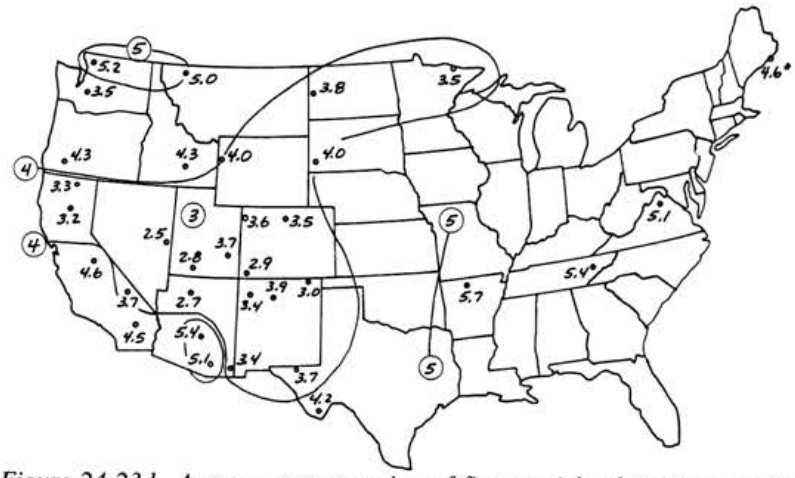


*Figure 24-23d Average concentration of fine particle absorption coefficient ($Mm^{-1}$) from the NPS network, 1983 - 1986 (Eldred et al., 1987).*

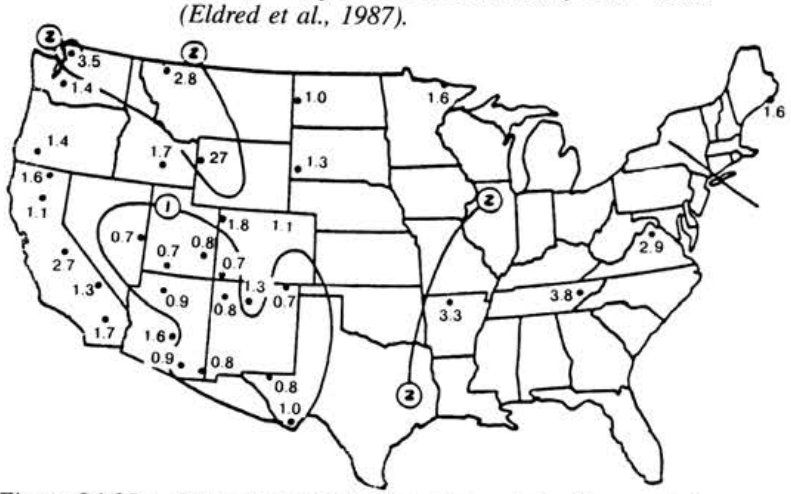


*Figure 24-23e Average concentration of remaining fine particle mass ($\mu g/m^3$) from the NPS network, 1983 - 1986 (Eldred et al., 1987).*

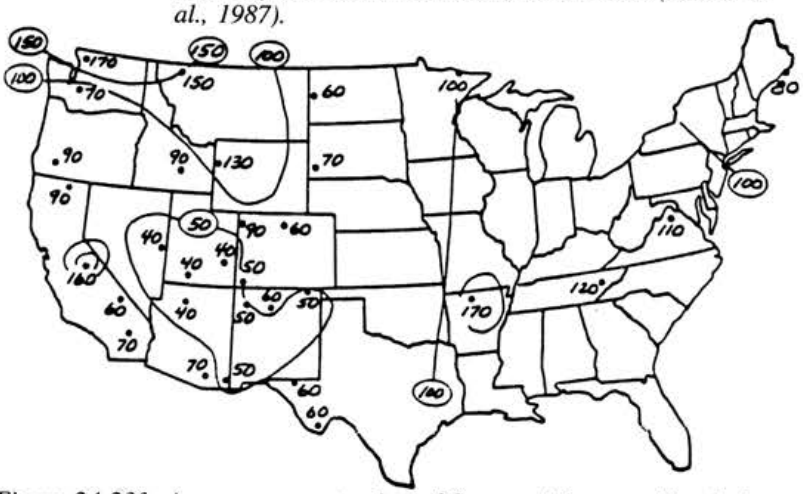


*Figure 24-23f Average concentration of fine particle nonsulfate hydrogen ($ng/m^3$) from the NPS network, 1983 - 1986 (Eldred et al., 1987).*

(specifically the desert/mountain Southwest) and the rural East (specifically the area south of the Great Lakes and east of the Mississippi):

- Sulfate concentrations are a factor of about six higher in the rural East than in the rural West.
- Organic aerosols and elemental carbon are both about a factor of two higher in the rural East. (Note that this conclusion also agrees with the data for 19 rural sites reported by Shah *et al.*, 1986).
- Fine nitrate aerosols (presumably ammonium nitrate) and fine soil aerosols are about the same in the rural East and West. (For nitrates, the concentration is about 0.5 to 1.0 $\mu g/m^3$; see discussion of denuder nitrate data in Section 4.2 and Appendix E.)

It is of interest to relate the East-West aerosol differences to the East-West visibility dichotomy. As noted earlier, light extinction levels are about a factor of six higher in the rural East than the rural West. This visibility difference is mostly due to the greater sulfate concentrations in the East which interact with the higher humidity of the East to produce dense sulfate-water hazes. Based on the extinction budget analysis of Section 4.4, one can conclude that—of the 500% increase in extinction for the East relative to the West—about 300% is due to the increased contribution from sulfates.

### 3.3.2 Seasonal Patterns

Three sets of results are currently available showing seasonal visibility patterns on a national basis. The first consists of quarterly medians of the NPS automated camera data for 1986-1988 (see listing in Appendix F). The second involves quarterly averages[3] of United States airport data for 1975 - 1983, reported as part of the historical trend analysis in Section 3.4 (see later Figure 24-30; Husar, personal communication 1989). The third, also by Husar (personal communication 1989), involves January and July averages at United States and Canadian airports from 1979 to 1983 (see Figures 24-24a and 24-24b).

Examining all three data sets reveals only one extremely strong seasonal feature occurring on the large geographical scale—the summertime maximum in extinction coefficient (minimum in visibility) over the region south of the Great Lakes and east of the Mississippi. Figure 24-25 illustrates the seasonal pattern in median light extinction

[3] Note that the NPS seasonal quarters are winter (Dec - Feb), spring (Mar - May), summer (Jun - Aug), and fall (Sep - Nov). On the other hand, the airport data in Section 3.4 pertain to calendar quarters—winter (Jan - Mar), etc.

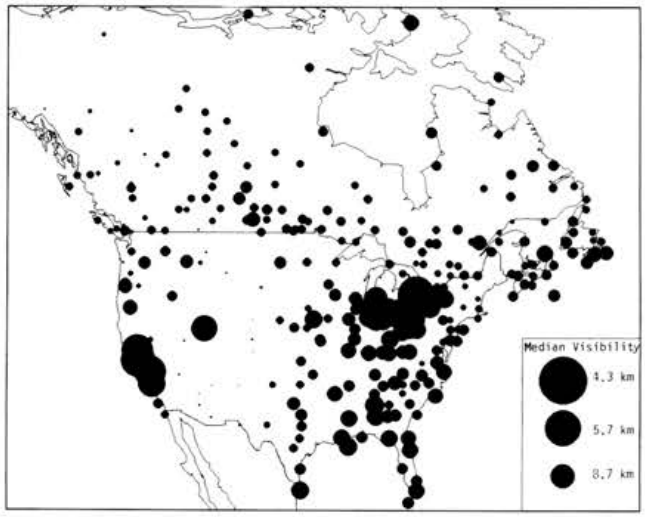


*Figure 24-24a Median airport visibilities for January, averaged over 1979 - 1983 (Husar, personal communication 1989).*

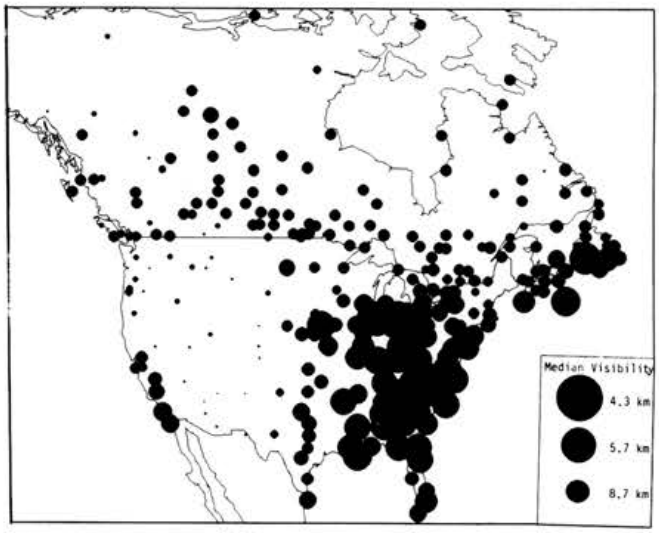


*Figure 24-24b Median airport visibilities for July, averaged over 1979 - 1983 (Husar, personal communication 1989).*

for the two NPS sites in this region. The summertime peak is very obvious. Figure 24-26 shows median airport visibilities during the summer at suburban/nonurban locations for the mid-1970's (Trijonis, 1982a). Comparing this map to the annual data in Figure 24-20, it is apparent that summertime visibility is significantly lower than annual visibility throughout the eastern region in question.

The predominant cause of the summertime haze peak in the East is the summertime maximum in sulfate concen-

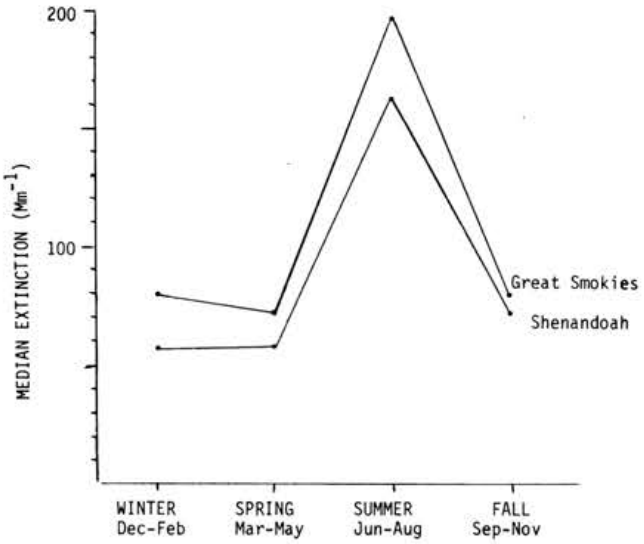


*Figure 24-25 Seasonal pattern in median light extinction at two eastern NPS automated camera sites, 1986 - 1988.*

trations. The NPS aerosol data show that sulfates (the major cause of light extinction in the East; see Section 4) are nearly twice as high in the summer as during the remainder of the year. Figure 24-27 shows seasonal patterns in other data sets for extinction, fine particle mass, and sulfates (Trijonis, 1982a).

None of the three sets of currently available results are adequate for a definitive analysis of the more subtle seasonal visibility patterns in New England, Canada, and the western two-thirds of the United States. The NPS data involve biases due to treatment of days when targets are snow covered (see earlier discussion).[4] The airport results by Husar are problematic in the West (due to lack of sufficiently distant targets at some sites and due to limited resolution in the reported results) and are sometimes restricted to only two months (January and July). A definitive analysis must await revised analysis of the NPS camera data and airport visibility data or, better yet, analysis of the transmissometer data from the new NPS monitoring system.

Not withstanding these limitations, a few patterns do seem to emerge. For example, it is well established that there is a summertime visibility minimum in Arizona and southern California (Trijonis, 1982b; Trijonis *et al.*, 1988; Dietrich and Molinar, personal communication 1989; Husar, personal communication 1989; Lewis, personal communication 1989). Minimum visibility occurs during the fall and winter in the northern two-thirds of Cali-

[4] Note that correcting for any bias could make the summer peak in Figure 24-25 all the stronger.

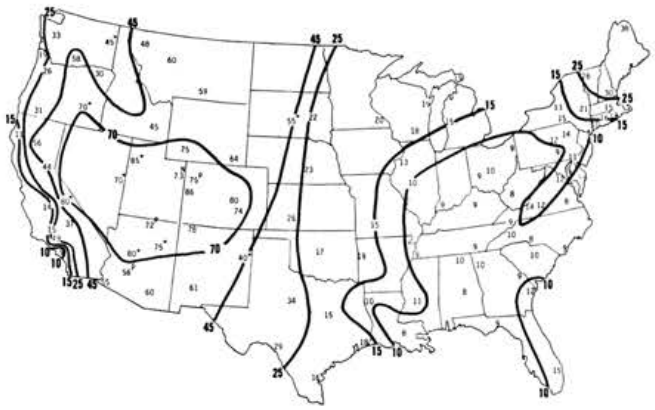

*Figure 24-26 Summertime median midday range (in miles) at suburban/nonurban airports in the United States, 1974 - 1976 (Trijonis, 1982a). P: based on photographic photometry data; N: based on nephelometry data; *: based on uncertain extrapolation of visibility frequency distribution. Note: All data are included with no restrictions on meteorology.*

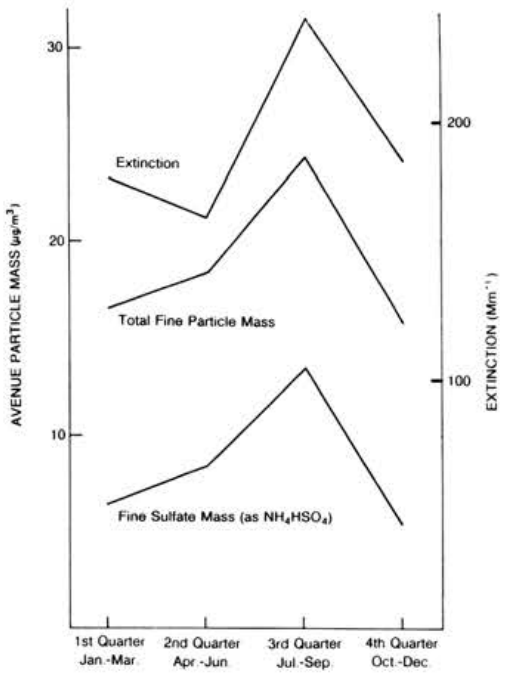


*Figure 24-27 The seasonal patterns in sulfates, fine particle mass, and light extinction for rural areas of the eastern United States (Trijonis, 1982). Note: Fine particle mass and fine sulfate mass data are averages over five rural EPA dichotomous sampler sites (Will cty, IL; Jersey cty, IL; Monroe cty, IL; Erie cty, NY; and Durham cty, NC). The light extinction data are estimated from seasonal median visibilities (using a Koschmeider constant of 3.0) at eight rural airports.*

fornia, the Pacific Northwest, and the northern mountain states (Trijonis, 1982b; Dietrich and Molinar, personal communication 1989; Husar, personal communication 1989). The winter/fall visibility minimum is especially strong in the central valley of California (Trijonis, 1982b; Husar, personal communication 1989; see Figures 24-24a and 24-24b).

Figures 24-28a through 24-28e illustrate national geographical patterns on a seasonal basis for fine mass, sulfur, elemental carbon, soil, and remaining mass. The most obvious seasonal feature for both fine mass and sulfur is the summer peak in the East. Fine mass and sulfur tend to peak during the summer in many parts of the country, but the summer maximum is especially strong in the East. Elemental carbon does not display very strong seasonality. Fine soil, a small component of light extinction (see Section 4), is greatest in the summer and spring nationwide. Remaining mass—possibly a reflection of organic aerosols—tends to peak in the summer at most locations.

### 3.3.3 Statistical Distribution of Visibility

So far in this section, annual and seasonal visibility levels have been expressed in terms of "typical" values, *i.e.* averages or medians. It is also of interest to examine the statistical distribution of visibility, especially with respect to worst-case values (greatest light extinction levels). A comprehensive study of the statistical distribution of worst-case visibility levels was conducted by Gins *et al.* (1981) using midday observations from 28 carefully selected airports. Gins *et al.* sorted the data for meteorology—eliminating midday observations with fog, precipitation, blowing clouds, etc.—and used appropriate methods for estimating percentiles from airport-type data. They applied three statistical methods to relate worst-case percentiles to media values:

1. frequency distribution functions (exponential, Weibull, lognormal, and gamma),
2. regression models, and
3. observed ratios of upper percentiles to medians.

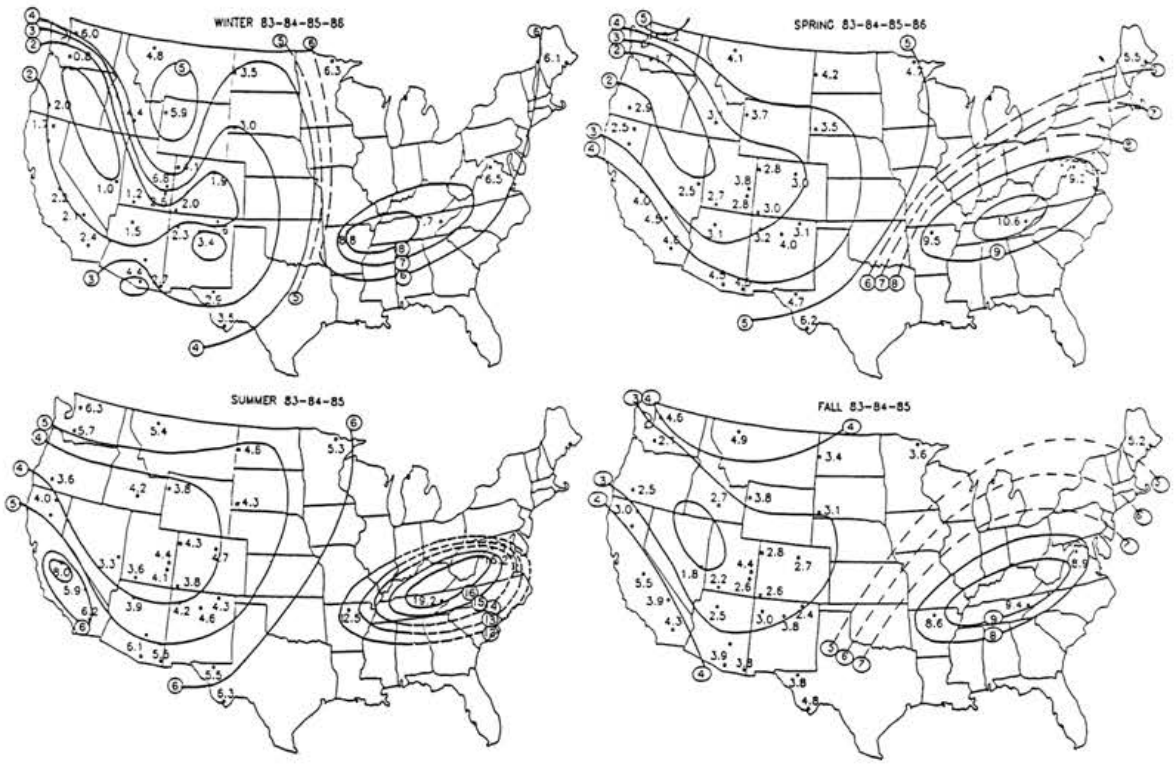


*Figure 24-28a Geographical patterns in aerosol concentrations by season—fine mass (μg/m³) (Eldred et al., 1987; Eldred, personal communication 1989).*

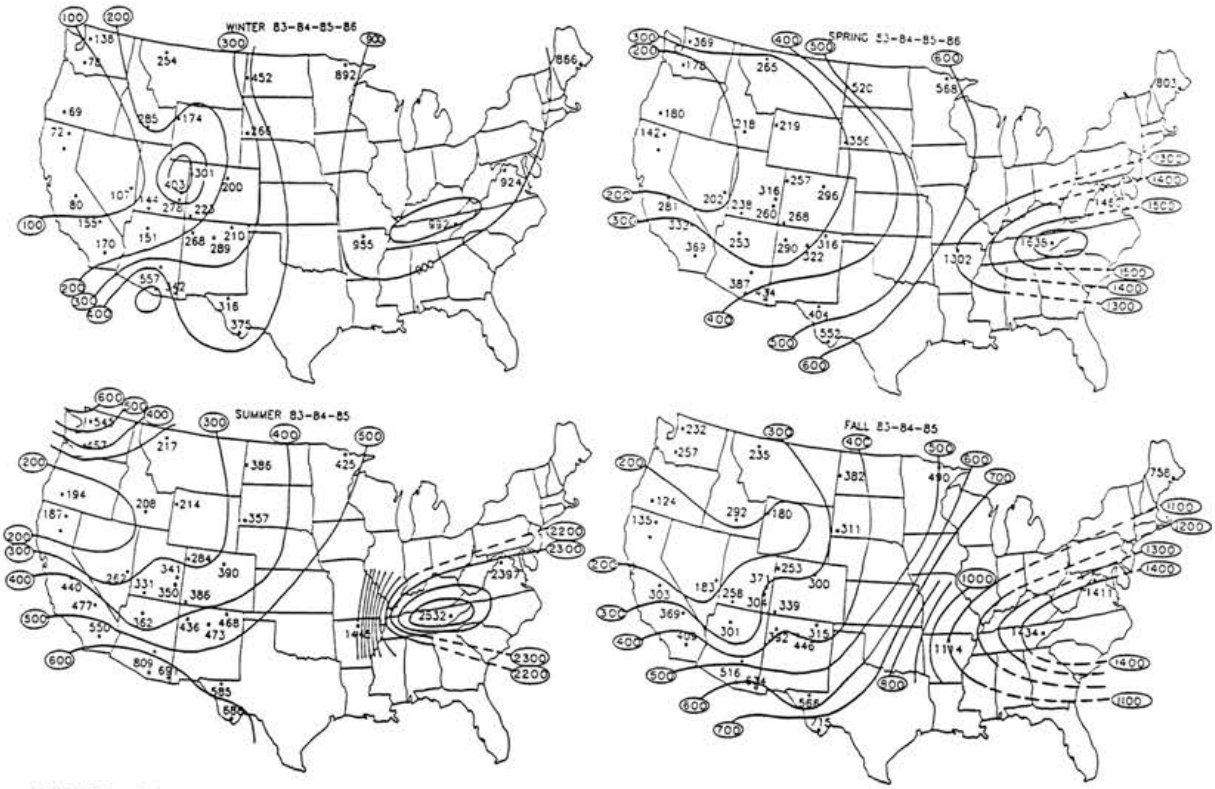


*Figure 24-28b Geographical patterns in aerosol concentrations by season—fine sulfur (ng/m³) (Eldred et al., 1987; Eldred, personal communication 1989).*

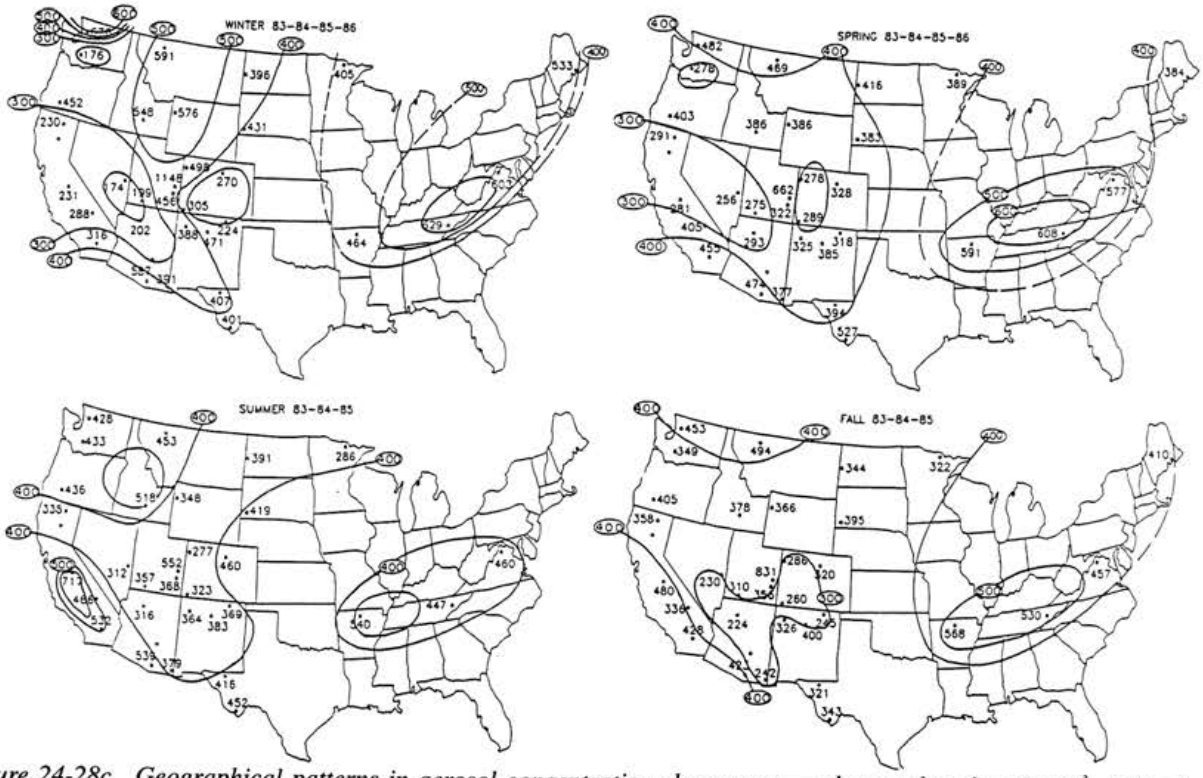


*Figure 24-28c Geographical patterns in aerosol concentrations by season — elemental carbon (ng/m³) (Eldred et al., 1987; Eldred, personal communication 1989).*

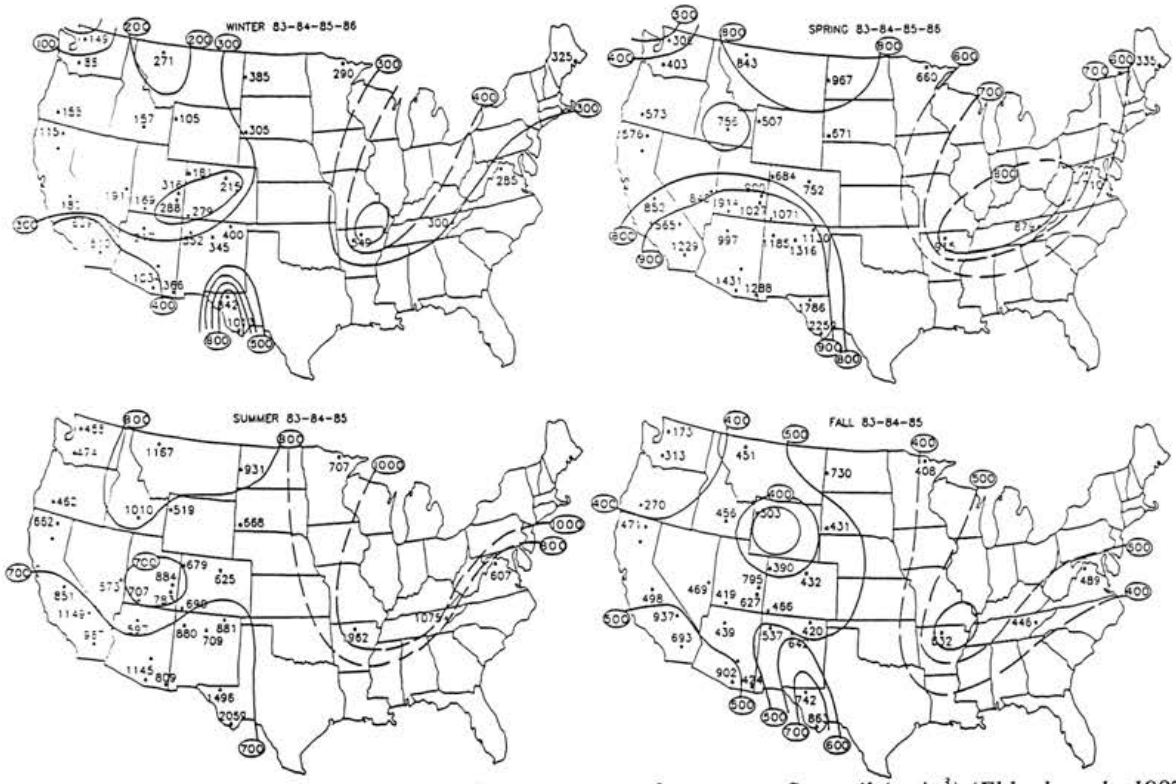


*Figure 24-28d Geographical patterns in aerosol concentrations by season—fine soil (ng/m³) (Eldred et al., 1987; Eldred, personal communication 1989).*

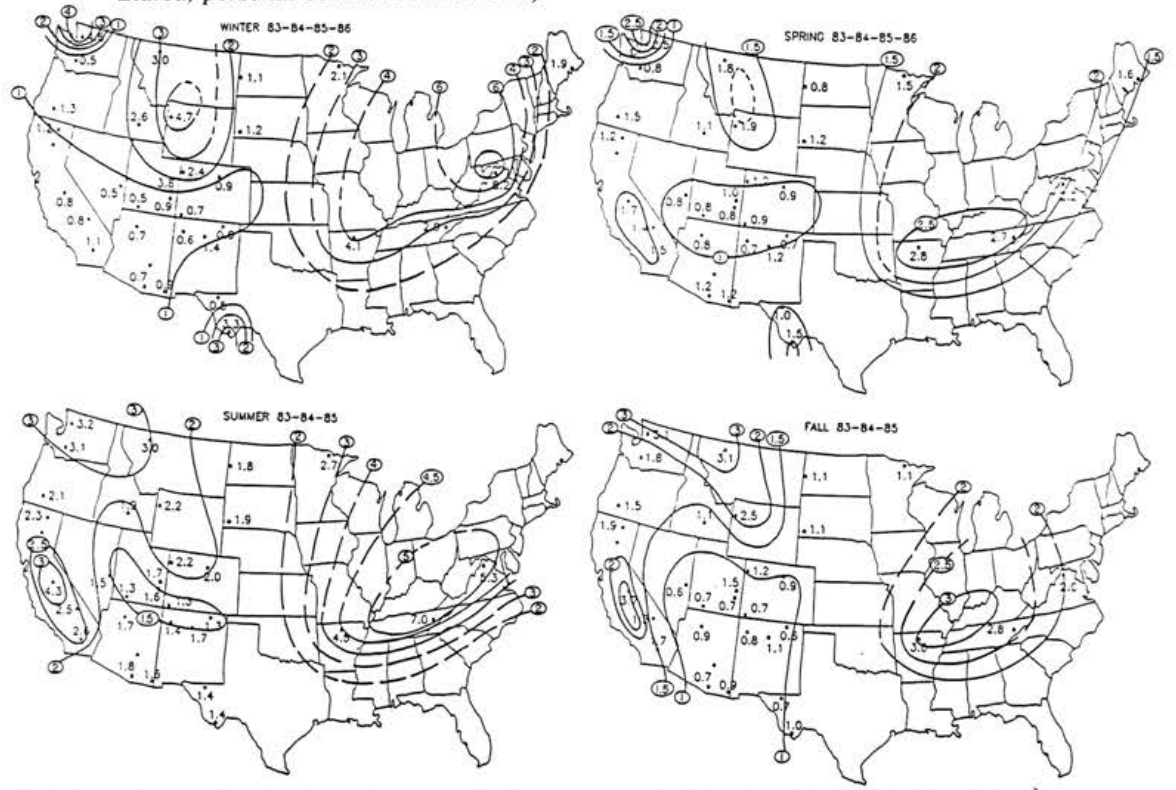


*Figure 24-28e Geographical patterns in aerosol concentrations by season—remaining mass (μg/m³) (Eldred et al., 1987; Eldred, personal communication 1989).*

Concluding that a simple ratio model was adequate, they characterized the relationship between worst-case and median extinction levels according to the ratios. Table 24-8 summarizes their results for various percentiles (90th to 99th), four regions of the country, and the four calendrical quarters.

Table 24-8 shows that median extinction levels are less than 99th percentiles by a factor of about 3.5 to 7; less than 95th percentiles by a factor of 2.5 to 4; and less than 90th percentiles by a factor of 2 to 3. This last factor (2 to 3) can be compared to the results of other studies because several researchers have published median and 90th percentile values. Among ll WRAQS sites in the West, Tombach *et al.* (1987a) reported ratios of 1.5 to 2 based on nephelometry data; 1 to 6 based on human observer data; and a range of two to greater than ten based on teleradiometer data. Among 44 NPS automated camera sites in the West, Air Resources Specialists (1988) and Dietrich and Molinar (personal communication 1989) found 90th/50th percentile extinction ratios of 1.5 to 2.5. Based on airport data using four readings per day and no meteorological sorting—Trijonis (1979) derived ratios of 1.5 to 4 for 17 western sites. For the East, Air Resources Specialists (1988) and Dietrich and Molinar (1989 personal communication) reported ratios of 2 to 3 among six NPS camera sites, while Trijonis and Yuan (1978) found ratios of 2.5 to 4.5 for 12 airport data sets.

Some of the results in the last paragraph indicate a greater variability in the 90th/50th percentile ratio than suggested by Table 24-8. This is partly due to the fact that Table 24-8 includes only one type of measurement (airport observations) and represents averages over groups of sites. Gins *et al.* (1981), in fact, noted significant variability in the ratios from site to site.

If one is interested in the statistical distribution of visibility at a particular site and not in the average statistical distribution for a large region, it evidently is important to collect site specific data. Also, in the future, it will be of interest to characterize statistical distributions using the newer and more accurate instrumental methods for measuring extinction.

The ratios in Table 24-8 can be considered as representing the "episodicity" of light extinction (haze) levels. It is interesting to note that the East has the highest episodicity, and that annual episodicity in the East is greater than episodicity within individual seasons. This partly reflects the strong seasonality of light extinction levels in the East (*i.e.*, the strong summertime maximum in haziness contributes to the annual episodicity). Another interesting feature is that episodicity in the East is stronger in the summer than in the winter. This means that the seasonal pattern in the East (*i.e.* the summertime peak) is even stronger for worst-case conditions than it is for average conditions. A similar situation may exist at many Western sites which tend to exhibit highest average extinction levels in the winter (see Section 3.2) as well as highest episodicity in the winter (see Table 24-8).

## 3.4 HISTORICAL VISIBILITY TRENDS

*R. Husar*

### 3.4.1 Visibility Trend Data Base

The visibility trend data consist of prevailing visibility measurements at 137 United States sites (basically airports) for which records exist since about 1948. A problem with airport visibility measurements is that there is always a furthest marker beyond which the visual range is not resolved. This translates to a lower threshold value or truncation for the distribution of the computed extinction coefficient. For this reason, nonparametric statistical indices such as percentiles of data are more useful. The 25th, 50th, 75th, and 90th percentiles of the extinction coeffficient were calculated monthly for each station to yield the trend data set.

The utility of the computed percentile values is demonstrated in Figure 24-29. For Souix City, IA, the trend graph shows that the threshold extinction coefficient dropped from 160 to 80 $Mm^{-1}$ in 1968. Since the 50th percentile was originally near the high initial threshold, the median would drop at that time. The 90th percentile, however, appears to be a robust reliable measure which is above the threshold influence; it indicates an increase in extinction over the period. Thus, depending on whether one follows the 50th or 90th percentiles, one would arrive at opposite conclusions about the trend. In the data set presented below, the percentile trends for each location were examined for such anomalous behavior. Stations in the West are most affected by reporting thresholds. For locations east of the Mississippi, the 75th percentile was almost always above the threshold.

The extinction coefficient is calculated by eliminating data obtained during fog and precipitation and by using a Koschmeider constant of 3.9. This value may not be appropriate for airport data, but any correction would just involve a constant and would not affect patterns and trends. Extinction coefficient, rather than visual range, is used to facilitate comparisons with emission trends. Also, in the discussion, the term haziness is used interchangeably with extinction coefficient.

### 3.4.2 Visibility Trend Maps

A summary of haze trend patterns is given in Figure 24-30. The specific parameter that is plotted is the 75th percentile. While this is unconventional, it constitutes a

*Table 24-8. Average Ratios of Selected Percentiles to the Median for Extinction Coefficients: 1974 - 1976 (Gins et al., 1981)*

| Period | Percentile | National | Pacific | Rocky Mountain | Central | Eastern |
|---|---|---|---|---|---|---|
| Annual | 90 | 2.40 | 2.50 | 2.25 | 2.04 | 2.85 |
| | 91 | 2.51 | 2.64 | 2.37 | 2.11 | 2.96 |
| | 92 | 2.63 | 2.80 | 2.50 | 2.18 | 3.08 |
| | 93 | 2.77 | 3.01 | 2.65 | 2.27 | 3.22 |
| | 94 | 2.95 | 3.26 | 2.82 | 2.36 | 3.40 |
| | 95 | 3.15 | 3.56 | 3.03 | 2.48 | 3.60 |
| | 96 | 3.41 | 3.94 | 3.33 | 2.62 | 3.84 |
| | 97 | 3.79 | 4.49 | 3.79 | 2.81 | 4.16 |
| | 98 | 4.39 | 5.25 | 4.49 | 3.08 | 4.85 |
| | 99 | 5.43 | 6.50 | 5.88 | 3.60 | 5.83 |
| Jan-Mar | 90 | 2.51 | 2.70 | 3.01 | 1.99 | 2.32 |
| | 91 | 2.62 | 2.80 | 3.15 | 2.06 | 2.41 |
| | 92 | 2.73 | 2.92 | 3.30 | 2.13 | 2.50 |
| | 93 | 2.86 | 3.05 | 3.50 | 2.21 | 2.60 |
| | 94 | 3.02 | 3.25 | 3.74 | 2.30 | 2.71 |
| | 95 | 3.22 | 3.50 | 4.03 | 2.40 | 2.88 |
| | 96 | 3.49 | 3.82 | 4.44 | 2.51 | 3.10 |
| | 97 | 3.91 | 4.38 | 5.12 | 2.66 | 3.37 |
| | 98 | 4.51 | 5.07 | 6.17 | 2.87 | 3.80 |
| | 99 | 5.57 | 6.34 | 7.74 | 3.57 | 4.45 |
| Apr-Jun | 90 | 2.27 | 2.02 | 2.15 | 2.17 | 2.74 |
| | 91 | 2.36 | 2.07 | 2.25 | 2.24 | 2.85 |
| | 92 | 2.45 | 2.12 | 2.36 | 2.33 | 2.96 |
| | 93 | 2.56 | 2.19 | 2.50 | 2.42 | 3.09 |
| | 94 | 2.69 | 2.27 | 2.65 | 2.54 | 3.25 |
| | 95 | 2.85 | 2.36 | 2.84 | 2.67 | 3.44 |
| | 96 | 3.04 | 2.48 | 3.09 | 2.84 | 3.65 |
| | 97 | 3.28 | 2.62 | 3.45 | 3.00 | 3.94 |
| | 98 | 3.67 | 2.81 | 3.87 | 3.27 | 4.47 |
| | 99 | 4.42 | 3.14 | 5.24 | 3.80 | 5.21 |
| Jul-Sep | 90 | 2.18 | 2.05 | 1.81 | 2.08 | 2.81 |
| | 91 | 2.26 | 2.13 | 1.89 | 2.16 | 2.91 |
| | 92 | 2.35 | 2.21 | 1.97 | 2.24 | 3.01 |
| | 93 | 2.46 | 2.31 | 2.05 | 2.33 | 3.17 |
| | 94 | 2.59 | 2.43 | 2.16 | 2.43 | 3.37 |
| | 95 | 2.75 | 2.56 | 2.30 | 2.56 | 3.61 |
| | 96 | 2.94 | 2.71 | 2.46 | 2.72 | 3.89 |
| | 97 | 3.16 | 2.87 | 2.66 | 2.90 | 4.23 |
| | 98 | 3.47 | 3.08 | 3.01 | 3.13 | 4.67 |
| | 99 | 4.04 | 3.44 | 3.67 | 3.50 | 5.51 |
| Oct-Dec | 90 | 2.54 | 3.17 | 2.68 | 1.89 | 2.47 |
| | 91 | 2.64 | 3.32 | 2.81 | 1.95 | 2.56 |
| | 92 | 2.76 | 3.49 | 2.96 | 2.00 | 2.66 |
| | 93 | 2.89 | 3.68 | 3.14 | 2.07 | 2.76 |
| | 94 | 3.05 | 3.92 | 3.35 | 2.14 | 2.88 |
| | 95 | 3.23 | 4.18 | 3.60 | 2.22 | 3.01 |
| | 96 | 3.47 | 4.51 | 3.97 | 2.30 | 3.18 |
| | 97 | 3.88 | 4.97 | 4.77 | 2.41 | 3.40 |
| | 98 | 4.45 | 5.50 | 5.91 | 2.56 | 3.79 |
| | 99 | 5.46 | 6.45 | 7.86 | 2.85 | 4.49 |

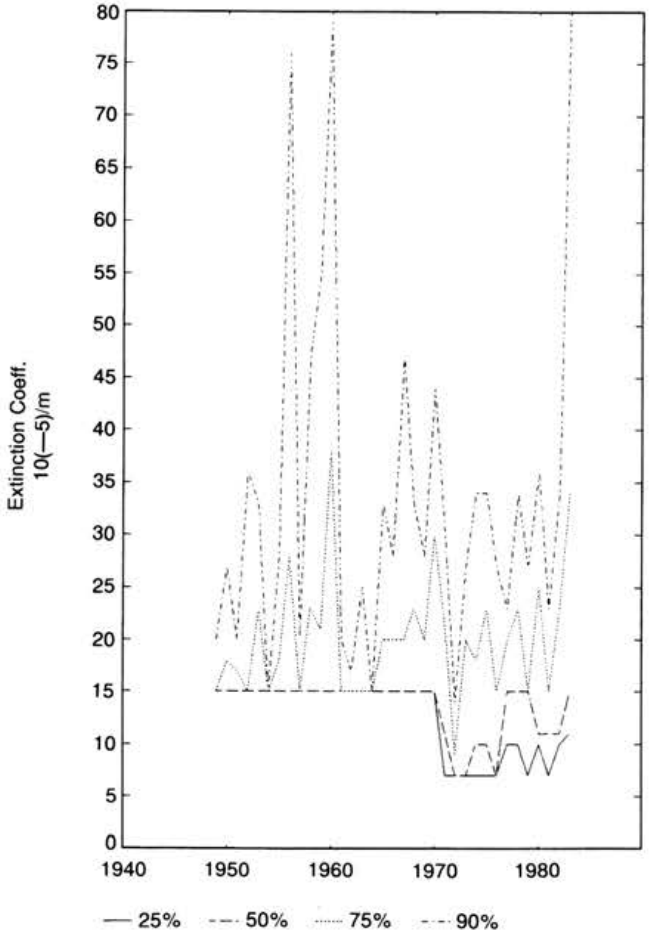


*Figure 24-29 Trends of percentiles of extinction coefficient at Sioux City, IA.*

safer approach than plotting the 50th percentile because it does not require any extrapolations or other adjustments to the data. The 16 maps represent four time periods and four seasons. The selected time periods are centered around 1950, 1960, 1970, and 1980, while the four calendrical quarters are January - March, April - June, July - September, and October - December.

The first quarter haziness, shown in the top row of maps, demonstrates that the worst visibility is in the area surrounding the Great Lakes, while the best visibility is in Arizona and New Mexico. There is evidence of declining overall winter visibility in the Gulf states. The visibility over the California-Oregon coast became worse up through the 1950's and 1960's, but evidently improved somewhat in the 1970's.

In the second quarter, a significant increase in extinction coefficient is exhibited over the United States east of the Rockies. Around 1950, the low visibility region was confined to the Ohio and Mississippi valleys. By the 1980's, much of the eastern United States was covered with springtime haze.

The most significant changes are noted for the third quarter (Munn, 1973; Trijonis and Yuan, 1978; Husar *et al.*, 1981; Husar, 1986 and 1988; Sloane, 1982a, 1982b, 1983b, and 1984b; Trijonis, 1982a). The visibility in the southeastern states (south of the Ohio River) showed the most significant decline.

Fourth quarter haziness exhibits a pattern similar to the first quarter, both qualitatively and quantitively. The outstanding feature is the poor visibility over the west coast states and those surrounding the Great Lakes. It is also interesting to note the decline of haziness in the Great Lakes region and the increase over the southeastern states.

The above regional changes in haziness are enlightening in that broad regions, such as the northeast and southwest, show coherent trends. However, the trends are significantly different between the northeast and southeast. In order to emphasize this difference, regional and seasonal trends are displayed in Figure 24-31. This figure shows the aggregate for the Northeast (including Indiana, Ohio, Pennsylvania, New York, Kentucky, West Virginia, and New England) compared to the aggregate for the Southeast (states south of the Ohio River and east of the Mississippi). In the Northeast, winter haze shows a 25% decline, while in the Southeast, there is a 40% increase. The summer haziness in the industrialized Northeast shows an increase up to the mid-1970's followed by a decline since. In the southeastern states, on the other hand, there is an 80% increase in summer haziness occurring mainly in the 1950's and 1960's.

Figure 24-32 compares the annual haze trends for the Northeast and Southeast. In the Northeast, there is virtually no change in the annual haziness, but the Southeast shows a 60% increase over the 35 year monitoring period. The annual haziness for the entire eastern United States shows a 25% increase over the period of record, with most of the change occurring in the 1950's and 1960's and no significant trend since about 1970. It is evident that averaging the haze data over the entire eastern United States and over the entire year obscures significant regional and seasonal differences.

### 3.4.3 Regional/Local Visibility Trends

As discussed in Section 3.3.1, visibility in large metropolitan areas is generally lower than the surrounding regional background. The difference depends on the size of and location of urban/industrial area, the season, and the decade of observation (Trijonis, 1982a).

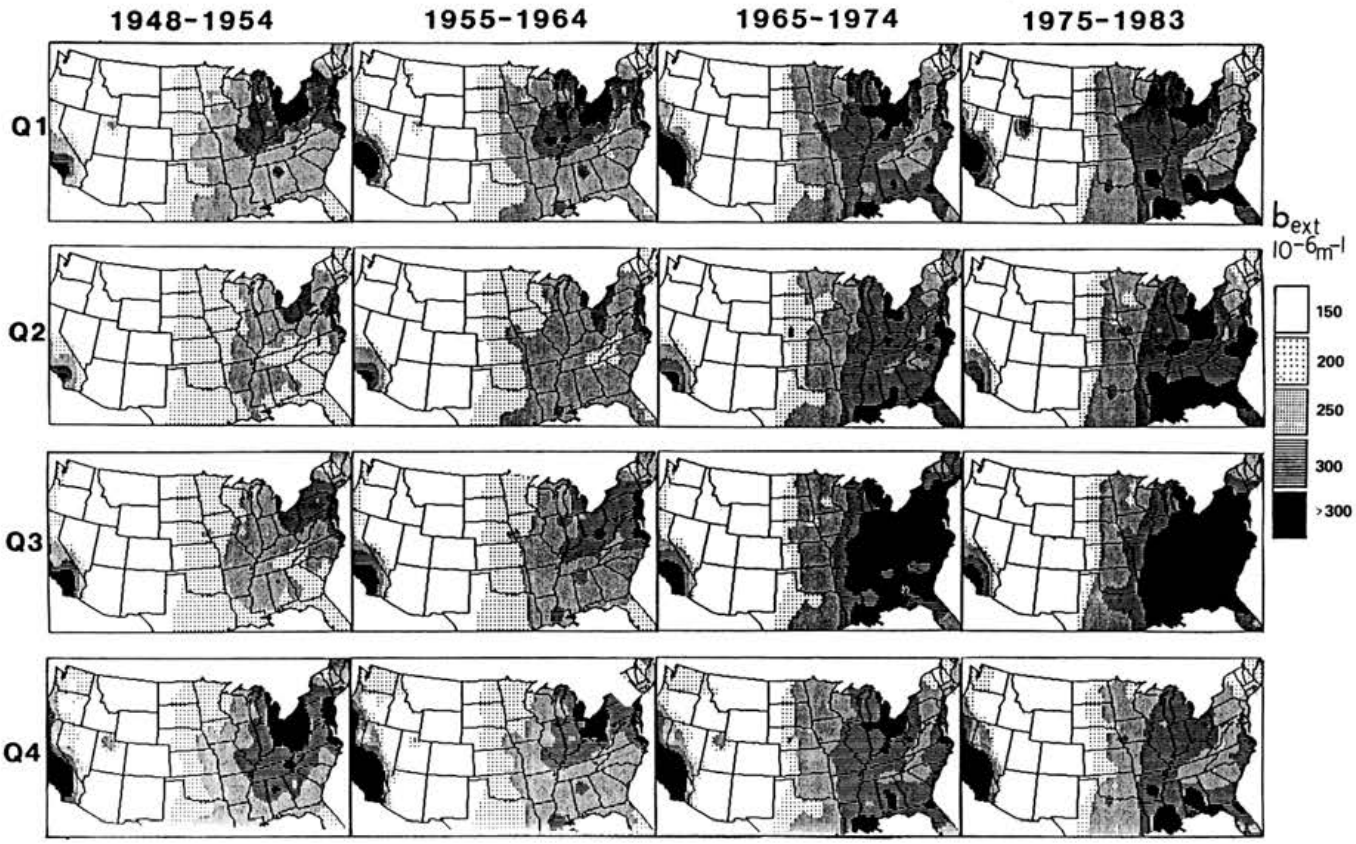


*Figure 24-30 United States trend maps for the 75th percentile extinction coefficient (derived from air visual range data) for the calendrical quarters: winter (Q1), spring (Q2), summer (Q3), and fall (Q4).*

Figures 24-33a and 24-33b illustrate the regional/local trend of extinction coefficient (75th percentile) at four locations in the vicinity of New York City (Newark, NJ; New York JFK, NY; New York La Guardia, NY; and Providence, RI). In the winter season (Figure 24-33a), La Guardia airport shows the highest haziness and Providence the lowest. A downward trend can be observed for each site. It is evident that the difference between the sites was highest in the 1950's and 1960's and diminished by the 1980's. The large differences in winter visibility among these nearby sites prior to 1970 suggest strong local influences that have diminished after the 1970's. Evidently, the winter haze became more regional in character.

The summertime haze trend for the above sites shows an upward trend in the 1950's and 1960's and a decrease since then. Historically, the summertime difference in extinction coefficient between the sites is less pronounced than in the winter. Evidently, the summertime haziness has been regional in character since the 1940's. This might be attributed to more intense atmospheric mixing in the summer.

### 3.4.4 Historical Relationship Between $SO_x$ Emissions and Visibility

Because sulfates are currently the major contributor to light extinction in the east, it is of interest to compare visibility trends in the east to sulfur oxide emission trends. The comparison should be separated by northeast versus southeast and winter versus summer in light of the strong regional and seasonal differences discussed previously.

The emission trends for the comparison base have been compiled by Husar (1988) using the historical yearly emission data by Gschwandtner *et al.* (1985) and Husar (1986) as well as the historical monthly emission data by Knudson (1985). Figures 24-34a and 24-34b illustrate the historical emission trends (by region and season) since 1860. The emissions are expressed as million tons of

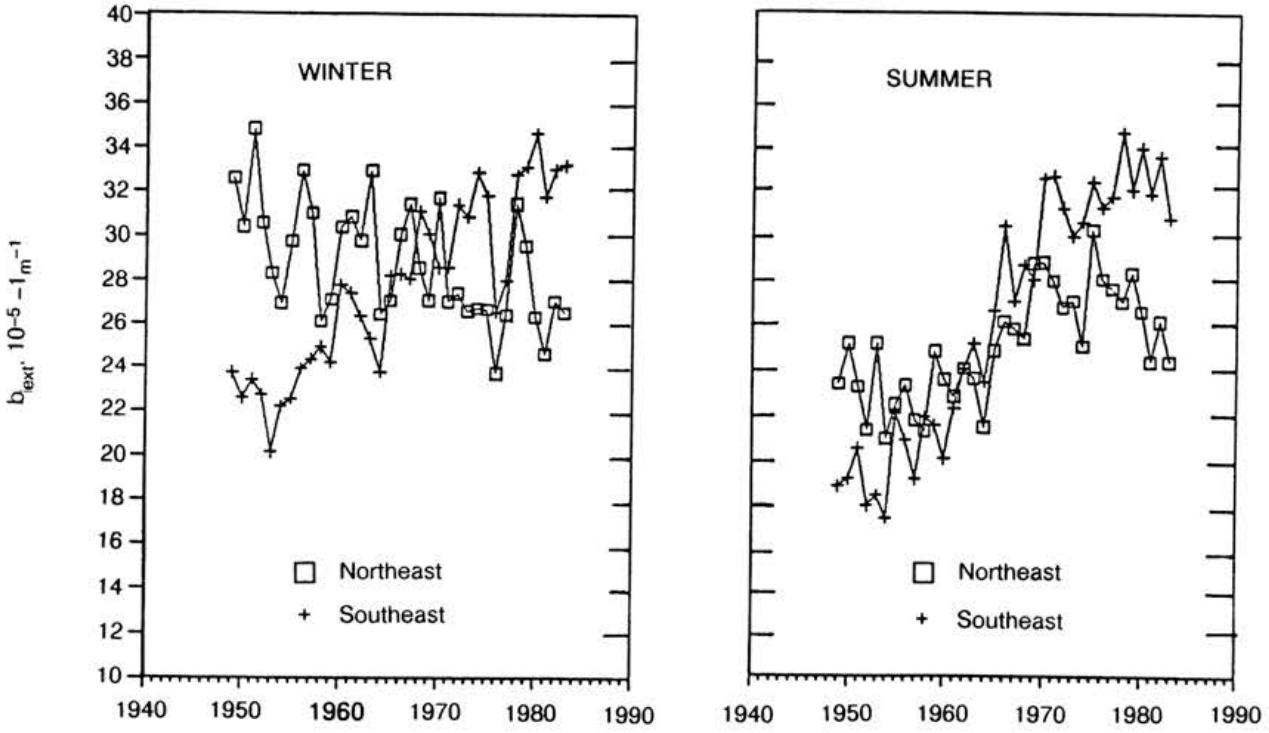


*Figure 24-31 Trends of winter and summer 75th percentile extinction coefficient for the Northeast and for the Southeast.*

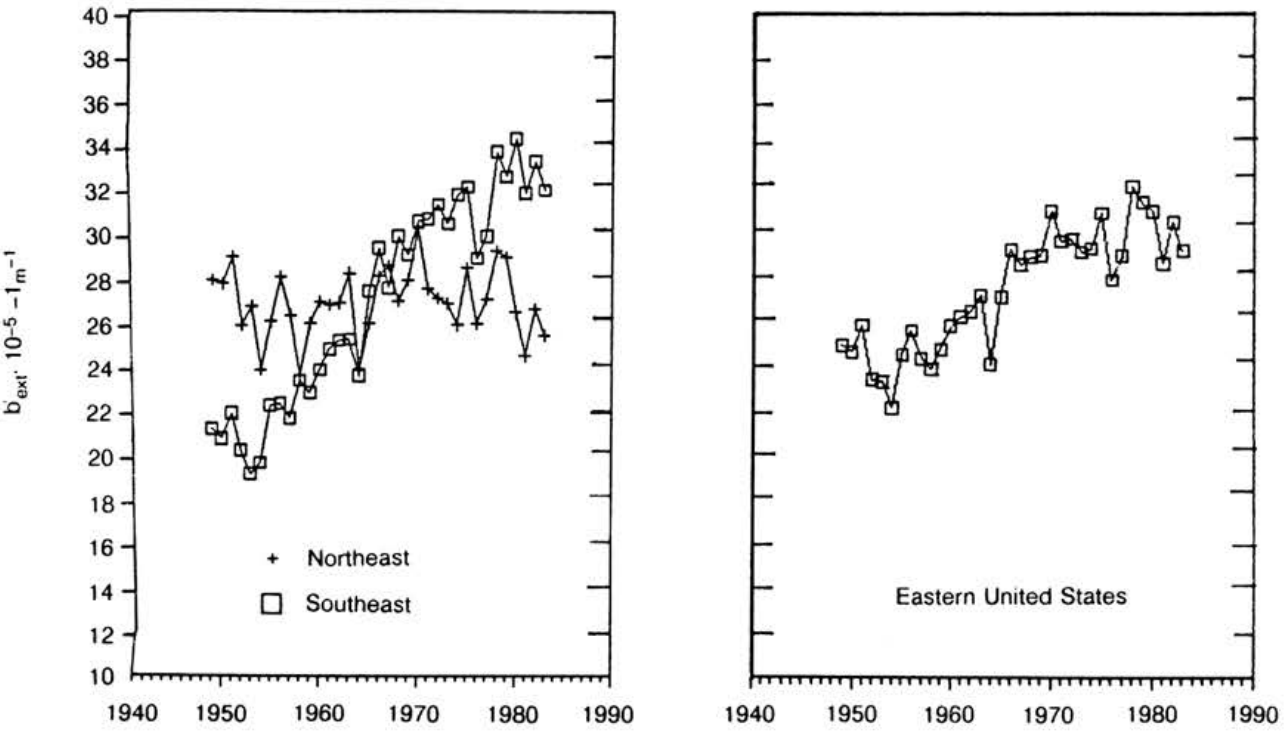


*Figure 24-32 Trends of annual 75th percentile extinction coefficient for the Northeast and the Southeast. The right-hand graph shows the annual average haze trend for the entire eastern United States.*

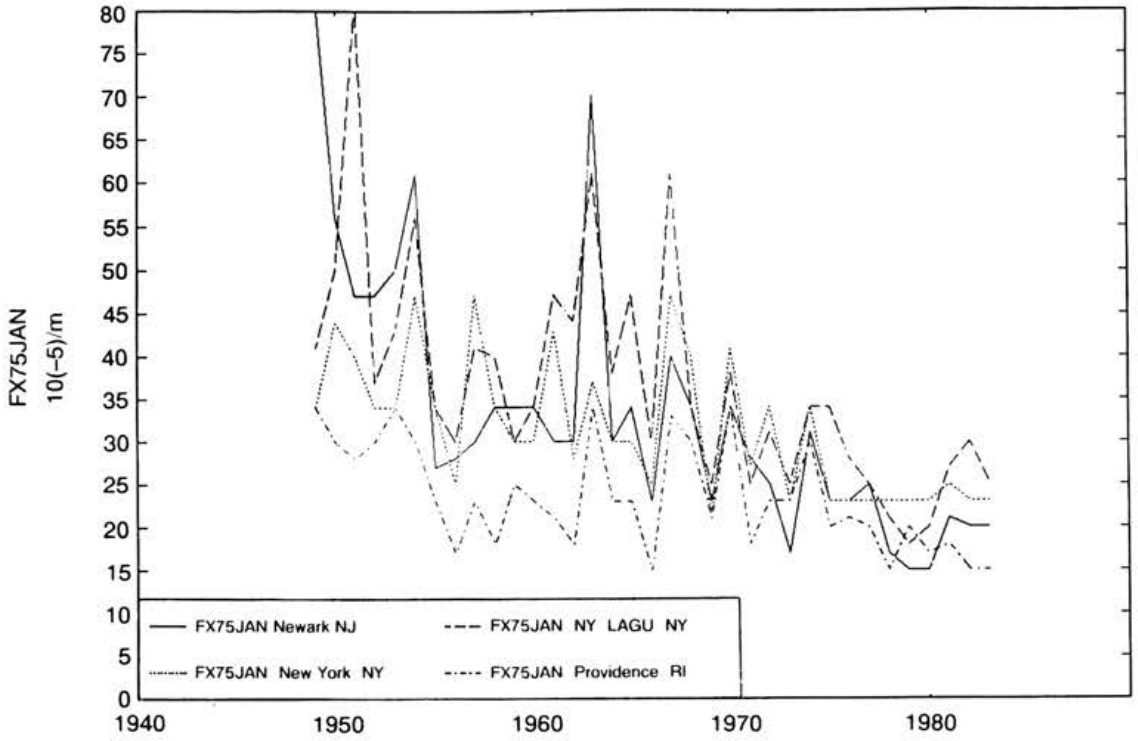


*Figure 24-33a Extinction coefficient (75th percentile) trends for four stations in the vicinity of New York City, NY, during the winter months.*

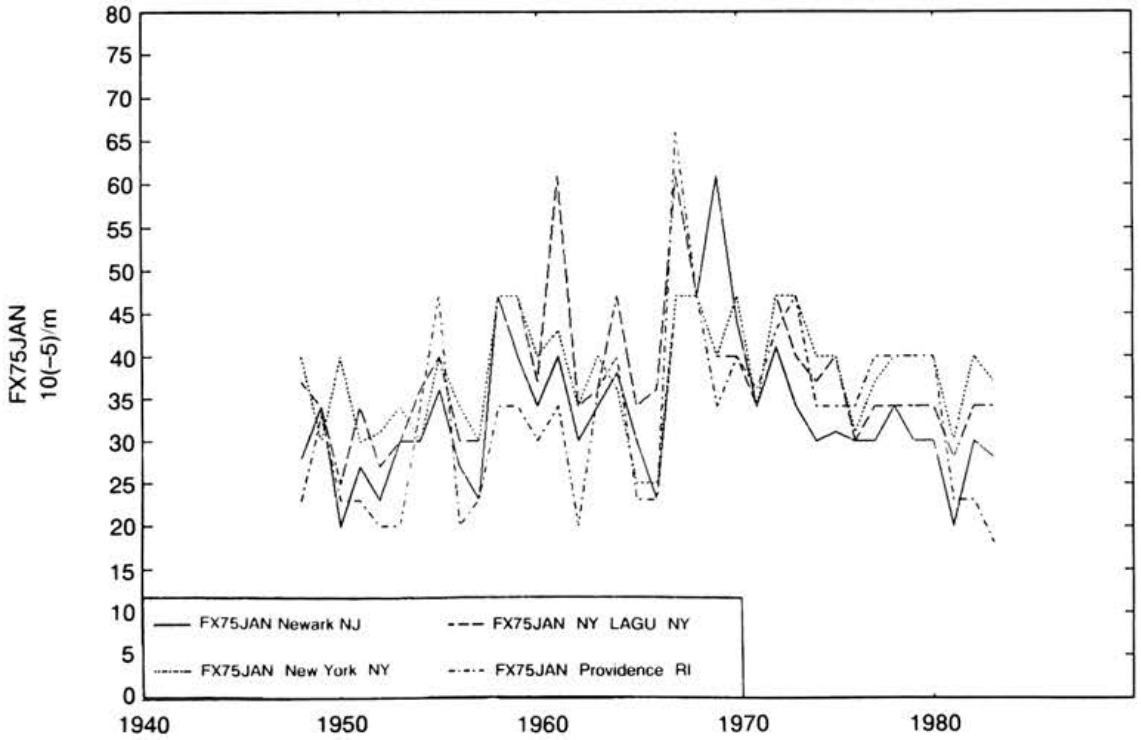


*Figure 24-33b Extinction coefficient (75th percentile) trends for four stations in the vicinity of New York City, NY, during the summer months.*

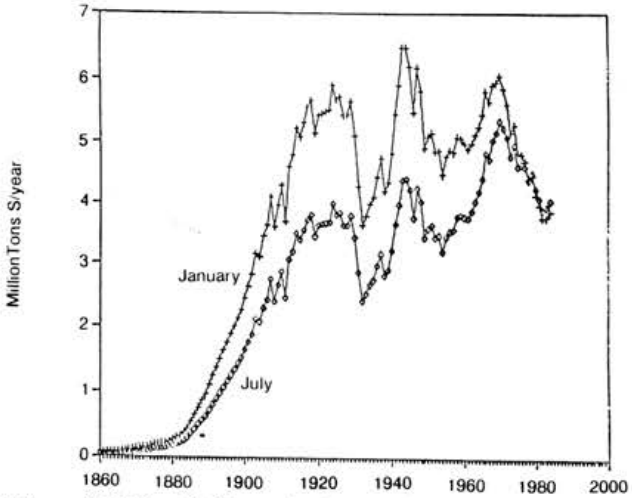


*Figure 24-34a Sulfur emission trends for January (+) and July (◊) for northeastern United States.*

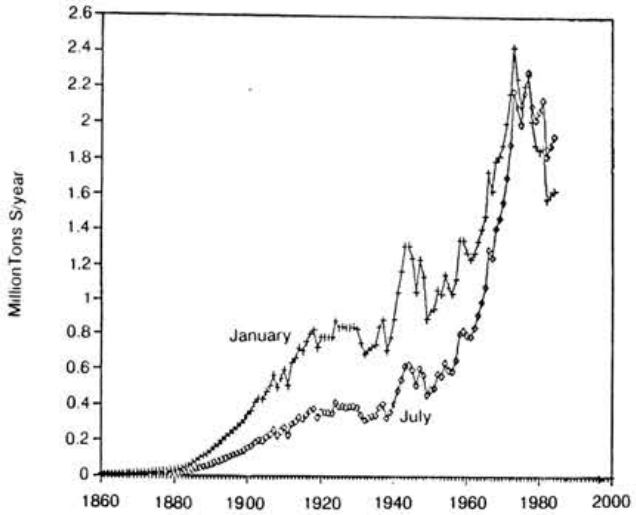


*Figure 24-34b Sulfur emission trends for January (+) and July (◊) for southeastern United States.*

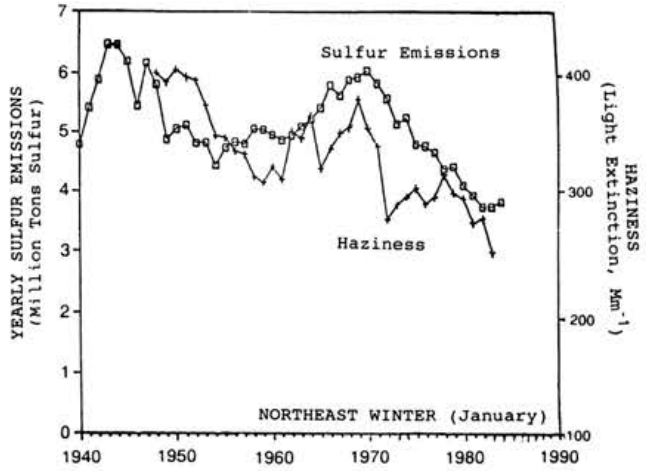


*Figure 24-35a Comparison of sulfur emission trends (◊) and extinction coefficient (+) for the northeastern region during the winter months.*

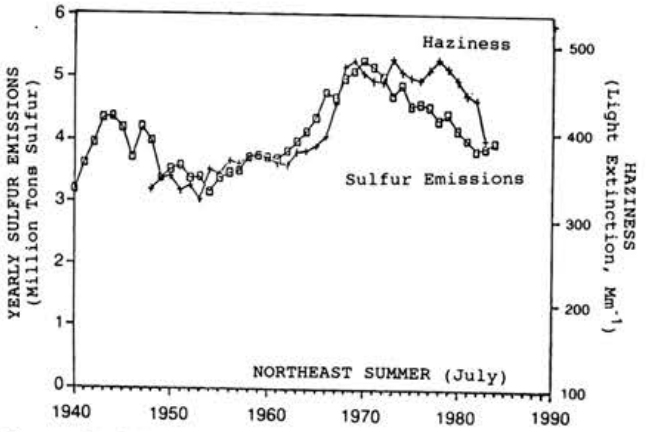


*Figure 24-35b Comparison of sulfur emission trends (◊) and extinction coefficient (+) for the northeastern region during the summer months.*

sulfur/year. The areas are 1.2 and 1.1 million km$^2$ for the northeast and southeast, respectively. Hence, the emissions units on the graphs can be interpreted approximately as grams of sulfur per square meter per year.

The computerized visibility trend data cover only the period since 1948. For this emission trend comparison, the visibility trends have been smoothed by using three-year moving averages. It should be noted that the general trend patterns are not sensitive to variations in defining "northeast" versus "southeast".

The trends of haze and sulfur emissions for the northeast in the winter (January) are depicted in Figure 24-35a. The emissions show a peak in the 1940's and in the early 1970's followed by a significant decline into the 1980's. Overall, there is a general decline during the 40-year period. The winter haziness also exhibits a general decline, but shows more year to year fluctuations.

The corresponding trends for the summer season (July) are illustrated in Figure 24-35b. The summer emissions again show the two peaks, but the peak around 1970 is more pronounced. Also, the decline since 1970 is not as significant as the decline of winter emissions. The summer haziness in the northeast shows the lowest values

in the 1950's and 1960's with a significant increase in the late 1960's. Since about 1970, there is no significant decline except for 1983. Overall, the emission and haze trends show certain correspondences, particularly in the 1950's and 1960's, but they deviate somewhat since the 1970's.

The winter haze and emission trends for the southeast are shown in Figures 24-36a and 24-36b. Winter emissions rise moderately until the early 1970's, when a slight decline begins. The winter haziness also shows a moderate increase up to the early 1970's. The dip in winter haziness around 1977 has no correspondence in the emission trends. The comparison of summer sulfur emissions and haziness for the southeast is found in Figure 24-36b. There is a remarkable correspondence, increasing values from the late 1940's through the early 1970's followed by a leveling off since then.

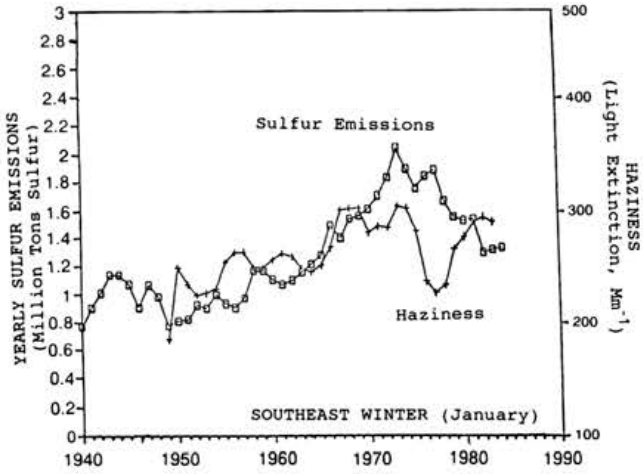


*Figure 24-36a Comparison of sulfur emission trends (□) and extinction coefficient (+) for the southeastern region during the winter months.*

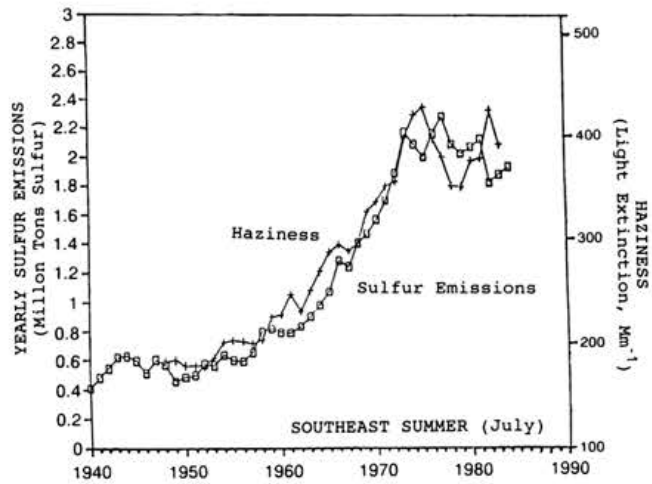


*Figure 24-36b Comparison of sulfur emission trends (□) and extinction coefficient (+) for the southeastern region during the summer months.*

The statistical relationship between historical sulfur emissions and extinction coefficient is further illustrated as a scatterplot in Figure 24-37. Here, yearly emissions and extinction coefficient are aggregrated over the entire East (states east of the Mississippi). In Figure 24-37, the correspondence between yearly sulfur emissions and yearly extinction coefficient is fairly close. As noted previously, the relationship between extinction coefficient and sulfur emissions depends on region and season. However, one aspect that is the same for both regions and both seasons is that a 50% change in sulfur emissions from current levels is statistically associated with about a 30% change in light extinction.

In conclusion, these data show that trends in the seasonal sulfur emissions provide a plausible explanation for the observed seasonal trends of atmospheric extinction coefficient over the eastern United States. However, such qualitative comparisons do not provide conclusive evidence of a cause-effect relationship. Also, the pattern of haze and sulfur emissions for the northeast and southeast tend to deviate at times. The causes of such deviations may include variabilities due to meteorology as well as poten-

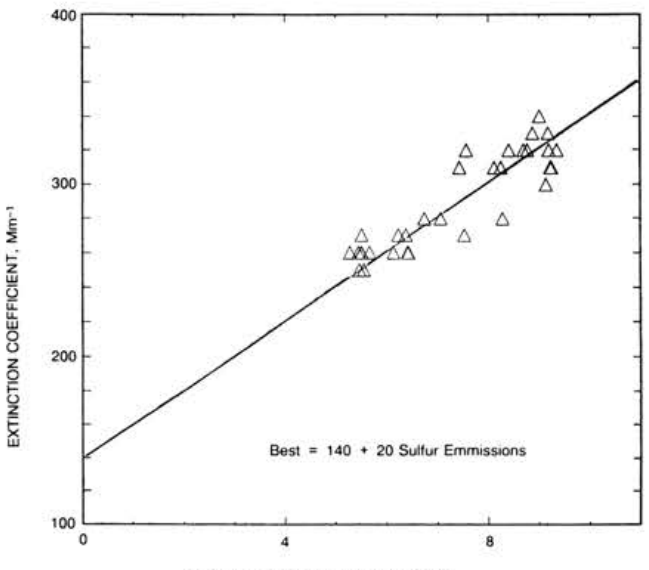


*Figure 24-37 Relationship between yearly extinction coefficients and yearly sulfur emissions for the entire East.*

tial errors in both emissions and visibility data. Finally, a one-to-one relationship cannot be expected since the haziness in one region may be influenced somewhat by emissions in the neighboring regions. A more detailed emission-haze trend analysis could be conducted using a regional haze model that incorporates both the changes in emissions as well as meteorological data for individual years. Both emissions and wind field data are available for such retrospective model studies.

From these data, it may be concluded that the haziness over the eastern United States since the late 1940's has been dominated by sulfur emission sources. Although the relative significance of other emissions and other chemical species that influenced visibility has not been quantified in the current analysis, it is not expected that these other species—organics, soot, nitrates, etc.—would have the same seasonal trend variations as sulfur emissions (*i.e.*, a strong historical decrease in the winter relative to the summer). Also, these trend results are consistent with the extinction budget results of Section 4.0 which shows that sulfates are currently the dominant contributor to light extinction in the East.

## 3.5 NATURAL BACKGROUND CONDITIONS FOR VISIBILITY/AEROSOLS

*J.C. Trijonis*

The purpose of this section is to estimate natural background levels of light extinction. Natural background visibility will, of course, vary with season, daily meteorology, and geography. Here, we consider the extinction levels associated with natural aerosols on an *annual average* basis, excluding factors such as precipitation, blowing snow, fog, etc. Geographically, one major division is made—East (basically up to one tier of states west of the Mississippi) and West (basically the desert/mountain areas of the Mountain and Pacific time zones). There is a strong dichotomy between these two regions in terms of vegetation, relative humidity, and current visibility levels.

Within each of the two major subregions, one would expect some spatial variations in natural aerosol levels. This is especially true at coastlines, where seaspray particles become important and relative humidity increases. The natural aerosol and visibility levels reported here do not apply to shoreline areas. Also, one would expect higher organic aerosols in the Southeast than in the Northeast and in the Pacific Northwest than in the desert Southwest (Altshuller, 1983) The values reported here are intended as overall spatial averages for the East and for the arid areas of the West.

Natural light extinction consists of only two significant components—Rayleigh scatter by air molecules and scatter by aerosols. On the average, natural background levels of absorption by $NO_2$ (EPA, 1982) and absorption by elemental carbon (see results below) are both negligible. For Rayleigh scatter in the East, we use a sea-level value of 12 $Mm^{-1}$. For the West, a value of 11 $Mm^{-1}$ is chosen to account for the higher average altitude.

Appendix A characterizes the natural background aerosol by estimating natural concentrations for each of the six major components of ambient fine aerosols: sulfates, organics, elemental carbon, ammonium nitrate, soil dust, and water (Trijonis, 1982a and 1982b). The estimates of natural concentrations are based on three types of information:

1. compilations of natural versus man-made emission levels
2. ambient measurements in remote areas (especially in the Southern hemisphere)
3. regression studies using man-made and/or natural tracers.

The left-hand side of Table 24-9 summarizes the results. In addition to the six fine particle components, a natural background level for coarse particles is also presented (see Appendix A for details).

In order to calculate contributions to light extinction, the particle mass concentrations must be multiplied by extinction efficiencies per unit mass. The extinction efficiencies presented in the center of Table 24-9 are based on the literature review by Trijonis *et al.* (1987 and 1988). Because water is treated explicitly and separately, the scattering (extinction) efficiencies for sulfates, nitrates, and organics represent "dry" conditions. The scattering efficiency for water is relatively high (5 $m^2/g$) because of the relatively low density of water.

On the right hand side of Table 24-9, natural light extinction levels are estimated as 26 $\pm$ 7 $Mm^{-1}$ (a little more than twice Rayleigh scatter) in the East and 17 $\pm$ 2.5 $Mm^{-1}$ (about 1.5 times Rayleigh scatter) in the West. These correspond to standard visual ranges of 150 $\pm$ 45 km in the East and 230 $\pm$ 35 km in the West. The major contributors to natural extinction levels in the East are Rayleigh scatter (46%), organics (22%), and water (19%). The major contributors in the West are Rayleigh scatter (64%), soil dust (including coarse particles) (14%), and organics (11%).

The error bounds in the previous paragraph have been determined by applying error propagation techniques to the uncertainties in the natural aerosol concentrations (see Table 24-9) and in the extinction efficiencies (assuming a relative error of plus or minus one-third). The overall errors are not that high, especially in the West, because Rayleigh scatter, a large component, is known with relative certainty.

*Table 24-9. Average Natural Background Levels of Aerosols and Light Extinction*

| | Average Concentration | | Error Factor | Extinction Efficiencies[a] | Extinction Contributions | |
|---|---|---|---|---|---|---|
| | East $\mu g/m^3$ | West $\mu g/m^3$ | | $m^2/g$ | East $Mm^{-1}$ | West $Mm^{-1}$ |
| FINE PARTICLES (≤2.5 μm) | | | | | | |
| Sulfates (as $NH_4 HSO_4$) | 0.2 | 0.1 | 2 | 2.5 | 0.5 | 0.2 |
| Organics | 1.5 | 0.5 | 2 | 3.75 | 5.6 | 1.9 |
| Elemental Carbon | 0.02 | 0.02 | 2-3 | 10.5 | 0.2 | 0.2 |
| Ammonium Nitrate | 0.1 | 0.1 | 2 | 2.5 | 0.2 | 0.2 |
| Soil Dust | 0.5 | 0.5 | $1^1/_2$ -2 | 1.25 | 0.6 | 0.6 |
| Water | 1.0 | 0.25 | 2 | 5 | 5.0 | 1.2 |
| COARSE PARTICLES (2.5-10 μm) | | | | | | |
| | 3.0 | 3.0 | $1^1/_2$ -2 | 0.6 | 1.8 | 1.8 |
| | | | RAYLEIGH SCATTER | | 12 | 11 |
| | | | | TOTAL | 26 ± 7 | 17 ± 2.5 |

[a] The extinction efficiencies are based on the literature review by Trijonis et al. (1986 & 1988). All the extinction efficiencies represent particle scattering, except for elemental carbon where the 10.5 $m^2/g$ value is assumed to consist of 9 $m^2/g$ absorption and 1.5 $m^2/g$ scattering. Note that the 0.6 $m^2/g$ value for coarse particles is a "pseudo-coarse scattering efficiency" representing the total scattering by all ambient coarse particles (≤ 2.5 μm) divided by the coarse particle mass between 2.5 and 10 μm.

## 3.6 EXISTING CONDITIONS AND HISTORICAL TRENDS FOR CLIMATIC EFFECTS OF AEROSOLS

*R. Charlson*

While there are many methods for measuring the climatically relevant properties of aerosols, there is no complete measurement system for climate assessment. There is almost no standardization of instruments and methods (other than some optical ones). There is no continuity of data acquisition, and—with the exception of turbidity, remote light scattering, and lidar—there is no agency currently operating an appropriate monitoring system. This section will review the existing methods for acquiring data on aerosol properties as they influence climate, the meager existing data base, and the lack of detectability of trends (due in large part to the lack of measurement capability).

### 3.6.1 Monitoring Methods

Table 24-10 presents a list of currently available methods for measurement of aerosol properties as they influence climate. This list is organized according to the divisions in Section 2.2.3. It is further subdivided as to measurements at a point, those over an air column, and those made remotely from aircraft or satellites.

With one exception, the methods in Table 24-10 do not measure a climatic effect but rather provide data from which climatic effects can be calculated. The exception is the pyranometer which measures directly the loss of total solar irradiance (direct plus diffuse) under clear skies. However, even then, two of the main direct effects—albedo with clear sky and absorption/emission of infrared radiation—can only be quantified indirectly through radiative transfer computations.

Monitoring methods for visibility and aerosols are discussed in Section 3.1, and the reader is referred to that section for an analysis of those methods. Here, the focus will be on methods used in monitoring programs directed specifically at climate effects of aerosols.

Much of the climate-related data for the United States and the world consists of turbidity (optical depth) measurements acquired with hand-held sun photometers. It is necessary to be severely critical of the bulk of these data because of serious instability and drift in the sun photometers. Further difficulties exist with calibrating the

*Table 24-10. Methods for Measuring Climatic Effects of the Atmospheric Aerosol*

1. Direct effect on visible radiation at one point in space (all are functions of wavelength).

| VARIABLE | METHOD |
|---|---|
| **B**sp | Integrating nephelometer |
| **B**abs | Difference of **B**ext - **B**sp |
| **B**ap | Integrating plate or integrating sandwich, light extinction by filter samples |
| **B**ext | Transmissometer, visual range (Lv = 4/**B**ext) |
| **B**sp as f(RH) | Humidity controlled nephelometer or visual range data stratified by RH |
| **B**sp | Polar nephelometer or partial integrating nephelometer |
| ωp | **B**sp/**B**ext |
| **B**/(ϕ) | Polar nephelometer |
| Extinction components | Measure size distribution and chemical composition (to possible complex refractive index) and use Mie formalism for ϕsp, ϕap, etc. |

2. Direct effect on infrared radiation.

| VARIABLE | METHOD |
|---|---|
| Extinction | Measure size distribution components and chemical composition; calculate via Mie formalism or measure infrared flux divergence |

3. Column integrals.

| VARIABLE | METHOD |
|---|---|
| Optical depth or turbidity as f (wavelength) | Sun-photometer; pyrheliometer (broad-based or monochromatic multiwavelength) |
| Total solar radiation | Pyranometer |
| Diffuse radiation | Shaded pyranometer |

4. Remote sensing of direct effects.

| VARIABLE | METHOD |
|---|---|
| **B**(180) | Lidar (at some laser wavelength) |
| Clear-sky reflectance/albedo | Satellite borne radiometers |

Note: All require Mie calculations and assumptions regarding size distribution and refractive index or angular scattering function.

5. Indirect cloud effects.

| VARIABLE | METHOD |
|---|---|
| CCN concentrations | Cloud chamber at known super-saturation, S |
| CCN concentrations as f (S) (super-saturation spectrum or CCN spectrum) | Cloud chamber with variable S |
| Ice nucleus concentration | No proven method |

6. Other quantities:

| VARIABLE | METHOD |
|---|---|
| CN(condensation nuclei) concentration | Condensation nucleus counter |

instruments, especially at low values of optical depth. As a result of these instrumental difficulties, much if not most turbidity data is of suspect quality, even some of the data that are officially archived by the National Climatic Data Center at Asheville, NC. Thus, it is necessary to utilize these data with caution, particularly data from sites with low aerosol loadings.

Substantial amounts of nephelometer and condensation nuclei (CN) data are available for four remote observations sites operated by the NOAA in the Geophysical Monitoring for Climatic Change Program (GMCC). The nephelometer measurements of Bsp at four wavelengths permit estimation of submicrometer aerosol concentration and provide a crude index of particle size distribution. These data could be useful as ground truth for satellite mapping of optical depth as a function of wavelength and as inputs to climate models. However, relatively little use has been made of them to date. The integrating nephelometers in use by GMCC all are of the same design and are calibrated against well characterized Rayleigh scattering gases. As a result, these data can be considered to be standardized and not seriously influenced by drift, changes in instrument design, or operating protocol. The CN data provide a useful index of the degree of departure from clean background conditions. However, they do not convey any directly useable information regarding climatic effects. Methods other than above are not widely implemented in either United States or international monitoring programs.

Some measurements are available for cloud condensation nuclei (CCN). However, there is a wide range of methods in use, and very few intercomparisons have ever been conducted (none recently). Thus, there is no generally accepted sampling methodology. Because of the calculated sensitivity of climate to CCN concentrations, this is a particularly critical shortcoming of the present measurement programs.

For the future, there is considerable promise that remote sensing methods will find substantial application in the study of climatic effects by aerosols. Lidar already has been used to locate and map stratospheric plumes from volcanic eruptions, Arctic haze, and various tropospheric plumes. The lidar backscatter coefficient, $\beta$ (180), can be quantified and related to the other integral optical properties in climate models.

Similarly, clear-sky radiance measured from satellites can provide a basis for calculating optical depth as a function of wavelength via the Mie formalism. However, no standard or proven method exists for doing this. The present operational programs will require substantial testing against ground truth prior to being fully accepted. Equally important as these clear-sky observations are satellite mapping of clouds and cloud properties. Current research using multiple wavelengths shows promise for quantifying the role of CCN in controlling cloud albedo.

## 3.6.2 Survey of Existing Data Bases

The number, quality, duration, and extent of data bases for most of the climatic properties of aerosols are extremely limited. Nonetheless, these data are sufficient to demonstrate the importance of direct effects on solar radiation. Other climatic effects (infrared and cloud) are much less well demonstrated and are current topics of research. The main climatic data sets acquired by United States agencies are from the NOAA/EPA turbidity network and the NOAA/GMCC network. In addition to describing these two networks, this section discusses global measurements and data needs. Visibility and aerosol data sets are summarized in Section 3.2.

### 3.6.2.1 North American Turbidity/Optical Depth Data

Since the beginning of the NOAA-EPA network in 1960, there have been between 10 and 46 observing sites, with only a few maintained continuously. The original Volz sun-photometers were replaced with NOAA J-series units in 1982, when the network was reduced to ten sites (all of which are still operating). The network has grown since to include 17 sites.

From 1960 to 1972, there was little documentation of instrument drift and calibration, and data quality for that period is questionable. Between 1972 and 1982, as the calibration process and instrumentation evolved, the data are officially labeled as of "unknown" quality by NOAA. From mid-1982 to the present, the data are considered to be of "high quality".

Figure 24-38, a map of optical depth for June 1983 through July of 1986, shows the 10 sites operating then. The station density and geographical extent clearly do not provide complete coverage of the United States. However, most of the sites have been chosen in rural areas that are not immediately impacted by local sources or large cities, so they probably are reasonably representative of nonurban areas out to a hundred or few hundred kilometers in radius.

### 3.6.2.2 GMCC Remote Location Aerosol Data

Besides the four-wavelength nephelometers and CN counters at each of the four baseline sites (Barrow, Mauna Loa Observatory, Samoa, and South Pole), an extensive set of solar radiation measurements are performed at GMCC sites from which a variety of aerosol parameters can be extracted. Unfortunately, none of the baseline sites is located at mid-latitude or near sea level, so none of the GMCC remote turbidity/optical

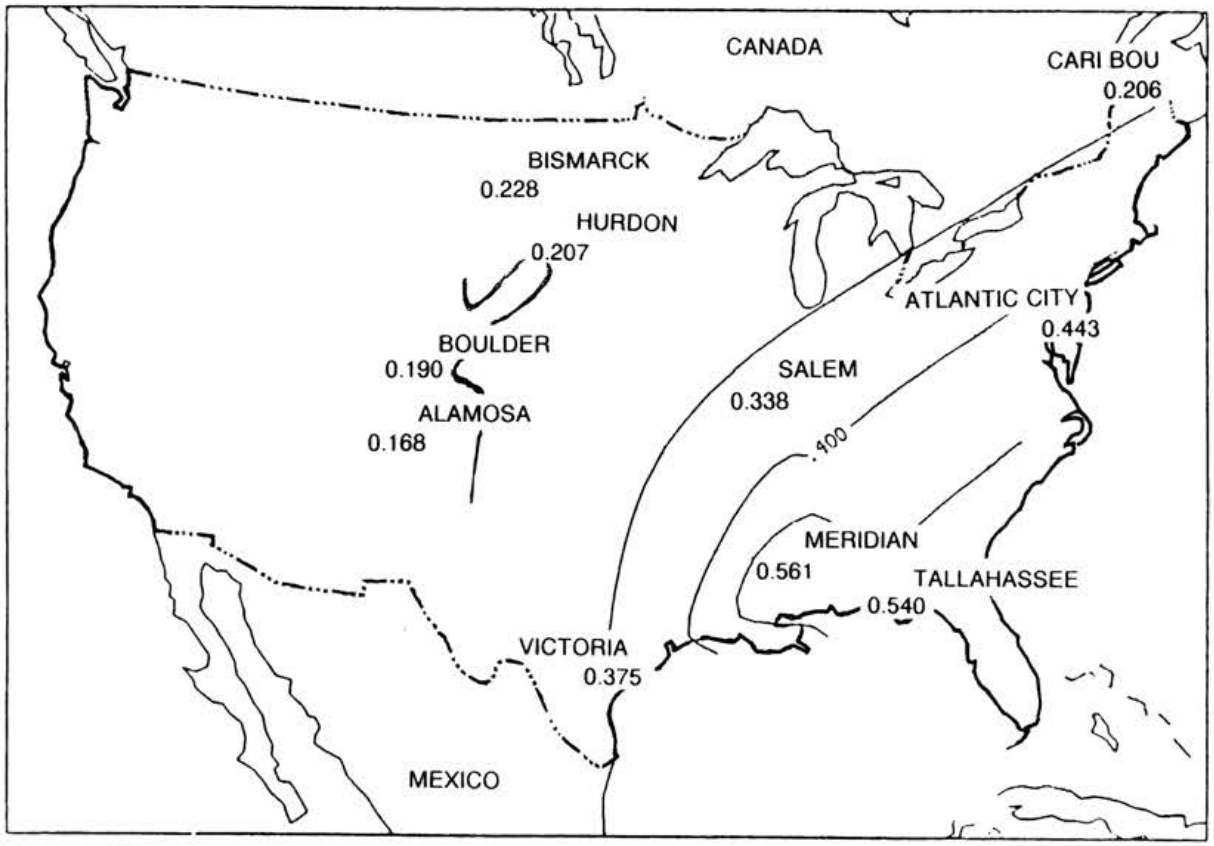


*Figure 24-38 Isopleths of aerosol optical depth for 380 nm wave length for June through July 1983 - 1986 from the recent high quality NOAA data base (map provided by NOAA).*

depth data can be used as a record of the background against which continental pollution can be assessed. However, recent Australian data for optical depth at remote marine sites does allow an approximate assessment of natural background and hence, the degree of departure over our continent.

### 3.6.2.3 Global Data

Even if the available turbidity data were of high quality, the fact that such data can only be acquired on land precludes observing the global distribution of aerosol properties. In principle, shipboard sun-photometry could be performed routinely. However, the difficulty of maintaining quality control in such data might be insurmountable. The only hope for global data in the future are satellite-borne radiometers and, perhaps, airborne instruments.

Satellite data are subject to considerable uncertainty due to the necessity of either assumptions regarding size distribution and refractive index, and/or empirical calibration of optical depth via simultaneous ground based sun-photometry (with all its errors).

In addition, drift of the sensitivity of satellite radiometers and changes in instruments over the years preclude any current attempt to sense trends from satellites. Difficulties exist over land due to changing albedo (*e.g.*, growth of vegetation, snow, plowing, etc.). However, oceans and large lakes present a sufficiently constant low albedo to allow estimation of optical depth.

The satellite-derived maps that presently are available from NOAA are in the process of being corrected and have not yet been thoroughly tested against corrected ground truth data. However, synoptic scale plumes of aerosol can be mapped and the background marine aerosol can be sensed. After a thorough evaluation of accuracy, detection limits, drift, and calibration, satellite radiometers will provide the needed global view, at least over the oceans.

The Background Air Pollution Monitoring Network (BAPMON) sun-photometer network that was established in the 1970's by WMO (in cooperation with the NOAA and EPA) suffers from the same instrumental errors and drift as the United States network. This network is

potentially very important because it could provide the much-needed ground truth for satellite observations. However, the "unknown quality" of current and past data preclude any analysis of these records.

Sampling of aerosol particles has been carried out internationally in a variety of short and long-term measurement programs. However, there is a wide range of methods in use, with no formal international intercomparisons of the methods. The chief problem in relating mass concentration data from various workers and various government programs is the lack of control of the size discrimination of the samplers, primarily the upper cut size which often is not known.

### 3.6.2.4 Nonexistent But Necessary Data

Despite the quality and continuity limitations of the sun photometry data, such data do allow estimation of the magnitude of current solar irradiance loss (as will be discussed later). However, there are no routine data at all for the major indirect effect of aerosols—their acting as CCN. Referring to Table 24-10, it is clear that very few of the possible climatic measurements actually are being performed as a part of any national or international monitoring effort. The most important missing data for tropospheric aerosols would appear to be:

- CCN concentrations, both temporally and geographically,
- data for assessing the role of soil dust in infrared interactions, and
- simultaneous and contiguous chemical data to allow identification of the sources of aerosol particles that cause increased optical depth.

Standardization of samplers and protocols is also required, especially for CCN and international aerosol measurements.

## 3.6.3 National Turbidity Data

Before introducing maps of the optical depth for the continental United States, it is instructive to examine the magnitude of the controlling quantities, particle scattering and particle absorption, as measured in intensive field experiments by Weiss (1980). Table 24-11 reveals that levels of both scattering and absorption are highest in cities, but that the values in rural areas of the eastern United States are not remarkably lower, other than for urban smog episodes.

Figures 24-39 and 24-40 summarize the key geographical and temporal features of the historical optical depth (turbidity) records. Similar results were published earlier by Flowers *et al.* (1969). Keeping in mind the instrumental difficulties mentioned in Section 3.6.2, the outstanding features clearly are a summertime maximum of aerosol optical depth in the Tennessee/Ohio Valleys. The maximum optical depth is so large ($\delta p = 0.5$) that the instrumental uncertainty ($\Delta\delta p = 0.02$ with a drift properly corrected) is inconsequential. As pointed out by Husar *et al.* (1981) and Trijonis *et al.* (1986), these geographical and temporal features are quantitatively consistent with those derived from visibility data and sulfate aerosol data.

It is of interest to inquire whether the optical depth data are consistent with other aerosol and optical data in terms

*Table 24-11. Scattering Coefficient (**B**sp), Absorption Coefficient (**B**ap), and Albedo of Single Scatter (ωp) for Selected Locations and Times (Weiss, 1980; Clarke and Charlson, 1985)*

| Category/Site | **B**sp ($10^{-6}$ $m^{-1}$) | **B**ap ($10^{-6}$ $m^{-1}$) | ωp | No. of Obs. |
|---|---|---|---|---|
| | *URBAN* | | | |
| Seattle, WA (Industrial) | 50 | 27 | 0.65 | 43 |
| Portland, OR | 109 | 86 | 0.56 | 159 |
| St Louis, MO (St Louis Univ) | 75 | 50 | 0.6 | 50 |
| Denver, CO (Henderson) | 49 | 49 | 0.5 | 13 |
| Denver, CO (Trout Farm) | 70 | 60 | 0.54 | 23 |
| Phoenix, AZ | 210 | 118 | 0.64 | 20 |
| Denver, CO (Winter 1978) | 100 | 64 | 0.61 | 103 |
| Seattle,WA (Residential) | 38 | 10 | 0.79 | 69 |
| St Louis, MO (Residential) | 117 | 37 | 0.76 | 50 |
| | *RURAL* | | | |
| Tyson, MO (1973) | 67 | 19 | 0.78 | 96 |
| Tyson, MO (1975) | 51 | 12 | 0.81 | 52 |
| Milford, MI | 46 | 17 | 0.73 | 8 |
| Hall Mountain, AR | 40 | 6 | 0.87 | 62 |
| Puget Sound, WA | 24 | 6 | 0.80 | 23 |
| Above Flagstaff, AZ | 19 | 1.2 | 0.94 | 4 |
| Mesa Verde, CO | 12 | 1.2 | 0.91 | 4 |
| Abastumani Obs. (USSR) | 46 | 5.7 | 0.89 | 40 |
| Mauna Loa Obs., HI (Apr-Jun 82) | 1.6 | 0.12 | 0.93 | 33 |
| Mauna Loa Obs., HI (Jul-Dec 82) | 0.81 | 0.06 | 0.93 | 112 |

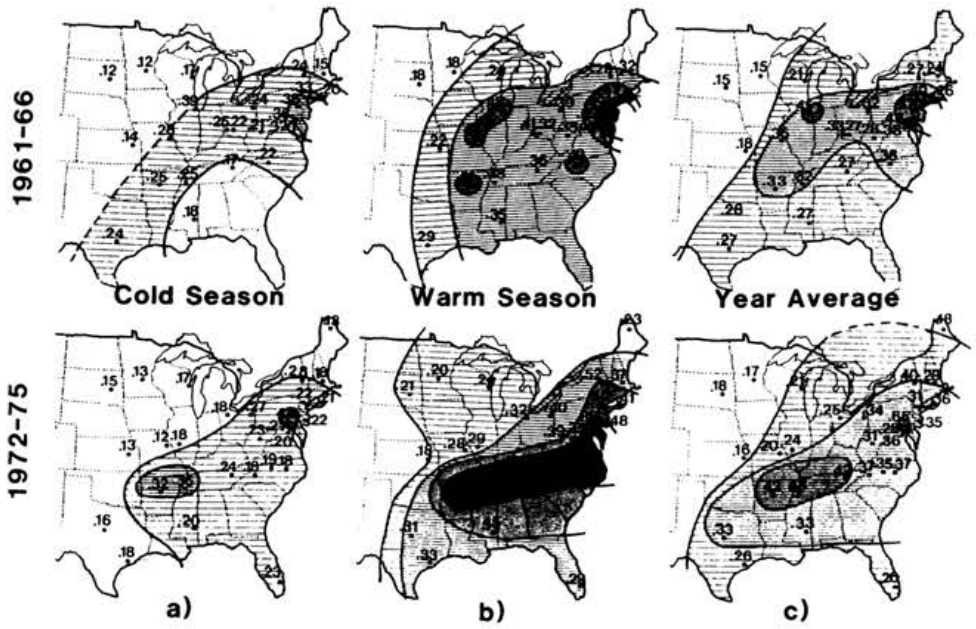


*Figure 24-39 Spatial distribution of vertical optical depth at 0.5 μm in 1961 - 1966 (top) and 1972 - 1975 (bottom) from 26 sites. a = cold season (Oct - Mar); b = warm season (Apr - Sep); c = yearly average (Husar et al., 1981).*

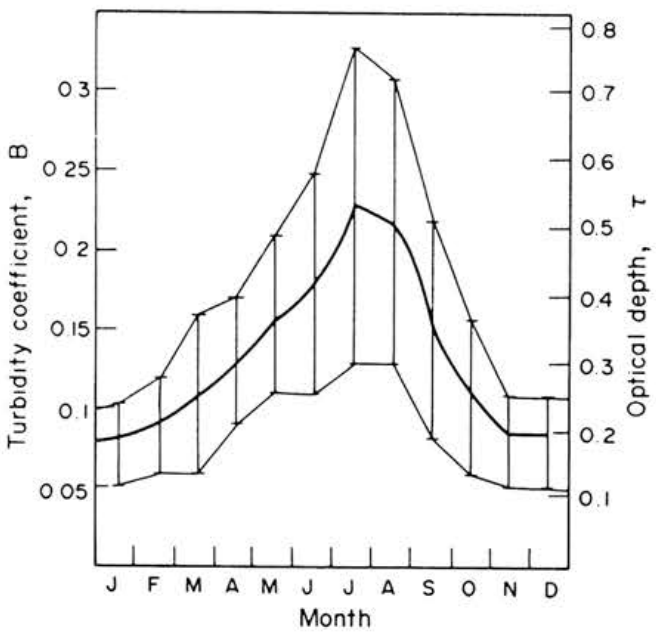


*Figure 24-40 Seasonal pattern of the monthly average optical depth (τ) or turbidity coefficient of B = 2.3 τ at 26 eastern United States sites during 1972 -1975 (Husar et al., 1981).*

of overall magnitude. As shown in the top part of Table 24-12, the optical depth values for the eastern United States (about 0.4) agree with measured particle extinction (about 140 $Mm^{-1}$), if one assumes a mixing height of 3 km. Furthermore, as shown at the bottom of Table 24-12, the measured aerosol optical depths are quite consistent with the total irradiance loss measured by Ball and Robinson (1982).

The current uncertainty in the United States turbidity data, specified for the case of the sun directly overhead, is 0.005 to 0.04 depending on the instrument, observer, *etc.* (DeLuisi and Reddy, personal communication 1989). This uncertainty is inversely proportional to path length through the atmosphere and thus would be half as much for a path length double the perpendicular distance. However, the data prior to 1982 - 1983 are stated by NOAA as of "unknown quality". Thus, the published analyses by Flowers *et al.* (1969), Husar *et al.* (1981), *etc.*—all of which depended on these earlier data—must be considered to have "unknown" uncertainty. It seems unlikely that the general features of the geographical distribution would be sensitive to such uncertainties. Similarly, the seasonal cycle in Figure 24-40 must be real; this cycle is also very evident in visibility data (see Sections 3.3.2 and 3.4). However, the time trend implicit in Figure 24-40 must be questioned.

*Table 24-12. Empirical Comparison for Industrial Regions*

RURAL AEROSOL EXTINCTION COEFFICIENT:

$\mathbf{B}_P$ = 140 $Mm^{-1}$, about 10% of which is absorption (see Sections 3.3.1 and 4.1)

AEROSOL OPTICAL DEPTH:

Assume: H = 3 km = 0.003 $Mm^{-1}$ (height of haze layer)

then: $\delta p = (140) \times (0.003) = 0.4$ (in agreement with turbidity data)

ENERGY LOSS:

Assume: 15% of scattering lost to space (see Figure 24-4) and $\mathbf{B}sp \approx 0.9\ B_P$

then: $0.15 \times \delta sp = 0.15 \times (0.9 \times 0.4) =$ 5% loss of irradiance to scatter

Assume: $\mathbf{B}ap \approx 0.1 \times \mathbf{B}_P = 14\ Mm^{-1}$

then: $\delta ap = \mathbf{B}ap\ H = 14 \times 0.003 =$ 4% loss due to absorption

Total loss = 9%, on the order of the 7.5% value measured by (Ball and Robinson, 1982)

It would be very useful to have documentation for the error in the United States turbidity data similar to that published for Australian turbidity data (Forgan, 1985). Prior to the discovery of instrumental error, the mean optical depth at Cape Grim, Tasmania, was reported to be about 0.12. After 1985, the earlier values have been deleted, and the newer values are closer to 0.05, a correction by more than a factor of two. It is significant that at an optical depth of 0.1 or greater, aerosol does measurably reduce solar irradiance and therefore alter regional climate; whereas at 0.05 or less, the aerosol is of marginal importance.

### 3.6.4 Lack of Data for Historical Trends

While some measurements of the climatically relevant properties of aerosol have been made, and while there is evidence that aerosol does reduce solar irradiance and influence regional climate (see Section 5.2), historical measurements are not of sufficient duration or quality to demonstrate how these effects grew over the course of industrial development.

It is necessary to infer that these effects must have occurred in and downwind of industrial regions from theoretical calculations, chemical aerosol data, background aerosol data, trends in visibility data, and historical records from ice cores.

# SECTION 4

# CONTRIBUTIONS TO LIGHT EXTINCTION

The preceding sections have dealt with concepts, measurements, patterns, and trends for light extinction and aerosols. The present section relates light extinction to aerosol composition, focusing specifically on the extinction contributions of sulfur and nitrogen oxides. The focus on sulfur and nitrogen oxides reflects the context of this document, which treats improved visibility as a collateral benefit of controls directed at acid deposition. This focus seems appropriate despite the facts that carbonaceous and other species also contribute to extinction and that some of the optically active sulfur and nitrogen oxides are not themselves acidic.

Section 4.1 first resolves total extinction into the components identified in Sections 2.2: scattering and absorption, by gases and by fine and coarse particles. This first level of resolution is accessible by direct measurement. Only fine particle scattering requires further detailed analysis, because the contribution of sulfur and nitrogen oxides to each of the other components is either overwhelming (gas absorption) or minor (gas scattering, particle absorption, and coarse-particle scattering). Sections 4.2 and 4.3 then examine the chemical composition of fine particles and the contributions of individual species to scattering. The individual contributions cannot be measured directly and in general are not even well defined. Nonetheless, despite these difficulties, it is possible to draw certain broad conclusions concerning the optical importance of sulfates and nitrates.

As discussed in Section 2.2, atmospheric optical properties are multidimensional and are not completely characterized just by the extinction at some representative wavelength. However, reflecting current apportionment practice, the present section does not address such important factors as path radiance and the dependence of extinction on wavelength. These other factors affect both atmospheric visibility and the apportionment of visible effects among atmospheric constituents. As a simple example, the relative importance of $NO_2$ is greatly increased if one considers discoloration rather than visual range, or extinction in the blue rather than in the green. Richards (1987 and 1990) has pointed out that the individual components of extinction carry useful information on some of these additional dimensions—information on albedo, scattering asymmetry, and wavelength dependence. To allow this information to be incorporated in the NAPAP Integrated Assessment, estimates are derived for species contributions to both total extinction and individual extinction components.

## 4.1 THE CONTRIBUTION OF FINE-PARTICLE SCATTERING TO TOTAL EXTINCTION

*W. White*

Visibility measurements and computations often assume, implicitly or explicitly, that scattering by fine particles is the dominant contributor to non-Rayleigh extinction. This section reviews the empirical evidence for this assumption. The importance of fine scattering is relevant in the context of sulfur and nitrogen oxide emissions because

- 90% or more of the sulfate measured in typical continental air is carried by fine particles, and ammonium nitrate is predominantly fine (Milford and Davidson, 1987), and
- atmospheric sulfates and ammonium nitrate interact with visible light almost entirely through scattering, with little or none of the energy lost to absorption.

### 4.1.1 A Survey of Budgets for Total Extinction

Tables 24-13 and 24-14 present extinction budgets derived from field studies which obtained data sufficient to estimate the fractional contribution of fine particle scattering to total non-Rayleigh extinction. The criteria for inclusion are that studies supply all of the following data:

- Particle scattering measured by unheated nephelometry. It is generally possible to guarantee only that samples were not intentionally preheated, as actual temperatures within the instrument were not usually reported.
- Some basis for apportioning measured scattering to fine and coarse particles, usually a size-resolved measurement of particle mass.
- Total non-Rayleigh extinction, from either direct measurement or the sum of absorption and scattering. Transmissometry or black-target teleradiometry is required for total extinction measurements; absorption can be measured with an integrating plate or estimated from the elemental carbon concentration.

The field programs summarized in Tables 24-13 and 24-14 employed a variety of measurement systems. The data from these differing configurations have been reduced to a common basis through accounting proce-

*Table 24-13. A Survey of Total Extinction Budgets*

| Totals ($Mm^{-1}$) | | Individual Components ($Mm^{-1}$) | | | | Remarks |
|---|---|---|---|---|---|---|
| **Be** | SUM | **Bsf** | **Bsc** | **Bap** | **Bag** | Location- Period - Reference |
| | | | | *RURAL EAST* | | |
| 163[a] | 156 | 122 | 8[p] | 11 | 3 | Research Triangle Park, NC - 1979 summer day - 1 |
| 184[a] | 197 | 169[e,i] | 6[r] | 7 | 2 | Logan, OH - 1980 summer[aa] day - 2 |
| - | 308 | 280[d,e] | 4[p] | 10 | 1 | Luray, VA - 1980 summer 24h - 3 |
| - | 190 | 162[d] | 4 | 9[u] | 2 | Lewes, DE - 1982 summer 24h - 4 |
| - | 103 | 70[d] | 3 | 12[u] | 5 | Lewes, DE - 1982-83 winter 24h - 4 |
| | | | | *URBAN EAST* | | |
| 232[b] | 238 | 172[j] | 11[p] | 30 | 11 | Houston, TX - 1980 summer day - 5 |
| - | 273 | 209[d] | 8[p] | 25[u] | 18 | Detroit, MI - 1981 summer 24h - 6 |
| | | | | *RURAL WEST* | | |
| - | 45[g] | 18[f,m] | 10[f,m] | 4[u] | 2[y] | China Lake, CA - 1979 year 24h - 7 |
| - | 48 | 23 | 6 | 6 | 2[x] | China Lake, CA - 1984-85 year 24h - 8 |
| - | 54 | 29 | 5 | 7 | 2[x] | Edwards AFB, CA - 1984-85 year 24h - 8 |
| - | 40 | 18 | 4 | 5 | 1[y] | Fort Irwin, CA - 1984-85 year 24h - 8 |
| - | 29[g] | 13 | 4[l] | 2 | 0[w] | Zilnez Mesa, AZ - 1979 summer[bb] 24h - 9 |
| h,c | - | h | h | - | - | Meteor Crater, AZ - 1985 fall day - 10 |
| 16[c] | 17 | 5 | 0[p] | 2[uv] | 0[y] | Grand Canyon, AZ - 1986-87 winter 24h - 11 |
| - | 21 | 9 | 1[p] | 0[u] | 0[y] | Grand Canyon, AZ - 1986-87 year 24h - 12 |
| 28[c] | 30 | 12 | 1[p] | 5[uv] | 2[x] | Page, AZ - 1986-87 winter 24h - 11 |
| - | 21 | 8 | 2[p] | 1[u] | 0[y] | Page, AZ - 1986-87 year 24h - 12 |
| - | 20 | 8 | 1[p] | 0[u] | 0[y] | Bryce Canyon, UT - 1986-87 year 24h - 12 |
| - | 27 | 10[k] | 4[n] | 1[u] | 0[y] | Spirit Mountain, NV - 1985-86 year 24h - 13 |
| - | 26 | 12 | 3[p] | 1[u] | 0[y] | Spirit Mountain, NV - 1986-87 year 24h - 12 |
| - | 23 | 8 | 2[p] | 1[u] | 0[y] | Meadview, AZ - 1986-87 year 24h - 12 |
| - | 24 | 9 | 2[p] | 1[u] | 0[y] | Prescott, AZ - 1986-87 year 24h - 12 |
| | | | | *URBAN WEST* | | |
| - | 219 | 106[d,e] | 12[q] | 66 | 24 | Commerce City, CO - 1978-79 winter 24h - 14 |
| 89[b] | - | 48[j] | 11[o,s] | - | 10 | Commerce City, CO - 1981-82 winter day - 15 |
| - | 120 | 66[j] | 13[o,s] | 20[t] | 10 | Commerce City, CO - 1981-82 winter day - 16 |
| - | 159 | 93[j] | 18[o,s] | 25[t] | 12 | Commerce City, CO - 1981-82 winter night - 16 |
| 140[c] | 159 | 64[e,i] | 18[s] | 39 | 25 | Denver, CO - 1987-88 winter gas[cc] 24h - 17 |
| 107[c] | 116 | 37[e,i] | 13[s] | 30 | 26 | Denver, CO - 1987-88 winter coal[cc] 24 h - 17 |
| - | 326 | 230[i] | 26[q] | 36 | 21 | Los Angeles, CA - 1982 summer day - 18 |
| - | 270 | 188[i] | 28[q] | 21 | 20 | Riverside, CA - 1982 summer day - 18 |
| - | 308 | 170[d,f] | 54 | 49[u] | 23 | Azusa, CA - 1984 summer day - 19 |
| - | 259 | 165[d,f] | 23 | 34[u] | 24 | Pasadena, CA - 1984 summer day - 19 |
| - | 302 | 206[d,f] | 32 | 34[u] | 18 | Upland, CA - 1984 summer day - 19 |
| - | 97 | 46[i] | 12[q] | 17 | 9 | San Jose, CA - 1982 summer day - 18 |

This table surveys studies which provide data sufficient to estimate the fractional contribution of fine particle scattering to total non-Rayleigh extinction. This table is intended as support for the accompanying Table 24-14.
Studies conducted during individual seasons were of limited duration, typically a month or less, and should not be assumed climatologically representative. The terms "day, night, and 24h" indicate that the samples were collected during daylight, nighttime, or all hours.

QUANTITIES:

**Be** Measured total extinction at 525 nm or 550 nm.

SUM Sum of extinction components at 525 nm: **Bsf** + **Bsc** + **Bap** + **Bag** + $\mathbf{B}_R$.

**Bsp** Particle scattering measured by unheated nephelometer.

**Bsf** Fine particle ($D_p$ <2.5 μm) scattering at 525 nm from nephelometer measurement corrected for partial response to coarse particles: **Bsp** - **Bsc**/2 unless otherwise noted. Instruments are MRI 156x/159x unless otherwise noted and are calibrated as recommended by Ruby and Waggoner(1981).

(Continued)

*Table 24-13. (Continued)*

**Bsc** Coarse particle scattering from measured coarse mass: $0.6(m^2/g)$ x CM [2.5 μm< $D_p$ <10 μm) unless otherwise noted.
**Bap** Particle absorption, from integrating plate measurement unless otherwise noted.
**Bag** $NO_2$ absorption at 525 nm: 0.53 ($Mm^{-1}$/ppb) x $NO_2$ at 1 atm and 0° C.
$\mathbf{B_R}$ Rayleigh scattering at 525 nm: 13.1 $Mm^{-1}$ at 1 atm and 25° C.

NOTES:
[a] **Be** measured by black-target teleradiometry at 550 nm.
[b] **Be** measured by black-target teleradiometry at 525 nm.
[c] **Be** measured by active transmissometry at 550 nm.
[d] **Bsp** measured by MRI 155x nephelometer with an effective wavelength of 475 nm: **Bsf** (525 nm) = **Bsf** (475 nm)/1.18, based on Angstrom exponent of 1.5 for **Bsf**.
[e] **Bsp** incorporates author's subsequent recalibration.
[f] **Bsp** incorporates reviewer's recalibration (x273/298).
[g] $\mathbf{B_R}$ changed from author's value for consistency with elevation.
[h] No absolute values reported. Reported **Bsp/Be** regression slope is multiplied in present work by 3/2, the approximate ratio of measured extinction to Rayleigh scattering when the nephelometer indicated no particle scattering, to correct for inflation of transmissometer readings by atmospheric turbulence. **Bsf/Bsp** = 0.8 was directly measured by placing a cyclone separator ahead of the nephelometer.
[i] Nephelometer temperature rise reported to be 2° C or less.
[j] Nephelometer temperature rise reported to be 4° C or less.
[k] **Bsf** = **Bsp** - 0.7 **Bsc**, because **Bsc** includes scattering from fine portion of coarse mode.
[l] **Bsc** calculated from particle size distribution and Mie theory.
[m] **Bsc/Bsf** calculated from particle size distribution and Mie theory. Fine-coarse cutpoint is 2.0 μm.
[n] **Bsc** from regression analysis, includes scattering from fine portion of coarse mode.
[o] **Bsc** derived from author's estimate of nephelometer truncation error.
[p] **Bsc** calculated from CM [2.5 μm< $D_p$ <15 μm] assuming CM10/CM15 = 0.7.
[q] **Bsc** calculated from CM [2.5 μm< $D_p$ <30 μm] assuming CM10/CM30 = 0.4.
[r] **Bsc** estimated from CM measurements at other locations.
[s] Nephelometer inlet reported to pass coarse ($D_p$ <15 μm) particles.
[t] **Bap** incorporates authors' adjustment to measured value.
[u] **Bap** calculated from measured elemental carbon: 10 ($m^2/g$) x EC.
[v] A second elemental carbon measurement yielded concentrations 1/5 as great. The authors preferred the larger values because these balanced **Be** and SUM.
[w] **Bag** from $NO_2$ measurements aloft.
[x] **Bag** from incomplete $NO_2$ measurements.
[y] **Bag** estimated from $NO_2$ measurements at other locations or times.
[aa] Ohio averages include all observations, not just those made under conditions favorable to teleradiometry.
[bb] Zilnez Mesa averages exclude day (July 5) dominated by smoke from wildfires.
[cc] 1987-88 Denver $SO_2$ emissions were halved during alternating two week periods by coordinated coal-gas fuel switching.

REFERENCES:
1. Dzubay and Clubb (1981).
2. Ellestad and Speer (1981). Data for **Bsp** and **Bap** from Ellestad (personal communication 1989).
3. Ferman et al. (1981).
4. Wolff et al. (1986).
5. Dzubay et al. (1982).
6. Wolff et al. (1982b).
7. Ouimette et al. (1981).
8. Trijonis et al. (1988).
9. Data are from Macias et al. (1981a) and Richards et al. (1981). The atypicality of the omitted sampling period is identified in Macias et al. (1981b).
10. Regression of **Bsp** on **Be** from Malm et al. (1987b), as corrected in Malm et al. (1989). Value for **Bsf/Bsp** from Tombach et al. (1986).
11. Malm et al. (1989).
12. SCENES data from R. Lewis (personal communication 1989). The program is described by Mueller et al. (1986) and McDade and Tombach (1987).
13. White and Macias (1990). Elemental carbon data from White (personal communication 1989).
14. Groblicki et al. (1981) and Wolff et al. (1981).
15. Lewis and Dzubay (1986).
16. Lewis et al. (1986).
17. Watson et al. (1988, 1989).
18. Appel et al. (1985).
19. Larson and Cass (1989). Data for **Bsp** from Larson (personal communication 1989).

*Table 24-14. Contributions to Non-Rayleigh Extinction*[a]

| %(**Be**-$\mathbf{B_R}$) | % (SUM - $\mathbf{B_R}$) | | | | |
|---|---|---|---|---|---|
| **B**sf | **B**sf | **B**sc | **B**ap | **B**ag | Remarks<br>Location and Period |
| | | | | *RURAL EAST* | |
| 75[b] | 85 | 5 | 8 | 2 | Research Triangle Park, NC - 1979 summer day |
| 91[b] | 92 | 3 | 4 | 1 | Logan, OH - 1980 summer day |
| - | 95 | 1 | 3 | 0 | Luray, VA - 1980 summer 24h |
| - | 91 | 2 | 5 | 1 | Lewes, DE - 1982 summer 24h |
| - | 78 | 3 | 13 | 5 | Lewes, DE - 1982-83 winter 24h |
| | | | | *URBAN EAST* | |
| 79 | 77 | 5 | 13 | 5 | Houston, TX - 1980 summer day |
| - | 80 | 3 | 10 | 7 | Detroit, MI - 1981 summer 24h |
| | | | | *RURAL WEST* | |
| - | 54 | 30 | 12 | 5 | China Lake, CA - 1979 year 24h |
| - | 62 | 16 | 17 | 5 | China Lake, CA - 1984-85 year 24h |
| - | 66 | 12 | 17 | 5 | Edwards AFB, CA - 1984-85 year 24h |
| - | 63 | 15 | 18 | 5 | Fort Irwin, CA - 1984-85 year 24h |
| - | 71 | 19 | 10 | 0 | Zilnez Mesa, AZ - 1979 summer 24h |
| 67[b] | - | 36[c] | - | - | Meteor Crater, AZ - 1985 fall day |
| 63[b] | 68 | 6 | 21 | 5 | Grand Canyon, AZ - 1986-87 winter 24h |
| - | 83 | 12 | 3 | 3 | Grand Canyon, AZ - 1986-87 year 24h |
| 57[b] | 60 | 4 | 25 | 10 | Page, AZ - 1986-87 winter 24h |
| - | 75 | 14 | 7 | 4 | Page, AZ - 1986-87 year 24h |
| - | 84 | 11 | 2 | 3 | Bryce Canyon, UT - 1986-87 year 24h |
| - | 65 | 26 | 6 | 3 | Spirit Mountain, NV - 1985-86 year 24h |
| - | 74 | 17 | 6 | 3 | Spirit Mountain, NV - 1986-87 year 24h |
| - | 72 | 19 | 6 | 3 | Meadview, AZ - 1986-87 year 24h |
| - | 74 | 18 | 5 | 3 | Prescott, AZ - 1986-87 year 24h |
| | | | | *URBAN WEST* | |
| - | 51 | 6 | 32 | 12 | Commerce City, CO - 1978-79 winter 24h |
| 61 | - | 12[c] | - | 11[c] | Commerce City, CO - 1981-82 winter day |
| - | 61 | 12 | 18 | 9 | Commerce City, CO - 1981-82 winter day |
| - | 63 | 12 | 17 | 8 | Commerce City, CO - 1981-82 winter night |
| 46[b] | 44 | 12 | 27 | 17 | Denver, CO - 1987-88 winter gas 24h |
| 35[b] | 35 | 12 | 29 | 24 | Denver, CO - 1987-88 winter coal 24h |
| - | 74 | 8 | 12 | 7 | Los Angeles, CA - 1982 summer day |
| - | 73 | 11 | 8 | 8 | Riverside, CA - 1982 summer day |
| - | 58 | 18 | 16 | 8 | Azusa, CA - 1984 summer day |
| - | 67 | 9 | 14 | 10 | Pasadena, CA - 1984 summer day |
| - | 71 | 11 | 12 | 6 | Upland, CA - 1984 summer day |
| - | 54 | 15 | 20 | 11 | San Jose, CA - 1982 summer day |

[a] Quantities are as defined in Table 24-13, but are presented here as a percent of total non-Rayleigh extinction **B**sf + **B**sc + **B**ap + **B**ag. Fine particle scattering **B**sf is given in terms of both directly measured and summed totals; other components are given in terms of summed totals unless otherwise noted. All values are at 525 nm as in Table 24-13.

[b] **B**sf (550 nm) = **B**sf (525 nm) * 0.93, based on Angstrom exponent of 1.5.

[c] Given as %(**B**e - $\mathbf{B_R}$).

dures which are documented in the captions and notes. Many of the adjustments involved are inexact, but nevertheless they serve to mitigate known biases. The experimental basis for the accounting scheme is briefly reviewed in the following paragraphs. The measurement techniques themselves are described in Section 3.1.

Scattering by fine particles can be measured directly by sampling behind a cyclone separator. Most data have been taken without cyclones, however, so that the proportion of observed scattering attributable to fine particles must be estimated from other size-resolved measurements. This estimate is a poorly determined factor in the budgeting process. One approach is to analyze, by multiple regression, the empirical dependence of observed scattering on fine and coarse mass. However, the regression approach does not work well in practice because the net effect of coarse particle concentrations on ratios of measured scattering to fine mass is small (Lewis, 1981; Ozkaynak *et al.*, 1985), so that measured scattering by both coarse and fine particles is statistically associated with fine particle mass. Alternatively, size-resolved scattering can be estimated theoretically from particle size distributions if these are available. However, the scattering/mass ratios of irregular coarse particles may depart significantly from those of Mie theory spheres (Hill *et al.*, 1984).

Fine particle scattering in Tables 24-13 and 24-14 is generally derived from measured particle scattering and estimated coarse particle scattering according to **B**sf = **B**sp - **B**sc/2. The assumption that the nephelometer responds to half the coarse particle scattering is consistent with the results of Hasan and Lewis (1983) and Trijonis *et al.* (1988). The scattering attributable to coarse particles has received little experimental attention. Trijonis *et al.* (1988) report nephelometer measurements with and without a cyclone which indicate a scattering/mass ratio of **B**sc/CM (2.5 μm $<D_p<$ 10 μm) = 0.6 $m^2/g$ in the Mojave desert. The regression estimate of **B**sc/CM (2.5 μm $<D_p<$ 15 μm) = 0.46 $m^2/g$ obtained by White and Macias (1988) for southern Nevada is consistent with this value when the differing definitions of coarse mass are taken into account. (Both results given here are corrected for nephelometer response.) Coarse scattering is generally scaled from coarse mass according to the Mojave ratio **B**sc/CM10 = 0.6 $m^2/g$, using the mass ratios CM10/CM15 = 0.7 (Rodes and Evans, 1985) and CM10/CM30 = 0.4 (Rodes *et al.*, 1985) to convert measurements with differing diameter cuts.

Most of the nephelometer data were collected by narrowband instruments with an effective wavelength of about 525 nm, and this wavelength is adopted as the standard in Tables 24-13 and 24-14. Data from older instruments, which measure scattering over a broad band centered at about 475 nm, are adjusted as follows. Scattering is first resolved into fine and coarse particle components as described above. Fine particle scattering is then adjusted using the ratio **B**sf(475)/**B**sf(525) = 1.18 given by Ruby and Waggoner (1981) for an aerosol with **B**sf $(\lambda) \propto \lambda^{-1.5}$. The Angstrom exponent of 1.5 is representative of Los Angeles smog (Charlson *et al.*, 1972) and desert Southwest aerosols (Richards *et al.*, 1981). No adjustment is made to coarse particle scattering, which is essentially independent of wavelength (Porch *et al.*, 1973).

Particle absorption values are taken from integrating plate measurements or elemental carbon concentrations. The wavelengths of integrating plate measurements were not always reported. They usually lay in the range 500 nm - 550 nm, and no adjustment has been attempted. Where absorption measurements are unavailable or suspect, particle absorption is estimated from the elemental carbon concentration using the specific absorption **B**ap(525)/EC = 10 $m^2/g$. This round number is consistent with careful measurements of diesel exhaust (Japar *et al.*, 1984) and urban aerosol (Adams *et al.*, 1989).

Absorption by gases is calculated from the $NO_2$ concentration using the specific absorption **B**ap(525)/$NO_2$ = 0.26 $m^2/g$ (Dixon, 1940). Mass concentrations of $NO_2$ are seldom reported, so the **B**ag values in Tables 24-13 and 24-14 are generally derived by adjusting reported **B**ag to the standard wavelength. Many of these values may be affected by ambiguities in the usage of "standard conditions"; they are based on the paper by Hodkinson (1966) which tabulates Dixon's results in volume specific terms ($km^{-1}$/ppm) without noting that these refer to 0 °C at 1 atm. No attempt is made to compensate for interferences by $HNO_3$ and organic nitrates in the $NO_2$ measurement (Winer *et al.*, 1974). Rayleigh scattering at 525 nm is taken to be 13.1 $Mm^{-1}$ at 25 °C and 1 atm (Ruby and Waggoner, 1981); the values in Tables 24-13 and 24-14 are generally derived by adjusting reported values to the standard wavelength.

### 4.1.2 Results

Table 24-14 supports the conclusion that scattering by fine particles is generally the dominant contributor to non-Rayleigh extinction. Fine particle scattering accounts for the majority of the total in all studies outside of downtown Denver. The fractional contribution of fine scattering to non-Rayleigh extinction exhibits a consistent regional pattern; it is more than 75% in all of the eastern studies, and less than 75% in all but two of the western studies (the unpublished SCENES data from Grand Canyon and Bryce Canyon).

Tables 24-13 and 24-14 show good balances for those studies which measured total extinction both directly and by component, lending credibility to both the extinction

and scattering measurements. Note should nonetheless be taken of the potential for inadvertent water losses in some "unheated" nephelometers and the uncertainty in estimates of coarse particle scattering.

There are major gaps in the spatial and seasonal coverage of Tables 24-13 and 24-14. The eastern studies include only two in urban areas and only one outside of summer, and the western studies include none in the north.

## 4.2 THE CHEMICAL COMPOSITION OF FINE PARTICLES

*W. White*

As noted in Section 2.1, ambient fine particulate matter is usually dominated by six major fractions: water, sulfates, elemental carbon, organic carbon, ammonium nitrate, and soil dust. This section reviews the relative abundance of the major light scattering species in this mix.

### 4.2.1 A Survey of Mass Balances from Visibility Studies

Table 24-15 presents mass balances derived from field studies of scattering and fine-particle composition. The criteria for inclusion are that a study supply all of the following data:

- fine-particle mass
- particle scattering measured by heated or unheated nephelometry
- fine-particle sulfur or sulfate
- fine or total carbon or organic carbon.

Particle mass is usually measured after equilibrating the sample to a standard relative humidity of 40 - 50%. The mass measured in this state is not generally that of the ambient particles, which may carry large quantities of

*Table 24-15. A Survey of Fine Particle Haze Composition*

| Concentration | | Composition (%FM) | | | | | |
|---|---|---|---|---|---|---|---|
| **B**sfd ($Mm^{-1}$) | FM ($\mu g/m^3$) | SLF | NTR | ORG | .SUM | CHEM | Remarks Location - Period - Reference |
| | | | | *RURAL EAST* | | | |
| 181[a] | 46 | 63 | 1 | 31[h] | 95 | >99[o] | Abbeyville, LA - 1979 summer 24h - 21 |
| 130[a] | 26 | 62 | 1 | 25 | 88 | 99 | Luray, VA - 1980 summer 24h - 3 |
| 81[a] | 17 | 59 | - | 34 | 96[l] | 105 | Lewes, DE - 1982 summer 24h - 4 |
| 55[a] | 15 | 49 | - | 22 | 74[l] | 87 | Lewes, DE - 1982-83 winter 24h - 4 |
| 115[a] | 20 | 66 | 1 | 9 | 76 | 86 | Lenox, MA - 1984 summer 24h - 22 |
| | | | | *URBAN EAST* | | | |
| 135 | 43 | 54 | 1 | 15[i] | 70 | 79 | Houston, TX - 1980 summer day - 5 |
| 133[a] | 36 | 53 | 1 | 32 | 86 | 97 | Detroit, MI - 1981 summer 24h - 6 |
| | | | | *RURAL WEST* | | | |
| 17[b] | 11 | 25[q] | 2[q] | 17 | 44 | 63 | China Lake, CA - 1979 year 24h - 7 |
| 22 | 8 | 25 | 8[f,g] | 35 | 69 | 97 | China Lake, CA - 1984-85 year 24h - 8 |
| 26 | 9 | 31 | 17[f,g] | 30 | 77 | 97 | Edwards AFB, CA - 1984-85 year 24h - 8 |
| 17[b] | 7 | 29 | - | 24 | 59[l] | 92 | Fort Irwin, CA - 1984-85 year 24h - 8 |
| 13[b] | 6 | 42[q] | 3[q] | 29 | 74 | 84 | Zilnez Mesa, AZ - 1979 summer[u] 24h - 9 |
| 18 | 5 | 42 | 2 | 33 | 80[m] | 93[p] | Sunshine, AZ - 1981-82 year day - 23 |
| 5[c] | 1 | 47 | 8[f] | 14 | 69 | 108 | Grand Canyon, AZ - 1986-87 winter 24h - 11 |
| 8[b] | 3 | 46 | - | 20 | 69[l] | 101 | Grand Canyon, AZ - 1986-87 year 24h - 12 |
| 11[c] | 3 | 39 | 9[f] | 40 | 89 | 116 | Page, AZ - 1986-87 winter 24h - 11 |
| 8[b] | 4 | 42 | - | 24 | 70[l] | 102 | Page, AZ - 1986-87 year 24h - 12 |
| 8[b] | 3 | 43 | - | 19 | 65[l] | 94 | Bryce Canyon, UT - 1986-87 year 24h - 12 |
| 23 | 5 | 40 | 5 | 35 | 89[m] | 110[p] | Blythe, CA - 1981-82 year day - 23 |
| 10[b] | 4 | 40 | - | 20 | 67[l] | 101 | Spirit Mountain, NV - 1985-86 year 24h - 13 |
| 11[b] | 4 | 40 | - | 21 | 68[l] | 100 | Spirit Mountain, NV - 1986-87 year 24h - 12 |
| 8[b] | 4 | 45 | - | 22 | 72[l] | 101 | Meadview, AZ - 1986-87 year 24h - 12 |

(Continued)

*Table 24-15. (Continued)*

| Concentration | | Composition (%FM) | | | | | |
|---|---|---|---|---|---|---|---|
| **B**sfd ($Mm^{-1}$) | FM ($\mu g/m^3$) | SLF | NTR | ORG | SUM | CHEM | Remarks Location - Period - Reference |
| 9[b] | 3 | 56 | - | 23 | 84[l] | 101 | Prescott, AZ - 1986-87 year 24h - 12 |
| 14 | 8 | 43 | 1 | 19 | 64[m] | 77[p] | Sierra Vista, AZ - 1981-82 year day - 23 |
| 13 | 4 | 40 | 1 | 30 | 73[m] | 91[p] | Encino, NM - 1981-82 year day - 23 |
| 10 | 5 | 27 | 1 | 28 | 59[m] | 75[p] | Walsenburg, CO - 1981-82 year day - 23 |
| 17 | 6 | 17 | 2 | 31 | 56[m] | 66[p] | Ouray, UT - 1981-82 year day - 23 |
| 15 | 5 | 29 | 3 | 30 | 68[m] | 82[p] | Delta, UT - 1981-82 year day - 23 |
| 10 | 6 | 15 | 1 | 20 | 39[m] | 57[p] | Fish Creek Ranch, NV - 1981-82 year day - 23 |
| 10 | 5 | 22 | 1 | 33 | 58[m] | 77[p] | Pathfinder, WY - 1981-82 year day - 23 |
| 21 | 5 | 27 | 6 | 39 | 83[m] | 97[p] | Little Butte, ID - 1981-82 year day - 23 |
| 17 | 4 | 27 | 2 | 41 | 73[m] | 81[p] | Harlowton, MT - 1981-82 year day - 23 |
| | | | | *URBAN WEST* | | | |
| 64[a] | 40 | 14 | 20 | 25 | 59 | 89 | Commerce City, CO - 1978-79 winter 24h - 14 |
| 43 | 19 | 17 | 17[f] | 32[j] | 66 | 81 | Commerce City, CO - 1981-82 winter day - 16 |
| 61 | 23 | 11 | 11[f] | 44[j] | 66 | 82 | Commerce City, CO - 1981-82 winter night -16 |
| 43[d] | 24 | 9 | 27[f] | 44 | 81 | 106 | Denver, CO[v] - 1987-88 winter gas[w] 24h - 17 |
| 25[d] | 14 | 13 | 19[f] | 58 | 91 | 126 | Denver, CO[v] - 1987-88 winter coal[w] 24h - 17 |
| 148 | 62 | 29 | 17[f] | 35[k,t] | 81 | >86[o] | Los Angeles, CA - 1982 summer day - 18 |
| 130 | 48 | 20 | 37[f] | 35[k,t] | 92 | >97[o] | Riverside, CA - 1982 summer day - 18 |
| 113[a,d] | 74 | 14[q] | 2[q] | 27 | 66[n] | >72[o] | Azusa, CA - 1984 summer day - 19 |
| 110[a,d] | 56 | 18[q] | 3[q] | 32 | 75[n] | >79[o] | Pasadena, CA - 1984 summer day - 19 |
| 135[a,d] | 58 | 15[q] | 3[q] | 27 | 66[n] | >71[o] | Upland, CA - 1984 summer day - 19 |
| 41[e] | 13 | 35 | - | 32 | >66 | >76 | Dallas, TX[x] - 1986-87 winter day - 24 |
| 44[e] | 19 | 20 | - | 43 | >62 | >68 | Dallas, TX[x] - 1986-87 winter night - 24 |
| 54 | 19 | 9[s] | 17[s] | 64 | 90 | 106 | Albuquerque, NM[y] - 1982-83 winter day - 25 |
| 196 | 54 | 3[s] | 6[s] | 79 | 88 | 97 | Albuquerque, NM[y] - 1982-83 winter night - 25 |
| 68[a] | 22 | 15[r] | 10[r] | 38[t] | 63 | >76[o] | Portland, OR[z] - 1977-78 year 24h - 26 |
| 41 | 22 | 10 | 20[f] | 50[kt] | 80 | >87[o] | San Jose, CA - 1982 summer day - 18 |

QUANTITIES:

**B**sfd Dry fine-particle ($D_p$ <2.5 μm) scattering at 525 nm, from nephelometer measurement corrected for partial response to coarse particles as in Table 24-13. Instruments are heated MRI 156x/159x unless otherwise noted, and are calibrated as recommended by Ruby and Waggoner (1981).

FM Measured fine-particle ($D_p$ <2.5 μm) mass concentration.

SLF Mass conc. of fine-particle sulfate species, collected on Teflon unless otherwise noted: 1.375 $[SO_4^{2-}]$f (ammonium sulfate).

NTR Mass conc. of fine-particle nitrate species, collected on Teflon unless otherwise noted: 1.29 $[NO_3^-]$f (ammonium nitrate).

ORG Mass conc. of fine-particle organic species, collected on quartz unless otherwise noted: 1.4$[C_{org}]$f.

SUM Mass conc. of major accumulation-mode fractions: SLF + NTR + ORG.

CHEM Mass conc. of chemically-resolved fine-particle fractions: SUM + CRUST + $[C_{ele}]$f.

CRUST Mass conc. of fine-particle crust: if not calculated by author, then [Si]f/0.28 or [Fe]f/0.05.

NOTES:

[a] **B**sp measured by MRI 155x nephelometer, with an effective wavelength of 475 nm: **B**sfd (525 nm) = **B**sfd (475 nm)/1.18, based on Angstrom exponent of 1.5 for **B**sfd.

[b] **B**sfd estimated from **B**sf assuming ratio **B**sfd/**B**sf = 19/20 from reference 8.

[c] **B**sfd estimated from **B**sf assuming ratio **B**sfd/**B**sf = 9/10.

[d] **B**sfd estimated from **B**sf assuming ratio **B**sfd/**B**sf = 2/3 from references 13, 15, and 17.

[e] **B**sc estimated from measurements at other locations.

(Continued)

*Table 24-15. (Continued)*

[f] $NO_3^-$ collected by filter pack behind a $HNO_3$ denuder.
[g] $NO_3^-$ averaged from incomplete measurements.
[h] Fine $C_{org}$ estimated by author from total $C_{org}$.
[i] Fine $C_{org}$ and $C_{ele}$ derived from fine C and Bap.
[j] Fine $C_{org}$ estimated from total $C_{org}$ assuming $C_{org}$ size distribution from reference 13.
[k] Fine $C_{org}$ estimated from total $C_{org}$ size assuming $C_{org}$ distribution from reference 18.
[l] Totals include $NO_3^-$ estimated from denuder/filter-pack measurements at other locations.
[m] Ambient nitrate in totals estimated as 3x measured nitrate (White and Macias, 1987).
[n] Ambient nitrate in totals estimated from denuder measurements of reference 17: NTR = 0.25 x FM.
[o] No crustal elements were measured.
[p] Crust estimates increased by factor 1.3 determined by regression (White and Macias, 1989).
[q] $NO_3^-$ and $SO_4^{2-}$ collected on Nuclepore filters.
[r] $NO_3^-$ and $SO_4^{2-}$ collected on cellulose acetate filters.
[s] $NO_3^-$ and $SO_4^{2-}$ collected on quartz filters.
[t] $C_{org}$ collected on glass fiber filters.
[u] Zilnez Mesa averages exclude day (July 5) dominated by smoke from wildfires.
[v] Downtown Denver data are from the Federal site.
[w] 1987-88 Denver $SO_2$ emissions were halved during the alternating two-week periods by coordinated coal-gas fuel switching.
[x] Dallas data are from the CAMS 5 site.
[y] Albuquerque data are from the Zuni site.
[z] Portland data are from all four sites.

REFERENCES:

1 through 19 as in Table 24-13.
21. Wolff et al. (1982b).
22. Wolff (1987) and Wolff and Korsog (1989).
23. Tombach et al. (1987b) and White and Macias (1987 & 1989). Averages from White (personal communication 1989).
24. Einfeld and Dattner (1988).
25. Zak et al. (1984).
26. Shah et al. (1984). Average CM/FM from Shah (personal communication 1989).

unbound (hygroscopic) water under humid conditions. Neither, however, is the measured mass necessarily that of dry particulate matter.

The amount of water associated with an equilibrated sample depends strongly on the concentration and composition of the sulfate fraction. At 50% relative humidity, well below the deliquescence point of $(NH_4)_2SO_4$, $H_2SO_4$ can still hold more than its weight in water (Pierson *et al.*, 1989). When special precautions are taken to preserve sample acidity, water can account for a third or more of the measured mass (Pierson *et al.*, 1989). Most field programs allow any acid in the sample to be neutralized by atmospheric and laboratory $NH_3$, in which case little or no difference is observed between masses measured at moderate and very low relative humidity (Lewis and Macias, 1980).

The counterpart of sample equilibration in optical measurements is the use of heated inlets on nephelometers, as described in Section 2. Most of the studies in Table 24-15 measured "dry" scattering in this manner. Fine particle scattering at the standard 525 nm wavelength is derived from these measurements as described in Section 4.1.2. Several studies measured both dry and ambient scattering, and the resulting dry/ambient ratios are used to adjust data from studies which used only unheated nephelometers.

Ammonium nitrate, a major constituent of fine particles in some areas, is difficult to sample accurately. Most visibility field studies now collect nitrate on Teflon filters, thereby eliminating the positive artifacts from adsorbed $HNO_3(g)$ which corrupted early data (Spicer and Schumacher, 1977). Ammonium nitrate is easily lost from the particulate phase, however, so samples collected on Teflon filters yield only lower bounds for ambient concentrations (Appel *et al.*, 1981; Shaw *et al.*, 1982). Accurate measurement of ambient $NH_2NO_3$ generally requires sampling behind a $HNO_3$ denuder with a filter pack for total $NO_3^-$.

Carbon samples are generally collected on quartz filters for various thermal analyses. Some gas-phase organics

adsorb on these filters, producing a positive artifact which can be substantial depending on the sampling conditions (Cadle *et al.*, 1983; White and Macias, 1989; McMurry and Zhang, 1989; Hering *et al.*, 1989). Additionally, the various methods for separating organic and elemental carbon provide differing operational definitions of these fractions (Cadle *et al.*, 1983; Malm *et al.*, 1989).

Crustal elements such as Si are generally determined by X-ray analyses such as XRF and PIXE. Interlaboratory comparisons show systematic differences of as much as a factor of two between the values returned by different groups for the same samples (Tombach *et al.*, 1987).

Chemical concentrations in Table 24-15 are presented in terms of presumed compounds rather than measured analytes. The same conversion factors are used for all studies. All sulfur is given as $SO_4^=$ (Lewis and Macias, 1980; Macias *et al.*, 1981a and 1981b), and $SO_4^=$ and $NO_3^-$ are given respectively as $(NH_4)_2SO_4$ and $NH_4NO_3$. Where they are available, $NH_4^+$ concentrations are usually consistent with this convention. Organic carbon is scaled by a factor of 1.4 to include associated hydrogen and oxygen, consistent with measurements of urban smog particles (Grosjean and Friedlander, 1975) and natural hydrocarbon reaction products (Graedel, 1978). Crustal elements such as Si are scaled by their average abundance in the continental crust (Mason and Moore, 1982).

### 4.2.2 Results

The mass balances obtained in Table 24-15 are generally satisfactory, in spite of the measurement difficulties noted in Section 4.2.1. Sulfates and organics are consistently the major contributors to fine-particle mass. Together with nitrates (which are major constituents in western cities), they typically accounted for three quarters of the observed total.

Figure 24-41 shows that both sulfates and organics were empirically associated with dry scattering: studies with high average concentrations of either fraction tended to yield high average scattering coefficients. The linear regression (n = 48) of study average **B**sfd on study average $[SO_4^=]f$ and $[C_{org}]f$ accounts for ($r^2$ =) 95% of the observed variance in dry fine particle scattering. The addition of $[NO_3^-]_f$ and other explanatory variables does not improve this fit, and the regression on total fine mass accounts for only 78%. The observed association between $C_{org}$ and **B**sfd is reassuring given the concerns raised in Section 4.2.1 over $C_{org}$ sampling artifacts, as the **B**sfd measurement is made *in situ*. (The association of **B**sfd with $C_{org}$ does not rest solely on the influential point in the lower right hand corner of the figure. Deletion of this point, which represents nighttime measurements during two winter months in Albuquerque, lowers $r^2$ from 0.948

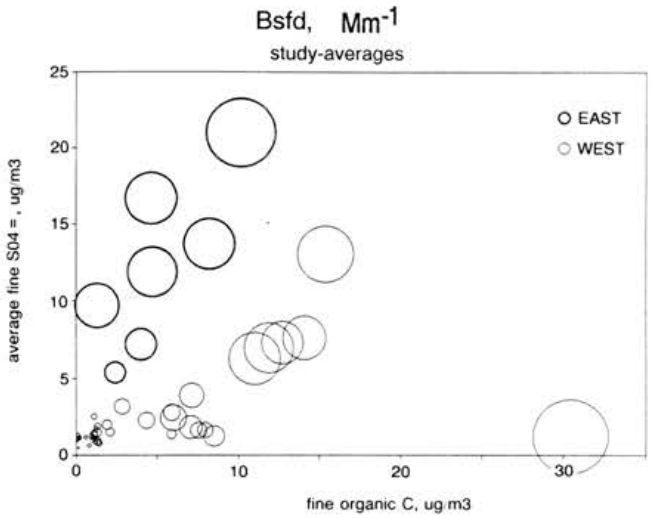


*Figure 24-41 The relationship, over all studies in Table 24-15, of dry scattering to sulfate and organic carbon. Each circle corresponds to one line in Table 24-15. The circle's center indicates the study's mean fine particle sulfate and organic carbon concentrations. The circle's radius is proportional to the study's mean dry fine particle scattering. The sulfate and organic carbon concentrations together account for 95% of the observed variance in Bsfd. Eastern and western studies are distinguished as indicated.*

to 0.945 and shifts the ordinary least squares regression relationship from **B**sfd = 1.8 + (6.6 ± 0.4) $[SO_4^=]f$ + (5.5 ± 0.3) $[C_{org}]f$ to **B**sfd = 3.0 + (7.1 ± 0.5) $[SO_4^=]f$ + (4.7 ± 0.5) $[C_{org}]f$).

Table 24-15 and Figure 24-41 show a clear East-West difference in the relative abundance of sulfates. Fine sulfates consistently account for half or more of the measured fine mass in the East and less than half in the West. Within the West, there are further differences. Sulfates account for 40 - 45% of the fine mass on the Colorado plateau but only 10 - 20% in western cities. Organics, the next most abundant constituent overall, exhibit no obvious gradients. Measured nitrate concentrations are significant only in the West. As in Tables 24-13 and 24-14, unpublished SCENES data provide the chief exception to these generalizations (in this case, a sulfate concentration accounting for the majority of fine particle mass at Prescott).

Table 24-15 and Figure 24-41 provide sparse coverage of the East, including only two urban studies and one non-summer study. The importance of sulfates in this region

has been amply documented, however, by large-scale monitoring programs which lacked scattering or carbon measurements. Table 24-16 presents results from two such networks, together with preliminary data from a new visibility monitoring program. The sulfate/mass ratios are consistent with those observed in the intensive studies of Table 24-15, and exhibit no clear spatial pattern.

## 4.3 APPORTIONING FINE-PARTICLE SCATTERING TO CHEMICAL FRACTIONS

*W. White*

The extinction and particle mass budgets of Sections 4.1 and 4.2 are well formulated, however difficult they may be to determine. Individual entries are unambiguously defined, relevant to certain control strategies, and—at least in principle—open to direct measurement. More fundamentally, those budgets are legitimate in the sense that the totals are the sums of the entries..

The present section addresses the problem of relating particle scattering to particle composition. The relationship is conventionally presented as another budget, the entries representing the scattering associated with individual species. In contrast to the earlier apportionments, however, the entries in such scattering "budgets" can be defined in various ways, are impossible to measure, and need not be additive.

### 4.3.1 Aerosol Microstructure and the Theoretical Basis for Apportionment

The theoretical legitimacy of particle scattering budgets depends on the manner in which particulate matter is physically partitioned into species. The scattering increments contributed by distinct particles are additive, whereas the scattering increments contributed by distinct fractions within the same particle are not (Feynman *et al.*, 1963).

Two particulate species are said to be externally mixed if they are carried by disjoint particle populations. Fine and coarse particles, which constitute disjoint populations by definition, provide a trivial example of externally mixed species. Fine particle and coarse particle scattering are thus additive, as tacitly assumed in Section 4.1, and are

*Table 24-16. Fine Particle Sulfate Contents From Monitoring Networks in the Rural East*[a]

| Network | Site | Annual | | Summer | |
|---|---|---|---|---|---|
| | | FM($\mu g/m^3$) | SLF/FM(%) | FM($\mu g/m^3$) | SLF/FM(%) |
| NPS[b] | Acadia, ME | 6 | 46 | 6 | 39 |
| SURE[c] | Montague, MA | 17 | 43 | 26 | 51 |
| SURE | Scranton, PA | 17 | 48 | 27 | 47 |
| SURE | Fort Wayne, IN | 20 | 41 | 22 | 61 |
| SURE | Duncan Falls, OH | 21 | 53 | 25 | 58 |
| SURE | Indian River, DE | 19 | 43 | 23 | 64 |
| NPS | Shenandoah, VA | 10 | 57 | 16 | 55 |
| SURE | Lewisburg, WV | 16 | 52 | 19 | 62 |
| SURE | Rockport, IN | 24 | 47 | 26 | 56 |
| SURE | Research Triangle Park, NC | 19 | 45 | 23 | 49 |
| NPS | Great Smokey Mountains, TN | 12 | 52 | 19 | 49 |
| SURE | Giles County, TN | 19 | 51 | 21 | 49 |
| EFPVN[d] | Look Rock, TN | 13 | 59 | 23 | 53 |
| NPS | Buffalo River, AR | 10 | 52 | 13 | 47 |
| | Average | 16 | 49 | 20 | 53 |
| | Standard Deviation | 5 | 5 | 5 | 7 |

[a] Quantities are as in Table 24-15.

[b] National Park Service Particulate Monitoring Network (Eldred et al., 1987; Malm, personal communication 1990). Data cover the period 6/82-5/86; summer data are from June, July, and August. Values are averages and ratios of averages.

[c] Sulfate Regional Experiment (Mueller and Hidy, 1983). Annual data are from the "intensive" months October 1977, January 1978, April 1978, July 1978; summer data are from August 1977 and July 1978. Values are averages and ratios of averages.

[d] Eastern Fine Particle Visibility Network (Evans, personal communication 1990). Values are medians and ratios of medians for 1988 data.

legitimately resolved in the extinction budgets of Tables 24-13 and 24-14.

Two species are said to be internally mixed if individual particles contain both species. Water, for example, is internally mixed with its hygroscopic hosts. As illustrated below, the scattering increments contributed by internally mixed species are not generally additive and not legitimately resolvable in extinction budgets.

The relevance of the foregoing distinctions to the apportionment of extinction can be seen most clearly in the simplest of examples. Consider an aerosol of ultrafine (Rayleigh-scattering) particles, composed in equal parts of two species with identical optical characteristics. This aerosol can be assembled in a variety of ways. Figure 24-42 illustrates two simple alternatives, a pure external mix and a uniform internal mix. The distribution of species with respect to particle size is the same in either assemblage, all of each species being carried by doublets. The two microstructures are thus indistinguishable by bulk analyses, even if the latter are resolved by particle size.

Despite their initial similarity, the two models yield differing residues when one species is removed through control measures. The aerosol remaining from the external mixture consists of doublets, while that from the internal mixture consists of singlets. Because the scattering/volume ratio of Rayleigh particles is proportional to particle volume, the doublet aerosol scatters twice as much light.

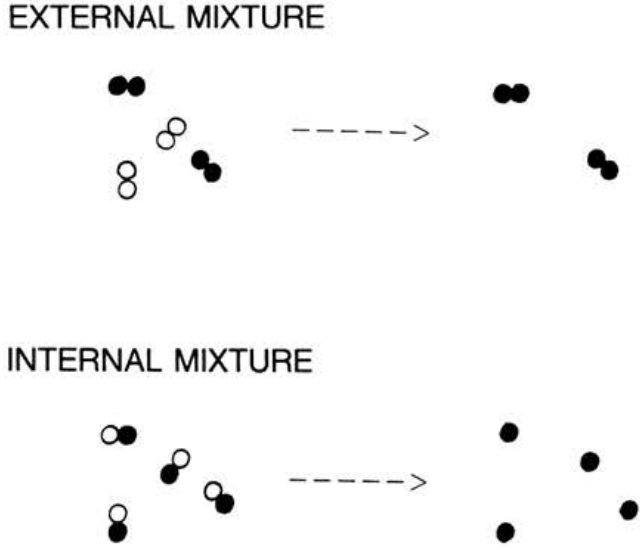


*Figure 24-42 Two distinct possibilities for the response of an aerosol to the removal of a constituent. The model aerosols are composed of two species, one of which (drawn in white) is eliminated by controlling emissions. The initial aerosols have identical size-resolved chemical compositions, but the remaining aerosols consist of doublets in the external mixture model, singlets in the internal mixture model.*

The scattering from the internally mixed aerosol of Figure 24-42 can be apportioned in differing ways. The simplest approach is to attribute half of the total scattering to each species, on the basis of symmetry. The budget entries then sum correctly, but they fail to predict the consequences of control (elimination of either species eliminates three quarters of the original scattering). An alternative accounting can be based on the scattering decrements/increments produced by removing/adding species. This approach illuminates the consequences of controls, but it does not yield a budget in which the parts sum to the whole: $3/4 + 3/4 > 1$.

The differing accounting schemes yield identical apportionments for the externally mixed aerosol in Figure 24-42, both procedures attributing half of the total scattering to each species. Fundamentally, this consistency arises from the fact that the externally mixed aerosol can be viewed as a mechanical mixture of physically distinct sub-aerosols, each with its own well defined extinction coefficient.

The theoretical basis for the apportionment of particle scattering in a general setting is developed by White (1986). In general, the scattering decrement is not even proportional to the volume decrement. (In the Rayleigh regime, for example, $\Delta \mathbf{B}sp/\mathbf{B}sp = (\Delta V/V)\ (2 - \Delta V/V)$ for internally mixed species of identical optical characteristics.) The ratio of scattering decrement to volume decrement, known as scattering efficiency, depends in a complex manner on the optical characteristics and particle size distributions of both the species removed and the species left behind. The nonlinearities arising from such factors are of limited magnitude, however. The coupling between particle size and concentration multiplies efficiencies by a factor between 2/3 and 2, approaching the extreme values only in the large and small particle limits where efficiencies approach zero. Figure 24-43 shows how calculated efficiencies vary with particle size and microstructure for one simple but representative class of aerosols generalizing the example shown in Figure 24-42.

The non-additivity of the scattering contributed by sulfates in a specific observed aerosol has been quantified by Sloane (1986). Using an internal mixture model based on impactor measurements of the Detroit aerosol, Sloane finds scattering efficiencies about 10% higher than would be calculated from the equivalent external mixture model. This value may be representative of the urban East, but is likely to be low for the arid West where sulfate is typi-

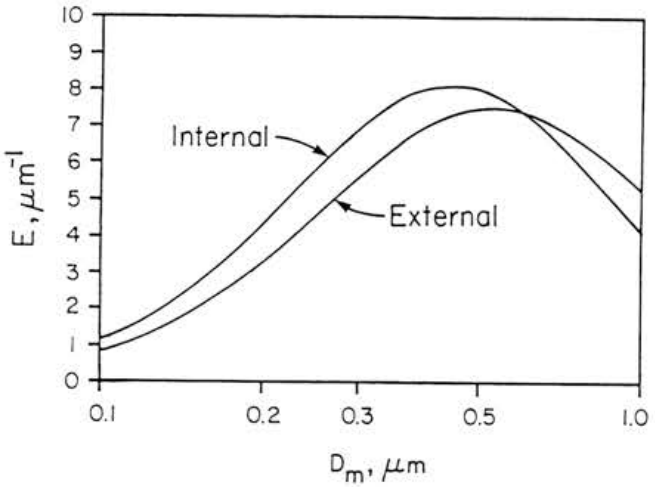


*Figure 24-43 Calculated scattering efficiencies at 550 nm of externally and internally mixed particle species. The scattering efficiency E (scattering contribution/volume contribution) is plotted as a function of the volume-median particle diameter $D_M$. The distribution of volume with respect to particle size is log normal with geometric standard deviation 1.6, and the refractive index of both species is 1.5. The scattering efficiency of an externally mixed species is determined by that species' volume distribution. The scattering efficiency of an internally mixed species is affected by its relative abundance in the aerosol and by the distribution of the remaining material with respect to particle size; the curve shown here is for a species contributing half of the total volume and distributed like the rest of the aerosol.*

cally carried by smaller particles. Sloane's detailed estimate is consistent with the simpler calculation shown in Figure 24-43, where the scattering efficiency in the internal mixture model is similarly enhanced by about 10% at the mass median diameter (about 0.45 μm at 60% RH) of Detroit sulfate. In the West, where mass median diameters in the range 0.2 - 0.3 μm are common (Hering *et al.*, 1981; Hering and Friedlander, 1982; Ouimette *et al.*, 1981; Watson *et al.*, 1988), the non-additivity indicated by Figure 24-43 rises to 25% - 35%.

Empirical evidence on the actual microstructure of ambient aerosols is limited, but indications are that reality is more complex than the idealizations on which existing models have been based. The most detailed measurements to date are those of Buseck and coworkers in the vicinity of Phoenix (Post and Buseck, 1984; Anderson *et al.*, 1988); their single particle analyses show sulfates to be associated with other species in a variety of different particle types but also show a significant minority of particles containing no detectable sulfur. The finding that sulfate is internally mixed with much of the remaining aerosol is as expected, given its *in situ* production in atmospheric reactions. The finding that some particles contain no sulfate is consistent with measurements at other locations that show substantial fractions of the fine particle mass to be contributed by hydrophobic particles (Covert and Heintzenberg, 1984; Harrison, 1985; McMurry and Stolzenburg, 1989).

The discussion has so far proceeded on the assumption that the removal of one species from a particle does not affect the masses of the remaining species in that particle. Figure 24-44 suggests some possible alternatives to such passive external and internal mixtures:

- Species 1 and 2 may be mutually antagonistic in the particulate phase, so that the removal of Species 2 permits additional condensation by Species 1. The scattering efficiencies in this case can be small or even negative. Such antagonism appears to exist between sulfates and nitrates (Harker *et al.*, 1977), sulfuric acid taking the cation from ammonium nitrate and liberating nitric acid to the gas phase. The effect of such competition is to attenuate the benefits of sulfate control in nitrate rich environments (Pilinis, 1989).
- Species 2 may be an active nucleus which depresses the equilibrium vapor pressure of Species 1. Under unsaturated conditions, the partial removal of Species 2 then eliminates Species 1 in the same proportion. In this manner, the scattering efficiency of hygroscopic species such as sulfuric acid and its ammonium salts are inflated by water (Garland, 1969; Covert *et al.*, 1972). That is, the scattering decrements to be expected from sulfur controls are leveraged by reduced liquid water concentrations.
- The equilibrium vapor pressure of Species 1 may be so low that its particulate-phase abundance is limited by gas-phase production rather than the availability of nuclei. The scattering efficiency of Species 2 is then diminished because the partial removal of Species 2 concentrates the condensation of Species 1 on fewer nuclei, increasing the mean particle size of the remaining aerosol (White and Husar, 1980). The gas-phase production of sulfuric acid in hazy air probably illustrates this phenomenon (McMurry and Friedlander, 1979). Under such conditions,

increasingly tight controls on primary particle emissions may have little impact on total scattering.

- Species 2 may physically coat the more volatile Species 1. Under unsaturated conditions, contributions from the imprisoned species then augment the scattering efficiency of the coating. Husar and Shu (1975) and Chang and Hill (1980) presented electron micrographs evidence suggesting that pollutant films may retard the evaporation of coastal fogs in the Los Angeles basin, and Rubel and Gentry (1984) have directly demonstrated stabilization of water droplets by partially evaporated organic coatings in the laboratory. The mass of the coating is a tiny fraction of the total, and control of the species involved could thus yield vastly disproportionate reductions in scattering.

Taken together, the examples of Figure 24-44 indicate that the scattering decrement produced by a given control strategy depends not only on the microstructure of the particulate phase but also on the relationship of the particulate phase to the gas phase.

### 4.3.2 Apportionment Strategies

It is clear from the preceding section that any "budget" resolving scattering by fine particles into the contributions of their constituent species must be somewhat inexact. Budgets are so familiar, however, and seem so natural a way of summarizing results, that they are difficult to avoid. The present section derives a set of fine particle scattering budgets which are explicitly inexact, yet informative in their gross features.

The soundest estimates of the scattering attributable to individual chemical species are those computed using models fitted to the size-resolved composition of the observed aerosol. Such models explicitly simulate the physical cause and effect relationship and the best utilize all of the data available on the aerosol's properties. It must be recognized, however, that even the most fundamental of these models incorporate important assumptions about particle structure, condensed water, and other unobserved aspects of the aerosol (White, 1986).

In practical terms, the most severe limitation of model derived apportionments is that they have not yet been generated for many locations. Comprehensive studies accounting for condensed water have been presented only for Denver (Sloane, 1983a and 1984a; Watson *et al.*, 1988) and Detroit (Sloane and Wolff, 1985; Sloane, 1986 and 1988), and only the most recent of these (Sloane, 1986 and 1988; Watson *et al.*, 1988) fully account for the effects of internal mixing. Even the simpler studies,

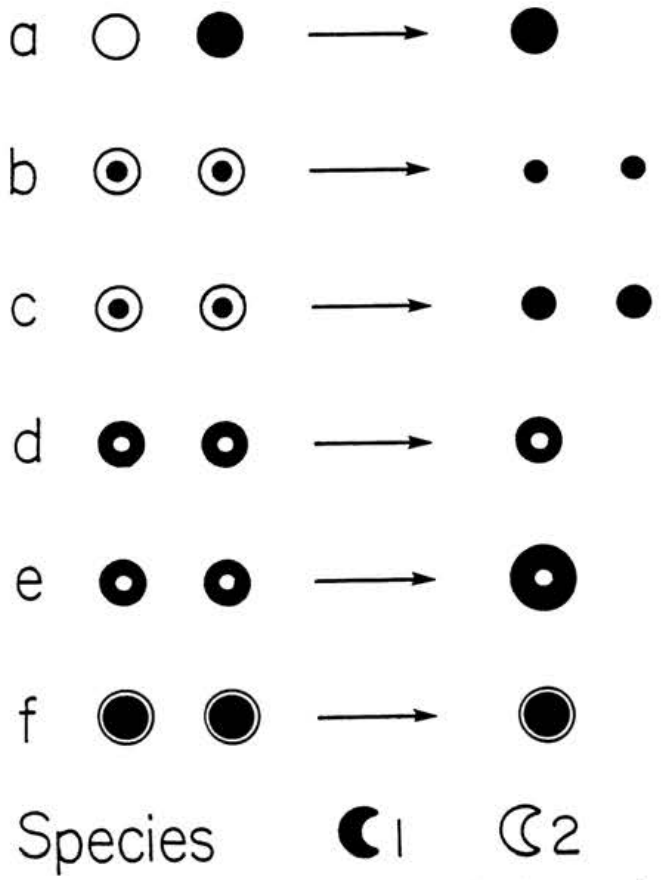


*Figure 24-44 The response of an aerosol to the removal of a constituent. Some examples are (a) non-volatile species, externally mixed; (b) non-volatile species, internally mixed; (c) species mutually antagonistic in the particulate phase; (d) condensate and nuclei, nuclei-limited; (e) condensate and nuclei, condensate-limited; and (f) volatile species coated by non-volatile species.*

which neglect water and the effects of internal mixing, have been presented only for the Mojave Desert (Ouimette *et al.*, 1981; Ouimette and Flagan, 1982; Trijonis *et al.*, 1988) and northern Arizona (Macias *et al.*, 1981a and 1981b; Malm *et al.*, 1987a).

A much wider range of apportionment estimates is available from multiple regression analyses of the empirical relationship between extinction and aerosol composition. Such studies are too numerous to list conveniently, but follow a standard methodology developed by White and Roberts (1977), Cass (1979), Trijonis (1979), and Groblicki *et al.* (1981). In this approach, the statistical association of observed scattering with observed aerosol composition is used to estimate the scattering efficiencies of individual species. Model simulations show the proce-

dure to yield usefully accurate results under favorable conditions (Sloane, 1988). An important liability is that the availability of standard software makes it easy to perform regression under unfavorable conditions.

Regression derived apportionments are vulnerable to a variety of systematic and random errors. At the most basic level, there is the problem that meteorologically driven fluctuations of the existing aerosol may be unrepresentative of the perturbations produced by control measures (White, 1986). A more practical difficulty is that regression results can be biased by errors in the measurements, even though the errors are themselves random; standard regression estimates tend to overrate the contributions of precisely measured species like sulfates and underrate those of poorly characterized species like organics (White and Macias, 1987). The high degree of intercorrelation commonly found among aerosol fractions can make regression estimates very sensitive to the choice of species to be included in the analysis (Sloane, 1983a). The resulting range of outcomes is broadened by the random error inherent in any sample statistic, error which is understated by standard estimates (White, 1989). A practical consequence of such indeterminacy is that the final selection of regression models is based in part on the plausibility of the results they generate, making the corresponding apportionments less objective than they may appear.

Several recent studies have addressed the difficulties noted above by basing scattering apportionments on nominal scattering efficiencies synthesized from a variety of estimates (Trijonis *et al.*, 1988; Watson *et al.*, 1989; Malm *et al.*, 1989). A similar approach is used in this review to derive consistent apportionments from heterogeneous data sets. Scattering by dry particles is prorated among all species on the basis of their mass concentrations, with species concentrated in the secondary accumulation mode assumed to scatter more efficiently than others. Scattering by condensed water is then prorated among hygroscopic species on the basis of their mass concentrations. To give some idea of their uncertainty, the resulting apportionments are presented for a range of assumptions about species size distributions and hygroscopicity. As the contributions of different species are not necessarily additive, the assumptions underlying high and low estimates are not necessarily complementary.

Table 24-17 summarizes the scheme used here to estimate scattering by fine particle sulfates and organics from the data in Tables 24-13 and 24-15. The low and high estimates are neither absolute bounds based on physical law, nor statistical confidence limits based on rigorous analysis of the uncertainties identified in Section 4.3.1. Instead, they are intended as indications of the ranges within which results from diverse apportionment schemes would fall. The main point to be drawn in Section 4.3.3 from these computations is that certain features of the fine particle scattering budget are quite insensitive to the details of the accounting method.

The low estimate for sulfates' contribution assumes that sulfates, nitrates, and organics all scatter twice as efficiently as the remaining fine aerosol, and that sulfates,

*Table 24-17. Apportionment Scheme for Fine Particle Scattering*[a]

| | Low Estimates | High Estimates |
|---|---|---|
| Dry Sulfates<br>**B**sfd (SLF) | [2SLF/(SLF+NTR+ORG+FM)]**B**sfd | [2SLF/(SLF+FM)]**B**sfd |
| Associated Water<br>**B**sfw (SLF) | [SLF/(SLF+NTR+0.5ORG)](**B**sf-**B**sfd) | [SLF/(SLF+NTR)](**B**sf-**B**sfd) |
| Ambient Sulfates<br>**B**sf (SLF) | **B**sfd(SLF) + **B**sfw(SLF) | **B**sfd(SLF) + **B**sfw(SLF) |
| Dry Organics<br>**B**sfd (ORG) | [ORG/(SLF+FM)]**B**sfd | [3ORG/(2ORG+SLF+FM)**B**sfd |
| Associated Water<br>**B**sfw (ORG) | 0 | [0.5ORG/(SLF+NTR+0.5ORG)](**B**sf-**B**sfd) |
| Ambient Organics<br>**B**sf (ORG) | **B**sfd(ORG) + **B**sfw(ORG) | **B**sfd(ORG) + **B**sfw(ORG) |

[a] Figures 24-45 and 24-46 illustrate the scattering attributed to sulfates and organics if observed scattering is prorated by mass according to the range of assumptions summarized here.

nitrates, and half of the organics are hygroscopic. The reasoning behind the low dry value is that sulfates are consistently found in the accumulation mode, wherever the other secondary species may be. The high estimates for sulfates' contributions assumes that sulfates alone scatter twice as efficiently as all other fine aerosol, and that only sulfates and nitrates are hygroscopic. For some studies, the high dry value corresponds to efficiencies in the upper range of those theoretically possible for plausible sulfate size distributions.

The low estimate for organics' contribution assumes that organics and other non-sulfate species scatter half as efficiently as sulfates, and that organics are hydrophobic. In part, the low dry value reflects uncertainties over organic particle size distribution and the role of sampling artifacts. The high estimate for organics' contribution assumes that organics scatter thrice, and sulfates twice, as efficiently as the remaining fine aerosol, and that organics are half as hygroscopic as sulfates and nitrates. The organics sulfate differential in the high dry value represents the differing specific volumes of fractions with similar refractive indices.

All estimates acknowledge the known affinity of the major sulfate and nitrate species for water, together with the uncertain composition and hygroscopicity of the organic fraction.

To help relate the apportionments derived here to those in the literature, Appendix H lists for each study the dry scattering efficiencies implicit in the present scheme. When making comparisons, it should be recognized that stated efficiencies can differ significantly from the effective efficiencies implicit in accompanying apportionments. This discrepancy arises from the common, but often undocumented, practice of adjusting calculated contributions so that they sum to the observed extinction. Varying conventions on extinction wavelength and mass accounting also affect stated values.

### 4.3.3 Results

Figures 24-45 and 24-46 display the scattering estimates derived from Tables 24-13, 24-15, and 24-17. Figure 24-45 shows scattering by sulfates and organics as a percentage of total fine particle scattering. Figure 24-46 replots these estimates as a percentage of non-Rayleigh extinction. The figures include all studies meeting the criteria of both Tables 24-13 and 24-15.

Certain patterns in the species scattering contributions clearly transcend the uncertainty of the estimates:

- In the eastern United States, fine particle scattering accounts for better than three-fourths of total non-Rayleigh extinction, and sulfates account for the majority of fine particle mass. The only other strongly hygroscopic fraction, ammonium nitrate, is found at very low concentrations. The conclusion that sulfates, and the water associated with them, are the dominant source of extinction in the East is therefore insensitive to the details of the apportionment procedure. Moreover, the calculations of Sloane (1986) suggest that the sulfate contribution is approximately additive. Although the values in Figures 24-45 and 24-46 represent only the two urban and two rural sites for which complete data are available, they are consistent with the particle data from other locations summarized in Tables 24-13 and 24-15.
- In the urban West, fine particle scattering accounts for less than two-thirds of non-Rayleigh extinction at most sites, and fine particle organics and nitrates are each as abundant as sulfates. The conclusion that sulfates are but one of several major sources of extinction in western cites is thus again insensitive to the details of the calculation and the probably significant non-additivity of the sulfate contribution. Although the values in Figures 24-45 and 24-46 represent only three different metropolitan areas, they are consistent with the composition data from other cities summarized in Table 24-15.

The results for the rural West show significant regional variations. The estimates for sulfate contributions to fine particle scattering are typically upwards of 50% in northern Arizona and southern Nevada and Utah, and less than 50% in the Mojave desert of California. The estimates for sulfate contributions to total non-Rayleigh extinction are especially heterogeneous. At China Lake they approach the low values obtained in western cities, while at some SCENES sites they approach the high values of the East. The entire northern two-thirds of the West is unrepresented in the scattering and extinction estimates due to a lack of ambient optical measurements. However, Table 24-15 shows a strong north-south gradient in fine particle composition, with sulfate/organic ratios from decreasing 2:1 in the south to 2:3 in the north.

## 4.4 SUMMARY
*W. White*

Table 24-18 condenses the individual estimates of the preceding sections into nominal budgets of the extinction associated with sulfur and nitrogen oxides. This table is patterned on an earlier review by Trijonis (1987) (Appendix E) which considered more narrowly the optical impacts of $NO_2$ and nitrates, examining several $NO_2$ and nitrate data sets not complete enough for inclusion here.

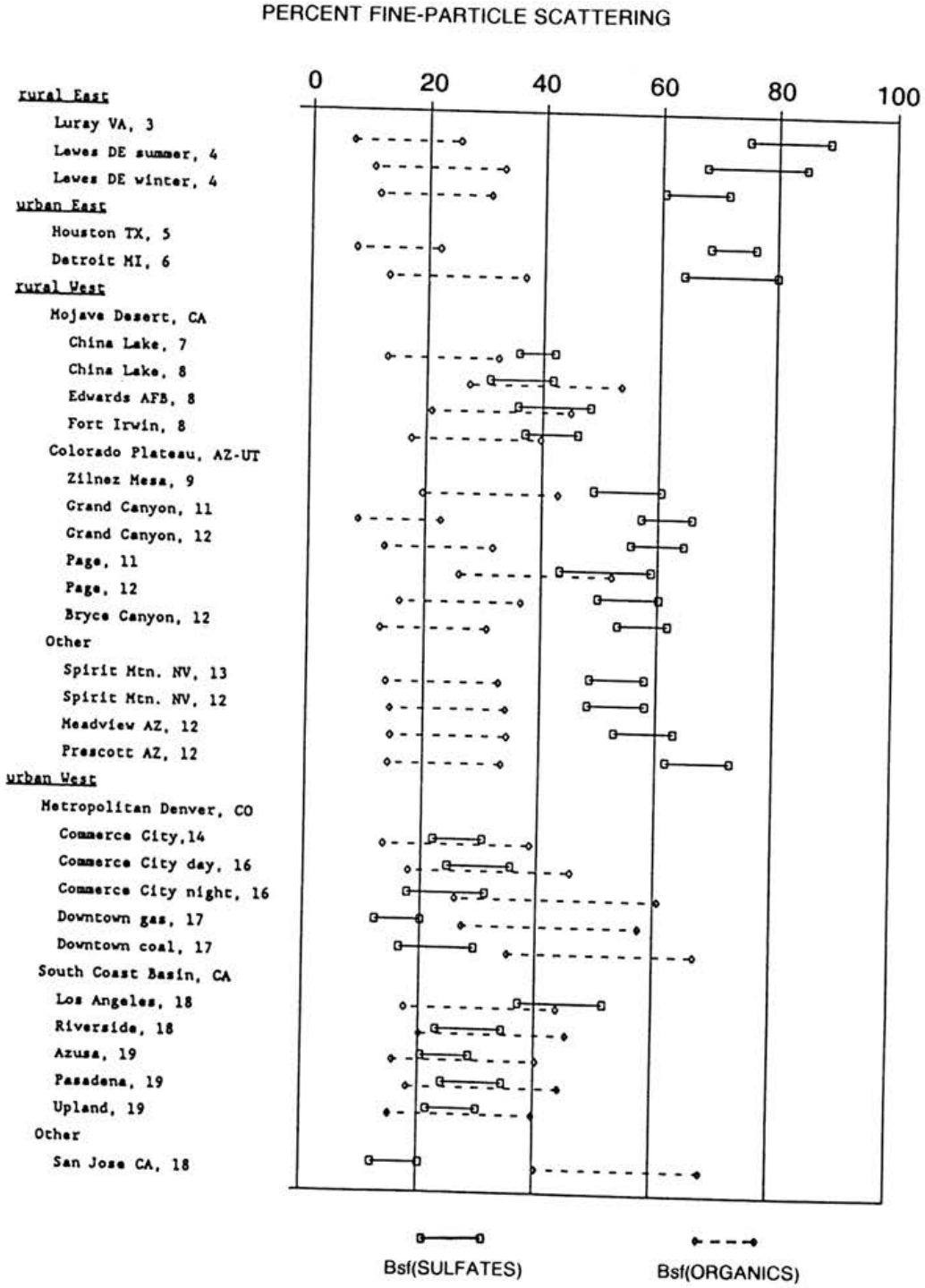


*Figure 24-45 Relative contributions of fine sulfates and organics to ambient fine particle scattering, according to a range of assumptions. Calculations are summarized in Table 24-17 and studies are as in Table 24-13.*

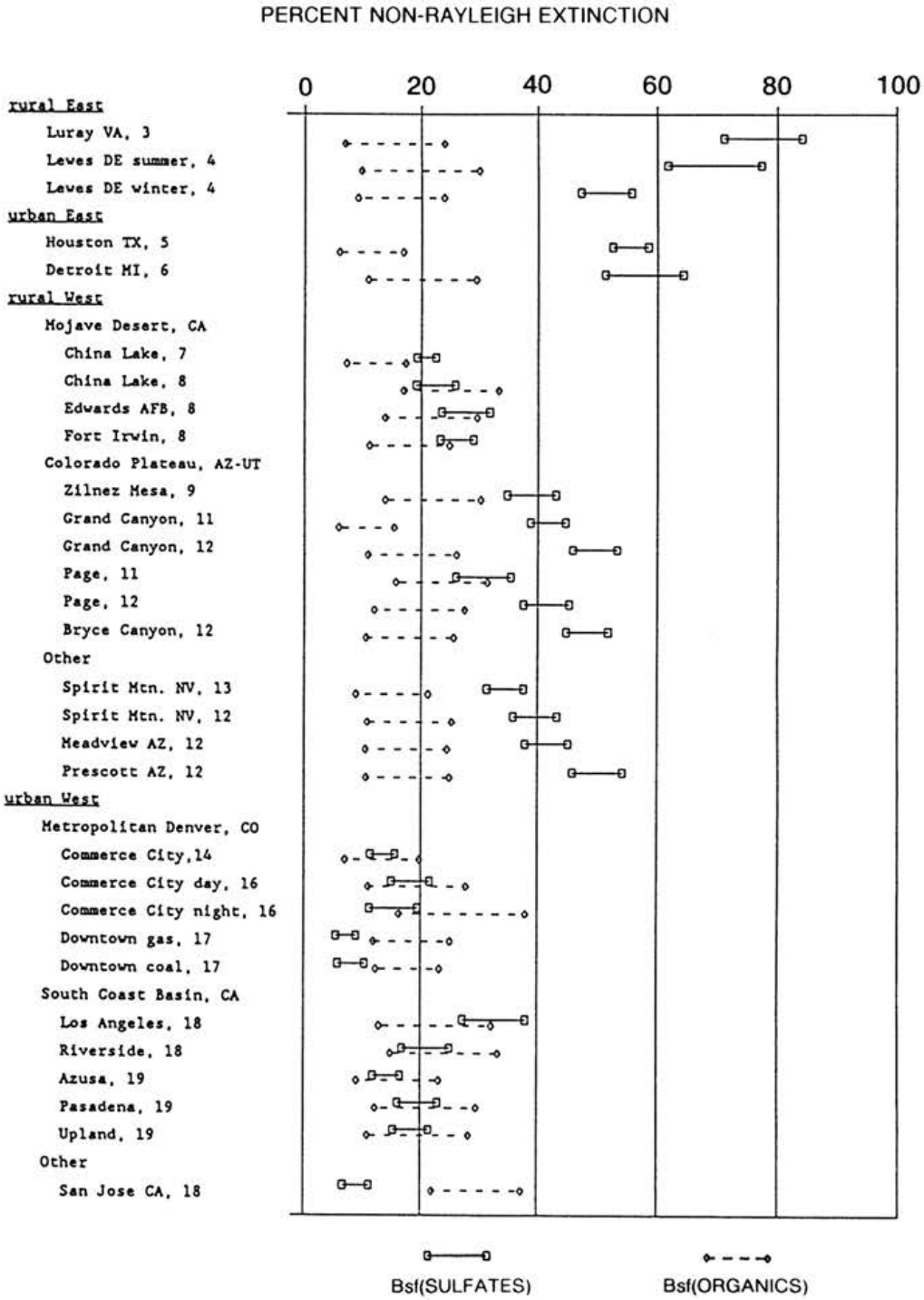


*Figure 24-46 Relative contributions of fine sulfates and organics to total non-Rayleigh extinction, according to a range of assumptions. Calculations are summarized in Table 24-17 and studies are as in Table 24-13.*

*Table 24-18. Budgets of the Extinction Associated with Sulfur and Nitrogen Oxides*[a]

| | Urban East | | | | Rural East | | |
|---|---|---|---|---|---|---|---|
| | $SO_x$ | $NO_x$ | Total Aerosol | | $SO_x$ | $NO_x$ | Total Aerosol |
| **B**sf | 55±10 | 4±3 | 75±10 | **B**sf | 60±10 | 4±3 | 85±10 |
| **B**sc | | | 5±3 | **B**sc | | | 3±2 |
| **B**ap | | | 13±5 | **B**ap | | | 8±5 |
| **B**ag | | 7±5 | 7±5 | **B**ag | | 3±2 | 3±2 |
| **Be-B**$_R$ | 55±10 | 10±6 | 100 | **Be-B**$_R$ | 60±10 | 7±4 | 100 |
| | **Urban West** | | | | **Rural West** | | |
| | $SO_x$ | $NO_x$ | Total Aerosol | | $SO_x$ | $NO_x$ | Total Aerosol |
| **B**sf | 15±5 | 15±10 | 60±15 | **B**sf | 30±20 | 6±6 | 70±15 |
| **B**sc | | | 12±5 | **B**sc | | | 17±10 |
| **B**ap | | | 18±10 | **B**ap | | | 10±10 |
| **B**ag | | 10±5 | 10±5 | **B**ag | | 3±3 | 3±3 |
| **Be-B**$_R$ | 15±5 | 25±10 | 100 | **Be-B**$_R$ | 30±20 | 10±7 | 100 |

[a] Values are given as percentages of total non-Rayleigh extinction at 525 nm.

The contributions of individual extinction components to the totals are taken from Table 24-14, while those of fine particle sulfates are taken from Figure 24-46. The values for $NO_2$ absorption are generally concordant with those in Appendix E except in the rural West, which Table 24-18 treats as a more remote environment than that considered in the earlier review. The contributions of fine particle nitrates are scaled to those of sulfates according to the nitrate/sulfate ratios in Table 24-15 and in the East are adjusted to take the findings of Appendix E into account. The entries are intended to be representative of annual averages in each geographical category, qualified by subjective estimates of the 68% (± 1 sigma) confidence limits corresponding to both scientific uncertainty and actual variability. All values are expressed as percentages of total non-Rayleigh extinction at 525 nm. It must be understood that a good deal of subjective judgment is involved in choosing representative values for quantities which are as sparely and unevenly sampled as those considered here.

The budgets of Table 24-18 are broken out in terms of individual extinction components, because different types of extinction have different effects on visibility (Richards, 1987 and 1990). As discussed in Section 4.3.1, the contributions of individual chemical fractions to particle scattering need not be additive. All of the entries are based on study averaged data, because these data are retrievable from the literature. They may imperfectly represent conditions on the clearest and haziest days, which may be valued more strongly by the human observer.

The accounting principle underlying the budgets of Table 24-18 is that all scattering by particulate sulfate and nitrate compounds is "associated" with emissions of sulfur and nitrogen oxides. Such an apportionment seems appropriate to this document, which treats improved visibility as a collateral benefit of controls on $SO_2$ or $NO_x$ emissions. It should be noted, however, that reducing $SO_2$ or $NO_x$ emissions is not necessarily the only way to reduce ambient sulfate and nitrate concentrations. In some western cities, for example, ammonia from cattle feedlots might be a more effective target for controlling ammonium nitrate, the dominant particulate nitrate species. Likewise, controlling hydrocarbons and/or nitrogen oxides to reduce urban ozone levels may reduce ambient sulfate concentrations by slowing the oxidation of $SO_2$ emissions. It should also be noted that this document has not addressed the functional relationship of the predominantly secondary sulfates and nitrates to emissions of $SO_2$ and $NO_x$. Controlling $SO_2$ and $NO_x$ may not always yield proportionate reductions in ambient sulfate and nitrate concentrations.

# SECTION 5

# EFFECTS OF ATMOSPHERIC OPTICAL CHARACTERISTICS

The purpose of this section is to summarize the current level of air pollution effects on light transmission in the atmosphere by comparing current effects with natural background. Section 5.1 deals with methodologies and results in regard to illustrating visibility effects. Section 5.2 deals with climate effects.

## 5.1 ASSESSMENT OF CURRENT VISIBILITY EFFECTS

*W. Malm*

A major challenge in assessing the effects that aerosol concentrations have on visibility is to link aerosol chemical and physical properties to the visual appearance of the scene as judged by the public. It is possible, with varying degrees of accuracy, to model or monitor the effect that pollutants, in combination with various lighting conditions, have on optical variables such as chromaticity, contrast, extinction coefficient, or visual range. Yet it is difficult for scientists and decision makers to "visually interpret" changes in any of these parameters for themselves, much less to quantitatively relate the changes to the general public's judgment of visual air quality.

Probably the easiest and most reliable way to illustrate changes that atmospheric and optical variables have on a scenic resource is through the use of photography. As discussed earlier in the report, studies have demonstrated that human response to photographs often is highly correlated with human judgment of the actual scene. As a result, photographs can serve as surrogates for reality when attempting to determine public response to changes in visual air quality.

In principle, if optical variables were measured at the same time color photographs were taken, it would be possible to establish a "data base" that would show pictorially the correspondence between measured values and the appearance of the scenic resource. The approach requires the gathering of data for a specific scene under a wide variety of atmospheric conditions and the careful collection of human responses to photographs of the different conditions. While such an approach has the potential for being most accurate in terms of characterizing the relationship between the visibility impacts and atmospheric properties, it does require collection of high quality atmospheric, photographic, and public response data.

An alternate to actually taking photographs in conjunction with optical measurements is to use "image processing" techniques to simulate the desired effect (Williams *et al.*, 1980; Malm *et al.*, 1983). This method employs results from atmospheric optical models designed to simulate the effects that changes in aerosol and optical parameters have on a scene. The "image processed" photographs can then be used in studies characterizing the human response to the visual degradation in an area as well as for "visual interpretation" of changes in atmospheric properties.

### 5.1.1 Review of Visibility Image Processing System (VIPS)

The use of image processing techniques to show the effect on visibility of adding aerosols or absorbing gases to the atmosphere was first done by Williams *et al.* (1980). Williams *et al.* used image processing to visually show the appearance of plumes with varying size, color, and contrast. Malm *et al.* (1983) developed a methodology for using image processing techniques to create photographs showing the effects of uniform haze on landscape features. Their original approach did not account for matrix effects of the colorwrite system (matrix effects refer to the fact that exposing film to green light will not only effect the "green" emulsion layer but also the "red" and "blue" layer and so forth), the change in color of sky and path radiance as a function of aerosol load, the explicit calculation of effects of ground reflectance on sky and path radiance, or the effects of multiple scattering. Over the years each of these problems have been addressed and can now be accounted for (Johnson *et al.*, 1988). Larson and Cass (1988) have also developed the capability to show effects of atmospheric aerosols on visibility and have applied them to the urban visibility problem in Pasadena, California. Figure 24-47 is a flow diagram outlining a visibility image processing system (VIPS).

### 5.1.2 Demonstration of VIPS

Figures 24-48, 24-49, 24-50, and 24-51 (Color Plates 24-1 and 24-2) are photographs of Grand Canyon National Park, AZ; Denver, CO; Shenandoah National Park, VA; and Chicago, IL, taken on days when the atmosphere was nearly free of visibility reducing particles. These photographs will be used to demonstrate the image processing technique by illustrating the effect of relative humidity on visibility conditions. Finally, an assessment of current visibility effects will be made by showing the difference between natural background conditions and current visibility levels.

**ORIGINAL IMAGE**

A 35 mm slide of a landscape feature representing a very clean atmosphere is required as a starting point for the process. The physical-chemical properties of the atmospheric aerosol at the time the slide was taken must be measured or estimated. If the slide was taken on a very clean day, the optical properties of naturally occurring atmospheric gases are assumed.

↓

**DIGITIZING IMAGE**

The selected image is digitized in three "colors" (red, green, and blue). That is, density measurements of the complete slide are made with a 25-micron aperture through three wide band filters. Each density measurement is represented by a digital number (DN) in the range of 0-255. A color file consists of 900 rows by 1350 columns of density measurements. The file representing all three colors consists of 3.6 million density values.

↓

**DISTANCE MASK**

All terrain features of the digital image are separated into distance categories based on the geography of the scene and the camera position.

↓

**COLOR CALIBRATION**

The system must be color calibrated not only for exposure *vs.* density characteristics, but also for color matrix effects. The color calibration incorporates characteristics of the film on which the original picture was recorded as well as the film used to reproduce the altered radiance field. The film is calibrated by exposing film to a series of known exposures that includes a variety of colors and brightness levels and measuring film response.

↓

**CALCULATION OF OPTICAL PROPERTIES OF AEROSOLS**

Models are used to calculate the scattering and absorption properties of the aerosol as a function of size, index of refraction, relative humidity, and other physical properties, such as the relative mix of different chemicals within one particle. The model used is one developed by Tsay et al. (1987). The model allows for externally mixed spherical aerosols as well as multicomponent aerosols that consist of a spherical core with shells of various thickness and physicochemical characteristics. Aerosol growth as a function of relative humidity is calculated following an approach outlined by Hanel (1976).

↓

**RADIATION TRANSFER MODELING**

Radiation transfer models are used to calculate new radiance fields as a function of aerosol properties. A doubling and adding radiation transfer model (Shettle and Feen, 1979) is used to calculate sky radiance fields when the optical depth is sufficiently large to allow a flat earth approximation to hold. Path radiance is then approximated using

$$N_r^* = N_s(1-T)$$

where $N_r^*$ and $N_s$ are the path and sky radiance, while T is the atmospheric transmittance between the observer and landscape feature over which the path radiance is to be calculated. For very clean atmospheres where earth curvature cannot be ignored and when path radiance is explicitly calculated, a Monte Carlo scheme is used to calculate these parameters (Tsay et al., 1987).

↓

**OUTPUTING MODIFIED IMAGE**

The calibrated DN values from the original slide, modeled sky radiance, path radiance, and distance mask are used to generate a new landscape radiance field which is output to a colorwrite system (Malm, 1983). The colorwrite system translates the new calibrated DN values into a color photograph or slide.

↓

**REVIEW AND VERIFICATION**

Finally, the computer generated slide is scanned with a microdensitometer to determine the accuracy of the simulated image. Integrated perceptual indices, such as just noticeable changes, can be calculated from the final density values (Malm and Pitchford, 1989; Carlson and Cohen, 1978).

*Figure 24-47 Flow diagram outlining image processing techniques.*

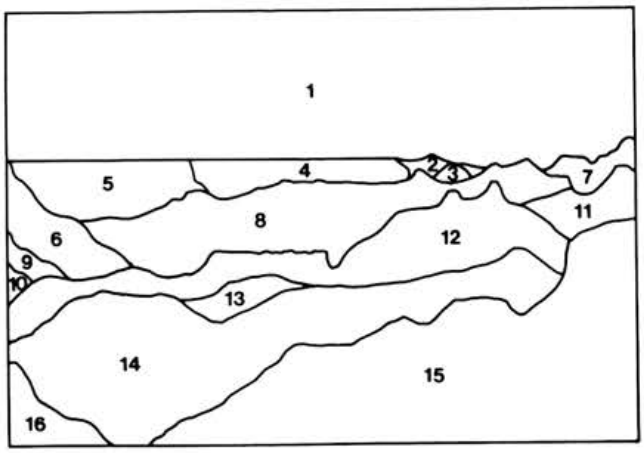


*Figure 24-52 Block diagram outlining the major landscape features of the photograph in Figure 24-48.*

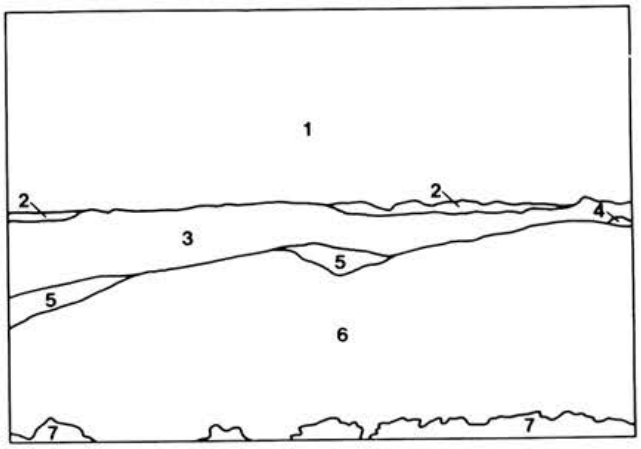


*Figure 24-54 Block diagram outlining the major landscape features of the photograph in Figure 24-50.*

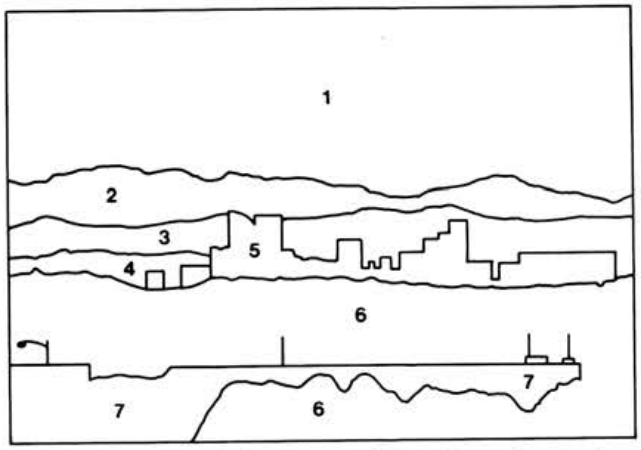


*Figure 24-53 Block diagram outlining the major landscape features of the photograph in Figure 24-49.*

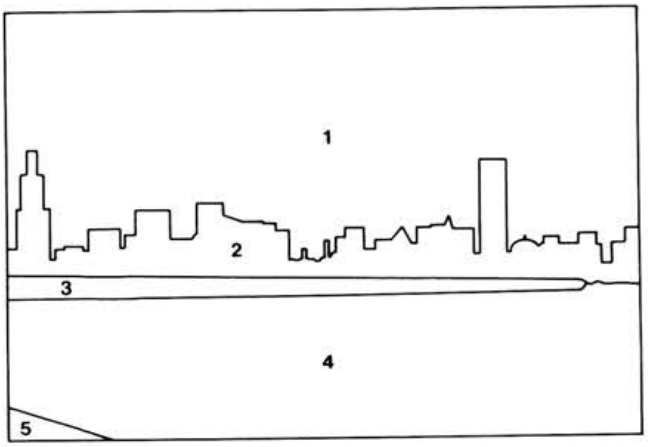


*Figure 24-55 Block diagram outlining the major landscape features of the photograph in Figure 24-51.*

Figures 24-52, 24-53, 24-54, and 24-55 show block diagrams outlining the major landscape features in each of the pictures, while Table 24-19 lists the distances to each feature. These figures form the "mask" used in the radiation transfer and modifying image sections of the VIPS.

The first demonstration utilizes Grand Canyon and Chicago to show the effect of relative humidity on visibility impairment. For Grand Canyon, the National Park Service (NPS) particulate data base was used to derive average summertime concentrations (1979-1985) of various dry aerosol species. The aerosols were broken out into three modes. The first mode consists of coarse mass *(2.5-15 microns)* and fine soil, the second mode is made up of only soot, while mode 3 is all in the fine mass *(0.0-2.5 microns)* size range. Mode 3 is made up of ammonium sulfate and other fine mass which is primarily organics and some nitrates. Table 24-20 shows the average summertime total mass as well as the percent mass each aerosol species contributes to the total mass. Mode 3 is the only mode considered to be hygroscopic. Since there hasn't been an aerosol characterization study carried out in Chicago, a number of assumptions had to be made for the Chicago scene. The aerosol mix and concentration levels measured in a Detroit, MI, special study were used as baseline dry aerosol levels for the Chicago case (Wolff *et al.*, 1982b). These values are also presented in Table 24-20.

*Table 24-19. Distance to Each Figure in Block Diagram of Photographs (Figures 24-52 through 24-55) and the Percent of Total Area Each Feature Comprises in Each Photograph.*

| Site | Feature | Average Distance (km) | Percent of Total Area |
|---|---|---|---|
| Grand Canyon | 1 | -- | 34.55 |
| | 2 | 124.0 | 0.17 |
| | 3 | 53.3 | 0.21 |
| | 4 | 49.4 | 1.34 |
| | 5 | 48.2 | 3.09 |
| | 6 | 45.6 | 1.27 |
| | 7 | 33.3 | 0.89 |
| | 8 | 33.1 | 7.82 |
| | 9 | 25.0 | 1.43 |
| | 10 | 18.7 | 0.50 |
| | 11 | 21.4 | 1.32 |
| | 12 | 15.8 | 8.25 |
| | 13 | 11.9 | 3.53 |
| | 14 | 9.5 | 10.37 |
| | 15 | 8.7 | 21.79 |
| | 16 | 8.2 | 3.47 |
| Denver | 1 | -- | 44.02 |
| | 2 | 66.5 | 7.15 |
| | 3 | 27.8 | 7.29 |
| | 4 | 23.2 | 2.42 |
| | 5 | 7.8 | 4.40 |
| | 6 | 4.0 | 10.38 |
| | 7 | 0.5 | 24.34 |
| Shenandoah | 1 | -- | 47.05 |
| | 2 | 80.0 | 0.54 |
| | 3 | 43.6 | 9.74 |
| | 4 | 15.0 | 0.38 |
| | 5 | 9.7 | 1.23 |
| | 6 | 4.0 | 35.62 |
| | 7 | 0.3 | 5.44 |
| Chicago | 1 | -- | 56.09 |
| | 2 | 2.7 | 10.47 |
| | 3 | 1.0 | 2.72 |
| | 4 | 0.5 | 29.15 |
| | 5 | 0.005 | 1.57 |

The coarse mode was considered to have a mass mean radius of *5.55 microns*, a geometric standard deviation of *2.5* and a density of *2.55 g/cm*$^3$, while the respective values for the fine mode are *0.12 microns*, *2.0*, and *1.75 g/cm*$^3$, respectively. The index of refraction for each mode, *1*, *2*, and *3*, was assumed to be *1.53+0.006i*; *1.7+0.008i*; and *1.9+0.6i*, respectively. Models developed by Tsay *et al.* (1987) and Hanel (1976) were used to estimate the associated water due to relative humidity, and other microphysical/optical properties. The aerosol growth as a function of relative humidity was calculated following an approach outlined by Hanel (1976). The interaction of radiation with a scattering/absorbing medium was calculated using Mie theory (Shettle and Fenn, 1979) and the assumption of spherical particles. The doubling and adding model was used to calculate sky radiance values, while Equation 1 was used to obtain path radiance.

Table 24-20 also lists average total mass, percent coarse and fine mass, fine soil, ammonium sulfate, soot, other fine mass, and water as a function of relative humidity. Relative humidity was varied from *0.0* to *98.0%*. Notice that at high relative humidities (*>90%*) water can be in excess of *50%* of the aerosol mass.

Table 24-21 lists average summertime atmospheric extinction at *550 nm*, percent change in extinction and visual range, and number of just noticeable changes between average summertime conditions at *RH = 40.0%* and a variety of RH levels. A just noticeable change (JNC) is determined by calculating contrast levels between all landscape features (edges) within the photograph as a function of changing radiance field. (The radiance field is a function of $b_{ext}$ and path radiance.) When any one of the contrast values reach a value that can be humanly observed, a just noticeable change has occurred. Notice that approximately a *5%* change in extinction usually evokes one JNC. The quadratic detection model, as outlined in Appendix D, is used to determine when a change in contrast of adjacent scenic features is perceptible. By definition, the JNC numbers are linearly proportional to how the human visual system responds to changes in visual air quality (Malm, 1985). It is emphasized that the JNC calculation using QDM has not been field validated and is only presented as an approximation to the amount of air pollution required to evoke a noticeable change in a scene.

Figures 24-56 through 24-60 (Color Plates 24-3 to 24-5) and 24-61 through 24-65 (Color Plates 24-6 to 24-8) photographically show the effect of changing RH from *40%* to *98%* for the Grand Canyon and Chicago. These figures dramatically demonstrate the synergistic role between RH and water soluble aerosols. The first picture in each series shows the visual air quality associated with average aerosol loadings but with low RH. Visual air quality, although not perfect, might be considered acceptable. However, as RH increases, the canyon virtually disappears, while Chicago's skyline becomes veiled in haze. Although the eastern United States has much higher levels of pollutants than does the West, it is the higher

*Table 24-20. Average Total Mass, Percent Coarse Mass, Fine Soil, Ammonium Sulfate, Soot, and Other Fine Mass and Water as a Function of Relative Humidity*

| Site | % RH | Mass Concentration ($\mu g/m^3$) | Coarse Mode | | Fine Mode | | | |
|---|---|---|---|---|---|---|---|---|
| | | | % Coarse | % Fine Soil | % Soot | % Sulfate | % Other | % $H_2O$ |
| Grand Canyon | 0 | 9.6 | 54.1 | 5.5 | 2.4 | 18.4 | 19.6 | 0.0 |
| | 40 | 9.6 | 53.7 | 5.5 | 2.4 | 18.3 | 19.5 | 0.7 |
| | 60 | 9.8 | 52.9 | 5.4 | 2.4 | 18.0 | 19.2 | 2.2 |
| | 80 | 11.4 | 45.3 | 4.6 | 2.0 | 15.4 | 16.4 | 16.3 |
| | 95 | 16.3 | 31.8 | 3.2 | 1.4 | 10.8 | 11.5 | 41.3 |
| | 98 | 24.6 | 21.1 | 2.2 | 0.9 | 7.2 | 7.6 | 61.0 |
| Chicago | 0 | 49.8 | 37.3 | 5.2 | 2.9 | 33.3 | 21.3 | 0.0 |
| | 40 | 50.2 | 36.9 | 5.2 | 2.9 | 33.0 | 21.1 | 1.0 |
| | 60 | 51.3 | 36.1 | 5.0 | 2.8 | 32.3 | 20.6 | 3.1 |
| | 80 | 63.7 | 29.1 | 4.1 | 2.3 | 26.0 | 16.6 | 21.9 |
| | 95 | 100.0 | 18.5 | 2.6 | 1.4 | 16.6 | 10.6 | 50.3 |
| | 98 | 161.5 | 11.5 | 1.6 | 0.9 | 10.3 | 6.6 | 69.2 |

*Table 24-21. Average Summertime Atmospheric Extinction at 550 nm.*[a]

| Site | RH | $B_{550}$ | $\% \Delta B_{ext}$ | $\% \Delta V_r$ | JNC |
|---|---|---|---|---|---|
| Grand Canyon | 40 | 0.0209 | 0.0 | 0.0 | 0 |
| | 60 | 0.0214 | 2.4 | -2.2 | 1 |
| | 80 | 0.0275 | 31.5 | -23.1 | 5 |
| | 95 | 0.0472 | 125.8 | -54.5 | 13 |
| | 98 | 0.0834 | 299.0 | -74.0 | 21 |
| Chicago | 40 | 0.0987 | 0.0 | 0.0 | 0 |
| | 60 | 0.1025 | 3.9 | -3.1 | 1 |
| | 80 | 0.1484 | 50.4 | -31.2 | 4 |
| | 95 | 0.2955 | 199.4 | -64.3 | 13 |
| | 98 | 0.5654 | 472.8 | -81.1 | 23 |

[a] Table shows percent change in extinction between average summertime extinction at RH = 40% and extinction at the specified RH; percent change in visual range between average summertime visual range at RH = 40% and visual range at specified RH; and number of just noticeable changes between photograph at RH = 40% and each photograph representing the various relative humidity levels.

eastern RH interacting with those pollutants that causes much of the dichotomy between eastern and western visibility.

A final demonstration of VIPS will be the pictorial representation of the difference between average natural and current visibility conditions. In Section 3.5, it is estimated that average natural background extinction in the East and West are $26 \pm 7\ Mm^{-1}$ and $17 \pm 2.5\ Mm^{-1}$, respectively. The associated estimates of aerosol species concentrations, water content, and their respective extinction efficiencies are presented in Table 24-9. To calculate a radiance field from these estimates, it is necessary to approximate a mass size distribution given the constraint that the fine particle mass extinction must add to $4.3\ Mm^{-1}$ in the West and $12\ Mm^{-1}$ in the East. Likewise, coarse mass extinction is estimated to be $1.8\ Mm^{-1}$ in both the East and West. An average RH of *80%* in the East and *60%* in the West is used, and it is assumed that organics, nitrates, and sulfates are equally hygroscopic.

The same optical model using three modes and respective indexes of refraction as previously is assumed. A dry fine mass mean radius of *0.20 microns*, geometric standard deviation of *2.0*, and density of *1.75 g/cm³* as well as a coarse mass mean radius of *5.55 microns*, geometric standard deviation of *2.5*, and density of *2.55 g/cm³* are consistent with the constraints outlined above.

Section 3.3.1 reports a current average extinction level of *230 $Mm^{-1}$* in the urban East, *150 $Mm^{-1}$* in the rural East, *120 $Mm^{-1}$* in the urban West, and *25 $Mm^{-1}$* in the rural West. Computer imaged photographs can be created comparing natural conditions to current average conditions by assuming appropriate aerosol size distributions and physicochemical properties. Grand Canyon (rural west), Denver (urban west), Shenandoah (rural east), and Chicago (urban east) will be used for these comparisons. For Grand Canyon, Denver, and Chicago the aerosols were assumed to have the same properties as the natural background cases but with increased fine mass concentrations to yield the estimated average current extinction levels. However, at Shenandoah the National Park Service has been monitoring atmospheric aerosols and visibility since 1982. The fine mass concentration and fraction of fine mass that is ammonium sulfate is presented in Table 24-16 for Shenandoah, Acadia, and Great Smoky Mountains National Parks. Therefore, the measured aerosol concentrations will be used to estimate average current extinction at Shenandoah.

The fine fraction is presumed to consist of ammonium sulfate, ammonium nitrate, light absorbing carbon, soil, and organics. Elemental sulfur was presumed to be due to ammonium sulfate; thus, fine ammonium sulfate mass was obtained by scaling elemental sulfur by *4.125*. Ammonium nitrate was estimated by assuming an ammonium nitrate-to-ammonium sulfate ratio of *0.15* for annual and *0.04* for summer. Fine soil was calculated by scaling crustal elements to account for their naturally occurring oxides. Finally, organic mass was obtained by subtracting ammonium sulfate, ammonium nitrate, fine soil, and light absorbing carbon from total fine mass.

A bimodal model, coarse and fine, lognormally distributed was used. A coarse mode with a mass median radius of *5.55 microns*, geometric standard deviation of *2.5*, and a density of *2.55 g/cc* was assumed, while the respective values for the fine mode were *0.2 microns*, *2.0*, *1.75 g/cc*. Fine soil was assumed to be on the tail of coarse mode, therefore, fine soil mass was added to coarse mass to obtain the coarse mode mass. The four remaining components of the fine fraction comprise the fine mode. The soot portion is associated with the mass of light absorbing carbon, while ammonium sulfate and nitrate are assumed to form one soluble component. Consistent with the discussion of extinction budgets in Section 4, two organic scenarios were considered. First none and secondly one half of the organic mass was assumed to be soluble.

Two water activity functions were used to simulate the growth of the soluble portion of the fine mode due to relative humidity. One water activity function was parameterized to reproduce growth curves published by Tang (1981); ammonium sulfate and ammonium nitrate mass were associated with this growth curve. Soluble organics, presumed to be less soluble than ammonium sulfate and ammonium nitrate, were associated with a water activity function parameterized to data published by Hanel (1976).

Since relative humidity was not gathered concurrently with the aerosol data, the effect of RH on extinction was calculated using 1988-1989 relative humidity data and assuming the RH distribution is independent of fine mass distribution. Table 24-22 presents a summary of the results of these calculations for Acadia, Shenandoah and Great Smoky Mountains National Parks. Listed in the table are the yearly average and summer total extinction as well as the fraction of total extinction that is associated with sulfates. The parenthetical values are for the case where one half of the organics are assumed water soluble.

Table 24-23 lists the average RH, atmospheric extinction, percent change in extinction/visual range, and the number of JNC's from natural conditions, while Figures 24-66 through 24-69 (Color Plates 24-9 to 24-12) show pictorially the difference between natural and average conditions. The differences are very dramatic in the rural East, urban East, and urban West. Although the difference is

*Table 24-22. Annual and Summer Average Atmospheric Extinction and Fraction of Extinction Associated with Sulfate for Three Eastern National Parks.*[a]

| NPS Site | Annual | | Summer | |
|---|---|---|---|---|
| | $B_{ext}$ ($km^{-1}$) | $\%B_{ext}$ (fSLF) | $B_{ext}$ ($km^{-1}$) | $\%B_{ext}$ (fSLF) |
| Acadia, ME | .062(.068) | 56(50) | .065(.076) | 53(46) |
| Shenandoah, VA | .110(.117) | 66(62) | .192(.218) | 77(68) |
| Great Smoky Mountains, TN | .116(.129) | 67(60) | .207(.240) | 74(64) |

[a] None of the organics and one-half of the organics were assumed to be water soluble. Parenthetical values are for the case where one-half of the organic mass are assumed water soluble.

*Table 24-23. Natural Conditions and Just Noticeable Changes for Urban West, Urban East, Rural West, and Rural East.*[a]

| Area/Site | % RH | $B_{550}(km^{-1})$ | % $B_{ext}$ | % SVR | JNC |
|---|---|---|---|---|---|
| Urban West (Denver) | 60 | 0.106 | 2617 | -88.0 | 27 |
| Urban East (Chicago) | 80 | 0.210 | 2000 | -90.9 | 18 |
| Rural West (Grand Canyon) | 60 | 0.012 | 207 | -36.8 | 8 |
| Rural East (Shenandoah) | 80 | 0.098 | 880 | -81.8 | 19 |

[a] Relative humidity, non-Rayleigh atmospheric extinction, percent change in non-Rayleigh, extinction and standard visual range from natural conditions and the number of just noticeable changes for urban west (Denver), urban east (Chicago), rural west (Grand Canyon), and rural east (Shenandoah).

less dramatic in the rural West, it is nevertheless quite perceptible.

The visibility image processing system is a continuously evolving technique and is somewhat constrained by limits of standard photographic methods and "colorwrite" systems. The system, including radiation transfer and Mie theory models, have not been validated with a field measurement program.

## 5.2 RELATIONSHIPS BETWEEN AEROSOLS AND CLIMATE

*R. Charlson*

### 5.2.1 Regional United States and Global Considerations—Direct Effects

While is easy to demonstrate that aerosol particles measurably reduce solar irradiance in industrial regions, the lack of data and inadequate spatial coverage preclude extending this demonstration to larger spatial scales. Ball and Robinson (1982) and Grassl (1988) consider the perturbation of the solar flux in the eastern United States and in the Arctic respectively. Using data that are similar to those in Table 24-12 and using simple radiation transfer theory, Ball and Robinson compared calculated and measured depletions and concluded that 24 stations in the eastern United States exhibit an annual average depletion of solar irradiance of *7.5%*. If the mean solar energy reaching the ground is *150 watt/m*$^2$ (night plus day, *50%* cloud cover), this amounts to a perturbation of the heat balance by around *10 watt/m*$^2$. A doubling of global $CO_2$ from *300* to *600 ppm* is calculated to yield a change of only plus *4 watt/m*$^2$ so that, *for such geographically limited industrial areas*, the absolute magnitude of the regional forcing by aerosol backscatter and absorption is calculated to be substantially larger than the greenhouse effect.

Grassl (1988) comes to similar conclusions from model calculations for Arctic haze, with changes in solar irradiance at the surface of up to *-8 watt/m*$^2$. Again, this is a large figure compared to published greenhouse forcings.

Putting aside the currently unanswerable question of the geographical distribution of the magnitude of cooling of the surface by industrial haze aerosol, it is clear that it is not globally or even hemispherically uniform. The three main industrial regions (eastern United States, Europe, and eastern Asia) each produce haze blobs over approximately *10*$^7$ *km*$^2$ for a total coverage of about *6%* of the earth. The global effect of these industrial regions may be estimated by distributing this aerosol evenly over the entire globe (Bolin and Charlson, 1976; Joseph *et al.*, 1973)—for a global forcing of about minus *0.6 watt/m*$^2$. This is not an inconsequential quantity globally (albeit much less than the increase due to a $CO_2$ doubling) and, of course, the regional irradiance losses are indeed substantial.

It is of interest to compare this anthropogenic perturbation against a natural background. Of course, this is not known for North America before industrialization. However, it can be estimated per the data in Section 3.5. If the continental natural background level of aerosol extinction is about *12 Mm*$^{-1}$, a layer three kilometers deep would produce an aerosol optical depth of *0.04*. This value is close to the present day observations of about *0.05* in clean southern hemispheric marine air (Forgan, 1985). Substantial uncertainty exists in this estimate and more and better data are warranted.

Much less is known regarding the direct infrared effects, for three reasons:

1. There are no routine measurements of the infrared aerosol optical depth.
2. Calculations of the infrared effects depend on assumptions regarding the aerosol size distribution and the complex refractive index of the particles as a function of size at super-micrometer wavelengths.

3. The refractive index of particles at these wavelengths is a strong function of the chemical composition of the particles (*e.g. NaCl* absorbs no infrared radiation while silicates are strong absorbers). Because the chemical composition is not well known, the infrared optical properties are very uncertain.

As a result, even the overall *sign* of the effect of dust aerosols on the net radiation balance cannot be given, and the importance relative to effects on solar radiation is very uncertain as well (Grassl, 1988).

### 5.2.2 Indirect Effects on Clouds

Although the Twomey effect of CCN population on cloud albedo was published in 1977, application of the theory to global and hemispheric climate and tests of the hypothesis have only developed recently. It is premature to draw any conclusions regarding this potentially strong climatic forcing (see Section 2.2.3). However, it is useful to review the current and fundamental literature.

Twomey (1977) and Twomey *et al.* (1984) presented calculations of the sensitivity of cloud albedo to droplet population, concluding that increased droplet concentrations increase albedo but that absorbers such as soot decrease it. Therefore, the sign of the effect of "pollution" could be either plus or minus. Recent data suggest that, for most of the globe, soot content is so low that the albedo should increase with increased pollution aerosol. Indeed, it has been known for decades that continental clouds (in populated regions) have higher droplet concentrations than those in remote marine areas ($10^3/cm$ versus $10^2/cm$).

Charlson *et al.* (1987) repeated Twomey's calculations for small changes in droplet concentrations, and also concluded that the sensitivity was high (see Section 2.3.2). Coakley *et al.* (1987 and 1988) and Grassl (1988) independently came to this same conclusion. Schwartz (1988) attempted to test this hypothesis relative to the assumption that there is an elevated non-seasalt sulfate concentration "throughout" the northern hemisphere due to oxidation of man-made $SO_2$. Schwartz found from the temperature record that the northern and southern hemispheres are warming at about the same rate. He deduced from cloud albedo data that the northern hemisphere clouds have about the same albedo as southern hemisphere clouds. He concluded that this lack of response indicates that temperature and albedo are not controlled by anthropogenic sulfates, contrary to the suggestions of Charlson *et al.* (1987), Coakley *et al.* (1987 and 1988), and Grassl (1988). Still other papers, currently in press, suggest that neither the temperature or cloud albedo data are sufficient for this test. Thus, it is necessary to leave open the question of northern hemispheric cooling by anthropogenic CCN.

### 5.2.3 Data and Methods for Estimating Climatic Effects

The above sections illustrate the necessarily uncertain approaches to estimating the current level of climatic effects. Only in the cases of solar irradiance and non-cloud albedo can the effects be measured directly, and common turbidity data measure only the solar beam irradiance and not the total. So, most of the climatically relevant data must be used in connection with theoretical models in order to deduce the magnitude of the effect.

The models that are used currently vary from the simplest, one dimensional heat balance (as in Section 5.2.1 above) that neglect the infrared and cloud effects, to two dimensional models including both visible and infrared direct effects and cloud effects, to full-blown global circulation models (GCM). The inclusion of regional non-cloud and CCN effects in these models is a current activity and results are not yet available. These modelling exercises are severely hampered by a lack of data.

### 5.2.4 Possible Implications of Aerosol Climatic Change

There is considerable uncertainty in quantifying the magnitude of climatic effects of anthropogenic aerosol. Both the preliminary assessment of Ball and Robinson (1982) and the recent papers on cloud albedo strongly suggest that large effects already may exist, but the quality and quantity of available data preclude fully understanding or demonstrating them. Nonetheless, it is important to assess the practical implications of these potentially large effects.

Robinson (1977) deduced that the direct effect on solar radiation should cause a moderation of the diurnal temperature cycle at the surface as well as the loss of solar radiation. The potential effect on crop growth is a shortening of the growing season. However, the loss of solar irradiance also might reduce heat stress for some plant species, so the overall importance to agronomy is not clear. An unpublished workshop by EPA in 1983 attempted to estimate the magnitude of change on the growing season. The conclusion was that the dominant effect would likely be a delay of the start of the season because solar irradiance is a major factor in thawing the frozen soil and in warming it to seed-germinating temperature. The current turbidities were calculated to shorten the growing season by about one week (Robinson, personal communication 1984).

There are certain to be still other potential consequences; but while their physical basis is clear, their magnitude is

still a matter of speculation. Change in heat balance over synoptic meteorological scales ($10^3$ *km*) may have a systematic influence on the location of weather systems and their paths across the continents. Changes in the vertical distribution of heating/cooling of the atmosphere produces changes in static stability with attendant changes in the amount and type of clouds. Changes in precipitation are thus possible due to changes in heat balance. This class of effects is separate from and in addition to modification of precipitation amount/type/location/frequency due to changes in CCN or IN.

# SECTION 6

# SUMMARY AND CONCLUSIONS

One of the important effects associated with acid precipitation related pollutants is interference with radiation transfer (light transmission) in the atmosphere. An obvious result of such interference is visibility degradation—the impairment of atmospheric clarity or of the ability to perceive form, texture, and color. Climate modification constitutes another, somewhat less obvious, result.

The links between the acid rain problem and radiation transfer effects, although indirect, are quite strong. The principal link is through sulfur dioxide emissions and sulfate aerosols. Sulfur dioxide, a major contributor to acidic deposition, produces sulfate aerosol (itself a fundamental component of acidic deposition). Sulfate aerosol, in turn, is an important contributor to visibility reduction—in fact, the dominant contributor in the eastern United States. A secondary link occurs through nitrogen oxide emissions—also a major contributor to acidic deposition—which produce gaseous nitrogen dioxide and, in combination with ammonia (which may be the controlling precursor emission), fine ammonium nitrate particles. Ammonium nitrate aerosol sometimes accounts for a significant fraction of visibility degradation, and nitrogen dioxide typically contributes a few percent of visibility reduction.

The purpose of this document is to review, evaluate, and synthesize the current scientific information regarding visibility (including climate). The intent is to provide a technically sound, peer-reviewed summary of the state of visibility science for use by NAPAP in addressing visibility issues. Of particular importance is the relationship of visibility to the air pollutants associated with acid deposition—*i.e.* the relationship of visibility to nitrogen dioxide, nitrate aerosols, and (especially) sulfate aerosols.

## 6.1 BASIC CONCEPTS

Visibility does not have a precise, universally accepted, definition. Historically, much of the interest in visibility came from aviation and military operations where the most important concept of visibility was the furthest distance at which an object could be discerned—the "visual range". Currently, much of the concern about visibility is related to the aesthetic change from air pollution—the inability to see form, texture, and color of scenic features. This document is mostly concerned with the later concept of visibility, degradation of aesthetics by air pollution, although considerable discussion is also given here to visual range.

Under a variety of viewing conditions, "visibility reduction" or "haziness" is directly proportional to reduction in atmospheric light transmittance. Light transmittance in the atmosphere is attenuated by scattering and absorption from both gases and particles. The extinction coefficient (**B**ext), which measures the total fraction of light that is attenuated per unit distance, is simply the sum of these four components: **B**ext = **B**sg + **B**ag + **B**sp + **B**ap, where s = scattering, a = absorption, g = gas, and p = particles. Because the extinction coefficient is an important fundamental optical variable, and because under a variety of viewing conditions it relates directly to how well a landscape feature can be seen, much of the discussion here centers around the concept of light extinction.

Another important issue to emphasize is that particles (aerosols) dominate light extinction except under extremely clean conditions, when natural scatter by air molecules (Rayleigh scatter) predominates. Thus, understanding visibility requires understanding the basic concepts of aerosol air quality. Two of the most important aerosol concepts with respect to visibility are size distribution and chemical composition. For visibility purposes, it is critical to distinguish fine particles ($\leq$ 2.5 $\mu$m) from coarse particles ($\geq$ 2.5 $\mu$m), because fine particles usually dominate visibility effects. The composition of ambient particulate matter consists basically of just six species: sulfates, organics, elemental carbon, ammonium nitrate, soil dust, and aerosol bound water. Among these six species, there are significant differences in sources, atmospheric behavior, size distributions, and visibility effects.

## 6.2 FINDINGS AND CONCLUSIONS

The following subsections summarize the major findings and conclusions of the Visibility State of Science/ Technology Report. Where appropriate, a qualitative uncertainty is attached to each of the conclusion paragraphs according to the following NAPAP uncertainty classification scheme:

- o = no basis
- * = limited information with major uncertainties
- ** = broad information with large or unknown uncertainty or limited information with little uncertainty
- *** = broad information with known but sometimes large uncertainty
- **** = ample and certain information.

### 6.2.1 Data Bases

Visibility monitoring includes measurements of aerosol, optical, and scene characteristics. Measurements of particle size and composition can be used to assess visibility cause/effect relationships. The most useful optical index, extinction coefficient, can be directly measured or estimated from monitoring data on scene characteristics.

Over the last decade, much progress has been made in aerosol and optical monitoring techniques. The techniques have been applied in numerous monitoring programs to greatly expand the understanding of aerosols and visibility. However, the most comprehensive sophisticated data sets have been acquired only in the rural West and a few large urban areas. In terms of geographic extent and period of record, the archive of airport visual range observations (which is subject to data quality limitations) is by far the most extensive visibility data base.

### 6.2.2 Contributions to Light Extinction

**** Scattering by fine particles is generally the dominant contributor to elevated extinction coefficients. Fine particle scattering typically accounts for 75 - 95% of non-Rayleigh extinction in the eastern United States and 50 - 80% of non-Rayleigh extinction in the western United States.

**** Sulfates and organics (with the addition of ammonium nitrates in western urban areas) typically account for about three-fourths of dry fine particle mass. Sulfuric acid and its ammonium salts are most important in the East, where they typically account for at least half of the total dry fine mass. In the West, sulfate contributions to fine mass are less, about 20 - 50% in rural areas and 10 - 20% in urban areas.

**** Although there are theoretical problems in defining precise extinction budgets for aerosol species, certain conclusions are clear. Sulfates are the dominant source of light extinction in the East, contributing slightly more than half of total extinction. This conclusion is insensitive to the details of the apportionment procedure. Sulfates are but one of several major sources of extinction in the West, a finding that is again robust. The relative importance of sulfates is greater in the rural West than in the urban West and varies significantly with region (apparently greatest in the southern interior).

### 6.2.3 Existing and Natural Background Conditions for Visibility/Aerosols

**** Figure 24-70, a map of median visual range for rural (suburban and nonurban) areas in the United States, illustrates the large difference between the East and West in rural visibility. Several data sources indicate that standard visual range in the rural mountain/desert areas of the Southwest averages about 130 to 190 km. In contrast, rural areas south of the Great Lakes and east of the Mississippi experience median standard visual range of about 20 - 35 km. Most of this factor-of-six East/West difference is due to greater sulfate concentrations in the East and their interaction with the higher humidity of the East.

**** With respect to seasonal visibility patterns, there is only one extremely strong feature occurring on a large geographical scale within the United States—the summertime maximum in extinction coefficient (minimum in visibility) over the region south of the Great Lakes and east of the Mississippi. The predominant cause of the summertime haze peak in the East is the summertime maximum in sulfate aerosol concentrations.

*** On the average, natural background standard visual range is estimated as 230 $\pm$ 35 km in the arid parts of the West and 150 $\pm$ 45 km in the East. Comparing the natural visibility levels with current visibility levels indicates that man-made contributions account for about one-third of the average extinction coefficient in the rural West and over 80% of the average extinction coefficient in the rural East. Under worst-case pollution episodes, man-made contributions would dominate in both regions.

### 6.2.4 Historical Visibility Trends

*** Airport observations of prevailing visibility can be used to investigate historical trends in haziness since the late 1940's. The observed trends show significant differences by regions and by season. The most salient feature in the trends is the increase of summertime haze in the eastern United States during the 1950's and 1960's. This increase is especially strong in the southeastern states.

*** In the eastern United States, there are generally good correspondences on a regional and seasonal basis between historical haze trends and historical SOx emission trends. Since the late 1940's, the northeast region has undergone a moderate decline in haziness and emissions during the winter and a moderate increase in both during the summer. Over the same period, the southeast region has experienced a moderate increase in emissions and haziness during the winter and a strong increase in both during the summer. The increasing trends for both emissions and haziness—*i.e.*, the summer case in the Northeast as well as the winter and summer cases in the Southeast—show the greatest rise during the 1950's and 1960's with a leveling off or decrease after the early 1970's. Viewed as a whole, the data suggest that haze trends for the eastern United States have been dominated by sulfur emission trends since the late 1940's.

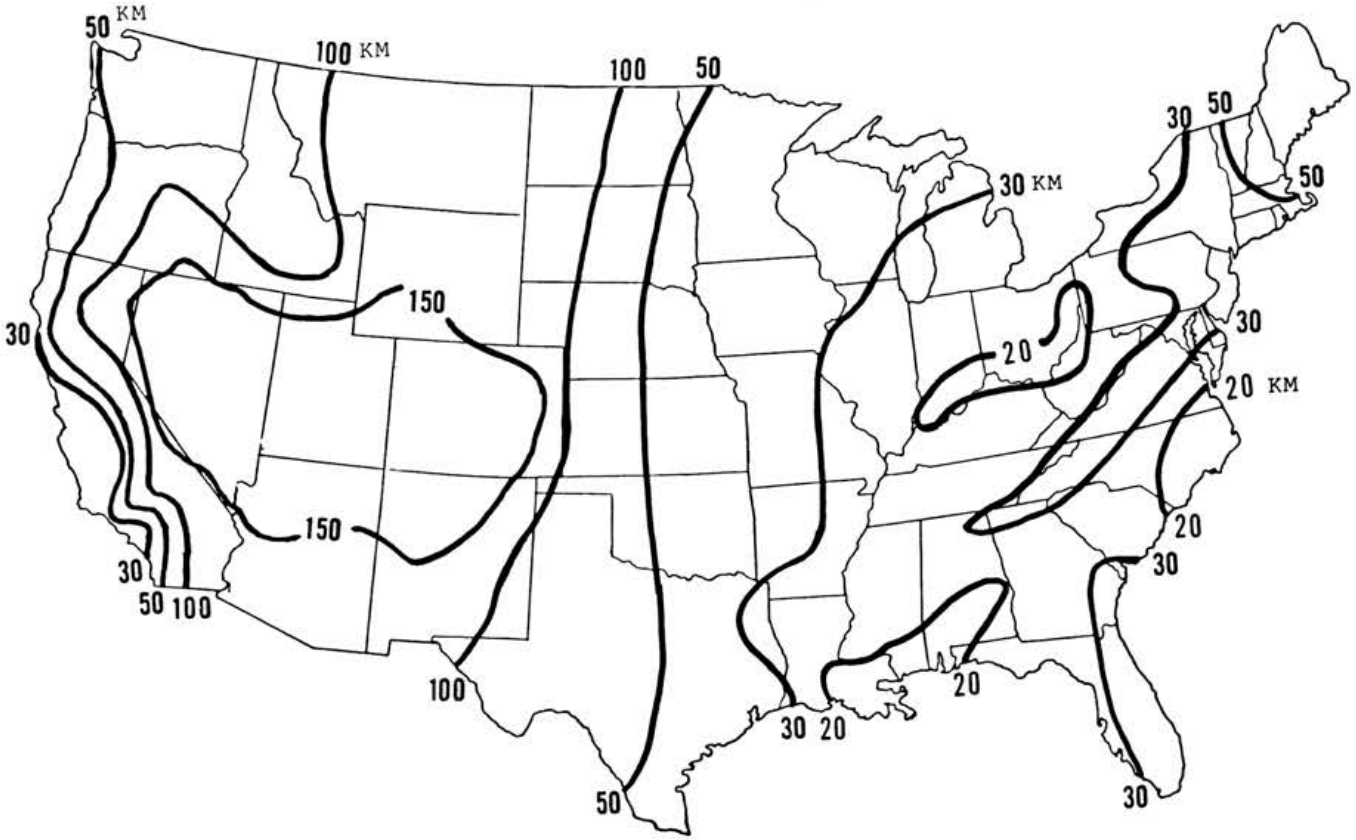


*Figure 24-70 Estimated standard median visual range (km) for rural (suburban/nonurban) areas of the United States. Notes: Values are based on airport median visual ranges factored by 1.3 to account for differences in detection thresholds in estimating standard visual range. Data included for all days (all weather conditions). Data are for 1974-1976, but recent studies indicate that current conditions are approximately the same as shown here.*

### 6.2.5 Characterization of Visibility

A full description of how images are transmitted through the atmosphere to an observer requires a knowledge of both the atmospheric transmittance (*i.e.*, the extinction coefficient) and the path radiance between the observer and the landscape feature of interest as well as the average brightness of the scene. These three variables combine to form what is known as the atmospheric modulation transfer function (*Mtf*).

*** Pollution control evaluations assume constant illumination conditions and usually involve situations where fine particle scattering is dominant. In this case, changes in the modulation transfer function are very closely related to changes in the extinction coefficient (because path radiance as well as transmittance is affected by changes in light scattering). Therefore, a knowledge of only the extinction coefficient can yield significant insight into how air pollution controls affect visibility. Furthermore, atmospheric transmittance relates well to how people judge scenic quality. Accordingly, extinction coefficient (or its reciprocal, standard visual range) is an important parameter in characterizing visibility.

** In addition to changes in extinction coefficient (or standard visual range), another method of quantifying visibility impairment is the number of cumulative "just notable changes" in scene appearance. The index, just noticeable changes, is scene specific, includes all aspects of the *Mtf* formulation, and relates directly to perception. The best way to communicate the visual effects is to create pictorial representations through image processing techniques. It should be noted, however, that the least certain part of visibility science is the part dealing with human perception and values; the JNC index and the photographic simulations are still subject to some uncertainties and scientific debate.

*** Figures 24-66 through 24-69 (Color Plates 24-9 to 24-12) illustrate the difference between natural and current average visibility for the urban East, rural East, urban West, and rural West, respectively. In the first three cases, the differences are very dramatic (representing 18 to 38 cumulative just noticeable changes). In the rural West, the differences are less dramatic, although still very perceptible (8 cumulative just noticeable changes).

### 6.2.6 Climate Relationships

** The *direct* climatic effects of fine particles are reflection of solar radiation back into space and absorbtion of solar radiation. Over an area of approximately $10^7$ $km^2$ in eastern North America (and evidently over similarly sized areas in Europe and eastern Asia), the average total decrease in solar radiation at the ground is on the order of 10 watt/$meter^2$ (about 7%). This effect acts opposite to the direct radiative effects of greenhouse gases.

* In addition to the direct radiative effect of fine particles, the potential exists for a large cooling effect due to the *indirect* role of man-made particles acting as cloud condensation nuclei and thereby increasing cloud albedo. There is also some potential for a direct heating effect by coarse dust particles.

The cloud albedo and coarse particle climatic effects are not well characterized. The overall meteorological consequences of the various aerosol effects on heat balance might be large but remains uncertain.

## 6.3 UNCERTAINTY

Compared to many other effects of air pollutants, visibility is fairly well understood. Unlike certain acid deposition effects that are multi-media, involve cumulative buildup, or are delayed, atmospheric optical parameters are instantaneous properties of atmospheric composition. The fundamental physics relating light extinction (and other optical parameters) to atmospheric gases and particles is well established. Also, light extinction is a simple linear sum of scattering and absorption by gases and particles. Furthermore, additional sub-divisions of light extinction contributions are either exactly additive (*e.g.* coarse versus fine particles) or approximately additive (*e.g.* allocations among chemical species). In fact, even before the past decade of visibility research, visibility was called the "best understood and most easily measured effect of air pollution" (Council on Environmental Quality, 1978). The most uncertain aspect of visibility science is the part dealing with human perception and values, *i.e.* the second link in the chain from air pollutant concentrations to atmospheric optics to human evaluations.

# SECTION 7

# RECOMMENDATIONS FOR FUTURE RESEARCH

This section provides a list of topics for future research in visibility studies. The list is organized according to the same six topics as in the Findings and Conclusions (Section 6.2):

1. measurement methods and data bases
2. existing and natural background conditions for visibility/aerosols
3. historical visibility trends
4. contributions to light extinction
5. characterization of visibility effects, and
6. climate effects.

## 7.1 MEASUREMENT METHODS AND DATA BASES

- Research should be intensified to develop methods that minimize particle sampling artifacts (especially for organics) and to develop *in situ* techniques for liquid water monitoring. There is also a need for nephelometers that do not modify the aerosol and for accurate methods to measure aerosol absorption.
- Additional intercomparison studies should be undertaken to aid in the evaluation of monitoring methods (especially for organics and elemental carbon). Monitoring reference methods should be developed that would promote the collection of comparable aerosol and visibility data nationwide.
- State-of-the-art visibility and aerosol monitoring should be geographically extended to allow a full national assessment of patterns and cause/effect relationships for visibility. Currently, there is a lack of comprehensive data sets for the northern half of the West, the southern part of the East, and the wintertime throughout the East.

## 7.2 EXISTING AND NATURAL BACKGROUND CONDITIONS FOR VISIBILITY/AEROSOLS

- National visibility maps and seasonal plots based on airport observations need to be updated with recent data, using appropriate techniques for handling the distribution functions and treating urban and rural areas separately. The spatial and seasonal visibility patterns based on airport data should be compared and reconciled with results based on the latest instrumental techniques for measuring visibility.
- Statistical distributions of visibility should be characterized using data from the latest instrumental methods.
- At least one year, preferably several years, of comprehensive visibility and aerosol data should be acquired at a few remote southern hemisphere sites to help provide a better understanding of natural background conditions.

## 7.3 HISTORICAL VISIBILITY TRENDS

- Visibility monitoring by the National Weather Service should be evaluated with respect to usefulness for visibility research. Prior to the replacement (in a few years) of human visibility observations at airports by forward scattering monitors, the impact of the change on trend analysis should be investigated.

## 7.4 CONTRIBUTIONS TO LIGHT EXTINCTION

- Data should be collected or assembled to allow the formulation of light extinction budgets for worst-case and best-case conditions as well as average conditions.
- Further work should be done to characterize the potential nonlinearities in the relationship between light scattering and concentrations of aerosol components.
- There is a need to compare light extinction budgets with total visibility budgets that include consideration of path radiance effects. The relative importance of fine-particle scattering, coarse-particle scattering, and absorption on path radiance should be characterized, and an empirical procedure should be developed for combining path radiance and extinction effects in a total visibility index.

## 7.5 CHARACTERIZATION OF VISIBILITY EFFECTS

- There is a need to quantify the role that path radiance plays in visibility impairment under a variety of lighting and atmospheric conditions. There is also a need to quantify the practical implications of path radiance in regard to control strategies directed at extinction coefficient.

- The laboratory work on "just noticeable" changes should be verified with field studies of the relationship between perceptible changes and air pollution levels.
- Field verification should be conducted regarding image processing techniques for visibility. The relationship between photographs and natural scene perception needs to be better understood.

## 7.6 CLIMATE EFFECTS

- The turbidity network should be improved and upgraded with stable instruments. Turbidity data should be interfaced with satellite measured irradiance to provide ground truth for the latter.
- A standard instrument is needed for measurement of cloud condensation nuclei. Such an instrument should be widely deployed to investigate the factors controlling population of cloud condensation nuclei.
- Turbidity, cloud condensation nuclei, and other climatological instruments should be acquired in a consistent manner over a decade or more for long-term trend analysis.
- Meteorological consequences of changes of heat balance due to regionally distributed aerosol should be investigated.
- Effects of climate changes on agronomy should be investigated.

# SECTION 8

# REFERENCES


**Ackerman, J.P. and O.B. Toon.** 1981. Absorption of visible radiation in atmosphere containing mixtures of absorbing and nonabsorbing particles. Appl. Optics 20:3661-3667.

**Adams, K.M., L.I. Davis Jr., S.M. Japar, and W.R. Pierson.** 1989. Real-time in situ measurements of atmospheric optical absorption in the visible via photoacoustic spectroscopy II: Validation for atmospheric elemental carbon aerosol. Atmos. Environ. 23:693-700.

* **Air Resource Specialists.** 1988. Visibility Monitoring and Data Analysis Report for Spring 1986 through Winter 1988 Monitoring Seasons. NPS contract #CX-0001-7-0010. National Parks Service, Fort Collins, CO.

**Altshuller, A.P.** 1982. Relationships involving particle mass and sulfur content at sites in and around St Louis, Missouri. Atmos. Environ. 16:837-843.

**Altshuller, A.P.** 1983. Review: Natural volatile organic substances and their effect on air quality in the United States. Atmos. Environ. 17:2131-2165.

**Altshuller, A.P.** 1985. Relationships involving fine particle mass, fine particle sulfur, and ozone during episodic periods at sites in and around St Louis, Missouri. Atmos. Environ. 19:265-276.

**Anderson, J.R., F.J. Aggett, P.R. Buseck, M.S. Germani, and T.W. Shattuck.** 1988. Chemistry of individual aerosol particles from Chandler, AZ, an arid urban environment. Environ. Sci. and Technol. 22:811-818.

**Appel, B.R., Y. Tokiwa, and M. Haik.** 1981. Sampling of nitrates in ambient air. Atmos. Environ. 15:283-289.

* **Appel, B.R., Y. Tokiwa, J. Hsu, L.E. Kothny, E. Hahn, and J.J. Wesolowski.** 1983. Visibility Reduction as Related to Aerosol Constituents. Report prepared for California Air Resource Board, by AIHL, Berkeley, CA.

**Appel, B.R., Y. Tokiwa, J. Hsu, L.E. Kothny, and E. Hahn.** 1985. Visibility as related to atmospheric aerosol constitutents. Atmos. Environ. 19:1525-1534.

**Atmospheric Environment.** 1981. Proceedings of EPA Symposium on "Plumes and Visibility - Measurements and Model Components", November 1980. Atmos. Environ. 15:1785-2646.

**Ball, R.J. and G.D. Robinson.** 1982. The origin of haze in the central United States and its effect on solar radiation. J. Appl. Meterol. 21:171-188.

**Barker, M.** 1976. Planning for environmental indicies: observer appraisals of air quality. In: K. Craig and E. Zube, eds. Perceiving Environmental Quality. Plenum Press, New York, NY.

**Bhardwaja, P.J., ed.** 1987. Visibility Protection: Research and Policy Aspects. Transactions of APCA Speciality Conference, September 1986, Grand Tetons National Park, WY. Air Pollution Control Assoc., Pittsburgh, PA.

**Blackwell, H.R.** 1946. Contrast thresholds of the human eye. J. Optical Soc. Amer. 36:624.

**Blumenthal, D., J. Trijonis, R. Kelso, M.L. Pitchford, and M. McGown.** 1987. Design and initial findings of the RESOLVE desert visibility study. In: P.J. Bhardwaja, ed. Visibility Protection: Research and Policy Aspects. Air Pollution Control Assoc., Pittsburgh, PA.

**Bolin, B. and R.J. Charlson.** 1976. On the role of the tropospheric sulfur cycle in the shortwave radiative climate of the earth. Ambio. 5:47-54.

* **Boswell, G.T.** 1975. How People Look at Pictures. University of Chicago Press, Chicago, IL.

**Brown, P.J., B.L. Driver, D. Bruns, and C. McConnell.** 1979. The outdoor recreation opportunity spectrum in wildland recreation planning: Development and application. In: Proceedings of first annual conference on recreation planning and development of the American Society of Civil Engineers, April 18-21, in Snowbird, UT.

**Bullrich, K.** 1964. Scattered radiation in the atmosphere, p. 99. In: Advances in Geophysics, 10. Academic Press, New York, NY.

**Cadle, S.H., P.J. Groblicki, and P.A. Mulawa.** 1983. Problems in the sampling and analysis of carbon particulate. Atmos. Environ. 17:593-600.

**Campbell, F.W.** 1983. Ambient stressors. Environ. and Behavior 15:355-380.

**Campbell, F.W. and J.J. Kulikowski.** 1986. Orientational selectivity of the visual cell of the cat. J. Physiol. (London) 187:437.

**Campbell, F.W. and J.G. Robson.** 1964. Application of fourier analysis to the modulation response of the eye. J. Opt. Soc. Amer. 54:581A.

**Campbell, F.W., B. Cleveland, G.F. Cooper, and C. Enroth-Cogell.** 1968. The spatial selectivity of the visual cells of the cat. J. Physiol.(London) 198:237.

*** Carlson, C.R. and R.W. Cohen.** 1978. Image Descriptors for Displays: Visibility of Displayed Information. RCA Laboratories, Princeton, NJ.

**Cass, G.R.** 1979. On the relationship between sulfate air quality and visibility with examples in Los Angeles. Atmos. Environ. 13:1069-1084.

**Chang, D.P.Y. and R.C. Hill.** 1980. Retardation of aqueous droplet evaporation by air pollutants. Atmos. Environ. 14:803-807.

**Charlson, R.J.** 1969. Atmospheric visibility related to aerosol and mass concentration. Environ. Sci. & Tech. 3:913-916.

**Charlson, R.J., D. S. Covert, Y. Tokiwa, and P.K. Mueller.** 1972. Multiwavelength nephelometer measurements in Los Angeles smog aerosol, III: Comparison to light extinction by $NO_2$. J. Colloid & Interface Sci. 39: 270-265.

**Charlson, R.J., D.S. Covert, and T.V. Larson.** 1984. Observations of the effect of humidity on light scattering by aerosols. In: L. Ruhnke and A. Deepak, eds. Hygroscopic Aerosols. A. Deepak Publishing, Hampton, VA.

**Charlson, R.J., J.E. Lovelock, M.O. Andreae, and S.G. Warren.** 1987. Oceanic phytoplankton, atmospheric sulfur, cloud albedo, and climate. Nature 326:655-661.

**Clarke, A.D. and R.J. Charlson.** 1985. Radiative properties of the background aerosol: Absorption component of extinction. Science 229:263-265.

**Coakley, J.A. Jr., R.L. Bernstein, and P.A. Durkee.** 1987. Effect of shipstack effluents on cloud reflectivity. Science 237:1020-1022.

**Coakley, J.A. Jr., R.L. Bernstein, and P.A. Durkee.** 1988. Effect of shipstack effluents on the radiative properties of marine stratocumulus: Implications for man's impact on climate, pp. 253-260. In: P.V. Hobbs and M.P. McCormick, eds. Aerosols and Climate. A. Deepak Publishing, Hampton, VA.

**Cohen, S., G.W. Evans, D. Stokols, and D.S. Krantz.** 1986. Behavior, Health, and Environmental Stress. Plenum Press, New York, NY.

*** Cooper, J.A., and J.G. Watson.** 1979. Portland Aerosol Characterization Study (PACS). Final report for Portland Air Quality Maintenance area advisory committee and Oregon Dept. of Environmental Quality.

**Core, J.E., N.R. Maykut, D. Weaver, J. Boylan and M. Hooper.** 1987. A summary of major findings from the Pacific Northwest regional aerosol mass apportionment study. In: P.J. Bhardwaja, ed. Visibility Protection: Research and Policy Aspects. Air Pollution Control Association, Pittsburgh, PA.

**Cornsweet, T.** 1970. Visual Perception. Academic Press, New York, NY.

*** Council on Environmental Quality.** 1978. Visibility Protection for Class I Areas, the Technical Basis. Washington, DC.

**Countess, R.J., G.T. Wolff, and S.H. Cadle.** 1980. The Denver winter aerosol - A comprehensive chemical characterization. J. Air Pollution Control Assoc. 30:1194.

**Countess, R.J., S.H. Cadle, P.J. Groblicki, and G.T. Wolff.** 1981. Chemical analysis of size-segregated samples of Denver's ambient particulate. J. Air Pollution Control Assoc. 31:247-252.

**Covert, D.S. and J. Heintzenberg.** 1984. Measurement of the degree of internal/external mixing of hygroscopic compounds and soot in atmospheric aerosols. Sci. Total Environ. 36:347-352.

**Covert, D.S., R.J. Charlson, and N.C. Ahlquist.** 1972. A study of the relationship of chemical composition and humidity to light scattering by aerosols. J. Appl. Meteorol. 11:968-976.

**Cunningham, M.** 1979. Weather, mood, and helping behavior: Quasi-experiments with the sunshine samaritan. J. Per. Soc. Psych. 37:1947-1956.

*** DeLuisi, D. and P. Reddy.** 1898. Personal communication. Geophysical Monitoring for Climatic Change program, NOAA, Washington, DC.

*** Dietrich, D. and J. Molinar.** 1989. Personal communication. Air Resources Specialists, Inc., Fort Collins, CO.

**Dixon, J.K.** 1940. The absorption coefficient of nitrogen dioxide in the visible spectrum. J. Chem. Physics 8:157-160.

*** Douglas, C.A. and L.L. Young.** 1945. Development of transmissometer for determining visual range. Tech. Dev. report #47. Civil Aeronautics Admin., Washington, DC.

**Dzubay, T.G. and K.W. Clubb.** 1981. Comparison of telephotometer measurements of extinction coefficients with scattering and absorption coefficients. Atmos. Environ. 15:2617-2624.

**Dzubay, T.G., R.K. Stevens, C.W. Lewis, D.H. Hern, W.J. Courtney, J.W. Tesch, and M.A. Mason.** 1982. Visibility and aerosol composition in Houston, TX. Environ. Sci. and Tech. 16:514-525.

*** Einfeld. W. and S. Dattner.** 1988. The Dallas Winter Visibility Study. Texas Air Control Board, Austin, TX.

*** Eldred, R.A.** 1989. Personal communication. University of California-Davis, Davis, CA.

* **Eldred, R.A. and T.A. Cahill.** 1988. IMPROVE Sampler Manual, version 2. Crocker Nuclear Lab - Air Quality Group, University of California, Davis, CA.

**Eldred, R.A., T.A. Cahill, P.J. Feeney, and W.C. Malm.** 1987. Regional patterns in particulate matter from the National Park Service Network, June 1982 to May 1986, pp. 386-396. In: P.S. Bhardwaja, ed. Visibility Protection: Research and Policy Aspects. Air Pollution Control Assoc., Pittsburgh, PA.

**Ellestad, T.G. and R.E. Speer.** 1981. Application of a telephotometer to visibility measurements in the eastern United States. Atmos. Environ. 15:2443-2449.

**Environmental Protection Agency.** 1979. Protecting Visibility: an EPA report to Congress. EPA report #450/5-79-008. Environmental Protection Agency, Stategies and Air Standards Division, Research Triangle Park, NC.

**Environmental Protection Agency.** 1982. Air Quality Criteria for Oxides of Nitrogen. EPA report #600/8-82-026. Research Triangle Park, NC.

**Evans, G.W. and S. Cohen.** 1987. Environmental stress. In: D. Stokols and I. Altman, eds. Handbook of Environmental Psychology. John Wiley and Sons, New York, NY.

**Evans, G.W. and S.V. Jacobs.** 1982. Air pollution and human behavior. In: G.W. Evans, ed. Environmental Stress. Cambridge University Press, New York, NY.

**Evans, G.W., S.V. Jacobs, and N.B. Frager.** 1982. Behavioral responses to air pollution. In: A. Baum and J. Singer, eds. Advances in Environmental Psychology, volume 4. Erlbaum, NY.

**Evans, G.W., S.V. Jacobs, D. Dooley, and R. Catalano.** 1987. The interaction of stressful life events and chronic strains on community mental health. Am. J. Comm. Psych. 15:23-24.

**Faugeras, O.D.** 1979. Digital color image processing within the framework of a human visual model. IEEE Trans. Acoust, Speech Sig. Process Vol. ASSP-27: 380-393.

**Ferman, M.A., G.T. Wolff, and N.A. Kelly.** 1981. The nature and sources of haze in the Shenandoah Valley/ Blue Ridge Mountain area. J. Air Pollution Control Assoc. 31:1074-1081.

**Faxvog, F.R. and D.R. Roessler.** 1975. Carbon aerosol visibility versus particle size distribution. Applied Optics 17:2612-2616.

**Feynman. R.P., R.B. Leighton, and M. Sands.** 1963. Lectures on Physics. Addison-Wesley, Reading, MA.

**Flowers, E.C., R.A. McCormick, and K.R. Kurfis.** 1969. Atmospheric turbidity over the United States. J. Appl. Meteorol. 8:953-962.

**Forgan, B.W.** 1985. Aerosol optical depth, p. 56. In: B.W. Forgan and P.J. Fraser, eds. Baseline 85. CSIRO Division of Atmospheric Research, Aspendale, Australia.

**Garland, J.A.** 1969. Condensation on ammonium sulfate particles and its effect on visibility. Atmos. Environ. 3:347-354.

**Gins, J.D., D.H. Nochumson, and J.C. Trijonis.** 1981. Statistical relationship between median visibility and conditions at worst-case impact on visibility. Atmos. Environ. 12:2451-2462.

**Graedel, T.E.** 1978. Chemical Compounds in the Atmosphere. Academic Press. New York, NY.

**Grassl, H.** 1988. Radiative effects of atmospheric aerosol particles, pp. 241-252. In: P.V. Hobbs and M.P. McCormick, eds. Aerosols and Climate. A. Deepak Publishing, Hampton, VA.

**Groblicki, P.J., G.T. Wolff, and R.J. Countess.** 1981. Visibility-reducing species in the Denver "Brown Cloud"-I: Relationships between extinction and chemical composition. Atmos. Environ. 15:2473-2484.

**Grosjean, D. and S.K. Friedlander.** 1975. Gas-particle distribution factor for organic and other pollutants in the Los Angeles atmosphere. J. Air Pollution Control Assoc. 25:1038-1044.

**Gschwandther, G., K.C. Gschwandtner, and K. Elridge.** 1985. Historic Emissions of Sulfur and Nitrogen Oxides in the United States from 1900 - 1980. EPA report #600/7-85-009a. Environmental Protection Agency, Research Triangle Park, NC.

**Hall, C.F. and E.L. Hall.** 1977. A nonlinear model for the spatial characteristics of the human visual system. IEEE Trans. Syst. Man. Sybern SMC-7:161-170.

* **Handler, A.** 1989. Annual Report on the Establishment and Operation of the Eastern Fine Particle Visibility Network. EPA report #600/3-89/026. Environmental Protection Agency, Research Triangle Park, NC.

**Hanel, G.** 1976. Radiative effects of atmospheric aerosol particles as functions of the relative humidity at thermodynamic equilibrium with the surrounding moist air, pp. 73-188. In: Advances in Geophysics, Volume 19. Academic Press, New York, NY.

**Hansen, A.D.A., B.A. Bodhaine, E.G. Dutton, and R.C. Schnell.** 1988. Aerosol black carbon measurements at the South Pole. Geophys. Res. Ltrs. 15:1193-1196.

**Harker, A.B., L.W. Richards, and W.E. Clark.** 1977. The effect of atmospheric $SO_2$ photochemistry upon observed nitrate concentrations in aerosols. Atmos. Environ. 11:87-92.

**Harrison, L.** 1985. The segregation of aerosols by cloud-nucleating activity—Part II: Observation of an urban aerosol. J. Climate and Appl. Meteorol. 24:312-321.

**Hasan, H. and T.G. Dzubay.** 1985. Size distribution of species and fine particles in Denver using a micro-orifice impactor. Aerosol Science & Tech.

**Hasan, H. and C.W. Lewis.** 1983. Integrating nephelometer response corrections for bimodal size distributions. Aerosol Sci. and Technol. 2:443-453.

* **Heisler, S.L., R.C. Henry, J.G. Watson, and G.M. Hidy.** 1980a. The 1978 Denver Winter Haze Study, Volume II. ERT document #P-5417-1. Environmental Research and Technology, Inc., Westlake Village, CA.

* **Heisler, S.L., R.C. Henry, and J.G. Watson.** 1980b. The Source of the Denver Haze in November and December of 1978. Paper 80-58.6, presented at the 73rd annual meeting of Air Pollution Control Assoc.

* **Heisler, S.L. and R. Baskett.** 1981. Particle Sampling and Analysis in the California San Joaquin Valley. ERT document #P-5381-701. Prepared for California Air Resources Board by Environmental Research & Technology, Inc., Westlake Village, CA.

**Henry, R.C.** 1977. The application of the linear system theory of visual acuity to visibility reduction by aerosols. Atmos. Environ. 11:697.

**Henry, R.C.** 1979. Modern psychophysics applied to visibility degradation. In: View on Visibility - Regulatory and Scientific. Air Pollution Control Assoc., Pittsburgh, PA.

**Henry, R.C.** 1986. Improved predictions of plume perception with a human visual system model. J. Air Pollution Control Assoc. 36:1353-1356.

**Henry, R.C.** 1987. Psychophysics, visibility, and perceived atmospheric transparency. Atmos. Environ. 21:159-164.

**Henry, R.C. and L.V. Matamala.** 1990. Prediction of color matches and color differences in the outdoor environment. In: C.V. Mathai, ed. Visibility and Fine Particles. Air and Waste Management Association, Pittsburgh, PA.

**Henry, R.C., J.F. Collins, and D. Hadley.** 1981. Potential for quantitative analysis of uncontrolled routine photographic slides. Atmos. Environ. 15:1959.

**Hering, S.V. and S.K. Friedlander.** 1982. Origins of aerosol sulfur size distributions in the Los Angeles basin. Atmos. Environ. 16:2647-2656.

**Hering, S.V., J.L. Bowen, J.G. Wengert, and L.W. Richards.** 1981. Characterization of the regional haze in the southwestern United States. Atmos. Environ. 15:1999-2009.

**Hering, S.V., B.R. Appel, W. Cheng, F. Salaymeh, S.H. Cadle, P.A. Mulawa, T.A. Cahill, R.A. Eldred, M. Surovik, D. Fitz, J.E. Howes, K.T. Knapp, L. Stockburger, B.J. Turpin, and J.J. Huntzicker.** 1989. Comparison of sampling methods for carbonaceous aerosols in ambient air. Aerosol Sci. Technol.

**Hidy, G.M.** 1975. Summary of the California aerosol characterization experiments. J. Air Pollution Control Assoc. 25:1106.

**Hidy, G.M., P.K. Mueller, D. Grosjean, B.R. Appel, and J.J. Wesolowski.** 1980. The Character and Origin of Smog Aerosols. Wiley-Interscience, New York, NY.

**Hill, S.C.** 1990. Measuring changes in aethestic values of the landscape. In: C.V. Mathai, ed. Visibility and Fine Particles. Air and Waste Management Association, Pittsburgh, PA.

**Hill, S.C., A.C. Hill, and P.W. Barber.** 1984. Light scattering by size/shape distributions of soil particles and spheroids. Applied Optics 23:1025-1031.

**Ho, W.W., G.M. Hidy, and R.M. Govan.** 1974. Microwave measurements of the liquid water content of atmospheric aerosols. J. Appl. Meteorol. 13:871-879.

**Hodkinson, J.R.** 1966. Calculations of color and visibility in urban atmospheres polluted by gaseous $NO_2$. Air & Water Pollution Intern. J. 10:137-144.

**Howell, E.R. and R.F. Hess.** 1978. The functional area for summation to threshold for sinusoidal gratings. Vision Res. 18:369-374.

**Husar, R.B.** 1986. Emission of sulfur dioxide and nitrogen oxides and trends for eastern North America. In: Acid Deposition Long-Term Trends, National Academy of Sciences, Washington, DC.

* **Husar, R.B.** 1988. Trends of Seasonal Haziness and Sulfur Emissions over the Eastern United States. Environmental Protection Agency, Research Triangle Park, NC.

* **Husar, R.B.** 1989. Personal communication. Washington University, St. Louis, MO.

* **Husar, R.B. and D.E. Patterson.** 1984. Haze Climate of the United States. Report #CR 810351. Environmental Protection Agency, Research Triangle Park, NC.

**Husar, R.B. and W.R. Shu.** 1975. Thermal analyses of the Los Angeles smog aerosol. J. Appl. Methodol. 14:1558-1565.

**Husar, R.B., J.M. Holloway, D.E. Patterson, and W.E. Wilson.** 1981. Spatial and temporal patterns of eastern United States haziness: A summary. Atmos. Environ. 15:1919-1928.

**Jaeckel, S.M.** 1973. Utility of color-difference formulas for match acceptability decisions. Appl. Optics 12:1299-1316.

*** Jaklevic, J.M., R.C. Gatti, F.S. Goulding, B.W. Loo and A.C. Thompson.** 1981. Aerosol Analysis for the Regional Air Pollution Study. EPA report #600/4-81-006. Environmental Protection Agency, Research Triangle Park, NC.

**Japar, S.M., A.C. Szkarlat, and W.R. Pierson.** 1984. The determination of the optical properties of airborne particle emissions from diesel vehicles. Sci. Total Environ. 36:121-130.

**Johnson, C.E., W.C. Malm, G. Persha, J.V. Molinar, and J.R. Hein.** 1984. Statistical comparisons between teleradiometer derived and slide derived visibility parameters. J. Air Pollution Control Assoc. 35:1261-1265.

**Johnson, C.E., W.C. Malm, J.V. Molenar, L. Mauch, J.R. Hein.** 1988. Improved methods for the computer-imaging of haze layers. Paper 88-56-3. Presented at the 81st annual meeting of the Air Pollution Control Assoc., June 19-24, in Dallas, TX.

**Jones, J.W. and G.A. Bogat.** 1978. Air pollution and human aggression. Psych. Reports 43:721-722.

*** Joseph, D.B., J. Metza, W.C. Malm, M.L. Pitchford.** 1987. Plans for IMPROVE: A federal program to monitor visibility in Class I areas. In: P.J. Bhardwaja, ed. Visibility Protection: Research and Policy Aspects. Air Pollution Control Assoc., Pittsburgh, PA.

**Joseph, J.H., A. Manes, and D. Ashbel.** 1973. Desert aerosols transported by Knamsinic depressions and their climatic effect. J. Appl. Meteorol. 12:792-797.

*** Knudson, D.A.** 1985. Estimated Monthly Emissions of Sulfur Dioxide and Oxides of Nitrogen for the 48 Contiguous States. 1975 - 1984. ANL/EES-TM-318. Department of Energy, Washington, DC.

**Larson, S.M. and G.R. Cass.** 1989. Characteristics of summer midday low-visibility events in the Los Angeles area. Environ. Sci. Technol. 23:281-289.

**Larson, S.M. and G.R. Cass.** 1988. Verification of image processing-based visibility models. Environ. Sci. Technol. 22:629.

*** Latimer, D.A., R.W. Bergstrom, S.R. Hayes, M.K. Liu, J.H. Seinfeld, G.Z. Whitten, M.A. Wojcik, and M.J. Hillyer.** 1978. The Development of Mathematical Models for the Prediction of Anthropogenic Visibility Impairment. EPA reports #4503-78-110a, b, & c. Environmental Protection Agency, Research Triangle Park, NC.

*** Latimer, D.A., T.C. Daniels, and H. Hogo.** 1980. Relationship between air quality and human perception of scenic areas. Publ. #4323. American Petroleum Institute, Washington, D.C.

**Latimer, D.A., H. Hogo, D.H. Hern, and T.C. Daniels.** 1983. Effects of visual range on the beauty of national parks and wilderness area vistas. In: R.D. Rowe and L.G. Chestnut, eds. Managing Air Quality and Scenic Resources at National Parks and Wilderness Areas.

**Lewis, C.W.** 1981. On the proportionality of fine mass concentration and extinction coefficient for bimodal size distributions. Atmos. Environ. 15:2639-2646.

*** Lewis, R.** 1989. Personal communication. Aero-Vironment, Inc., Pasadena, CA.

**Lewis, C.W. and T.G. Dzubay.** 1986. Measurement of light absorption extinction in Denver. Aerosol Sci. Technol. 5:325-336.

**Lewis, C.W. and E.S. Macias.** 1980. Composition of size-fractionated aerosol in Charleston, WV. Atmos. Environ. 14:185-194.

*** Lewis, C.W. and R.K. Stevens.** 1983. Comparison of Factors Influencing Visual Air Quality During the Winter in Denver, derived from measurements made by General Motors and Motor Vehicle Manufacturers Association in 1978 and Environmental Protection Agency in 1982. EPA Preliminary Report. Environmental Protection Agency, Research Triangle Park, NC.

**Lewis, C.W., R.E. Baumgardner, R.K. Stevens, and G.M. Russwurm.** 1986. Receptor modeling study of Denver winter haze. Environ. Sci. Technol. 20:1126-1136.

**Lioy, P.J., J.M. Daisey, N.M. Reiss, and R. Harkov.** 1983. Characterization of inhalable particulate matter, volatile organic compounds, and other chemical species measured in urban areas in New Jersey: Summertime episodes. Atmos. Environ. 17:2321-2330.

**Loomis, R.J., M.J. Kiphart, D.B. Garnard, W.C. Malm, and J.V. Molenar.** 1985. Human perception of visibility impairment. In: Proceedings of 78th annual meeting of Air Pollution Control Association, June 16-21, Detroit, MI.

**Lowry, E.M.** 1931. The photometric sensibility of the eye and the precision of photometric observations. J. Optical Society of America 21:32.

**Lowry, E.M.** 1951. The luminance discrimination of the human eye. J. of the Soc. of Motion Pictures and Television Engineers.

**Lundgren, D.A., M. Lippmann, F.S. Harris, W.E. Clark, W.H. Marlow, and M.D. Durham, eds.** 1979. Aerosol Measurements. University of Florida Press, Gainesville, FL.

* **Lyons, C. and I. Tombach.** 1979. Willamette Valley Field and Slash Burning Impact Air Surveillance Network Data Evaluation, Vol. 2. Final report prepared for Oregon Dept. of Environmental Quality by AeroVironment Inc., Pasadena, CA.

**Macias, E.S., J.O. Zwicker, J.R. Ouimette, S.V. Hering, S.K. Friedlander, T.A. Cahill, G.A. Kuhlmey, and L.W. Richards.** 1981a. Regional haze case studies in the southern United States I: Aerosol chemical composition. Atmos. Environ. 15:1971-1986.

**Macias, E.S., J.O. Zwicker, and W.H. White.** 1981b. Regional haze case studies in the southwestern United States II: Source contributions. Atmos. Environ. 15:1987-1997.

**Macias, E.S., T.L. Vossler, W.H. White.** 1987. Carbon and sulfate fine particles in the western United States. In: P.S. Bhardwaja, ed. Visibility Protection: Research and Policy Aspects. Air Pollution Control Assoc., Pittsburgh, PA.

* **Malm, W.C.** 1979. Visibility: a physical perspective. Presented at workshop on visibility values, Jan 28-Feb 1, at Fort Collins, CO.

**Malm, W.C.** 1985. An examination of the ability of various physical indicators to predict judgment of visual air quality. Presented at the 78th annual meeting of the Air Pollution Control Assoc., June 16-21, in Detroit, MI.

**Malm, W.C.** 1986. Review of techniques for measuring atmospheric extinction. In: Proceedings of 79th annual meeting of Air Pollution Control Assoc.

**Malm, W.C. and R.C. Henry.** 1987. Regulatory perspective of visibility research needs. In: Proceedings of 80th annual meeting of Air Pollution Control Assoc., June 21-26, in New York, NY.

**Malm, W.C. and M. Pitchford.** 1989. The use of an atmospheric quadratic detection model to assess change in aerosol concentrations to visibility. Paper 89-67.3. Presented to the 82nd annual meeting of the Air Pollution Control Assoc., June 25-30, in Anaheim, CA.

* **Malm, W.C. and E.G. Walther.** 1980. A Review of Instrument-Measuring Visibility-Related Variables. EPA report #600/4-80-016. Environmental Protection Agency, Research Triangle Park, NC.

**Malm, W.C., M. Kleine, and K. Kelley.** 1980a. Human perception of visual air quality (layered haze). Presented at the 1980 conference on visibility at the Grand Canyon.

**Malm, W.C., K.K. Leiker, and J.V. Molenar.** 1980b. Human perception of visual air quality. J. Air Pollution Control Assoc.

**Malm, W.C., K. Kelly, J. Molenar, and T. Daniels.** 1981. Human perception of visual air quality (uniform haze). Atmos. Environ. 15:1875.

**Malm, W.C., J. Molenar, and L.L. Chan.** 1983. Photographic simulation techniques for visualizing the effect of uniform haze on a scenic resource. J. Air Pollution Control Assoc. 33:126.

**Malm, W.C., P. Bell, and G.E. McGlothin.** 1984. Field testing a methodology for assessing the importance of good visual air quality. In: Proceedings of the 77th annual meeting of the Air Pollution Control Assoc., June 24-29, San Francisco, CA.

**Malm, W.C., T. Cahill, K. Gebhart, and A. Waggoner.** 1987a. Optical characteristics of atmospheric sulfur at Grand Canyon, AZ. In: P.S. Bhardwaja, ed. Visibility Protection: Research and Policy Aspects. Air Pollution Control Assoc., Pittsburgh, PA.

**Malm, W.C., G. Persha, R. Tree, R. Stocker, I. Tombach, and H. Iyer.** 1987b. Comparison of atmospheric extinction measurements made by a transmissometer, integrating nephelometer, and teleradiometer with natural and artificial black targets. In: P.S. Bhardwaja, ed. Visibility Protection: Research and Policy Aspects. Air Pollution Control Assoc., Pittsburgh, PA.

**Malm, W.C., D.M. Ross, R. Loomis, J. Molenar, and H. Iyer.** 1987c. An examination of the ability of various physical indicators to predict perception thresholds of plumes as a function of their size and intensity. In: P.J. Bhardwaja, ed. Visibility Protection Research and Policy Aspects. Air Pollution Control Assoc., Pittsburgh, PA.

* **Malm, W.C., K. Gebhart, D. Latimer, T. Cahill, R. Eldred, R. Pielke, R. Stocker, and J. Watson.** 1989. The Winter Haze Intensive Tracer Experiment. Report by National Parks Service, Fort Collins, CO.

**Mason, B. and C.B. Moore.** 1982. Principles of Geochemistry. John Wiley and Sons, New York, NY.

**Mathai, C.V., ed.** 1990. Visibility and Fine Particles. Transactions of AWMA specialty conference, October 1989, Estes Park, CO. Air and Waste Management Assoc., Pittsburgh, PA.

* **Mathai, C.V. and I.H. Tombach.** 1985. Assessment of the Technical Basis Regarding Regional Haze and Visibility Impairment. Final report prepared for the Utility Air Regulatory Group by Aerovironment Inc., Moniovia, CA.

**Mathai, C.V. and I.H. Tombach.** 1987. A critical assessment of atmospheric visibility and aerosol measurement in the eastern United States. J. Air Pollution Control Assoc. 37:700-707.

**McDade, C.E. and I.H. Tombach.** 1987. Goals and initial findings from SCENES. In: P.S. Bhardwaja, ed. Visibility Protection: Research and Policy Aspects. Air Pollution Control Assoc., Pittsburgh, PA.

**McMurry, P.H. and S.K. Friedlander.** 1979. New particle formation in the presence of an aerosol. Atmos. Environ. 13:1635-1651.

**McMurry, P.H. and M.R. Stolzenburg.** 1989. On the sensitivity of particle size to relative humidity for Los Angeles aerosols. Atmos. Environ. 23:497-507.

**McMurry, P.H. and X.Q. Zhang.** 1989. Size distributions of ambient organic and elemental carbon. Aerosol Sci. Technol. 10:430-437.

**Middleton, W.E.K.** 1952. Vision Through the Atmosphere. Toronto University Press, Toronto, Canada.

**Middleton, P., T.R. Stewart, and R.C. Dennis.** 1983. Modeling human judgment of urban visual air quality. Atmos. Environ.

**Middleton, P., T.R. Stewart, D. Ely, and C.W. Lewis.** 1984. Physical and chemical indicators of urban visual air quality. Atmos. Environ. 18:861-870.

**Mie, G.** 1908. Ann. Physik. Bd 2, 25, IV. Fogle, Netherlands.

**Milford, J.B. and C.I. Davidson.** 1987. The sizes of particulate sulfate and nitrate in the atmosphere—a review. J. Air Pollution Control Assoc. 37:125-134.

**Mueller, P.K. and G.M. Hidy.** 1983. The Sulfate Regional Experiment: Report of Findings. Report #EA-1901, Vols. 1, 2, & 3. Electric Power Research Institute, Palo Alto, CA.

**Mueller, P.K. and J.G. Watson.** 1982. Eastern Regional Air Quality Measurements, Vol. I. Report #EA-1914. Electric Power Research Institute, Palo Alto, CA.

**Mueller, P.K., D.A. Hansen, and J.G. Watson.** 1986. The Subregional Cooperative Electric Utility, Dept. of Defense, National Parks Service, and EPA (SCENES) study on visibility: An overview. Report #EPRI EA-4664-SR. Electric Power Research Institute, Palo Alto, CA.

**Munn, R.E.** 1973. Secular increases in summer haziness in the Atlantic provinces. Atmosphere 11:4.

**Nixon, J.K.** 1940. Absorption coefficient on $NO_2$ in the visibile spectrum. J. Chem. Phys. 8:157.

**NOAA.** 1982. An Overview of Applied Visibility Fundamentals Survey and Synthesis of Visibility Literature. FCM-R3-1982. National Oceanic and Atmospheric Administration, Washington, DC.

**Ouimette, J.R. and R.C. Flagan.** 1982. The extinction coefficient of multicomponent aerosols. Atmos. Environ. 16:2405-2419.

**Ouimette, J.R., R.C. Flagan, and A.R. Kelso.** 1981. Chemical species contributions to light scattering by aerosols at a remote arid site. In: E.S. Macias and P.K. Hopke, eds. Amer. Chem. Soc. Symposium Series 167: Atmospheric Aerosol.

**Ozkaynak. H., A.D. Schatz, G.D. Thurston, R.G. Isaacs, and R.B. Husar.** 1985. Relationships between aerosol extinction coefficients derived from airport visual range observations and alternative measures of airborne particle mass. J. Air Pollution Control Assoc. 35:1176-1185.

*** Pace, T.J., Jr., G. Watson, and C.E. Rhodes.** 1981. Preliminary interpretation of inhalable particulate network data. Presented at the 74th annual meeting of the Air Pollution Control Assoc.

**Patterson, E.E., J.M. Holloway, and R.B. Husar.** 1980. Historical Visibility over the Eastern United States: Daily and Quarterly Extinction Coefficient Contour Maps. EPA-600/3-80-043a. Environmental Protection Agency, Research Triangle Park, NC.

*** Pierson, W.R.** 1985. Personal communication. Ford Motor Company, Detroit, MI.

**Pierson, W.R., W.W. Brachaczek, T.J. Korniski, T.J. Truex, and J.W. Butler.** 1980a. Artifact formation of sulfate, nitrate, and hydrogen ion on backup filters: Allegheny Mountain experiment. J. Air Pollution Control Assoc. 30:30-34.

**Pierson, W.R., W.W. Brachaczek, T.J. Korniski, T.J. Truex.** 1980b. Ambient sulfate measurements on Allegheny Mountain and the question of atmospheric sulfate in the northeastern United States. Annals, New York Academy of Sciences 338:145-173.

**Pierson, W.R., W.W. Brachaczek, R.A. Gorse, S.M. Japar, J.M. Norbeck, and G.J. Keeler.** 1989. Atmospheric acidity measurements on Allegheny Mountains and the origins of ambient acidity in the northeastern United States. Atmos. Environ. 23:431-459.

**Pilinis, C.** 1989. Numerical simulation of visibility degradation due to particulate matter: Model development and evaluation. J. Geophys. Research.

**Pitchford, M. and M. McGown.** 1987. An approach for calculating inherent contrast of teleradiometer targets, pp. 490-498. In: P.J. Bhardwaja, ed. Visibility Protection: Research and Policy Aspects. Air Pollution Control Assoc., Pittsburgh, PA.

**Porch, W.M., D.S. Ensor, R.J. Charlson, and J. Heintzenberg.** 1973. Blue moon: Is this a property of background aerosol? Appl. Optics 12:34-36.

**Post, J.E. and P.R. Buseck.** 1984. Characterization of individual particles in the Phoenix urban aerosol using electron-beam instruments. Environ. Sci. Technol. 18:35-42.

* **Reisinger, L.M. and R.J. Valente.** 1984. Visibility and air quality impairment in the southeastern United States—1983. Paper #84-59.3. Presented at 77th annual meeting of the Air Pollution Control Association, San Francisco, CA.

* **Reisinger, L.M. and R.J. Valente.** 1985. Visibility and Other Air Quality Measurements made at the Great Smoky Mountains National Park. TVA/ON RED/ AWR-85/6. Tennessee Valley Authority, Muscle Shoals, AL.

* **Richards, L.W.** 1987. A Discussion of Atmospheric Optics Related to Visibility. Report #STI-96070-702-5D. Sonoma Technology Inc., Santa Rosa, CA.

**Richards, L.W.** 1990. Effect of atmosphere on visibiity. In: C.V. Mathia, ed. Visibility and Fine Particles. Air and Waste Management Association, Pittsburgh, PA.

**Richards, L.W. and M. Stoelting.** 1987. Experimental evaluation of the determination of atmospheric extinction by the measurement of the transmittance of radiance difference. In: P.J. Bhardwaja, ed. Visibility Protection Research and Policy Aspects. Air Pollution Control Assoc., Pittsburgh, PA.

* **Richards, L.W., G.R. Markowski, and N. Waters.** 1981. Comparison of nephelometer, telephotometer, and aerosol data in the Southwest. Paper No. 81-54.5. Presented at Air Pollution Control Assoc. annual meeting, June 1988.

**Robinson, G.D.** 1977. Effects of energy production: Particulates, pp.61-71. In: R.R. Revelle, ed. Energy and Climate. Panel on Energy and Climate, National Research Council, Washington, DC.

* **Robinson, G.D.** 1984. Personal communication. National Research Council, Washington, DC.

**Rodes, C.E. and E.G. Evans.** 1985. Preliminary assessment of 10 µm particulate sampling at eight locations in the United States. Atmos. Environ. 19:293-303.

**Rodes, C.E., D.M. Holland, L.J. Purdue, and K.A. Rehme.** 1985. A field comparison of PM10 inlets at four locations. J. Air Pollution Control Assoc. 35:345-354.

**Ross, D.M., W.C. Malm, and R.J. Loomis.** 1985. The psychological valuation of good visual air quality by national park visitors. In: Proceedings of 78th annual meeting of Air Pollution Control Assoc., June, Detroit, MI.

**Ross, D.M., W.C. Malm, and R.J. Loomis.** 1987. An examination of the relative importance of park attributes at several national parks. In: P.S. Bhardwaja, ed. Visibility Protection: Research and Policy Aspects. Air Pollution Control Assoc., Pittsburgh, PA.

**Ross, D.M., W.C. Malm, H.K. Iyer, and R.J. Loomis.** 1990. Human visual sensitivity to layered haze using computer generated images. In: Proceedings of Air and Waste Management Assoc. International specialty conference "Visibility and Fine Particles", October 15-19, 1989, Estes Park, CO.

**Ross, D.M., W.C. Malm, H.K. Iyer, and R.J. Loomis.** 1988. Human detection of layered haze using natural scene slides with a signal detection paradigm. In: Proceedings of 81st annual meeting of Air Pollution Control Assoc., June 19-24, Dallas, TX.

**Rotton, J. and J. Frey.** 1982. Atmospheric conditions, seasonal trends, nd psychiatric emergencies. In: Replications and Extensions. American Psychological Assoc., Washington, DC.

**Rotton, J., T. Barry, M. Milligan, and M. Fitzpatrick.** 1979. The air pollution experience and interpersonal aggression. J. App. Psych. 9:397-412.

**Rubel, G.O. and J.W. Gentry.** 1984. Measurement of the kinetics of solution droplets in the presence of absorbed monolayers: Determination of water accomodation coefficients. J. Phys. Chem. 88:3142-3148.

**Ruby. M.G. and A.P. Waggoner.** 1981. Intercomparison of integrating nephelometer measurements. Environ. Sci. Technol. 15:109-113.

**Schwartz, S.E.** 1988. Are global cloud albedo and climate controlled by marine phytoplankton? Nature 336:441-445.

* **Shah, J.J.** 1981. Measurements of Carbonaceous Aerosol Across the United States: Sources and Role in Visibility Degradation. Ph.D. Thesis, Oregon Graduate Center, Beaverton, Oregon.

**Shah, J.J., J.G. Watson, Jr., J.A. Cooper, and J.J. Huntzicker.** 1984. Aerosol chemical composition and light scattering in Portland, OR: The role of carbon. Atmos. Environ. 18:235-240.

**Shah, J.J., R.L. Johnson, E.K. Heyerdahl, and J.J. Huntzicker.** 1986. Carbonaceous aerosol at urban and rural sites in the United States. J. Air Pollution Control Assoc. 36:254-257.

**Shaw, R.W., Jr. and R.J. Paur.** 1983. Composition of aerosol particles collected at rural sites in the Ohio River Valley. Atmos. Environ. 17:2031-2044.

**Shaw, R.W., Jr., R.K. Stevens, J. Bowermaster, J.W. Tesch, and E. Tew.** 1982. Measurements of atmospheric nitrate and nitric acid: The denuder difference experiment. Atmos. Environ. 16:845-853.

**Shettle, E.P. and R.W. Fenn.** 1979. Models for the aerosols of the lower atmosphere and the effects of humidity variations on the optical properties. AFGL-TR-79-0214/

Environmental Research Paper #676. Air Force Geophysics Laboratory, Optical Research Division, Project 7670, Hanscon AFB, MA.

**Sloane, C.S.** 1982a. Visibility trends I: Methods of analysis. Atmos. Environ. 16:41-51.

**Sloane, C.S.** 1982b. Visibility trends II: Mideastern United States. Atmos. Environ. 16:2309-2321.

**Sloane, C.S.** 1983a. Optical properties of aerosols—comparison of measurements with model calculations. Atmos. Environ. 17:409-416.

**Sloane, C.S.** 1983b. Summertime visibility declines: Meteorological influences. Atmos. Environ. 17:763-774.

**Sloane, C.S.** 1984a. Optical properties of aerosols of mixed composition. Atmos. Environ. 18:871-878.

**Sloane, C.S.** 1984b. Meteorologically adjusted air quality trends: Visibility. Atmos. Environ. 18:1217-1229.

**Sloane, C.S.** 1985. Change in aerosol optical properties with change in chemical composition. In: Proceedings of 78th annual meeting of Air Pollution Control Assoc., June 16-21, Detroit, MI.

**Sloane, C.S.** 1986. Effect of composition on aerosol light scattering efficiencies. Atmos. Environ. 20:1025-1073.

**Sloane, C.S.** 1988. Forecasting visibility impairment: A test of regression estimates. Atmos. Environ. 22:2033-2045.

**Sloane, C.S. and G.T. Wolff.** 1984. Relating ambient visibility to aerosol composition. Paper #84-115.1. Presented at 77th annual meeting of Air Pollution Control Assoc., San Francisco, CA.

**Sloane, C.S. and G.T. Wolff.** 1985. Prediction of ambient light scattering using a physical model responsive to relative humidity: Validation with measurements from Detroit. Atmos. Environ. 19:669-680.

**Spengler, J.D. and G.D. Thurston.** 1983. Mass and elemental composition of fine and coarse particles in six United States cities. J. Air Pollution Control Assoc. 33:1162-1171.

**Spicer, C.W. and P.M. Schumacher.** 1977. Interferences in sampling atmospheric particulate nitrate. Atmos. Environ. 11:873-876.

**Stelson, A.W. and J.H. Seinfeld.** 1981. Chemical mass accounting of urban aerosol. Environ. Sci. Technol. 15:671-679.

**Stern, A.C., ed.** 1976. Air Pollution: Measuring Monitoring and Surveillance of Air Pollution, Vol. III. Academic Press, New York, NY.

**Stevens, R.K., T.G. Dzubay, G. Russworm, and D. Rickel.** 1978. Sampling and analysis of atmospheric sulfates and related species. Atmos. Environ. 12:55-68.

**Stevens, R.K., T.G. Dzubay, R.W. Shaw, W.A. McClenny, C.W. Lewis, and W.E. Wilson.** 1980. Characterization of aerosol in the Great Smoky Mountains. Environ. Sci. and Tech. 14:1491-1498.

**Stevens, R.K., T.G. Dzubay, C.W. Lewis, and R.W. Shaw.** 1984. Source apportionment methods applied to the determination of the origin of ambient aerosols that affect visibility in forested areas. Atmos. Environ. 18:261-272.

**Steward, T.R., P. Middleton, and D.W. Ely.** 1983. Urban visual air quality judgments: Reliability and validity. J. Environ. Psych. 3:129-145.

**Stewart, T.R., P. Middleton, M. Downton, and D. Ely.** 1984. Judgments of photographs versus field observations in studies of perception and judgment of the visual environment. J. Environ. Psych. 4:283-302.

**Szkarlat, A.C. and S.M. Japar.** 1981. Light absorption by airborne particles, Comparison of integrating plate and spectrophone techniques. Appl. Optics 20:1151-1161.

* **Tang, I.N.** 1981. Deliquescence properties and particle size change of hygroscopic aerosols. In: Generation of Aerosols and Facilities for Exposure Experiments. Ann Arbor Science Publishers, Ann Arbor, MI.

**Tang, I.N., W.T. Wong, and H.R. Munkelwitz.** 1981. The relative importance of atmospheric sulfates and nitrates in visibility reduction. Atmos. Environ. 15:2463.

**Tombach, I. and D. Allard.** 1983. Comparison of Visibility Measurement Techniques: Eastern United States. EPRI report #EA-3292. Electric Power Research Institute, Palo Alto, CA.

**Tombach, I.H., D.W. Allard, R.L. Drake, and R.C. Lewis.** 1987a. Western Regional Air Quality Studies: Visibility and Air Quality Measurements 1981-1982. EPRI report #EA-4903. Electric Power Research Institute, Palo Alto, CA.

**Tombach, I., D. Bush, W. Malm, and L.W. Richards.** 1987b. SCENES light extinction methods study, September-October 1985. In: P.S. Bhardwaja, ed. Visibility Protection: Research and Policy Aspects. Air Pollution Control Assoc., Pittsburgh, PA.

**Trijonis, J.C.** 1979. Visibility in the Southwest - an exploration of the historical data base. Atmos. Environ. 13:833.

**Trijonis, J.C.** 1982a. Existing and natural background levels of visibility and fine particles in the rural East. Atmos. Environ. 16:2431-2445.

**Trijonis, J.C.** 1982b. Visibility in California. J. Air Pollution Control Assoc. 32:165-169.

* **Trijonis, J.C.** 1987. National Relationship Between Visibility and $NO_x$ Emissions. Report by Santa Fe Research Corp., Bloomington, MN.

* **Trijonis, J.C. and K. Yuan.** 1978. Visibility in the Northeast: Long-Term Visibility Trends and Visibility/Pollutant Relationships. EPA report #600/3-78-075. Environmental Protection Agency, Research Triangle Park, NC.

* **Trijonis, J., G. Cass, G. McRae, Y.W.Y. Lim, N. Chang, and T. Cahill.** 1982. Analysis of Visibility, Relationships and Visibility Modeling/Monitoring Alternatives. Report for contract #A9-103-31, submitted to California Air Resources Board, Sacramento, CA.

**Trijonis, J.C., M. Pitchford, M. McGown, *et al.*** 1987. Preliminary extinction budget results from the RESOLVE program, pp. 872-883. In: P.J. Bhardwaja, ed. Visibility Protection Research and Policy Aspects. Air Pollution Control Assoc., Pittsburgh, PA.

**Trijonis, J.C., M. McGown, M. Pitchford, D. Blumenthal, P. Roberts, W. White, E. Macias, R. Weiss, A. Waggoner, J. Watson, J. Chow, and R. Flocchini.** 1988. RESOLVE Project Final Report: Visibility Conditions and Causes of Visibility Degradation in the Mojave Desert of California. NWC TP #6869. Naval Weapons Center, China Lake, CA.

* **Tsay, S., J.M. Davis, G.L. Stephens, S.K. Cox, and T.B. McKee.** 1987. Backward Monte Carlo Computations of Radiation Propagating in Horizontally Inhomogeneous Media, Part I: Description of Codes. Report by Cooperative Institute for Research in the Atmosphere, Colorado State University, Fort Collins, CO.

**Twomey, S.A.** 1977. Chapter 12, pp. 274-293. In: Atmospheric Aerosols. Elsevier Scientific Publishing Co., Amsterdam, Netherlands.

**Twomey, S.A., M. Piepgrass, and T.L. Wolfe.** 1984. An assessment of the impact of pollution on global cloud albedo. Tellus 36B:356-366.

* **Valente, R.J. and L.M. Reisinger.** 1983. Data Summary: Visibility and Ambient Air Quality in the Great Smoky Mountain National Park Research Project. TVA/ONR/AQB-83/4. Tennessee Valley Authority, Muscle Shoals, AL.

**vandeHulst, H.C.** 1981. Light Scattering by Small Particles. Dover Publications, New York, NY.

**Watson, J.G., J. Chow, and J.J. Shah.** 1981. Analysis of Inhalable and Fine Particulate Matter Measurements. EPA-450/4-81-035. Environmental Protection Agency, Research Triangle Park, NC.

* **Watson, J. G., J.C. Chow, L.W. Richards, S.R. Anderson, J.E. Houck, D.L. Dietrick.** 1988. The 1987-88 Metro Denver Brown Cloud Air Pollution Study Volumes I, II, & III. DRI report #8810.1F1, 8810.1F2, and 8810.1F3. Prepared for the greater Denver Chamber of Commence, Denver, CO.

* **Watson, J.G., J.C. Chow, L.C. Pritchett, L.W. Richards, D.L. Dietrich, J. Molenar, J. Faust, S.R. Andersen, and C.S. Sloane.** 1989. Comparison of three measures of visibility extinction in Denver, CO. Paper No. 89-151.4. Presented at Air Pollution Control Assoc. annual meeting, June 1989.

**Watson, J.G., J. Chow, and R.K. Stevens.** 1990. Survey of fine particle sampling systems used in visibility studies. In: C.V. Mathai, ed. Visibility and Fine Particles. Air and Waste Management Association, Pittsburgh, PA.

* **Weiss, R.E.** 1980. The Optical Absorption Properties of Suspended Particles in the Lower Troposphere at Visibile Wavelengths. Ph.D. Dissertation, University of Washington, Seattle, WA.

**Weiss, R.E., T.V. Larson, and A.P. Waggoner.** 1982. In situ rapid-response measurement of $H_2SO_4$ /$(NH_4)_2$ $SO_4$ aerosols in rural Virginia. Environ. Sci. and Technol. 16:525-532.

* **Whitby, K.T. and B. Cantrell.** 1976. Atmospheric aerosols - characteristics and measurements. In Session 29: Fine Particles at international conference on Environmental Sensing Assessment held in Las Vegas, NV, in Sept. 1976. Institute of Electrical and Electronics Engineers, New York, NY.

**Whitby, K.T., R.B. Husar, and B.Y.H. Liu.** 1972. The aerosol size distribution of Los Angeles smog. J. Colloid Interface Sci. 39:177-204.

**White, W.H.** 1986. On the theoretical and empirical basis for apportioning extinction by aerosols: a critical review. Atmos. Environ. 20:1659-1672.

**White, W.H.** 1989. Heteroscedasticity and the standard errors of regression esimates. In: J.G. Watson, ed. Receptor Models. Air Pollution Control Assoc., Pittsburgh, PA.

**White, W.H. and R.B. Husar.** 1980. A Lagrangian model of the Pasadena smog aerosol. In: G.M. Hidy *et al.*, eds. Advances in Environmental Science and Technology.

**White, W.H. and E.S. Macias.** 1987. On measurement error and the empirical relationship of atmospheric extinction to aerosol composition in the non-urban West. In: P.S. Bhardwaja, ed. Visibility Protection: Research and Policy Aspects. Air Pollution Control Assoc., Pittsburgh, PA.

**White, W.H. and E.S. Macias.** 1988. Light scattering by haze and dust at Spirit Mountain, NV. In: C.V. Mathai, ed. Visibility and Fine Particles. Air and Waste Management Assoc., Pittsburgh, PA.

**White, W.H. and E.S. Macias.** 1989. Carbonaceous particles and regional haze in the western United States. Aerosol Sci. Technol. 10:111-117.

**White, W.H. and P.T. Roberts.** 1977. On the nature and origins of visibility-reducing aerosols in the Los Angeles air basin. Atmos. Environ. 11:803-812.

**Williams, M.D., E. Treiman, M. Wecksung.** 1980. Plume blight visibility modeling with a simulated photographic technique. J. Air Pollution Control Assoc. 30:131.

**Winer, A.M., J.W. Peters, J.P. Smith, and J.N. Pitts, Jr.** 1974. Response of commercial chemi-luminescent NO/$NO_2$ analyzers to other nitrogen-containing compounds. Environ. Sci. Technol. 8:1118-1121.

**Winkler, P.** 1973. The growth of atmospheric aerosol particles as a function of the relative humidity II: Method and measurement at different locations. J. Research Atmos. 6:617-638.

**Wolff, G.T.** 1987. Visibility-reducing species in New England's Berkshire Mountains. In: P.S. Bhardwaja, ed. Visibility Protection: Research and Policy Aspects. Air Pollution Control Assoc., Pittsburgh, PA.

**Wolff, G.T. and P.E. Korsog.** 1989. Atmospheric concentrations and regional source apportionments of sulfate, nitrate, and sulfur dioxide in the Berkshire Mountains in western Massachusetts. Atmos. Environ. 23:55-65.

**Wolff, G.T., R.J. Countess, P.J. Groblicki, M.A. Ferman, S.H. Cadle, and J.L. Muhlbaier.** 1981. Visibility-reducing species in the Denver "Brown Cloud"-II: Sources and temporal patterns. Atmos. Environ. 15:2485-2502.

**Wolff, G.T., N.A. Kelly, and M.A. Ferman.** 1982a. Source regions of summertime ozone and haze episodes in the eastern United States. Water, Air, Soil Pollution 18:65-81.

**Wolff, G.T., M.A. Ferman, N.A. Kelly, D.P. Stroup, and M.S. Ruthkosky.** 1982b. The relationships between the chemical composition of fine particles and visibility in the Detroit metropolitan area. J. Air Pollution Control Assoc. 32:1216-1220.

**Wolff, G.T., N.A. Kelly, M.A. Ferman, and M.L. Morrissey.** 1983. Rural measurements of chemical composition of airborne particles in the eastern United States. J. Geophys. Res. 88:10,769-10,775.

*** Wolff, G.T., N.A. Kelly, M.A. Ferman, M.S. Ruthkosky, D.P. Stroup, and P.E. Korsog.** 1985a. Measurements of haze and fine particles at a rural site on the Atlantic coast. Paper 85-11.4. Presented at 78th annual meeting of the Air Pollution Control Assoc., Detroit, Michigan.

**Wolff, G.T., P.E. Korsog, D.P. Stroup, M.S. Ruthkosky, and M.L. Morrissey.** 1985b. The influence of local and regional sources on the concentration of inhalable particulate matter in southeastern Michigan. Atmos. Environ. 19: 305-313.

**Wolff, G.T., N.A. Kelly, M.A. Ferman, M.S. Ruthkosky, D.P. Stroup, and P.E. Korsog.** 1986. Measurements of sulfur oxides, nitrogen oxides, haze, and fine particles at a rural site on the Atlantic coast. J. Air Pollution Control Assoc. 36:585-591.

*** Zak, B.D., W. Einfeld, H.W. Church, G.T. Gay, A.L. Jensen, J. Trijonis, M.D. Evey, P.S. Homann, and C. Tipton.** 1984. The Albuquerque Winter Visibility Study, Volume I: Overview and Data Analysis. Sandia Report SAND 84-0173/1. Sandia National Laboratory, Albuquerque, NM.

**Ziedner, M. and M. Shechter.** 1988. Psychological responses to air pollution: some personality and demographic correlates. J. Environ. Psych. 8:191-208.

---

* Indicates publication is an internal report, or not peer reviewed, or not readily available.

# APPENDIX A

# CHARACTERIZATION OF NATURAL BACKGROUND AEROSOL CONCENTRATIONS

## A.1 INTRODUCTION
*J.C. Trijonis*

This appendix develops estimates of annual average aerosol concentrations under natural background conditions for the eastern and western United States. As noted in Section 3.5, the East values represent an average over the area up to one tier of states west of the Mississippi. The West values represent an average for the mountain/desert regions of the western United States.

Natural background concentrations are estimated for coarse particle (2.5 to 10 μm) and for six major components of fine aerosols (≤ 2.5 μm): sulfates, organics, elemental carbon, ammonium nitrate, soil dust, and water. Following the procedures of Trijonis (1982), the natural background concentrations are estimated based on three types of information:

1. compilations of natural versus man-made emission levels,
2. ambient measurements in remote areas (especially in the southern hemisphere, and
3. regression studies using man-made and/or natural tracers.

Table 24A-1 summarizes the results of the analysis. The following subsections explain the results for each of the aerosol components.

*Table 24A-1. Natural Background Levels of Aerosols*

| | Ave. Conc. | | Error |
|---|---|---|---|
| | East μg/m$^3$ | West μg/m$^3$ | Factor |
| Fine Particles (≤ 2.5 μm) | | | |
| Sulfates (as $NH_4HSO_4$) | 0.2 | 0.1 | 2 |
| Organics | 1.5 | 0.5 | 2 |
| Elemental Carbon | 0.02 | 0.02 | 2-3 |
| Ammonium Nitrate | 0.1 | 0.1 | 2 |
| Soil Dust | 0.5 | 0.5 | 1.5-2 |
| Water | 1.0 | 0.25 | 2 |
| Coarse Particles (2.5-1.0 μm) | 3.0 | 3.0 | 1.5-2 |

## A.2 FINE ORGANICS
*J.C. Trijonis*

Organic particles are an important component of the natural fine aerosol. Unfortunately, substantial uncertainty exists regarding concentrations for natural organic aerosols. For one, there has been a long standing paradox (Altshuller, 1983), with emission rate calculations suggesting potentially large concentrations of plant wax and turpene-derivative aerosols (Duce, 1978; Beauford *et al.*, 1977; Rasmussen and Went, 1965) but with ambient studies finding little direct evidence of significant natural organic aerosols (Crittenden, 1976; Daisey *et al.*, 1979; Shaw *et al.*, 1983). Second, there are uncertainties regarding sampling procedures for organic aerosols—in terms of negative artifacts, positive artifacts, and blank determinations. Third, as seen below, the relevant ambient studies do not provide consistent conclusions regarding natural organic aerosols.

The analysis below will be separated into West and East. Throughout the discussion, organic particle concentrations will be defined and reported as 1.5 times organic carbon concentrations.

For the West, we have chosen a value of 0.5 μg/m$^3$ for natural background fine organics (with an error factor of approximately two). This conclusion is based on the following considerations:

- The RESOLVE visibility study (Trijonis *et al.*, 1988) in the Mojave desert of California included measurements of carbon isotope ratios and analyses of organic molecular composition in order to investigate the origins of organic aerosols. The study concluded that, on an annual basis, 80% ± 15% of the organic aerosol was anthropogenic. Noting that the average organic aerosol concentrations were 3 μg/m$^3$, one derives a natural organic aerosol level of 0.6 ± 0.45 μg/m$^3$.
- Using particle filters from three Arizona sites of the SCENES study, Mazurek *et al.* (1988) investigated organic molecular composition via solvent extraction and high resolution gas chromatography. Assuming that one-half of non-petroleum (contemporary) organics are solvent extractable, non-petroleum organic concentrations averaged only about 0.2 to 0.3 μg/m$^3$. About three-fourths of this was wood smoke, which may itself have a large man-made component. These findings sug-

gest a natural organic aerosol concentration as small as 0.1 to 0.2 $\mu g/m^3$.

- Currently, average fine organic concentrations at remote sites in the West range from about 1 to 2 $ug/m^3$ (Bhardwaja, 1987; Eldred *et al.*, 1987; Macias *et al.*, 1987; Shah *et al.*, 1986; Sutherland and Bhardwaja, 1987; Trijonis *et al.*, 1988). Currie *et al.* (1984) have performed carbon dating at three remote western sites, finding about two-thirds to seven-eights of carbon particles being contemporary. This indicates an upper bound to natural organic particles on the order of 1 to 1.5 $\mu g/m^3$. The upper bound may be very loose, however, due to potential contributions from man-made wood smoke.

For the East, we have chosen a value of 1.5 $\mu g/m^3$ for natural fine organics, again with an uncertainty factor of about two. The relevant considerations are as follow:

- Currently, fine organic aerosol concentrations over the rural east average about 4 $\mu g/m^3$ (Shah *et al.*, 1986; Huntzicker *et al.*, 1986; Trijonis, 1982). For the Ohio Valley, Huntzicker *et al.* (1986) have concluded that combustion is the "principal source" of these organic aerosols because the organic mass fraction correlates very highly ($R^2$ = 0.62 to 0.73) with the elemental carbon mass fraction but negligibly with the mass fraction of a plant wax tracer. Nationally, a similar conclusion is reached by Shah *et al.* (1986) based on high correlations of organic and elemental carbon. Furthermore, Cachier *et al.* (1986), in characterizing continental contributions to fine carbon in the marine atmosphere, have concluded that carbon from combustion predominates in the northern hemisphere whereas the southern hemisphere primarily reflects biogenic emissions. If we arbitrarily define "principal source" or "predominate" as "more than two-thirds", these results suggest that less than 1.3 $\mu g/m^3$ of the current 4 $\mu g/m^3$ is biogenic.
- In review articles concerning organic aerosol concentrations in remote areas, Duce (1978) and Hahn (1980) interpret available information as suggesting a remote continental background of 1.5 to 2.25 $\mu g/m^3$ for fine organics in the northern hemisphere.
- Recent measurements suggest that fine organic aerosol concentrations in tropical rain forests are on the order of 10 $\mu g/m^3$ (Cachier *et al.*, 1985; Talbot *et al.*, 1988). Tropical rain forests are major global source areas for organic aerosols, because of both biomass burning and high biogenic activity. Although these higher concentrations are not directly relevant to background organics in the United States (they exceed current, evidently man-made dominated concentrations by a factor of 2.5!), they do point out the possibility of significant contributions from natural organic aerosol sources.

## A.3 FINE SULFATES

*J.C. Trijonis*

The estimates of natural background fine sulfates in Table 24A-1 are 0.2 $\mu g/m^3$ for the East and 0.1 $\mu g/m^3$ for the West. These estimates are based on the reasoning and data in the three paragraphs below. In all discussions, sulfate mass concentrations are reported in terms of $NH_4HSO_4$ equivalents.

- The emission inventory for the NAPAP Interim Assessment indicates that natural sources of gaseous sulfur (both terrestrial and marine) account for about 3% of total emissions east of the Mississippi (Placet and Streets, 1987). Combining this with the fact that current fine sulfate concentrations are 5 to 10 $\mu g/m^3$ in the rural East and 1 to 2 $\mu g/m^3$ in the rural West (Trijonis, 1982; Eldred *et al.*, 1987; Macias *et al.*, 1987; also see aerosol composition data in Section 4) suggests that natural background sulfate levels are on the order of 0.2 $\mu g/m^3$ in the East and 0.1 $\mu g/m^3$ in the West. In terms of internal consistency, it is worthwhile to note that natural source emission *density* is estimated to be twice as great in the East than the West. The potential error in this estimation procedure is quite high, however, because natural emissions have an overall uncertainty factor of three.
- Rural sulfate levels in the southern hemisphere may be indicative of natural background levels because man-made $SO_2$ emissions are on an order of magnitude less in the southern hemisphere than in the northern hemisphere (Curris and Hirschler, 1980; Varhelyi, 1985; Dignon and Hameed, 1989). Lawson and Winchester (1979) reviewed data from 11 rural southern hemisphere sites and found average sulfate concentrations in the range of 0.04 to 0.6 $\mu g/m^3$, with most sites in the range 0.1 to 0.3 $\mu g/m^3$. Subsequent data for various southern hemisphere sites have shown a similar range, 0.05 to 0.8 $\mu g/m^3$ (Andreae, 1982; Adams *et al.*, 1983; Annegarn *et al.*, 1983; Khemani, 1985; Talbot *et al.*, 1988; Clairac *et al.*, 1988). It should be noted, however, that even at remote southern hemisphere locations, anthropogenic influences may be non-negligible. Also, tropical rain forests may be more significant emitters of sulfur compounds than North American forests because of the greater biological activity level.

- Shaw (1985) estimated a natural background of 0.15 to 0.4 $\mu g/m^3$ in central Alaska by regressing sulfate against elemental carbon (a presumed anthropogenic tracer) and interpreting the zero intercept as the background value. Maenhaut *et al.* (1979) reported an average concentration of 0.2 $\mu g/m^3$ for Antarctica.

The uncertainty level of the natural background estimates for sulfates are judged to be about a factor of two. This uncertainty is not important to the calculation of natural background visual range because sulfates constitute such a small portion of the natural background aerosol.

## A.4 FINE ELEMENTAL CARBON

*J.C. Trijonis*

Two considerations indicate the average concentration of natural background elemental carbon (EC) is very small:

- The average concentration of elemental carbon at extremely remote locations is very minute, *i.e.*, 0.006 $\mu g/m^3$ at Mauna Loa, 0.003 $\mu g/m^3$ at the South Pole, 0.004 $\mu g/m^3$ in the North Pacific, 0.03 $\mu g/m^3$ in the North Atlantic, and 0.04 $\mu g/m^3$ in the Arctic (Clarke, 1984; Twohy *et al.*, 1989).
- The only significant natural source for elemental carbon is apparently wildfire. Combining the NAPAP emissions inventory for particulate matter with estimates of the fraction of emissions that constitute fine elemental carbon (Cass *et al.*, 1982; Trijonis, 1984; Shah, 1986) indicates that forest fires plus prescribed burning together account for about 2.8% of emissions. Noting that current elemental carbon concentrations in rural areas average about 0.2 to 1.0 $\mu g/m^3$ (Trijonis, 1982; Macias *et al.*, 1987; Eldred *et al.*, 1987) suggests that elemental carbon concentrations from wild fires average only about 0.005 to 0.03 $\mu g/m^3$, even if one counts prescribed burns as wild fires.

In Table 24A-1, we have assumed an average natural background concentration for fine elemental carbon of 0.02 $\mu g/m^3$. The uncertainty in this value, a factor of two to three, is unimportant to the calculation of natural background visibility because of the very small contribution from natural elemental carbon.

## A.5 FINE AMMONIUM NITRATE

*J.C. Trijonis*

The estimate of natural background fine ammonium nitrate concentration is 0.1 $\mu g/m^3$ for both the East and West. This estimate is based on the following considerations:

- Fine aerosol nitrate concentrations (expressed an $NH_4NO_3$ equivalents) are on the order of 0.1 $\mu g/m^3$ in equatorial/southern hemisphere rain forests (Clairac *et al.*, 1988; Talbot *et al.*, 1988). This value (0.1 $\mu g/m^3$) may represent an upper bound for the United States because the tropical rain forest are considered to be major natural source areas for the precursors of nitrate aerosols (Kaplan *et al.*, 1988; Talbot *et al.*, 1988).
- The NAPAP Interim Assessment emission inventory (Placet and Streets, 1987) indicates that natural $NO_x$ emissions are 4.5 times as great as natural gaseous sulfur emissions on a molar basis. Adjusting for molecular weights of ammonium nitrate versus $NH_4HSO_4$, this suggests the "potential" for three times as much natural fine nitrate as natural fine sulfate—a potential on the order of 0.3 to 0.6 $\mu g/m^3$ fine nitrate based on our estimates of natural sulfate concentrations. However, it is expected that the production of fine nitrate aerosols should be relatively much lower than the production of fine sulfates because of three reasons:

  (1) Fine ammonium nitrate will accumulate only where there is sufficient ammonia to neutralize all sulfuric acid to ammonium sulfate (Wolff, 1984), and natural background ammonia emissions may not always be sufficient to accomplish that neutralization (Placet and Streets, 1987).

  (2) Nitrogen should deposit out of the atmosphere more rapidly than sulfur because of the very high reactivity of the intermediate product $HNO_3$.

  (3) Partly related to the lack of ammonia and the high reactivity of $HNO_3$, nitrate aerosols in remote regions often occur substantially—if not predominately—in the coarse rather than the fine size range (Talbot *et al.*, 1988; Clairac *et al.*, 1988; Khemani *et al.*, 1985; Hoff *et al.*, 1983; Savoie and Prospero, 1982), evidently due to reactions of $HNO_3$ with coarse crustal or sea-salt particles.
- Total (fine and coarse) nitrate concentrations (as $NH_4NO_3$) in remote marine areas have been found to average about 0.2 $\mu g/m^3$ in the southern hemisphere, 0.3 $\mu g/m^3$ in the equatorial region, and 0.4 $\mu g/m^3$ in the northern hemisphere (Huebert, 1980; Huebert and Lazrus, 1980). However, it is expected that these concentrations are predominately in the coarse particle size range (Huebert, personal communication 1989; Milford and Davidson, 1987).
- One might *a priori* expect higher natural background fine nitrates in the East that in the West

because the soils of the East are more biologically active, thereby emitting more ammonia and $NO_x$. However, because of the complexity introduced by interactions with the sulfur cycle, it is not obvious what the spatial pattern would actually be. Here, we arbitrarily assume the same concentrations for the East and West.

The judgmental uncertainty in our estimate for natural fine ammonium nitrate is about a factor of two. This uncertainty is unimportant to the calculations of natural background light extinction because of the insignificant contributions from nitrates.

## A.6 FINE SOIL AND COARSE MASS

*J.C. Trijonis*

With respect to soil dust, it is difficult, if not impossible, to calculate rigorously how much is natural wind blown dust versus how much is anthropogenic dust (*e.g.*, dust raised by traffic, construction, and agriculture or by wind action over surfaces disturbed by human activity). Here, we will arbitrarily assume that half of current fine soil concentrations are natural and half are anthropogenic. Fortunately, the potential error in this assumption (about a factor of 1.5 to 2) is not critical because fine soil dust is a relatively minor contributor to natural background light extinction. Because fine soil concentrations are approximately 1 $\mu g/m^3$ for both the East and West (Sutherland and Bhardwaja, 1987; Eldred *et al.*, 1987; Trijonis, 1982; also see aerosol composition data in Section 4), our assumption yields a natural fine soil concentration of 0.5 $\mu g/m^3$.

Coarse mass will be considered in conjunction with the fine soil category because soil dust is usually the dominant contribution to coarse mass. Current coarse mass concentrations (between 2.5 and 10 $\mu m$ in diameter) at "remote" sites generally average about 3 to 10 $\mu g/m^3$ in both the East and the West (see Section 4). For natural background coarse mass, we will adopt a value of 3 $\mu g/m^3$ for both East and West (about half of the midpoint of the concentration range). *A priori*, one might expect more natural soil dust in the West than the East, but this might be compensated by greater coarse organic mass in the East. The error in this background value, about a factor of 1.5 to 2, is not critical to the calculations of natural background visual ranges (although coarse mass is important with respect to natural *non-Rayleigh* extinction levels in the West).

## A.7 AEROSOL WATER

*J.C. Trijonis*

Trijonis (1982) compiled data to show that the annual average fine aerosol in the rural East currently consists of approximately 9 $\mu g/m^3$ sulfates (as $NH_4HSO_4$), 4 $\mu g/m^3$ organics, 1 $\mu g/m^3$ elemental carbon, 1 $\mu g/m^3$ crustal, and 1 $\mu g/m^3$ nitrates. Based on thermodynamic considerations (Tang, 1981) as well as measurements made with microwave waterometers, nephelometers, and multi-stage cascade impactors (Hidy *et al.*, 1974; Stelson and Seinfold, 1981; Covert *et al.*, 1972; Countess *et al.*, 1981; Ferman *et al.*, 1981), he concluded that this model ambient aerosol contains an average of about 11 $\mu g/m^3$ of water. In order to estimate natural background levels of water, he proposed two procedures—one for a low estimate and one for a high estimate. The low estimate is based on the assumption that the water is attached only to the electrolyte (sulfate and nitrate) portion of the aerosol, while the high estimate is obtained by assuming that the water is attached equally to all components of the aerosol.[1] Multiplying the 11 $\mu g/m^3$ water concentration by the ratio of natural/current aerosol mass concentrations (either for sulfates plus nitrates or for total fine mass) yields natural background estimates of 0.3 $\mu g/m^3$ and 1.6 $\mu g/m^3$ for fine aerosol water. As noted in Table 24A-1, we have adopted a value of 1 $\mu g/m^3$ as the estimate for the natural background level of fine aerosol water. The overall uncertainty is judged to be about a factor of two.

Natural background water for the West can be computed by comparisons with the East taking into account both the lower natural aerosol levels in the West (see Table 24A-1) and the lower relative humidity (on the order of 40% - 60% rather than 70% - 75%). Three comparison calculations have been made:

1. Assuming water concentrations are proportional to total dry aerosol mass and the function $RH/[1-RH]^2$
2. Assuming water concentrations are proportional to sulfate plus nitrate mass and the function $RH/[1-RH]$
3. Assuming water concentrations are proportional to sulfate and nitrate mass and the RH function given by Tang (1981).

These three methods yield estimates of 0.2 $\mu g/m^3$, 0.25 $\mu g/m^3$, and 0.14 $\mu g/m^3$ natural fine water for the West, respectively. These values should be slight underestimates because the relative humidity correction includes not only

[1] The first estimate is low relative to the second because the natural aerosol is especially low relative to the current aerosol in terms of the sulfate and nitrate compounds.

[2] Assuming water concentration is proportional to $RH/(1-RH)$ is equivalent to assuming total scattering for the hygroscopic part of the aerosol is proportional to $1/(1-RH)$.

the subtraction of water scattering mass but also shifts in scattering efficiency. A value of 0.25 $\mu g/m^3$ has been chosen for the West in Table 24A-1.

## A.8 REFERENCES

**Adams, F., P. VanEspen, and W. Maenhaut.** 1983. Aerosol composition at Chacaltaya, Bolivia, as determined by size-fractionated sampling. Atmos. Environ. 17:1521-1536.

**Altshuller, A.P.** 1983. Review: Natural volatile organic substances and their effect on air quality in the United States. Atmos. Environ. 17:2131-2165.

**Andreae, M.O.** 1982. Marine aerosol chemistry at Cape Grim, Tasmania, and Townsville, Queensland. J. Geophys. Res. 87:8857.

**Annegarn, H.J., R.E. VanGrieken, D.M. Biddy, and F. Von Blottnitz.** 1983. Background aerosol composition in the Namib Desert, south west Africa (Namibia). Atmos. Environ. 17:2045-2053.

**Beauford, W., J. Barber, and A.R. Barringer.** 1977. Release of particles containing metals from vegetation into the atmosphere. Science 195:571-573.

**Bhardwaja, P.J., ed.** 1987. Visibility Protection: Research and Policy Aspects. Air Pollution Control Assoc., Pittsburgh, PA.

**Cachier, H., P. Buat-Menard, M. Fontugne, and J. Rancher.** 1985. Source terms and source strengths of the carbonaceous aerosol in the tropics. J. of Atmos. Chem. 3:469-489.

**Cachier, H., P. Buat-Menard, M. Fontugne, and R. Chesselet.** 1986. Long-range transport of continentally-derived particulate carbon in the marine atmosphere: evidence from stable carbon isotope studies. Tellus 38b:161-177.

**Cass, G.R., P.M. Bonne, and E.S. Macias.** 1982. Emissions and air quality relationships for atmospheric carbon particles in Loion and atmospheric aerosols in an equatorial forest area. J. Atmos. Chem. 6:301-322.

**Clairac, B., R. Delmas, B. Cros, H. Cachier, P. Buat-Menard, and J. Servant.** 1988. Formation and chemical composition of atmospheric aerosols in an equatorial forest area. J. Atmos. Chem. 6:301-322.

*** Clarke, A.D.** 1987. Aerosol Light Absorption by Soot in Remote Environments. University of Hawaii, Honolulu, HI.

**Clarke, A.D., R.E. Weiss, and R.J. Charlson.** 1984. Elemental carbon aerosols in the urban, rural, and remote-marine troposphere and in the stratosphere: inferences from light absorption data and consequences regarding radiative transfer. Sci. Total Environ. 36:97-102.

**Countess, R.J., S.H. Cadle, P.J. Groblicki, and G.T. Wolff.** 1981. Chemical analysis of size-segregated samples of Denver's ambient particulate. J. Air Pollution Control Assoc. 31:247-252.

**Covert, D.S., R.J. Charlson, and N.C. Ahlquist.** 1972. A study of the relationship of chemical composition and humidity to light scattering by aerosols. J. Appl. Meteorol. 11:968-976.

*** Crittenden, A.L.** 1976. Analysis of Atmospheric Organic Aerosols by Mass Spectroscopy. EPA Grant No. R801119, NTIS Ecological Research Series report PB 258 822.

**Curris, C.F. and M.M. Hirschler.** 1980. Atmospheric sulfur: natural and man-made sources. Atmos. Environ. 14:1263-1278.

**Currie, L.A., G.A. Klouda, and K.J. Voorhees.** 1984. Atmospheric carbon: the importance of accelerator mass spectrometry. Nuclear Instruments and Methods in Phys. Res. V(b):371-379.

*** Daisey, J.M., B. Naumann, and T.J. Kneip.** 1979. Trends in Particulate Organic Matter at a Rural New York Sampling Station. New York Medical Center, New York, NY.

**Dignon, J. and S. Hameed.** 1989. Global emissions of nitrogen and sulfur oxides from 1860 to 1980. J. Air Pollution Control Assoc. 39:180-186.

**Duce, R.A.** 1978. Speculations on the budget of particulate and vapor phase non-methane organic carbon in the global troposphere. Pageoph 16:244-273.

**Eldred, R.A., T.A. Cahill, P.J. Feeney, and W.C. Malm.** 1987. Regional patterns in particulate matter from the National Park Service Network, June 1982 to May 1986, pp. 386-396. In: P.S. Bhardwaja, ed. Visibility Protection: Research and Policy Aspects. Air Pollution Control Assoc., Pittsburgh, PA.

**Ferman, M.A., G.T. Wolff, and N.A. Kelly.** 1981. The nature and sources of haze in the Shenandoah Valley/ Blue Ridge Mountain area. J. Air Pollution Control Assoc. 31:1074-1081.

**Hahn, J.** 1980. Organic constituents of natural aerosols. Annals NY Academy of Sci. 338:359-376.

**Hidy, G.M. *et al.*** 1974. Characterization of Aerosols in California. Rockwell International Science Center report for contract No. 358. California Air Resources Board, Sacramento, CA.

---

* Nonpeer-reviewed sources.

**Hoff, R.M., W.R. Leaitch, P. Fellin, and L.A. Barrie.** 1983. Mass size distributions of chemical constituents of winter Arctic aerosols. J. Geophys. Res. 88:10947.

**Huebert, B.J.** 1980. Nitric acid and aerosol nitrate measurements in the equatorial Pacific region. Geophys. Res. Ltrs. 7:325-328.

*** Huebert, B.J.** 1989. Personal communication. University of Rhode Island, RI.

**Huebert, B.J. and A.L. Lazrus.** 1980. Tropospheric gas-phase and particulate nitrate measurements. J. Geophys. Res. 85:7322-7328.

**Huntzicker, J.J., E.K. Heyerdahl, S.R. McDow, J.A. Rau, W.H. Priest, and C.S. MacDougall.** 1986. Combustion as the principal source of carbonaceous aerosol in the Ohio River valley. J. Air Pollution Control Assoc. 36:705-709.

**Kaplan, W.A., S.C. Wofsy, M. Keller, and J.M. deCosta. 1988.** Emission of NO and deposition of $O^3$ in a tropical forest system. J. Geophys. Res. 93:Feb 29.

**Khemani, L.T., G.A. Monin, M.S. Naik, P.S. Prakasa Rao, R. Kumar, and Bh.V. Ramana Murty.** 1985. Trace elements and sea salt aerosols over the sea areas around the Indian subcontinent. Atmos. Environ. 19:277.

**Lawson, D.R. and J.W. Winchester.** 1979. Atmospheric sulfur aerosol concentrations and characteristics from the South American continent. Science 205:1267-1269.

**Macias, E.S., T.L. Vossler, W.H. White.** 1987. Carbon and sulfate fine particles in the western United States. In: P.S. Bhardwaja, ed. Visibility Protection: Research and Policy Aspects. Air Pollution Control Assoc., Pittsburgh, PA.

**Maenhaut, W., W.H. Zoller, R.A. Duce, and G.L. Hoffman.** 1979. Concentration and size distribution of particulate trace elements in the south polar atmosphere. J. Geophys. Res. 84:2421-2431.

*** Mazurek, M.A., G.R. Cass, and B.R.T. Simoneit.** 1988. Quantification of the Source Contributions to Organic Aerosols in the Remote Desert Atmosphere. RP 1630-11. Environmental Quality Laboratory, California Institute of Technology, Pasadena, CA.

**Milford, J.B. and C.I. Davidson.** 1987. The sizes of particulate sulfate and nitrate in the atmosphere—a review. J. Air Pollution Control Assoc. 37:125-134.

**Placet, M. and D.G. Streets.** 1987. NAPAP Interim Assessment, Volume II: Emissions and Controls. National Acid Precipitation Assessment Program, Washington, DC.

**Rasmussen, T.A. and F.W. Went.** 1985. Volatile organic material of plant origin in the atmosphere. Proceedings of the NY Academy of Sciences 9:1207.

**Savoie, D.L. and J.M. Prospero.** 1982. Particle size distribution of nitrate and sulfate in marine atmosphere. Geophys. Res. Ltrs. 9:1207.

**Shah, J.J.** 1986. Review of Emissions Inventory for the Three Counties in Southeast Desert Air Basin. Nero and Associates, Portland, OR.

**Shah, J.J., R.L. Johnson, E.K. Heyerdahl, and J.J. Huntzicker.** 1986. Carbonaceous aerosol at urban and rural sites in the United States. J. Air Pollution Control Assoc. 36:254-257.

**Shaw, R.W., A.L. Crittenden, R.K. Stevens, D.R. Cronn, and V.S. Titor.** 1983. Ambient concentrations of hydrocarbons from conifers in atmospheric gases and aerosols measured in Soviet Georgia. Environ. Sci. Technol. 17:389-395.

**Stelson, A.W. and J.H. Seinfeld.** 1981. Chemical mass accounting of urban aerosol. Environ. Sci. Technol. 15:671-679.

**Sutherland, J.L. and P.S. Bhardwaja.** 1987. Composition of the aerosol in northern Arizona and southern Utah, pp. 373-385. In: P.S. Bhardwaja, ed. Visibility Protection: Research and Policy Aspects. Air Pollution Control Assoc., Pittsburgh, PA.

**Talbot, R.W., M.O. Andreae, T.W. Andreae, and R.C. Harris.** 1988. Regional aerosol chemistry of the Amazon Basin during the dry season. J. Geophys. Res. 93:1499-1508.

*** Tang, I.N.** 1981. Deliquescence properties and particle size change of hygroscopic aerosols. In: Generation of Aerosols and Facilities for Exposure Experiments. Ann Arbor Science Publishers, Ann Arbor, MI.

**Trijonis, J.C.** 1982. Existing and natural background levels of visibility and fine particles in the rural East. Atmos. Environ. 16:2431-2445.

**Trijonis, J.C.** 1984. Effects of diesel vehicles on visibility in California. Sci. Total Environ. 36:131-140.

**Trijonis, J.C., M. McGown, M. Pitchford, D. Blumenthal, P. Roberts, W. White, E. Macias, R. Weiss, A. Waggoner, J. Watson, J. Chow, and R. Flocchini.** 1988. RESOLVE Project Final Report: Visibility Conditions and Causes of Visibility Degradation in the Mojave Desert of California. NWC TP 6869. Naval Weapons Center, China Lake, CA

**Twohy, C.H., A.D., Clarke, S.G. Warren, L.F. Radke, and R.J. Charlson.** 1989. Light absorbing material extracted from cloud droplets and its effect on cloud albedo. J. Geophys. Res. Feb 89.

---

* Nonpeer-reviewed sources.

**Varhelyi, G.** 1985. Continental and global sulfur budgets, I: anthropogenic $SO_2$ emissions. Atmos. Environ. 19:1029-1040.

**Wolff, G.T.** 1984. On the nature of nitrate in coarse continental aerosols. Atmos. Environ. 18:977-981.

# APPENDIX B

# VISUAL RANGE CONCEPT

## B.1 EQUATIONS

*W. Malm*

Equation 24-16 can be rewritten as

$$C_r = C_o({}_sN_o / {}_sN_r)e^{-\overline{B}_{ext} r} \qquad \textbf{(B-1)}$$

where $\overline{B}_{ext}$ is the average extinction over sight path $r$, and it is assumed the background is the sky (${}_bN_o = {}_sN_o$ *and* ${}_bN_r = {}_sN_r$). If $\overline{B}_{ext}$ is constant and if ${}_sN_o/{}_sN_r = 1$, Equation B-1 reduces the familiar Koschmeider relationship

$$C_r = C_o e^{-\overline{B}_{ext} r}. \qquad \textbf{(B-2)}$$

Solving Equation B-1 for $\overline{B}_{ext}$ yields

$$\overline{B}_{ext} = \frac{1}{r} \ln(C_r / C_o \gamma) \qquad \textbf{(B-3)}$$

where $\gamma = {}_sN_o/{}_sN_r$. It should be emphasized that $\overline{B}_{ext}$ is the average extinction coefficient of the atmosphere between the observer and target when they are separated by a distance equal to $r$.

Let $V_r \equiv r$ be the distance from a feature at which a threshold contrast of $\varepsilon$ is achieved. Equation B-3 can then be written as

$$V_r = \frac{1}{\overline{B}_{ext,V_r}} \ln \frac{|Co|\gamma}{\varepsilon}. \qquad \textbf{(B-4)}$$

This relationship is the defining equation for a "monochromatic" visual range of an object with an inherent contrast equal to $C_o$. In this equation, $\overline{B}_{ext,V_r}$ is the average attenuation coefficient between the observer and a target which is at a distance sufficient to reduce its apparent contrast to $\varepsilon$. It is not the same $\overline{B}_{ext}$ as determined by Equation B-3 unless $C_r = \varepsilon$ and $r$ is equal to the visual range ($\overline{B}_{ext}$ may not be constant in space). For a black object, $C_o = -1 (|C_o| = 1)$, Equations B-3 and B-4 become

$$\overline{B}_{ext} = -r^{-1} \ln(C_r / \gamma) \qquad \textbf{(B-5)}$$

$$V_r = \ln(\gamma/\varepsilon)/\overline{B}_{ext,V_r}. \qquad \textbf{(B-6)}$$

In addition, if the earth is assumed flat, if the aerosol is horizontally homogeneous, if the object is viewed at a zenith angle of 90°, and if the object is viewed under a cloudless sky, then $\gamma = 1$ (the sky radiance at the target and sky radiance at the observation point are equal) and $\overline{B}_{ext} = \overline{B}_{ext,V_r} = B_{ext}$. If these assumptions are met, Equation B-6 yields

$$V_r = -\ln(\varepsilon / B_{ext}). \qquad \textbf{(B-7)}$$

Sometimes this equation is further simplified by ignoring the absorption component of the extinction coefficient or assuming that it is equal to zero. Then,

$$V_r = -\ln(\varepsilon / B_s). \qquad \textbf{(B-8)}$$

Equations B-7 and B-8 allow measurements of the scattering or extinction coefficient (transmissometers, polar and integrating nephelometer measurements) to be interpreted in terms of an equivalent visual range, or conversely for airport visual range to be interpreted as extinction coefficients.

Much of the early visibility perception research concentrated on quantifying $\varepsilon$ in Equation B-8. $\varepsilon$ is the brightness contrast between an object and its background that is "just noticeable" or visible.

In response to these needs, the Tiffany experiment examined contrast thresholds of circular objects as a function of size, positive and negative contrast, background illumination, and duration of viewing (Blackwell, 1946; Taylor, 1964). Others have examined the magnitude of apparent contrast of natural targets required to be just visible (Duntley, 1948; Horvath and Noll, 1969; Hering *et al.*, 1971; Douglas and Young, 1945; Middleton, 1952). Results of these studies are summarized in Table 24B-1 and are reviewed in some detail by Gordon (1979). Average contrast thresholds vary from a low of *0.02* to a maximum of *0.055*.

*Table 24B-1. The Contrast and Angular Size of Detection Relationship Based Upon 0.33 Second Viewing Time, a 99% Probability, and a Lack of Knowledge of Target Position of ±4° or More*

| Reference | Average or Range | Contrast[a] $C_r$ | Angular Size of Target (Minutes of Arc) |
|---|---|---|---|
| Douglas & Young (1945) | average | 0.055 | 6.5 |
| | minimum | 0.110 | 3.0 |
| | maximum | 0.029 | 28.0 |
| Duntley (1948) | average | 0.055 | 6.5 |
| Middleton (1952) Ottawa | average | 0.042 | 10.0 |
| | +1 STD $C_r$ | 0.073 | 4.5 |
| | -1 STD $C_r$ | 0.011 | >120.0 for $\Delta t$ >0.33 sec[b] |
| Middleton (1952) Mount Washington | average | 0.034 | 20.0 |
| | +1 STD $C_r$ | 0.056 | 6.3 |
| | -1 STD $C_r$ | 0.012 | >120.0 for $\Delta t$ >0.33 sec[b] |
| Horvath & Noll (1969) Observer I | average | 0.030 | 24.0 |
| Horvath & Noll (1969) Observer II | average | 0.042 | 10.0 |
| Hering et al. (1971) Black Targets | average | -0.020 | 30.0 |
| Hering et al. (1971) Antenna Towers | average | ≥0.055 | <6.5 |

[a] $C_r = \frac{{}_tN_r - {}_bN_r}{{}_bN_r}$ where ${}_tN_r$ = target radiance and ${}_bN_r$ = background radiance.

[b] $\Delta t$ = viewing time.

## B.2 REFERENCES

**Blackwell, H.R.** 1946. Contrast thresholds of the human eye. J. Opt. Soc. Amer. 36:624.

**Douglas, C.A. and L.L. Young.** 1945. Development of a Transmissometer for Determining Visual Range. CCA Tech. Dev. Rept. No. 47. US Dept of Commerce, Washington, DC.

**Duntley, S.Q.** 1948. The reduction of apparent contrast by the atmosphere. J. Opt. Soc. Amer. 38:179-191.

**Gordon, J.I.** 1979. Daytime visibility, a conceptual review. Report No. 11, November 1979 AFGL-TR-79-0257, SIO Ref. 80-1. University of California (Scripps Institution of Oceanography-Visibility Laboratory), San Diego, CA.

**Hering, W.S., J.S. Muench, and H.A. Brown.** 1971. Field Test of a Forward Scatter Visibility Meter. AFCRL-71-0315. Air Force Cambridge Research Laboratories, Hanscom Field, Bedford, MA.

**Horvath, H. and K.E. Noll.** 1969. The relationship between atmospheric light scattering coefficient and visibility. Atmos. Environ. 3:543-550.

**Middleton, W.E.K.** 1952. Vision Through the Atmosphere. University of Toronto Press, Toronto, Ontario, Canada.

**Taylor, J.H.** 1964. Use of visual performance data in visibility prediction. App. Opt. 3(5):562.

# APPENDIX C

# EQUIVALENT CONTRAST AND ATMOSPHERIC MODULATION TRANSFER FUNCTION

## C.1 EQUIVALENT CONTRAST
*W. Malm*

Although a typical landscape projected on the human retina is two-dimensional, for purposes of simplicity the following discussion will be carried out in one dimension. The generalization to two dimensions is straightforward.

It has been shown that for discrimination tasks the variation of a mean square radiance field is the significant psychophysical variable (Carlson and Cohen, 1978). Consider the simple sine-wave superimposed on a background radiance field

$$N(x) = \frac{N_m + N_b}{2} + \frac{N_m - N_b}{2} \cos(2\pi f x) \qquad \text{(C-1)}$$

where $N_m$ and $N_b$ are radiance values associated with the peak and trough of a sine-wave, respectively. The mean square radiance associated with Equation 24-4 can be shown to equal

$$\overline{N}^2 = \overline{N}^2 + 1/2\ m^2\ \overline{N}^2 \qquad \text{(C-2)}$$

where $m$ is the modulation contrast, $m=(N_m-N_b)/(N_m+N_b)$, $\overline{N}$ is the average image radiance, and $(1/2)\ m^2\overline{N}^2$ is the mean square radiance fluctuation.

More complicated one dimensional images can be represented as weighted sums of light and dark bars of various frequencies and intensities. Mathematically,

$$N_r(x) = a_o + \sum_{n,n\neq o} a_n e^{in2\pi f_o x} \qquad \text{(C-3)}$$

where $N_r(x)$ is the one dimensional image radiance field at an observer image distance $r$, $a_o$ is average image radiance $\overline{N}$, and $a_n$ are the weighting factors associated with various sinusoid frequencies $n2\pi f_o$. The second term, $\sum_{n,n\neq 0} a_n e^{in2\pi f_o x}$, is the modulation of average image radiance $a_o$. The modulation contrast of a given sinusoid is just $a_n/a_o$. Calculation of the mean square radiance associated with Equation 24-6 yields

$$\overline{N_r^2} = a_o^2 + \sum_n |a_n|^2 \qquad \text{(C-4)}$$

Comparison of Equation C-2 to Equation C-3 suggests that the second term in each of these equations can be set equal to each other to yield

$$1/2\ m^2\ \overline{N}^2 = \sum_n |a_n|^2 \qquad \text{(C-5)}$$

Solving for $m$ gives

$$C_{eq} \equiv m = \frac{\sqrt{2\sum_n |a_n|^2}}{\overline{N}} \qquad \text{(C-6)}$$

where $C_{eq}$ is defined to be average image equivalent contrast. $C_{eq}$ is essentially the average sine-wave modulation contrast associated with the amplitude of the various spatial frequencies that make up the image. $C_{eq}$ is sensitive to changes in both edge sharpness and sizes of image structure.

For the discriminative tasks such as the determination of visibility impairment, it is convenient to somewhat modify Equation C-6 to better reflect the workings of the human visual system. There is considerable evidence that the visual system behaves as if it were fourier decomposing the scene into channels or adjacent bands of spatial frequency and processing these bands independently (Campbell and Robson, 1964; Campbell *et al.*, 1968; Campbell and Kulikowski, 1966). If it is the desire to explicitly understand the response of the human visual system to image modification, then Equation C-6 can be rewritten as follows:

$$C_{eq,i} = \frac{\sqrt{2\sum_{\Delta n} |a_n|^2}}{\overline{N}} \qquad \text{(C-7)}$$

where $i$ refers to the *ith* human visual system channel and the sum over $\Delta n$ under the square root sign is carried out for those frequencies that correspond to *ith* human channel.

## C.2 MODULATION TRANSFER FUNCTION
*W. Malm*

The modulation contrast, $m = a_n/a_o$, is modified in accordance with Equations 24-15 and 24-12. The effect of an increase in atmospheric aerosol concentration on the average radiance field is to reduce the average radiance by a factor equal to the atmospheric transmittance $T$ while adding path radiance $N_r^*$:

$$a_o' = a_o T + N_r^* \qquad \text{(C-8)}$$

where $a_0'$ is the new average radiance. On the other hand, the modulation term, $a_n e^{in2\pi f_n x}$, is only reduced by a factor equal to $T$. This is because radiance differences are attenuated equally by an amount equal to the atmospheric transmittance (see Equation 24-13), thus the effect of an increase in atmospheric aerosol concentration on Equation C-3 is

$$N_r'(x) = a_o T + N_r^* + T \sum_n a_n e^{i2\pi n f_o x} \qquad \textbf{(C-9)}$$

where $N_r'(x)$ is the one dimensional radiance field after an increase in atmospheric aerosol load. The modulation contrast of any sinusoid is then

$$m' = Ta_n / (a_o T + N_r) \qquad \textbf{(C-10)}$$

and the transfer of modulation contrast is

$$M_{tf,a} = m'/m = \frac{1}{1 + N_r^*/a_o T} \qquad \textbf{(C-11)}$$

Provided atmospheric turbulence does not interfere with transfer of modulation contrast, Equation C-11 is independent of spatial frequency and is the general form for the atmospheric contrast transmittance in spatial frequency space. It is more commonly referred to as the modulation transfer function of the atmosphere (Malm, 1985).

## C.3 REFERENCES

**Campbell, F.W. and J.J. Kulikowski.** 1966. J. Physiol. (London) 187:437.

**Campbell, F.W. and J.G. Robson.** 1964. J. Opt. Soc. Amer. 54:581A.

**Campbell, F.W., B. Cleveland, G.F. Cooper, and C. Enroth-Cogell.** 1968. J. Physiol. (London) 198:237.

**Carlson, C.R. and R.W. Cohen.** 1978. Image Descriptors for Displays: Visibility of Displayed Information. RCA Laboratories, Princeton, NJ.

**Malm, W.C.** 1985. An examination of the ability of various physical indicators to predict judgment of visual air quality. Proceeding of 78th annual meeting of Air Pollution Control Assoc., Detroit, MI. June 16-21, 1985.

# APPENDIX D

# THE QUADRATIC DETECTION MODEL

## D.1 QUADRATIC DETECTION MODEL

*W. Malm*

A quadratic detection model, proposed by Carlson and Cohen (1978), has been used to predict thresholds of perceived image sharpness in video type image display devices. The basic hypothesis of the model is that in order to perceive a change in the appearance of a scene with a given error rate, the change in the mean square luminance per unit frequency, integrated over any single human visual system channel, must be a constant fraction of the interfering signal. Mathematically,

$$C_f(\upsilon)^2 - C_i(\upsilon)^2 = C_T(\upsilon)^2 + k(\upsilon)C_i(\upsilon)^2 \qquad \textbf{(D-1)}$$

where $C_f(\upsilon)^2$ - $C_i(\upsilon)^2$ are the frequency dependent final and initial equivalent sine wave contrast, respectively, $C_T(\upsilon)$is the threshold contrast and $k(\upsilon)$ is a constant fraction at each frequency. $C_f$, $C_i$ and $C_T$ are modulation contrasts defined as

$$C \equiv \frac{N_1 - N_2}{N_1 + N_2} \qquad \textbf{(D-2)}$$

where $N_1$ and $N_2$ are the maximum and minimum radiance values of a brightness field that is varied in accordance with a sine wave response. Equation D-1 is in the form of a contrast discrimination model and can be used to predict just noticeable changes in scenic brightness structure.

The frequency dependent equivalent modulation contrast can be calculated using

$$C_f(\upsilon) = \sqrt{2\phi(\upsilon)/a_o} \qquad \textbf{(D-3)}$$

where $\phi(\upsilon)$ is the perceived power spectra of the scene under investigation and can be calculated by taking the spatial fourier transform of the brightness field (Malm, 1985). $a_o$ is the average scenic brightness. The value of the proportionality constant $k(\upsilon)$ was obtained from contrast discrimination experiments under conditions where the initial contrast is much greater than threshold contrast (Carlson and Cohen, 1978). The constant $k(\upsilon)$ as a function of spatial frequency is shown in Figure 24D-1. Notice that $k(\upsilon)$ increases as spatial frequency increases. $k(\upsilon)$ is slowly varying with changes in experimental condition and procedure. In some experiments, display luminance was varied over four orders of magnitude, with the resulting change in contrast required for detection varying by less than a factor of three.

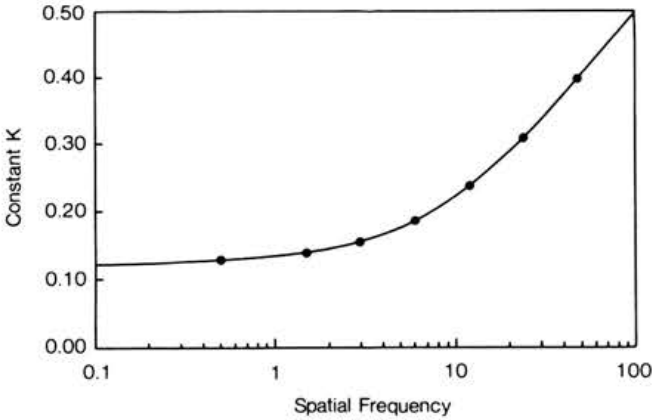


*Figure 24D-1 Proportionality constant required for determination of detection thresholds plotted as a function of spatial frequency.*

Carlson and Cohen (1978) have also shown that the equivalent contrast, $C_{eq}$, for an edge is given by

$$C_{eq,e} = 0.14 C_{edge} \qquad \textbf{(D-4)}$$

for any frequencies above 1.5 cycles/degree.

$C_{edge}$, the modulation contrast between two adjacent landscape features, or between a landscape feature and the sky, is given by

$$C_{edge} = \frac{N_{1_1} - N_{1_2}}{N_{1_1} + N_{1_2}} \qquad \textbf{(D-5)}$$

where $N_{1_1}$ and $N_{1_2}$ are the radiance values associated with two adjacent landscape features.

If the change in scene equivalent contrast is a result of addition or subtraction of atmospheric aerosol, initial and final contrast are related to each other by

$$C_f(\upsilon) = M_{tf}\, C_i(\upsilon) \qquad \textbf{(D-6)}$$

where $M_{tf}$ is the atmospheric modulation transfer function given by

$$M_{tf} = \frac{1}{1 + N_r^* / a_o T} \qquad \textbf{(D-7)}$$

$a_o$ is the average scene luminance. $T$ *and* $N_r^*$ are the atmospheric transmittance and path radiance between the object being viewed and the observer, respectively (Malm and Henry, 1987). Substituting Equation D-6 into Equation D-1 and solving for $M_{tf}$ yields

$$M_{tf} = C_T^2(\upsilon)/C_i^2(\upsilon) + k + 1. \qquad \textbf{(D-8)}$$

Given the above equations, just noticeable changes presented in this report are calculated using the following:

- Identify all contrast edges in the photograph. This includes contrast edges between contiguous features as well as any feature outlined against the sky.
- Calculate the equivalent contrast between all edges using Equations D-4 and D-5 as a function of incremental changes in aerosol concentration.
- When the difference between the square of initial and final contrasts are greater or equal to the right side of Equation D-1, a JNC has been reached.
- Repeat the calculation until the desired amount of aerosol has been added or subtracted from the atmosphere.

The value used for $k$ is *0.158* and $C_T$ was set equal to *0.0035*. These values correspond to a threshold apparent contrast, $(N_1\text{-}N_2)/N_2$, of a large landscape feature as seen against the horizon sky of approximately *0.05*. A suprathreshold apparent contrast change of approximately *0.02* of some contrast edge within landscape will usually evoke a just noticeable change. Furthermore, a change in extinction coefficient of approximately *5%* will evoke a just noticeable change in most landscapes.

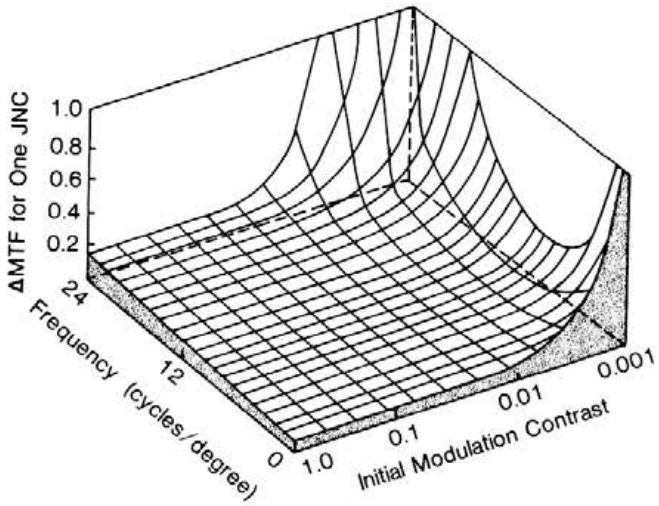


*Figure 24D-2 Change in modulation transfer function surface as a function of initial modulation contrast and spatial frequency.*

## D.2 REFERENCES

**Carlson, C.R. and R.W. Cohen.** 1978. Image Descriptors for Displays: Visibility of Displayed Information. RCA Laboratories, Princeton, NJ.

**Malm, W.C.** 1985. An examination of the ability of various physical indicators to predict judgment of visual air quality. Proceedings of 78th annual meeting of Air Pollution Control Assoc., Detroit, MI. June 16-21, 1985.

**Malm, W.C. and R.C. Henry.** 1987. Regulatory perspective of visibility research needs. Proceedings of 80th annual meeting of Air Pollution Control Assoc., New York, NY. June 21-26, 1987.

# APPENDIX E

# THE EFFECT OF NITROGEN DIOXIDE AND AMMONIUM NITRATE ON NATIONWIDE VISIBILITY

**from "National Relationship Between Visibility and NOx Emissions" by John Trijonis, Santa Fe Research Corporation, Bloomington, Minnesota 55438.**

## E.1 INTRODUCTION
*J.C. Trijonis*

Nitrogen oxide emissions affect visibility (*i.e.* contribute to light extinction) in two important direct ways, via the product of gaseous $NO_2$ concentrations and fine particle ammonium nitrate concentrations. Only these two direct influences will be considered here. There is a third direct effect, production of coarse nitrate particles. However, coarse particle nitrate contributions to extinction can generally be assumed negligible because coarse particle scattering is a relatively small part of total extinction and because nitrates usually constitute only a small fraction of coarse particle mass (Trijonis *et al.*, 1988). Nitrogen oxide emissions additionally can affect light extinction indirectly, *e.g.*, by influencing ozone photochemistry which in turn affects sulfate aerosol production. Such indirect effects will also be neglected.

The objective is to estimate the percentage of national light extinction that is currently attributable to gaseous $NO_2$ and fine ammonium nitrate. In implementing the approach, there is a need for geographic and demographic disaggregation. A literature review concerning the contributions of gaseous $NO_2$ and particle nitrate to light extinction suggests that four basic divisions are appropriate—East versus West, and metropolitan versus rural. These divisions are defined in Figure 24E-1.

Subjective uncertainty analysis is included as part of the approach to this study. The uncertainty in the contributions of $NO_2$ and nitrates to light extinction is estimated individually for each of the four divisions. All uncertainties are intended to represent $\pm$ one standard error (equivalent to 68% confidence level).

## E.2 $NO_2$ CONTRIBUTIONS TO LIGHT EXTINCTION
*J.C. Trijonis*

The percentage contribution of nitrogen dioxide to light extinction coefficient can be computed from simultaneous data on $NO_2$ concentrations and total light extinction. Light absorption from $NO_2$ at the visible wavelength of 550 nm is calculated from the $NO_2$ concentrations using a simple physical constant, 0.33 $Mm^{-1}$ per ppb. The $NO_2$ absorption can then be divided by total light extinction to yield the percentage $NO_2$ contribution.

Table 24E-1 presents results for the four geographic and demographic divisions. As indicated in the table, there are two types of data that can be used for the analysis. The first type involves special field programs which provide simultaneous, high quality data on $NO_2$ and total light extinction. The disadvantage to these data sets, however, is that they cover a limited number of sites and short time periods, with the latter drawback leading to seasonal biases and questions concerning statistical representativeness. The second type of data involves routine monitoring for $NO_2$ in conjunction with estimates of extinction based on studies of airport visibility data. These routine data sets cover several years at many locations but there are questions of data quality, especially with respect to the airport extinction data.[1] In compiling Table 24E-1, an attempt was made to include as many special field programs as possible by performing an extensive literature review regarding field studies. The routine $NO_2$ data were taken from printouts of all annual averages in the EPA SAROAD data base for the 1980's.

[1] There are three main data quality questions concerning extinction estimates derived from airport visibility measurements:

(1) The method for calculating extinction coefficient from airport median visual range (see footnote b of Table 24E-1) may be inaccurate on an overall average basis.

(2) There is imprecision in estimating extinction coefficient from airport median visual range due to variations in observation and reporting practices among airport weather personnel. Fortunately, however, imprecision tends to become a negligible factor when a large number of sites are included.

(3) The studies of airport data used herein are from the middle to late 1970's and the results may not be representative of the 1980's. This last limitation should not be severe, however, because trend data suggest only slight visibility changes from the 1970's to the 1980's (Trijonis, 1986). Also, with routine NO2 data, there may be interferences so that routine NO2 concentrations are biased low.

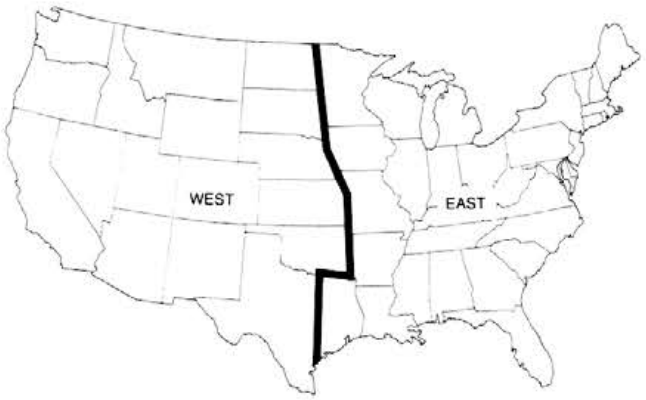


*Figure 24E-1 Definition of East versus West and metropolitan versus rural. METROPOLITAN AREA: An area of concentrated population exceeding approximately 100,000, including an important city (~ 50,000 population) and the suburban areas surrounding the city. RURAL AREA: Any non-metropolitan area.*

For each geographic/demographic division in Table 24E-1, the various data sets are in fairly good agreement. The most notable discrepancy is that the routine data base indicates higher $NO_2$ contributions than the special field data bases in rural areas. This might be due to detection limit errors in the routine data base at low $NO_2$ concentrations. Alternatively, the routine data base might represent more populated rural areas as opposed to remote rural areas.

A scrutiny of Table 24E-1, taking into account the potential errors and biases in the various data bases, leads to the following judgment as to $NO_2$ extinction contributions (including uncertainty bounds):

| | |
|---|---|
| Metropolitan west: | 8% ± 1.5% |
| Rural west: | 4% ± 2% |
| Metropolitan east: | 5% ± 1.5% |
| Rural east: | 2% ± 1.5% |

It should be stressed that the uncertainty bounds are intended to represent the potential errors in the average $NO_2$ contributions (not, for instance, the site-to-site or study-to-study standard deviations).

*Table 24E-1. Nitrogen Dioxide Contributions to Light Extinction*[a]

| Regions and Data Sets | Avg. $NO_2$ Conc. (ppb) | Avg. Total Ext. ($Mm^{-1}$) | % of Total Ext. from $NO_2$ |
|---|---|---|---|
| METROPOLITAN - WEST | | | |
| A. SPECIAL FIELD PROGRAMS | | | |
| 1. Appel et al. (1983): One month at Los Angeles and Riverside in the summer of 1982.[b] | S 49 | S 290 | S 6 |
| 2. Appel et al. (1983): One month at San Jose in the summer of 1982.[b] | S 19 | S 95 | S 7 |
| 3. Lewis et al. (1986): Three weeks at Denver in the winter of 1982.[b] | W 29 | W 150 | W 6 |
| 4. Groblicki et al. (1981): Four weeks at Denver in the winter of 1978.[b] | W 45 | W 190 | W 8 |
| 5. Zak et al. (1984): Two months at Albuquerque in the winter (Jan-Feb) of 1983. | W 29 | W 220 | W 4 |
| B. ROUTINE MONITORING DATA | | | |
| 1. Trijonis (1982): One to 16 years of data at 26 California metropolitan sites, mostly in the mid-1970's.[c] | 41 | 150 | 9 |
| 2. SAROAD Data: Three or more years of data at 62 metropolitan sites in the 1980's.[c] | 29 | 110 | 9 |
| RURAL - WEST | | | |
| A. SPECIAL FIELD PROGRAMS | | | |
| 1. RESOLVE Special Study (Trijonis et al., 1988): Thirteen weeks of sampling at Edwards AFB and China Lake, CA. | 3 | 50 | 2 |
| B. ROUTINE MONITORING DATA | | | |
| 1. SAROAD Data: Three or more years of data at 15 rural sites in the 1980's.[c] | 11 | 70 | 5 |

(Continued)

*Table 24E-1. (Continued)*

| Regions and Data Sets | Avg. $NO_2$ Conc. (ppb) | Avg. Total Ext. ($Mm^{-1}$) | % of Total Ext. from $NO_2$ |
|---|---|---|---|
| METROPOLITAN - EAST | | | |
| A. SPECIAL FIELD PROGRAMS | | | |
| 1. Hasan and Dzubay (1983): One week at Houston, TX in September 1980.[c] | S 24 | S 190 | S 4 |
| 2. Wolff et al. (1982): One week at Detroit in July 1981 | S 33 | S 230 | S 5 |
| B. ROUTINE MONITORING PROGRAMS | | | |
| 1. SAROAD Data: Three or more years of data at 85 metropolitan sites in the 1980's.[c] | 22 | 150 | 5 |
| RURAL - EAST | | | |
| A. SPECIAL FIELD PROGRAMS | | | |
| 1. Cadle et al. (1985): Eighteen weeks in northern Michigan in winter 1983-1984.[b] | W 2 | W 100 | S 7 |
| 2. Ferman et al. (1981): One month at Shenandoah Valley, VA in the summer of 1981.[c] | S 2 | S 280 | S 2 |
| B. ROUTINE MONITORING PROGRAMS | | | |
| 1. SAROAD Data: Three or more years of data at 25 rural sites in the 1980's. [c] | 13 | 150 | 3 |

[a] S/W: Data are restricted to a single season, summer (S) or winter (W). Results are seasonally biased and also may be nonrepresentative due to a small sample size.

[b] Reported extinction values are corrected for nephelometer wavelength, nephelometer calibration, missing coarse particle scattering, and/or Rayleigh scatter.

[c] Total extinction estimated from airport visibility data (Trijonis et al., 1985; Trijonis, 1982a & 1982b; Trijonis and Yuan, 1978a & 1978b). Average total extinction is estimated as 0.7 x [3.9/AMVR], where AMVR is airport median visual range (Trijonis et al., 1988).

## E.3 FINE PARTICLE AMMONIUM NITRATE CONTRIBUTIONS TO LIGHT EXTINCTION

*J.C. Trijonis*

Table 24E-2 summarizes results concerning the contribution of fine ammonium nitrate to light extinction. The organization of Table 24E-2 is similar to that of Table 24E-1, with the exception of the results for the metropolitan-west. There are so many nitrate data sets available for the metropolitan-west, that it seems more useful to organize them by city rather than by special studies versus routine monitoring.

In the case of nitrates, there are two important complications. First, unlike the case of $NO_2$ where the extinction efficiency is a well known physical constant, the extinction efficiency for fine ammonium nitrate aerosols depends on relative humidity and aerosol size distribution, and it has not been fully characterized. The extinction efficiencies for fine nitrates used here are explained in Footnotes a and d of Table 24E-2. Second, there are two useful measurement methods for fine nitrate particles, sampling with the denuder/nylon filter technique and sampling with Teflon filter. The denuder/nylon filter method provided a true representation of particle nitrates, but the amount of data available under this method is very limited, with respect to both sites and time periods covered. There is an abundance of data from Teflon filter sampling, but Teflon filters yield only a lower bound for particle nitrates because of the tendency for ammonium nitrate to volatilize from the filter. True particle nitrate tends to be about 20 - 50% higher than Teflon filter nitrate on an annual average basis (Appel, personal communication 1987; Stevens, personal communication 1987; John *et al.*, 1986; Mulawa and Cadle, 1985).

Based on a study of the results in Table 24E-2, it appears that reasonable estimates of fine ammonium nitrate contributions to extinction are as follows:

| | |
|---|---|
| Metropolitan west: | 15% ± 4% |
| Rural west: | 6% ± 2.5% |
| Metropolitan east: | 5% ± 2% |
| Rural east: | 5% ± 2% |

Again, the reader should note that the uncertainty bounds are intended to represent the potential errors in the overall conclusions regarding average fine ammonium nitrate contributions, not site-to-site standard deviations.

*Table 24E-2. Fine Particle Ammonium Nitrate Contributions to Light Extinction*[a]

| Regions and Data Sets | Avg. Fine $NO_3$ Conc. ($\mu g/m^3$) | Avg. Total Ext. ($Mm^{-1}$) | % of Total Ext. from $NO_3$ Aerosols |
|---|---|---|---|
| *METROPOLITAN - WEST* | | | |
| A. LOS ANGELES METROPOLITAN AREA | | | |
| 1. Appel et al. (1983): One month at Los Angeles and Riverside in summer of 1982.[b,c] | S 10.7 | S 290 | S 34 |
| 2. John et al. (1985): Four days for sampling at west Los Angeles in the summer of 1983.[d,e] | S 5.8 | S 180 | S 25 |
| 3. EPA IP Network: Two to five years of data at Azura, Los Angeles, and Riverside from 1979-1983.[e,f] | >3.1 | 210 | >12 |
| B. SAN FRANCISCO METROPOLITAN AREA | | | |
| 1. Appel et al. (1983): One month at San Jose in the summer of 1982.[b,c] | S 3.4 | S 95 | S 33 |
| 2. John et al. (1985): Four days of sampling at San Jose in the summer of 1982.[b,c] | S 1.4 | S 100 | S 11 |
| 3. EPA IP Network: Two to four years of data at Livermore, Richmond, San Francisco, and San Jose from 1979-1983.[e,f] | >1.5 | 100 | >11 |
| C. DENVER METROPOLITAN AREA | | | |
| 1. Lewis et al. (1986): Three weeks at Denver in the winter of 1982.[c,e] | W 2.2 | W 150 | W 11 |
| 2. Groblicki et al. (1981): Four weeks at Denver in the of 1978.[b,c] | W 6.1 | W 190 | W 14 |
| D. PORTLAND METROPOLITAN AREA | | | |
| 1. Shah et al. (1985): Approximately 30 days per site at four Portland area locations from summer 1977 to spring 1978.[b,c] | >1.8 | 110 | 7 |
| E. ROUTINE NITRATE DATA AT 32 METROPOLITAN LOCATIONS | | | |
| 1. EPA IP Network: One to five years of data at 32 metropolitan locations from 1979-1983.[e,f] | >1.17 | 100 | >9 |
| *RURAL - WEST* | | | |
| A. SPECIAL FIELD PROGRAMS | | | |
| 1. RESOLVE Special Study (Trijonis et al., 1988): Thirteen weeks of sampling at Edwards AFB and China Lake, CA.[b] | 0.9 | 50 | 9 |
| 2. John et al. (1985): Four days of sampling in mountains northeast of Los Angeles in summer of 1983.[d,e] | S 2.5 | S 140 | S 9 |
| 3. John et al. (1985): Four days of sampling in remote Kern County in summer 1982.[d,e] | S 0.9 | S 95 | S 5 |
| B. ROUTINE NITRATE DATA FROM TEFLON FILTERS | | | |
| 1. EPA IP Network: One to four years of data at 9 rural locations from 1979-1983.[e,f] | >0.3 | 40 | >4 |
| 2. WRAQS Network (White and Macias, 1987): One year at ll sites in the mountain/desert West in 1981-1982.[e,f] | >0.1 | 25 | >2 |
| *METROPOLITAN - EAST* | | | |
| A. SPECIAL FIELD PROGRAMS | | | |
| 1. Cadle (1985): One year at Warren, MI in 1981-1982.[e,f,g] | 1.2 | 190 | 7 |
| 2. Hasan and Dzubay (1983): One week at Houston, TX in September 1980.[c,e] | S >0.4 | 190 | S >2 |
| 3. Wolff et al. (1982): One week at Detroit in July 1981.[e,g] | S >0.2 | S 230 | S >1 |
| B. ROUTINE NITRATE DATA FROM TEFLON FILTERS | | | |
| 1. EPA IP Network: One to five years of data at 59 metropolitan locations from 1979-1983.[e,f] | >0.4 | 150 | >3 |

(Continued)

*Table 24E-2. (Continued)*

| Regions and Data Sets | Avg. Fine $NO_3$ Conc. ($\mu g/m^3$) | Avg. Total Ext. ($Mm^{-1}$) | % of Total Ext. from $NO_3$ Aerosols |
|---|---|---|---|
| *RURAL - EAST* | | | |
| A. SPECIAL FIELD PROGRAMS | | | |
| 1. Stevens (1987): Several months of sampling at Research Triangle Park, NC in the 1980's.[e,f] | 0.7 | 170 | 4 |
| 2. Pierson (1987); Mathai and Tombach (1987): One month of sampling at two rural sites in Pennsylvania in summer 1983.[c,e] | S 0.5 | S 280 | S 2 |
| 3. Stevens et al. (1980): One week at Smokey Mountains in September 1980.[e,f,h] | S 0.3 | S 200 | S 2 |
| 4. Cadle et al. (1985): Eighteen weeks in northern Michigan in winter 1983-1984.[e,f,g] | W 0.8 | W 100 | W 8 |
| B. ROUTINE NITRATE DATA FROM TEFLON FILTERS | | | |
| 1. EPA IP Network: One to four years of data at 9 rural sites from 1979-1983.[e,f] | >0.6 | 120 | >5 |

[a] Nitrate concentrations represent lower bound because samples were collected on Teflon filters. Note that lower bound on nitrate concentrations does not necessarily translate into a lower bound for nitrate contributions to extinction (third column) because of compensating effects in estimating nitrate scattering efficiency for some of the studies.
S/W: Data are restricted to a single season, summer (S) or winter (W). Results are seasonally biased and also may be nonrepresentative due to small sample size.

[b] Extinction efficiency for nitrates specific to this data set is derived in cited reference.

[c] Reported extinction values (and any propogated effect on $NO_3^-$ scattering efficiencies) are corrected for nephelometer wavelength, nephelometer calibration, missing coarse particle scattering, and/or Rayleigh scatter.

[d] Non-Rayleigh part of extinction for these California sites is estimated as five times measured fine particle mass as suggested by data from Trijonis et al. (1987), Appel et al. (1983), and Trijonis and Davis (1981).

[e] Nitrate aerosol is taken as 1.29 [$NO_3^-$] to account for mass of ammonium cation. Scattering efficiency for nitrate aerosol is then taken as 4 $m^2/g$ in rural West, 6 $m^2/g$ in urban West, and 8 $m^2/g$ in rural and urban East (Trijonis et al., 1988; Shah et al., 1984; Appel et al., 1983; and White, 1981).

[f] Total extinction is estimated from airport visibility data (Trijonis et al., 1985; Trijonis, 1982a & 1982b; Trijonis and Yuan, 1978a & 1978b). Average total extinction is estimated as 0.7 x [3.9/AMVR], where AMVR is airport median visual range (Trijonis et al., 1988).

[g] Fine aerosol nitrate is computed from total aerosol nitrate using simultaneously collected size distribution data for nitrates.

[h] Total extinction is also estimated at this site as nine times average fine particle mass based on data in Trijonis, 1982a.

## E.4 REFERENCES

**Appel, B.R.** 1987. Personal communication. Air and Industrial Hygiene Laboratory, California Dept. of Health Services, Berkeley, CA.

**Appel, B.R., Y. Tokiwa, J. Hsu, L.E. Kothny, E. Hahn, and J.J. Wesolowski.** 1983. Visibility reduction as related to aerosol constituents. California Air Resource Board report CA/DOH/AIHL/SP-29, Sacramento, CA.

**Cadle, S.H.** 1985. Seasonal variations in nitric acid, nitrate, strong aerosol acidity, and ammonia in an urban area. Atmos. Environ. 19:181-188.

**Cadle, S.H. *et al.*** 1985. Atmospheric concentrations and the deposition velocity to snow of nitric acid, sulfur dioxide, and various particulate species. Atmos. Environ. 19:1819-1827.

**Dzubay, T.G., R.K. Stevens, C.W. Lewis, D.H. Hern, W.J. Courtney, J.W. Tesch, and M.A. Mason.** 1982. Visibility and aerosol composition in Houston, Texas. Environ. Sci. & Technol. 16: 514-525.

**Ferman, M.A., G.T. Wolff, and N.A. Kelly.** 1981. The nature and sources of haze in the Shenandoah Valley/Blue Ridge mountain area. J. Air Pollution Control Assoc. 31:1074-1081.

**Groblicki, P.J., G.T. Wolff, and R.J. Countess.** 1981. Visibility-reducing species in the Denver "Brown Cloud"-I: Relationships between extinction and chemical composition. Atmos. Environ. 15:2473-2484.

**Hasan, H. and T.G. Dzubay.** 1983. Apportioning light extinction coefficients to chemical species in atmospheric aerosol. Atmos. Environ. 17:1573-1581.

* **John, W., *et al.*** 1985. Dry acid deposition on materials and vegetation: concentrations in ambient air. California Air Resources Board report CA/DOH/AIHL/SP-34. Sacramento, CA.

* **John, W., *et al.*** 1986. A new method for nitric acid and nitrate aerosol measurement using the dichotomous sampler. California Air Resources Board report CA/DOH/AIHL/R-304. Sacramento, CA.

**Lewis, C.W., R.E. Baumgardner, R.K. Stevens, and G.M. Russwurm.** 1986. Receptor modeling study of Denver winter haze. Environ. Sci. & Technol. 20:1126-1136.

**Mathai, C.V. and I.H. Tombach.** 1987. A critical assessment of atmospheric visibility and aerosol measurements in the eastern United States. J.Air Pollution Control Assoc.

**Mulawa, P.A. and S.H. Cadle.** 1985. A comparison of nitric acid and particulate nitrate measurements by the penetration and denuder difference methods. Atmos. Environ. 19:1317-1324.

**Pierson, W.R.** 1987. (Table 24 E-2, rural east, personal communication). Desert Research Institute, Reno, NV.

**Shah, J.J., J.G. Watson Jr., J.A. Cooper, and J.J. Huntzicker.** 1984. Aerosol chemical composition and light scattering in Portland, Oregon: The role of carbon. Atmos. Environ. 18:235-240.

**Stevens, R.K.** 1987. Personal communication. Atmospheric Sciences Laboratory, US Environmental Protection Agency, Research Triangle Park, NC.

**Stevens, R.K., T.G. Dzubay, R.W. Shaw, W.A. McClenny, C.W. Lewis, and W.E. Wilson.** 1980. Characterization of aerosol in the Great Smoky Mountains. Environ. Sci. & Technol. 14:1491-1498.

**Trijonis, J.C.** 1982a. Visibility in California. J. Air Pollution Control Assoc. 32:165-169.

**Trijonis, J.C.** 1982b. Existing and natural background levels of visibility and fine particles in the rural East. Atmos. Environ. 16:2431-2445.

**Trijonis, J.C.** 1986. Patterns and trends in data for atmospheric sulfates and visibility. Acid Deposition-Long Term Trends. National Academy of Sciences, Washington, D.C.

* **Trijonis, J.C. and M. Davis.** 1981. Development and application of methods for estimating inhalable and fine particle concentrations from routine Hi-Vol data. Prepared for California Air Resources Board contract #AO-076-32.

**Trijonis, J.C., M. Pitchford, M. McGown, *et al.*** 1987. Preliminary extinction budget results from the RESOLVE program, pp. 872-883. In: P.J. Bhardwaja, ed. Visibility Protection Research and Policy Aspects. Air Pollution Control Association, Pittsburgh, PA.

**Trijonis, J.C. and K. Yuan.** 1978a. Visibility in the Northeast. EPA report 600/3-78-075. Environmental Protection Agency, Research Triangle Park, NC.

**Trijonis, J.C. and K. Yuan.** 1978b. Visibility in the Southwest. EPA report 600/3-78-039. Environmental Protection Agency, Research Triangle Park, NC.

* **Trijonis, J.C., *et al.*** 1985. Air quality benefit analysis for Los Angeles and San Francisco based on housing values and visibility. Prepared for California Air Resources Board contract #A2-088-32.

**Trijonis, J.C., M.McGown, M. Pitchford, D. Blumenthal, P. Roberts, W. White, E. Macias, R. Weiss, A. Waggoner, J. Watson, J. Chow, and R. Flocchini.** 1988. RESOLVE Project Final Report: Visibility Conditions and Causes of Visibility Degradation in the Mojave Desert of California. NWC TP 6869. Naval Weapons Center, China Lake, CA.

* **White, W.H.** 1981. The role of particulate sulfates and nitrates in reducing visibility. Paper presented at Air Pollution Control Assoc. annual meeting in Philadephia, PA, June 1981.

**White, W.H. and E. Macias.** 1987. Particulate nitrate measurements in rural areas of the western United States. Atmos. Environ.

* **Zak, B.D., *et al.*** 1984. The Albuquerque Winter Visibility Study, Vol. 1: Overview and Data Analysis. Sandia National Laboratories report SAN84-0173/1, Albuquerque, NM.

* Nonpeer-reviewed sources.

# APPENDIX F

## QUARTERLY MEDIAN VISUAL RANGES FOR NATIONAL PARK SERVICE AUTOMATED CAMERA SITES, 1986 - 1988

| SITE | SEASONAL MEDIAN VISUAL RANGE (KM) Dec-Feb | Mar-May | Jun-Aug | Sep-Nov |
|---|---|---|---|---|
| Acadia Park, ME | 85 | 64 | 69 | 64 |
| Arches Park, UT | 140 | 158 | 189 | 166 |
| Bandelier Monument, NM | 171 | 154 | 156 | 178 |
| Big Bend Park, TX | 168 | 128 | 145 | 185 |
| Black Canyon Monument, CO | 134 | 146 | 159 | 140 |
| Bryce Canyon Park, UT | 243 | 182 | 184 | 189 |
| Bridger Wilderness, WY | 52 | 60 | 165 | 84 |
| Buffalo River, AR | 61 | 43 | 46 | 64 |
| Carlsbad Caverns Park, NH | 156 | 177 | 110 | 137 |
| Capulin Volcano, NM | 156 | 125 | 136 | 110 |
| Capitol Reef Park, UT | 102 | 144 | 172 | 158 |
| Chaco Culture NHP, NM | 155 | 168 | 166 | 162 |
| Chiricahau Monument, AZ | 170 | 162 | 134 | 166 |
| Colorado Monument, CO | 119 | 151 | 171 | 156 |
| Craig (BLM), CO | 75 | 123 | 148 | 107 |
| Crater Lake Park, OR | 105 | 83 | 148 | 66 |
| Craters of the Moon, ID | 66 | 129 | 140 | 128 |
| Death Valley Monument, CA | 203 | 133 | 92 | 117 |
| Dinosaur Monument, CO | 131 | 133 | 162 | 178 |
| Glacier Park, MT | 35 | 58 | 152 | 82 |
| Glen Canyon Area, AZ | 151 | 152 | 149 | 146 |
| Great Basin Park, NV | 225 | 174 | 195 | 138 |
| Green River Area, WY | 131 | 67 | 176 | 164 |
| Great Sand Dunes, CO | 158 | 123 | 114 | 140 |
| Great Smoky Mountains, TN | 49 | 54 | 20 | 50 |
| Grand Teton Park, WY | 18 | 119 | 127 | 94 |
| Guadalupe Mountains, TX | 150 | 120 | 106 | 125 |
| Isle Royale Park, MN | 24 | 49 | 66 | 58 |
| Jarbidge Wilderness, NV | 64 | 24 | 136 | 92 |
| Joshua Tree Monument, CA | 244 | 140 | 115 | 139 |
| Lava Beds Monument, CA | 154 | 146 | 158 | 112 |
| Lake Mead Area, NV | 234 | 143 | 156 | 149 |
| Lassen Volcanic Park, CA | 107 | 94 | 171 | 122 |
| Mesa Verde Park, CO | 166 | 152 | 156 | 164 |
| Mount Rainer Park, WA | 81 | 82 | 102 | 98 |
| Olympic Park, WA | 10 | 59 | 94 | 66 |
| Pinnacles Monument, CA | 162 | 114 | 132 | 114 |
| Point Reyes, CA | 65 | 50 | 36 | 28 |
| Redwood Park, CA | 91 | 69 | 42 | 50 |
| Rocky Mountain Park, CO | 136 | 110 | 144 | 132 |
| San Gorgonio Wilderness, CA | 266 | 101 | 127 | 140 |
| Shenandoah Park, VA | 70 | 68 | 24 | 54 |
| Superstitution Mountains, AZ | 234 | 185 | 153 | 166 |
| Theodore Roosevelt Park, ND | 198 | 93 | 133 | 120 |
| Voyageurs Park, MN | 75 | 99 | 172 | 106 |
| Weminuche Wilderness, CO | 98 | 112 | 150 | 137 |
| Wind Cave Park, SD | 209 | 119 | 152 | 147 |
| Yellowstone Park, WY | 55 | 24 | 96 | 63 |
| Yosemite Park, CA | 56 | 75 | 69 | 68 |
| Zion Park, UT | 184 | 156 | 172 | 164 |

NOTE: All data are included except for observations of snow-covered targets. Seasonal values represent averages of all quarterly medians available from 1986 to 1988. Quarterly medians are based on regressions fit to cumulative frequency plots (Data from Air Resources Specialists, 1988).

# APPENDIX G

# QUANTIFICATION OF COLOR DIFFERENCE

## G.1 QUANTIFICATION OF COLOR DIFFERENCE

*W. Malm*

The perception of color is not purely physical or purely psychological. It is the evaluation of radiant energy in terms that correlate with visual perception. The study of how the human observer responds to radiant energy of different wavelengths has been ongoing for some 200 years. Although many theories of color vision have been proposed, the Commission Internationale del'Eclairage (CIE), over a period of four decades, has set colorimeteric standards that form the basis of the so-called CIE method of color specification. While these standards are adequate for the evaluation of color in a controlled laboratory setting, they apparently do not accurately quantify color in natural settings. In this appendix, the CIE system will be briefly outlined, as well as new approaches to color quantification that may be more applicable to quantifying the effect of atmospheric particles and gases on natural landscape color.

The CIE chromaticity diagram is one way to quantify the concept of color. In a chromaticity diagram, the spectral distribution of light is first weighted with three functions corresponding to the spectral response of the human eye. For any color of light, there are three coordinate values that define a point in space. The projection of all possible points onto a unit plane ($x+y+z=1$) defines a two-dimensional shape called a chromaticity diagram (see Figure 24G-1). Monochromatic, or light at one wavelength, defines the outer edges of the diagram, and white light is located in the center. Any color can thus be represented by its coordinates ($x,y$), on the diagram.

Since the chromaticity diagram does not distinguish between differences in intensity (*e.g.*, between yellow and brown or white, gray, and black), chromaticity coordinates ($x,y$) must be used in conjunction with a descriptor of light intensity for a complete specification of color. Thus, a color solid can be formed by taking the two-dimensional chromaticity diagram and adding a third dimension perpendicular to this plane to represent brightness.

Figure 24G-2 is a drawing of a color solid. The brightness in such a coordinate system is usually specified by a value of $Y$ or by a parameter ($L^*$), which is directly proportional to the subjective perception of brightness and is related to $Y$ as follows:

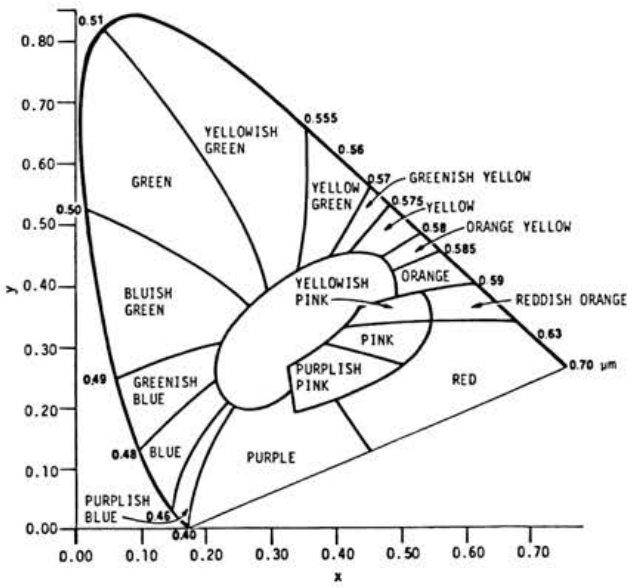


*Figure 24G-1 Chromaticity diagram.*

$$L^* = 25\ Y^{1/3} - 17. \qquad \textbf{(G-1)}$$

The Munsell color system is the most widely used means of specifying colors. In this system, colors are arranged by brightness (or value, which is $L^*/10$), hue (the shade of color—for example, yellow, red, green, or blue), and chroma or saturation (the degree of departure of a given hue from a neutral gray of the same value).

In 1976, the CIE adopted two color-difference formulas for calculating the perceived magnitude of color differences. Color differences are specified by a parameter, $\Delta E$, which is a function of the change in light intensity or value ($\Delta L^*$) and the change in chromaticity ($\Delta x,\Delta y$). The objective of the $\Delta E$ parameter is to provide a univariate measure of the difference between two arbitrary colors as perceived by humans. This parameter allows us to make quantitative comparisons of the perceptibility of two plumes, even though one may be a reddish discoloration viewed against a blue sky while, the other may be a white plume viewed against a dark forest canopy.

$\Delta E$ is related to the distance between two colors in a color space (*e.g.*, Figure 24G-2), with appropriate weights

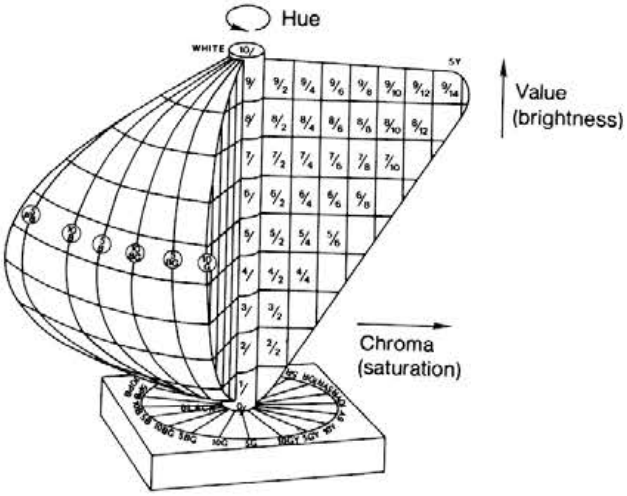


*Figure 24G-2 Representation of a color solid.*

given to the sensitivity of the human eye-brain system to the specific changes in chroma and saturation involved. In this way, color changes having equal $\Delta E$ values can be said to be equally perceptible.

The $\Delta E$ formalism has been used extensively (Latimer *et al.*, 1978; Latimer and Ireson, 1988) to predict the perceptibility of plumes viewed against a variety of backgrounds. However, the color space associated with $\Delta E$, developed under laboratory conditions using color "chips" and uniform backgrounds, may not be directly applicable to perception of color differences under natural conditions. Recent work by Henry has found that the eye brain system may be much more sensitive to color differences in a natural setting (Matamala and Henry, 1990) than predicted by the $\Delta E$ formalism. Furthermore, the $\Delta E$ formalism does not account for the change in plume perceptibility resulting from changes in plume size, shape, and edge sharpness.

A new quantitative parameter, $\Delta F$, has been developed by Henry and co-workers in recent years (Henry and Collins, 1982; Collins and Henry, 1984; Henry, 1986). This parameter is based on the human visual system model of Faugeras (1979), which incorporates the dependence of the human eye/brain system on spatial frequencies. The $\Delta F$ parameter, like $\Delta E$, is proportional to perception of color differences.

All previously described colormetric measurement schemes have serious shortcomings when applied to measurements of natural landscape colors. A major limitation associated with using a chromaticity diagram is deciding on the proper "white point", while the CIE color space requires a definition of $Y_m$, the $Y$ tristimulus value of some reference "white object" color stimulus (MacAdam, 1981). Both problems are centered around the inability to establish, in a natural environment, the chromatic adaptation state of the eye-brain system.

The retinex theory of color perception as proposed by Land seems to circumvent this problem (Land, 1977). He suggests that perceived lightness determinations of various colors are arrived at independently for "short", "middle", and "long" wavelength receptors by sequentially ratioing short, middle, and long wavelength energies at color edges. The ratioing is carried out in such a way as to yield a perceived color that is dependent on the lightest portion of the scene.

Malm *et al.* (1980) have shown how this theory can be modified to fit into the contrast formalism. Suppose that a vista element is viewed against a background blue sky. Then the perceived color is a vector sum of the contrast between the vista element and sky associated with the short, middle, and long wavelength receptors after adjusting each contrast to an equal lightness scale:

$$\hat{C}_c = \hat{C}_s + \hat{C}_m + \hat{C}_l \qquad \textbf{(G-2)}$$

where $\hat{C}_c$, $\hat{C}_s$, $\hat{C}_m$, and $\hat{C}_l$ are the overall color contrast, short, middle, and long wavelength receptor contrasts, respectively. The parameter $\hat{C}_c$ can be thought to be made up of lightness, hue, and saturation components. Numerical quantities can be associated with lightness, hue and saturation by rotating the cartesian ($C_s$, $C_m$ *and* $C_l$) space such that contrast values that satisfy $C_s = C_m = C_l$ form an achromatic contrast scale, $C_a$. Perpendicular distances from the achromate are defined to be saturation (SAT), and the angle around the achromate is defined to be hue.

For reference, Table 24G-1 lists Munsell, color contrast, and chromaticity numbers for a number of Munsell chips. For color contrast calculations the N9.0 Munsell chip was used as a reference against which short, middle, and long wavelength contrasts of various colored chips were calculated. Furthermore, the effect of atmospheric aerosol and gases on $\hat{C}_s$, $\hat{C}_m$, $\hat{C}_l$, and thus color, can be calculated using Equation G-2.

The above described color model does not incorporate the human visual system response to variation in spatial frequencies. Since there is strong evidence in favor of the existence of separate achromatic and chromatic channels in the human eye-brain system, each receiving its information from the same receptors, but processing it in different ways, it has been suggested that achromatic contrast be replaced with equivalent contrast, $C_m$, defined in

*Table 24G-1. Munsell Hue, Lightness and Chroma Color Indices for a Number of Munsell Color Chips. Also Listed for Reference are Corresponding Chromaticity Coordinates and Color Contrast Hue, Saturation and Achromatic Contrast Values.*

| Munsell Notation | | | Color Contrast | | | Chromaticity | |
|---|---|---|---|---|---|---|---|
| Hue | Lightness | Chroma | ϕm | Ca | SAT | X | Y |
| 6.1R | 5.1 | 1.8 | 203.5 | 0.49 | 0.02 | 0.34 | 0.32 |
| 5.1R | 5.0 | 8.0 | 217.1 | 0.55 | 0.11 | 0.44 | 0.32 |
| 4.8Y | 5.1 | 2.0 | 263.0 | 0.51 | 0.08 | 0.35 | 0.36 |
| 5.0Y | 6.9 | 12.0 | 263.8 | 0.46 | 0.50 | 0.47 | 0.49 |
| 6.4G | 5.0 | 2.1 | 296.3 | 0.50 | 0.05 | 0.26 | 0.34 |
| 5.3G | 4.9 | 9.8 | 300.0 | 0.51 | 0.12 | 0.23 | 0.43 |
| 5.4B | 5.0 | 2.0 | 63.4 | 0.45 | 0.74 | 0.28 | 0.30 |
| 7.5B | 4.0 | 9.9 | 66.3 | 0.52 | 0.22 | 0.16 | 0.20 |

the previous section, while saturation and hue remain unchanged. A modulation color contrast vector in this space can be represented as

$$\overline{C}_{mc} = \overline{C}_m + \overline{SAT} + \overline{HUE} \qquad \text{(G-3)}$$

This model has a number of advantages over other color or contrast models. It explicitly accounts for the sensitivity of the human visual system to variation in spatial frequencies, and secondly it incorporates the retinex theory to account for variation in illumination conditions found in a natural setting. Finally, the $C_{mc}$ vector is related to the modulation transfer function of the atmosphere in a simple and direct way.

## G.2 REFERENCES:

**Collins and Henry.** 1984. Incorporation of a Human Visual System Model in the Plume Visibility Model PLUVUE. Environmental Research and Technology, Inc., Newbury Park, CA. ERT Document No. P-B553-001.

**Faugeras, O.D.** 1979. Digital color image processing within the framework of a human visual model. IEEE Trans. Acoust., Speech Sig. Process. ASSP-27:380-393.

**Henry, R.C.** 1986. Improved predictions of plume perception with a human visual system model. J. Air Pollution Control Assoc. 36:1353-1356.

**Henry and Collins.** 1982. Visibility Indices: A Critical Review and New Directions. Environmental Research and Technology, Inc., Westlake Village, CA. ERT Document P-A771.

**Land, E.H.** 1977. The Retinex theory of color vision. Scient. Am. 237(6): 108.

**Latimer, D.A., R.W. Bergstrom, S.R. Hayes, M.K. Liu, J.H. Seinfeld, G.Z. Whitten, M.A. Wojcik, and M.J. Hillyer.** 1978. The development of mathematical models for the prediction of anthropogenic visibility impairment. EPA-450/3-778-110a, b, c. Environmental Protection Agency, Research Triangle Park, NC.

**Latimer, D.A. and R.G. Ireson.** 1988. Workbook for plume visual impact screening and analysis. EPA-450/4-88-015. Environmental Protection Agency, Research Triangle Park, NC.

**MacAdam, D.L.** 1981. Perceptual significance of colorimetric data for colors of plumes and haze. Atmos. Environ.

**Malm, W.C., K.K. Leiker, and J.V. Molenar.** 1980. Human perception of visual air quality. J. Air Pollution Control Assoc. 30(2).

**Matamala, L.V. and R.C. Henry.** 1990. Analysis of the Grand Canyon color matching experiment. In: C.V. Mathai, ed. Visibility and Fine Particles. Air and Waste Management Assoc., Pittsburgh, PA.

# APPENDIX H

# SCATTERING EFFICIENCIES AND ESTIMATED CONTRIBUTIONS

## H-1 DRY FINE-PARTICLE SCATTERING EFFICIENCIES

*W. White*

Listed below are the dry fine-particle scattering efficiencies ($m^2/g$) implied by the apportionment scheme of Table 24-17. Studies are as in Table 24-13.

| DRY SCATTERING EFFICIENCIES | **B**sfd/FM | **B**sfd(slf)/slf | | **B**sfd(org)/org | |
|---|---|---|---|---|---|
| | | low | high | low | high |
| *RURAL EAST* | | | | | |
| Luray, VA/3 | 4.93 | 5.2 | 6.1 | 3.0 | 7.0 |
| Lewes, DE/summer/4 | 4.86 | 5.0 | 6.1 | 3.1 | 6.4 |
| Lewes, DE/winter/4 | 3.58 | 4.1 | 4.8 | 2.4 | 5.6 |
| *URBAN EAST* | | | | | |
| Houston, TX/5 | 3.18 | 3.7 | 4.1 | 2.1 | 5.2 |
| Detroit, MI/6 | 3.74 | 4.0 | 4.9 | 2.4 | 5.2 |
| *RURAL WEST* | | | | | |
| Mojave Desert, CA | | | | | |
| China Lake/7 | 1.62 | 2.2 | 2.6 | 1.3 | 3.0 |
| China Lake/8 | 2.66 | 3.2 | 4.2 | 2.1 | 4.1 |
| Edwards AFB/8 | 2.92 | 3.3 | 4.5 | 2.2 | 4.6 |
| Fort Irwin/8 | 2.66 | 3.3 | 4.1 | 2.1 | 4.5 |
| Colorado Plateua, AZ-UT | | | | | |
| Zilnez Mesa/9 | 2.15 | 2.5 | 3.0 | 1.5 | 3.2 |
| Grand Canyon/11 | 3.39 | 4.0 | 4.6 | 2.3 | 5.8 |
| Grand Canyon/12 | 2.59 | 3.1 | 3.6 | 1.8 | 4.2 |
| Page/11 | 3.23 | 3.4 | 4.6 | 2.3 | 4.4 |
| Page/12 | 2.08 | 2.5 | 2.9 | 1.5 | 3.3 |
| Bryce Canyon/12 | 2.62 | 3.2 | 3.7 | 1.8 | 4.4 |
| Other | | | | | |
| Spirit Mountain, NV/13 | 2.37 | 2.8 | 3.4 | 1.7 | 4.0 |
| Spirit Mountain, NV/12 | 2.76 | 3.3 | 4.0 | 2.0 | 4.6 |
| Meadview, AZ/12 | 2.26 | 2.6 | 3.1 | 1.6 | 3.6 |
| Prescott, AZ/12 | 2.73 | 3.0 | 3.5 | 1.7 | 4.0 |
| *URBAN WEST* | | | | | |
| Metropolitan Denver, CO | | | | | |
| Commerce City/14 | 1.62 | 2.0 | 2.9 | 1.4 | 3.0 |
| Commerce City/day/16 | 2.27 | 2.7 | 3.9 | 1.9 | 3.8 |
| Commerce City/night/16 | 2.69 | 3.2 | 4.8 | 2.4 | 4.1 |
| Downtown/gas/17 | 1.81 | 2.0 | 3.3 | 1.7 | 2.7 |
| Downtown/coal/17 | 1.77 | 1.9 | 3.1 | 1.6 | 2.3 |
| South Coast Basin, CA | | | | | |
| Los Angeles/18 | 2.41 | 2.7 | 3.7 | 1.9 | 3.6 |
| Riverside/18 | 2.74 | 2.9 | 4.6 | 2.3 | 4.3 |
| Azura/19 | 1.53 | 1.8 | 2.7 | 1.3 | 2.7 |
| Pasadena/19 | 1.98 | 2.3 | 3.4 | 1.7 | 3.3 |
| Upland/19 | 2.32 | 2.8 | 4.0 | 2.0 | 4.2 |
| Other | | | | | |
| San Jose, CA/18 | 1.83 | 2.0 | 3.3 | 1.7 | 2.6 |

## H-2 ESTIMATED CONTRIBUTIONS TO FINE-PARTICLE SCATTERING

*W. White*

Listed below are estimated contributions (%) to fine-particle scattering shown in Figure 24-45. Studies are as in Table 24-13.

| ESTIMATED CONTRIBUTIONS | SULFATES | | ORGANICS | |
|---|---|---|---|---|
| | low | high | low | high |
| *RURAL EAST* | | | | |
| Luray, VA/3 | 75 | 89 | 7 | 25 |
| Lewes, DE/summer/4 | 68 | 85 | 11 | 33 |
| Lewes, DE/winter/4 | 61 | 72 | 12 | 31 |
| *URBAN EAST* | | | | |
| Houston, TX/5 | 69 | 76 | 8 | 22 |
| Detroit, MI/6 | 64 | 80 | 13 | 37 |
| *RURAL WEST* | | | | |
| Mojave Desert, CA | | | | |
| China Lake/7 | 36 | 42 | 13 | 32 |
| China Lake/8 | 31 | 42 | 27 | 54 |
| Edwards AFB/8 | 36 | 48 | 21 | 45 |
| Fort Irwin/8 | 37 | 46 | 18 | 40 |
| Colorado Plateau, AZ-UT | | | | |
| Zilnez Mesa/9 | 49 | 61 | 20 | 43 |
| Grand Canyon/11 | 57 | 66 | 9 | 23 |
| Grand Canyon/12 | 56 | 64 | 13 | 32 |
| Page/11 | 43 | 59 | 26 | 52 |
| Page/12 | 50 | 60 | 16 | 37 |
| Bryce Canyon/12 | 53 | 62 | 13 | 31 |
| Other | | | | |
| Spirit Mountain, NV/13 | 49 | 58 | 14 | 33 |
| Spirit Mountain, NV/12 | 48 | 58 | 14 | 34 |
| Meadview, AZ/12 | 53 | 63 | 15 | 34 |
| Prescott, AZ/12 | 62 | 73 | 14 | 33 |
| *URBAN WEST* | | | | |
| Metropolitan Denver, CO | | | | |
| Commerce City/14 | 22 | 30 | 14 | 39 |
| Commerce City/day/16 | 25 | 35 | 18 | 46 |
| Commerce City/night/16 | 18 | 31 | 26 | 61 |
| Downtown/gas/17 | 12 | 20 | 27 | 58 |
| Downtown/coal/17 | 17 | 29 | 35 | 67 |
| South Coast Basin, CA | | | | |
| Los Angeles/18 | 37 | 52 | 18 | 44 |
| Riverside/18 | 23 | 34 | 20 | 45 |
| Azura/19 | 20 | 29 | 16 | 40 |
| Pasadena/19 | 24 | 34 | 18 | 44 |
| Upland/19 | 22 | 30 | 15 | 40 |
| Other | | | | |
| San Jose, CA/18 | 12 | 20 | 40 | 69 |

## H-3 ESTIMATED CONTRIBUTIONS TO NON-RAYLEIGH EXTINCTION

*W. White*

Listed below are estimated contributions (%) to non-Rayleigh extinction shown in Figure 24-46. Studies are as in Table 24-13.

| ESTIMATED CONTRIBUTIONS | SULFATES | | ORGANICS | |
|---|---|---|---|---|
| | low | high | low | high |
| *RURAL EAST* | | | | |
| Luray, VA/3 | 71 | 84 | 7 | 24 |
| Lewes, DE/summer/4 | 62 | 77 | 10 | 30 |
| Lewes, DE/winter/4 | 47 | 56 | 9 | 24 |
| *URBAN EAST* | | | | |
| Houston, TX/5 | 53 | 59 | 6 | 17 |
| Detroit, MI/6 | 51 | 64 | 11 | 30 |
| *RURAL WEST* | | | | |
| Mojave Desert, CA | | | | |
| China Lake/7 | 19 | 23 | 7 | 17 |
| China Lake/8 | 19 | 26 | 17 | 33 |
| Edwards AFB/8 | 24 | 32 | 14 | 30 |
| Fort Irwin/8 | 23 | 29 | 11 | 25 |
| Colorado Plateau, AZ-UT | | | | |
| Zilnez Mesa/9 | 35 | 43 | 14 | 30 |
| Grand Canyon/11 | 39 | 45 | 6 | 15 |
| Grand Canyon/12 | 46 | 53 | 11 | 26 |
| Page/11 | 26 | 35 | 16 | 31 |
| Page/12 | 38 | 45 | 12 | 28 |
| Bryce Canyon/12 | 45 | 52 | 11 | 26 |
| Other | | | | |
| Spirit Mountain, NV/13 | 31 | 38 | 9 | 21 |
| Spirit Mountain, NV/12 | 36 | 43 | 11 | 25 |
| Meadview, AZ/12 | 38 | 45 | 10 | 25 |
| Prescott, AZ/12 | 46 | 54 | 11 | 25 |
| *URBAN WEST* | | | | |
| Metropolitan Denver, CO | | | | |
| Commerce City/14 | 11 | 16 | 7 | 20 |
| Commerce City/day/16 | 15 | 22 | 11 | 28 |
| Commerce City/night/16 | 11 | 19 | 16 | 38 |
| Downtown/gas/17 | 5 | 9 | 12 | 25 |
| Downtown/coal/17 | 6 | 10 | 12 | 23 |
| South Coast Basin, CA | | | | |
| Los Angeles/18 | 27 | 38 | 13 | 32 |
| Riverside/18 | 17 | 25 | 15 | 33 |
| Azura/19 | 12 | 16 | 9 | 23 |
| Pasadena/19 | 16 | 23 | 12 | 30 |
| Upland/19 | 15 | 21 | 11 | 28 |
| Other | | | | |
| San Jose, CA/18 | 7 | 11 | 22 | 37 |

## INDEX